Analysis of Selected Symbiosis Repressed Poplar Genes upon Ectomycorrhiza Formation

Dissertation

zur Erlangung des akademischen Grades eines
Doktors der Naturwissenschaften
-Dr. rer. nat.-

im Fachbereich 2 (Biologie/Chemie)
der Universität Bremen

vorgelegt von

Anneke Immoor

Bremen, August 2021

Analysis of Selected Symbiosis Repressed Poplar Genes upon Ectomycorrhiza Formation

Erster Gutachter:	Prof. Dr. Uwe Nehls
Zweite Gutachterin:	Prof. Dr. Rita Groß-Hardt
Datum des Kolloquiums:	05.10.2021

Danksagung

Diese Doktorarbeit zu schreiben wäre unmöglich gewesen ohne meinen Betreuer Prof. Dr. Uwe Nehls. Ich danke dir für dein Vertrauen in mich und die Chancen, die du mir durch meinen Wechsel in die molekulare Biologie ermöglicht hast. Ich konnte viel von deinem großen Wissen und unseren Diskussionen profitieren.

Großer Dank gebührt meinen ehemaligen und derzeitigen Kollegen. Danke Annette Hintelmann für deinen fortwährenden moralischen Support und dass du immer für mich dar warst. Du hältst alles am Laufen und hast immer den Überblick. Auch dir Thea möchte ich danken, für die gute Zusammenarbeit und deine gute Pflege unserer Pappel- und Pilzstämme. Danke Jonas Lucht, dass du mir auf meinen letzten Metern im Labor und am Mikroskop noch mal neue Motivation geschenkt hast. Ohne dich wäre ich in der Bildauswertung und Bearbeitung bei weitem nicht so weit gekommen. Nicht zu vergessen sind Jana Schnakenberg und Jana Müller: wir haben die schwierigsten Zeiten gemeinsam gemeistert!

Vielen Dank Rita Groß-Hardt, dass du dich bereit erklärt hast, diese Arbeit zu begutachten. Vielen Dank auch an Martin Diekmann, Annette Peter und Judith Giel, dass ihr in meiner Prüfungskommission sitzt.

Zu guter Letzt möchte ich mich bei meiner Familie bedanken. Ihr seid einfach immer für mich da. Ohne euch wäre ich nicht dort, wo ich jetzt bin. Auch könnte ich mir keine besseren Schwiegereltern wünschen. Lucas, ich weiß nicht, ob ich das alles ohne dich durchgestanden hätte. Du trägst so große Anteile an dieser Arbeit und ich konnte dich täglich mit meinen Problemen und Erfolgen erfreuen. Ich liebe dich.

Auch wenn sie es vermutlich nie lesen werden: danke an die Ponys Dukie und Charlie. Dafür, dass ihr so frech (oder süß) seid und mir immer geholfen habt, den Kopf für ein paar Stunden freizubekommen. Seit neustem hilft dabei auch unser Hund Morris. Danke!

Zusammenfassung

Damit eine Symbiose zwischen Ektomykorrhizen und Pflanzen stattfinden kann, muss die Struktur und Funktionalität von Feinwurzeln angepasst werden. Nur so kann der Stoffaustausch von Zucker gegen Nährstoffe und weitere Metabolite stattfinden. Die grundlegenden Prozesse dieser Anpassungen sind dabei in großen Teilen noch unerforscht. Auf dieser Grundlage wurden in vorangegangenen Studien durch genomweite Genexpressionsanalysen drei Pappel Gene identifiziert, deren Transkription in Mykorrhizen 20 – 100 -fach niedriger war. Es handelte sich dabei um ein Kalzium Bindeprotein (*Potri.2G2183*), einen Aminosäure Transporter (*Potri.2G0797*) und ein Enzym aus dem Fettstoffwechsel (*Potri.9G1040*). Um die Proteine zu charakterisieren und den Mechanismus der Regulierung herauszufinden, wurden die Promotoren in dieser Arbeit auf mögliche *cis* - Elemente untersucht. Dafür wurden Promotor-Reporter Konstrukte mit Fluoreszenzproteinen hergestellt und dann mittels Agrobakterien zur Behandlung von Komposit Pappeln verwendet. Als Grundlage für diese Analyse konnte im Rahmen dieser Arbeit durch einen Wechsel von pPLV zum pCXUN basierten Vektorrückrat die Transformationseffizienz der Pappeln um 69.8 % erhöht werden. Weiterhin wurde herausgefunden, dass weder die Orientierung der Fluoreszenz Kassetten auf der T – DNA, noch deren Größe einen messbaren Einfluss auf die Pflanzentransformationseffizienz haben. Dabei konnten Promoter Bereiche von *Potri.2G2183* und *Potri.2G0797* erfolgreich mittels PCR amplifiziert und trunkiert werden. Zur weiteren Charakterisierung der Promotoren, wurden diese und ihre Trunkierungen in eine eGFP-NLS Expressionskassette kloniert. Um potenzielle *cis* – Elemente durch Auswertung visueller Daten zu finden, wurde eine konstitutiv exprimierende tdTomato-NLS Expressionskassette in Tandem mit der Promoter Kassette geschaltet (Grün: Rot Verhältnis). Diese Verhältnisse können gegebenenfalls Aufschluss über Änderungen in der Genexpression durch die Mykorrhizierungen geben. Als Alternative zu diesen so genannten Doppelmarker Konstrukten aus eGFP und tdTomato wurde das Timer Protein DsRED-E5 etabliert. Weil das grüne Signal im Verhältnis zum roten Signal im Falle des Timer Proteins sehr schwach war, wurde die Bildaufnahme durch Variierung des der Kameraeinstellungen optimiert. In anschließenden Studien muss diese Methode nun auf Anwendbarkeit in Mykorrhizen getestet werden. Insgesamt muss die visuelle Quantifizierung noch weiter optimiert werden. Auch subzälluläre Lokalisierung der Gene basierend auf transienter Expression in Tabakblättern wurde durchgeführt. Da hier keine eindeutigen Signale detektiert werden konnten, muss das System weiter angepasst und optimiert werden.

Summary

Plant fine roots undergo several developmental and functional adaptations to allow for the association with ECM fungi and to enable bidirectional nutrient and metabolite exchange. To investigate the molecular basis of these processes, a set of 3 poplar genes that have been characterized as mycorrhiza repressed in previous studies (Nehls, unpublished), were used. These genes are supposed to code for (1) a calcium binding protein (*Potri.2G2183*), (2) an amino acid transporter (*Potri.2G0797*) and (3) a protein involved in lipid metabolism (*Potri.9G1040*). To be able to perform promoter analyses in composite poplar roots, the root transformation process was optimized. By switching from a pPLV to pCXUN vector backbones for *Agrobacterium* mediated T – DNA transfer, the transformation efficiency was substantially increased. Additionally, it could be shown, that neither the T – DNA size of single or double fluorescence protein cassettes, nor the orientation of the expression cassettes on the T – DNA impacted this overall transformation efficiency. To characterize their gene expression, promoter regions of all three genes were visually screened *in planta* for regulatory elements or possible transcription factor binding sites using promoter-reporter gene constructs. Thereby, a second constitutively expressed fluorescence cassette was introduced as a possible verification and reference method for visual evaluation of gene expression based on green: red ratios. Promoter regions of *Potri.2G0797* and *Potri.2G2183* were successfully amplified from genomic poplar DNA and a series of truncations was generated to identify possible *cis* - elements. It was possible to detect changes in expression patterns. However, the identified regions need further analysis to determine if they might control fine root dependent gene expression and gene suppression upon ectomycorrhizal symbiosis. As an alternative to double protein cassettes, a timer protein was successfully established as an additional tool for promoter analysis. Because the green signals were very weak compared to red, the image taking process was optimized by adapting the camera settings. Further studies need to verify the applicability of such ratio-based expression intensity measurements in mycorrhiza regulated gene expression. Furthermore, the whole system needs to be further optimized to obtain reliable and comparable results. The subcellular localization of the deduced proteins of these genes was tested *in planta* but was unsuccessful and thus needs further optimization processes.

Table of Contents

Danksagung I

Zusammenfassung II

Summary III

Table of Contents IV

List of Abbreviations IX

1 Introduction 1

- 1.1 General introduction 1
- 1.2 Ectomycorrhiza 1
  - 1.2.1 Ectomycorrhiza overview 1
  - 1.2.2 Ectomycorrhiza structure 2
  - 1.2.3 Ectomycorrhiza ecology 3
  - 1.2.4 Ectomycorrhiza function 5
- 1.3 The woody plant model organism *Populus spec.* 6
- 1.4 The ectomycorrhiza model organism *Pisolithus microcarpus* 7
- 1.5 Plant transformation methods 8
  - 1.5.1 Comparing stable to transient plant transformation 8
  - 1.5.2 Overview of Agrobacterium mediated plant transformation 9
  - 1.5.3 Binary vector systems as a tool for Agrobacterium mediated plant transformation 10
  - 1.5.4 The plant transformation vectors pGREEN and pCXUN 11
  - 1.5.5 Creating plant transformation vectors using Ligase independent cloning (LIC) 13
- 1.6 Gene regulation in Eukaryotes: Promoter analyses 14
  - 1.6.1 Overview of gene regulation in eukaryotes 14
  - 1.6.2 Eukaryotic promoter structure 14
  - 1.6.3 cis – element-based regulation of eukaryotic gene transcription 15
  - 1.6.4 Eucaryotic promoter stability 16
  - 1.6.5 Functional promoter analyses in Eukaryotes 17
- 1.7 Fluorescence protein reporter systems 18
  - 1.7.1 Fluorescence proteins 18
  - 1.7.2 Use for subcellular protein localization studies and promoter analysis 19
  - 1.7.3 Distinguishing autofluorescence from fluorescence protein signals 20
- 1.8 Study background 21

1.8.1 The poplar gene Potri.2G0797 21
1.8.2 The poplar gene Potri.2G2183 22
1.8.3 The poplar gene Potri.9G1040 23
1.9 Thesis aims and objectives 25
2 Material and Methods 26
2.1 Technical Equipment 26
2.1.1 Statistics 26
2.1.2 Microscopy 26
2.1.3 Image processing 27
2.1.4 Agarose gel electrophoresis 28
2.1.5 Sterile working benches 29
2.1.6 Centrifuges 29
2.1.7 Thermoshaker 29
2.1.8 OD_{600} measurements 29
2.1.9 Polymerase Chain Reaction (PCR) Thermocycler 29
2.1.10 Incubator 29
2.1.11 Sterilefiltration and autoclaving 30
2.2 Chemicals and Enzymes 30
2.3 Kits 33
2.4 Organisms 33
2.5 Cloning strategies 34
2.5.1 Intermediate cloning vector pJET1.2 34
2.5.2 Binary vectors pPLV and pCXUN 35
2.5.3 Promoters and terminators 36
2.5.4 Fluorescence proteins 36
2.5.5 Used primers 37
2.5.6 Conventional cloning: Dephosphorylating and Ligation steps 41
2.5.7 Ligase Independent Cloning (LIC) of promoter fragments 42
2.6 Lab protocols 43
2.6.1 Extraction of genomic DNA from Populus tremula x tremuloides 43
2.6.2 Polymerase chain reaction (PCR) 45
2.6.3 Agarose gel electrophoresis (Sambrook et al., 1989) 47
2.6.4 DNA quantification methods 48
2.6.5 Cloning of PCR fragments in the pJET 1.2 vector 48

2.6.6 Chemical competent *Escherichia coli* cells 48
2.6.7 Transformation of chemically competent E. coli 50
2.6.8 Plasmid isolation from *E. coli* using the Alkaline Lysis Method 50
1.1.12 Restriction digestion 52
2.6.9 Sanger Sequencing 52
2.6.10 Glycerol stocks 53
2.6.11 In silico cloning 53
2.6.12 Transformation of *Agrobacterium rhizogenes* modified from (Holsters et al., 1978) 53
2.6.13 Chemical competent Agrobacteria 54
2.6.14 Subcellular localization of proteins in Nicotiana benthamiana leaves 54
2.6.15 Transformation of Populus alba and P. tremula x tremuloides: Composite plants 55
2.6.16 Mycorrhization of transformed poplar fine roots 56
3 Results 58
3.1 Optimizing composite Poplar root transformation efficiencies 58
3.1.1 Establishing pCXUN as standard plant transformation vector for Composite plants 58
3.1.2 Does the orientation of the marker cassettes in the T – DNA impact the transformation efficiency of poplar roots? 64
3.2 Establishing DsRED-E5 as potential marker gene for *in planta* investigation of gene regulation in poplar 68
3.3 Determining promoter activity based on fluorescence intensities 71
3.3.1 Establishing camera settings for the analysis of promoter intensities based on images 71
3.3.2 Determining impacts on the comparability of fluorescence ratios 72
3.4 Comparing fluorescence ratios between first and second order root hair nuclei 74
3.5 Consistency of fluorescence expression levels in one transgenic root system 76
3.6 Characterization of *Potri.2G0797* 78
3.6.1 Subcellular protein localization of Potri.2G0797: Do introns matter? 78
3.6.2 Promoter analyses of Potri.2G0797 in a pCXUN backbone double marker system 80
3.6.3 Using different poplar hybrids for promoter analysis? 88
3.6.4 Fluorescence intensities in mycorrhized and non – mycorrhized fine - roots 89

3.7 Characterization of *Potri.2G2183* 92

  3.7.1 Subcellular protein localization of *Potri.2G2183* 92

  3.7.2 Promoter analyses of *Potri.2G2183* 92

3.8 Characterization of *Potri.9G1040* 97

  3.8.1 Promoter analyses and the identification of transcription factors of Potri.9G1040 97

4 Discussion 99

4.1 Establishing pCXUN as poplar root transformation vector 99

  4.1.1 Plant transformation efficiencies of the binary vectors pPLV and pCXUN 99

  4.1.2 Impacts of the orientation of the expression cassette in the pCXUN T-DNA 100

  4.1.3 Plant transformation efficiencies of single and double marker cassettes 102

4.2 Fluorescence reporters for the investigation of promoter activity 102

  4.2.1 Calibration of double fluorescence marker cassettes for promoter analysis 103

  4.2.2 The timer protein DsRED-E5 105

4.3 Epifluorescence microscopy-based quantification of fluorescence intensities 106

  4.3.1 Defining camera settings to obtain reliable fluorescence intensities 106

  4.3.2 Autofluorescence in fluorescence microscopy 107

  4.3.3 Impact of root orders on gene expression in poplar 108

  4.3.4 Gene expression patterns in roots of composite poplar plants 109

4.4 Promoter analysis of mycorrhiza regulated genes 110

  4.4.1 Promoter truncations as a step to find potential cis - elements 110

  4.4.2 Promoter analyses of *Potri.2G0797* 111

  4.4.3 Promoter analyses of *Potri.2G2183* 113

  4.4.4 Promoter analyses of *Potri.9G1040* 114

  4.4.5 Using different poplar hybrids for promoter analyses 114

4.5 Subcellular protein localization in tobacco leaves 115

  4.5.1 Heterologous expression in tobacco leaves 115

  4.5.2 Subcellular localization of *Potri.2G0797*, *Potri.2G2183* and *Potri.9G1040* 115

5 Outlook 118

6 Appendix and supplementary data 119

6.1 List of Tables 119

6.2 List of Figures 122

6.3 Construct verifications 136

  6.3.1 Verification of marker constructs in pCXUN for establishing experiments 136

6.3.2 Establishing DsRED-E5 137
6.3.3 Verifications of *Potri.2G0797* subcellular localization constructs 137
6.3.4 Verifications of *Potri.2G0797* promoter constructs 141
6.3.5 Verifications of *Potri.2G2183* subcellular localization 145
6.3.6 Verifications of *Potri.2G2183* promoter constructs 146
6.3.7 Verifications of *Potri.9G1040* promoter constructs 148
7 References 151
Versicherung an Eides Statt 173

List of Abbreviations

A	Adenosine
AAAP	Amino Acid/Auxin Permease
AAP3	Amino Acid Permease 3
ADP	Adenosine DiPhosphate
AGS	AGropine Synthase
APC	Amino acid – Polyamine Choline
ATP	Adenosine TriPhosphate
ATPase	enzyme that hydrolyses adenosine triphosphate to adenosine diphosphate
bp	basepairs
BSA	Bovine Serum Albumin
C	Carbohydrate
C (base)	Cytosine
CAM	Calmodulin
CamV 35S promoter	Cauliflower Mosaic Virus 35S Promoter
cDNA	complementary DNA
CDS	Coding Sequence
chv-genes	bacterial chromosomal virulence genes
cLSM	confocal Laser Scanning Microscope
CML	CalModulin Like
CPY	Casein hydrolysate-Peptone-Yeast extract medium
CTAB	CetylTrimethylAmmonium Bromide
CUS	CUcumopine Synthetase
CXE12	CarboXyl Esterase 12 protein
dCTP	deoxyCytidine TriPhosphate
ddH_2O	double distilled water
DEPC	DiEthyl PyroCarbonate
dGTP	deoxyGuanosine TriPhosphate
DTT	Dithiothreitol
DMSO	DiMethyl SulfOxide
DNA	DeoxyriboNucleic Acid
DNase	Desoxyribonuklease
dNTP	desoxyNucleoide TriPhosphates
DPSS	Diode Pumped Solid State Laser
dsDNA	double stranded DNA
DTT	DiThioThreitol
ECM	ECtoMycorrhiza
EF hand	helix-loop-helix structural domain
d	Effect size
ER	Endoplasmatic reticulum
EtBr	Ethidium bromide
EtOH	Ethanol
FP	Fluorescence Protein
G	Guanine
GABA	Gamma-AminoButyric Acid
gDNA	genomic DNA
GFP	Green Fluorescence Protein. dGFP = double GFP
HF	High fidelity
INRA	INstitut de la Recherche Agronomique
KCM	Potassium chloride - Calcium chloride - Magnesium chloride

kb	Kilobase
kDa	Kilo Dalton
LAS 2.0	Leica Application Suite Software 2.0
LB	Lysogeny Broth
LUT	Lookup Table
LIC	Ligase Independent Cloning
MAS	Mannopine Synthase
MES	2-(N-Morpholino)Ethanesulfonic acid
MHB	Mycorrhiza Helper Bacteria
M&M	Material and Methods
MMEJ	Microhomology Mediated End-Joining
MOPS	3-(N-morpholino)propanesulfonic acid
mRNA	messenger RNA
MS salts	Murashige and Skoog salts
MS6 medium	Murashige and Skoog medium
MSC	Multiple Cloning Site
NEB	New England Biolabs
NHEJ	Non-Homologous End Joining
NLS	Nuclear Localization Sequence
NOS	NOpaline Synthase
OCS	OCtopinse Synthase
OD	Optical Density
ORI	Origin of Replication
P	Phosphate
PIC	Preinitiation complex
PCR	Polymerase Chain Reaction
Potri.2G0797	poplar aminoacid transporter Potri.2G0797
Potri.2G0797	poplar aminoacid transporter Potri.2G0797
Potri.9G1040	poplar CXE12 family protein Potri.9G1040
Psd	Phosphatidylserine decarboxylase gene
RFP	Red Fluorescence Protein
Ri-plasmid	Root inducing plasmid
RNA	RiboNucleic Acid
RNAi	RNA interference
RNase	Ribonuclease
rol-genes	root-inducing genes
rpm	rounds per minute
rSAP	Shrimp Alkaline Phosphatase
RT	Room Temperature
RT-qPCR	Real Time quantitative Polymerase Chain Reaction
SD	Shine-Dalgarno sequence
SDS	Sodium dodecyl sulfate
SE	Standard error
SNL	Amino acid sequence for a peroxisome localization signal
ssDNA	single stranded DNA
Std	Standart deviation
SUS	SUccinamopine Synthase
sYFP	super Yellow Fluorescence Protein
T	Thymine
T - DNA	transfer DNA
T89	Populus tremula x tremuloides

TAE	Tris-Acetic acid-EDTA buffer
TATA-box	binding site for transcription factors in the promoter region of many genes
TBP	Transcription Factor Binding Protein
TF	Transcription Factor
Ti-plasmid	Tumor inducing plasmid
TS	Transcription Start
U	1 Unit of restriction enzyme will completely digest 1 µg of substrate DNA in a 50 µl reaction in 60 minutes
UTR	UnTranslated Region
UV	Ultraviolet
VIP	*vir*E2-Interacting Protein
vir-genes	virulence genes
xg	x-times the gravitational acceleration
(k/m) bp	(kilo/mega) base pairs
2,4-D	2,4-dichlorphenoxyacetic acid
2,4-DB	2,4-dichlorophenoxbutyric acid
2,4-methyl	methyl-2,4-dichlorphenoxy acetate

1 Introduction

1.1 General introduction

It is important to investigate forest systems for reasons that are economic in terms of wood production as well as ecologic with regard to large scale carbon sequestration (Nehls et al. 2010). Since most of current European forests consist of plants living in symbiosis with an ectomycorrhizal fungal partner, it is of great relevance to better understand the impacts of mycorrhiza on tree growth and health (Yang et al., 2015). This is particularly true for ecosystem management, restoration, forestry and agriculture (Tsai et al., 1994; Martin et al., 2007). Model organisms like *Populus spec*. on the plant site and *Pisolithus microcarpus* at the fungal site are useful to investigate the principals of mycorrhizal symbiosis.

1.2 Ectomycorrhiza

1.2.1 Ectomycorrhiza overview

Mycorrhizal interactions can be divided into seven groups, which mainly differ in their infection and growth pattern as well as plant and fungal partners (Massicotte et al., 1987; Sally and Smith, 2008). The focus of this study is on Ectomycorrhiza, which are most common in woody perennials of boreal and many temperate forest ecosystems (Martin and Nehls, 2009; Vayssières et al., 2015; Balestrini and Kottke, 2016). All in all, about 2 - 3 % of all land plants, mainly forest trees, are able to undergo such a symbiosis with ECM (ectomycorrhizal) soil fungi (Martin and Nehls, 2009; Nehls et al., 2010; Tedersoo et al., 2010). Thereby, ectomycorrhiza mycelia make up to 80% of the fungal body and 30% of the microbial biomass in forest soils (Allen, 1991; Fitter and Moyersoen, 1996; Wang and Qiu, 2006). Its formation mostly takes place in the upper soil layers at the interface of organic matter and mineral soil, where the mineralization processes are most active (Dahlberg, 2001). ECM might have helped land colonization because of their relatively high mineralization capacities (Allen, 1991; Fitter and Moyersoen, 1996; Wang and Qiu, 2006). They were found to have evolved repeatedly with different origins over the last 80 -180 million years (Martin, 2001; Bruns and Shefferson, 2004; Hibbett and Brandon Matheny, 2009). This broad time range cannot be further narrowed because nearly no fossilization of the soft fungal tissue can be recorded (Lepage et al., 1997). Thus, the complete recognition- and first colonization process is still poorly understood.

1.2.2 *Ectomycorrhiza structure*

Ectomycorrhiza fungi form large colonies that are interconnected with soil exploring hyphae. Generally, the colony of such a mycobiont is divided into three different functional networks and consists of **(1)** extra-radical hyphae, **(2)** a fungal sheath forming a mantle around plant fine roots and **(3)** intercellular hyphae forming the Hartig net (Martin and Nehls, 2009; Tedersoo et al., 2010). A visualization of these structures is given in **Figure 1**.

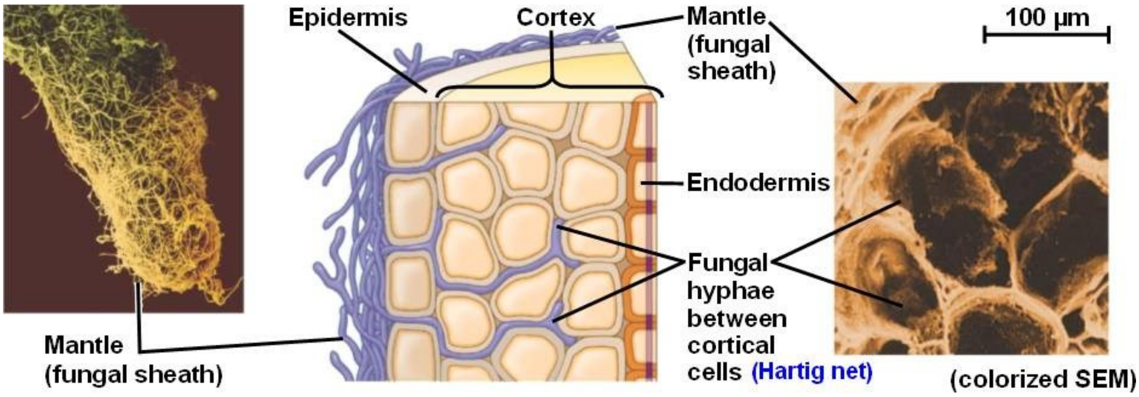

Figure 1. Overview of where the symbiosis of trees and ectomycorrhiza takes place. Atrebe10: "Basic morphology of a common ectomycorrhizal association", (https://commons.wikimedia.org/wiki/File:Ectomycorrhiza_illustration.jpg). Published at Wikimedia commons, 19.07.2021, Licensed under Attribution Share Alike 3.0 Unported license (https://creativecommons.org/licenses/by-sa/3.0/deed.en). SEM = Scanning Electron Microscope.

A plant fine root is colonized as soon as a mantle and Hartig net are formed. Thereby, almost every fine root of an ectomycorrhizal plant is colonized (Dahlberg, 2001; Majdi et al., 2001; Martin, 2001). In detail, the colonization process starts with spatially separated ectomycorrhizal hyphae and plant fine roots (Schaechter, 2009). After first contact, the hyphae wrap around the roots, aggregate, and form a fungal sheath. This mantle – like structure can get up to 40 µm thick in diameter and leads to a closed environment at the root surface. Because it can greatly resemble parenchymal tissue, it is referred to as pseudo-parenchyma in such cases (Schaechter, 2009). Originating from this mantle, a so called Hartig net is frequently formed where ingrowing hyphae (Intraradical hyphae) establish an intercellular network between the root- and fungal colony. When forming the Hartig net, the hyphae penetrate next to the root cap and grow in transverse direction to the root axis and into the space of the middle lamella (Blasius et al., 1986). Thereby, they grow with the apoplast of epidermal – and cortex cells (Massicotte et al., 1987; Sally and Smith, 2008). The penetration depth is plant species dependent, which is also true for strategies to increase the interaction surface, for example the elongation of epidermal cells (Blasius et al. 1986; Smith and Read 2010). It was shown that the fungal hyphae of the Hartig net have a transfer-cell like structure (coenocytic) without cell septation, resulting in a multinucleate status of the hyphae, which is thought to facilitate nutrient transport. Cells of the extraradical hyphae of ectomycorrhizal fungi form septa (Kottke and Oberwinkler, 1987). Outward extending hyphae also originate from the mantle and surround the roots in single, hydrophilic branches or collective, hydrophobic structures called rhizomorphs (Agerer 2001; Smith and Read 2010). The complexity of such a rhizomorph organization depends on different fungal exploration strategies, and organization types and can be directly correlated to long distance nutrient transport rates (Kammerbauer et al., 1989; Agerer, 2001; Smith and Read, 2010). Depending of the branching order of roots, death rate of fine roots and nutrient availability, ECM structures last for approximately one annual season (Dahlberg, 2001; Majdi et al., 2001; Martin, 2001). This is also correlated to the fact, that plant fine roots are short – lived and defined to be second or third order and not more than 2 mm in diameter (Helmisaari et al., 2000; Pregitzer et al., 2007; Zhu et al., 2018). However, fine – root life span was reported to be increased upon mycorrhization (Guo et al., 2008).

1.2.3 Ectomycorrhiza ecology

During ectomycorrhizal symbiosis, fungus derived minerals and nutrients that were mobilized from organic layers of the soil are exchanged with plant-derived carbohydrates gained from photosynthesis (Martin and Nehls, 2009; Nehls et al., 2010; Tedersoo et al., 2010). Because plants are naturally limited by nitrate and phosphate, the availability of nutrients through the fungal partner improves the plants ability to compete for habitats (Nehls et al., 2010). Overall, fungi can provide up to 68% of the host plants nitrogen need (Peay et al., 2007). Thereby, the fungus may be able to change the plants uptake capacity depending on the amount of available N (Corrêa et al., 2008). Additionally, the phosphate exchange to the plant directly correlates with the plant's growth (Jones et al., 1998). Thus, ECM plants were shown to grow much larger in the same amount of time compared to non-mycorrhized plants (Jones et al., 1998; Corrêa et al., 2008). The fungus on the other hand gains an advantage from the easily available carbohydrates of the plant. That is, because its own capacities to take up other sources than dead organisms or plant exudates are restricted, resulting in an inability to utilize complex carbohydrates (Nehls et al. 2010). Combined with the direct access of fungi to plant exudates at colonized roots, both symbionts can often occur at environments where both could not survive without the other (Nehls et al., 2010). Therefore, ECM are highly competitive in soil exploration, but each symbiont also has intra species competition.

On the fungal site, the timing of the colonization determines the dominant fungus in the species composition (priority effect), relating to the amount of root tips colonized per plant

(Kennedy et al., 2009; Kennedy, 2010). This process is fungal species dependent and can be influenced by many abiotic and biotic factors, such as soil moisture and pH value, or the number of competitors, host specificity and selective grazing by collembola (Mamoun and Olivier, 1993; Kennedy, 2010; Kanters et al., 2015). Thus, one tree can be mycorrhized by many fungi and one fungus can colonize many trees, forming a link between different plants and plant species. Such a network can expand over several square kilometres and may have major consequences on plant competitive interactions and performance (Dahlberg, 2001). It is assumed, that linkages of single trees through one fungus reduce plant competition and even promote forest recovery because of source-sink relationships. This underground "tree-talk" might be a foundational process in the complex adaptive nature of forest ecosystems (Stricker et al., 2015). However, this possibility and its extent highly depend on the compatibility of the given plant- and fungal community and environmental factors and is not fully understood and investigated yet (Arnebrant et al., 1993; Amaranthus and Perry, 1994; Simard et al., 1997; He et al., 2006; Deckmyn et al., 2014). Additionally, fungal species respond differently to certain stress conditions. These impacts on host tree sustainability and forest ecosystems also needs further evaluation (Khullar and Sudhakara Reddy, 2019).

ECM association can often buffer or overcome environmental problems for the plant either passively because of a closed environment evoked by the fungal mantle, or possibly also in an active way by for example transporting water to the roots with specialized fungal hyphae (Duddridge et al., 1980; Brownlee et al., 1983). Moreover, the fungal sheath forms a physical protection towards plant pathogens or heavy metals, mainly because one mantle can envelop many root tips at a time, but also because secondary metabolites of the fungus are assumed to act as a biochemical defence mechanism (Schaechter 2009; Colpaert et al. 2011). Even though ECM formation gains many advantages, it also leads to resource consuming adaptions in the plant. When comparing trees with and without ECM formation, the overall photosynthetic activity is enhanced by the symbiosis as the carbohydrate demand is higher compared to a tree that only produces carbohydrate (C) for itself. This relationship was discovered when *Laccaria bicolor* fruiting bodies of a fungal symbiont were removed, resulting in a decreased photosynthetic activity. In total, the plant loses up to 50 % of its photosynthetic carbohydrates to the fungus (Nehls et al. 2010). Therefore, it makes sense that plant and fungal partners both have influence on the exchange processes during symbiosis. Plants normally can prevent parasitism in controlling and restricting the carbohydrate fluxes, for example when the plant is more independent on the fungus because of high nitrogen (N) availability in the soil (Review: Nehls et al. 2010). On the other hand, most ECM fungi have the capability to switch between their C sources in dependence of seasonal impacts in terms of C-starvation, which is directly coupled to the photosynthetic activity of the symbiosis partner. Once photosynthetic rates are low, the fungus likely switches to a facultative transitory saprotrophic lifestyle to ensure a constant sugar supply (Nehls et al. 2010). Additionally, the fungal mantle can be utilized as an intermediate storage compartment around the roots (Massicotte et al., 1987). These dynamics help to be able to adapt to different environmental conditions (Massicotte et al., 1987).

Besides exploring the soil vegetative with their hyphae, ectomycorrhiza reproduce sexually via macroscopic sporocarps to complete their lifecycle (Johnson 1996). The building of fungal fruiting bodies is dependent on the allocation of carbohydrates, which is in return depending on the nutrient availability in the soil. The more nutrients are available up to eutrophication, the less allocation occurs, a process, which can lead to strong shifts in fungus compositions and belowground diversity (Högberg et al., 2010; Lilleskov et al., 2011; Wallander et al., 2011). In the end, both fungal morphological hyphae features, such as colour, extent of branching or the degree of complexity, and observing fruiting bodies in combination with molecular tools serve as a classification tool for ECM (Schaechter, 2009).

1.2.4 Ectomycorrhiza function

The extended nutrient and metabolite exchange within the fungal colony and between plants happens via outward extending hyphae (Nehls et al. 2010). Nutrient and carbohydrate transports are moved via a gradient, which is mainly evoked through glycolysis and intermediate carbohydrate storage pools at the plant-fungus interface (Nehls et al. 2010). All in all, the nutrient transport in ECM symbiosis takes place at the three different interfaces **(1)** soil - fungus, **(2)** fungus -apoplast and **(3)** apoplast – root-cell (Chalot and Brun 1998).

At **(1)**, one of the first factors that influence ECM formation are secondary metabolites that are excreted by plant roots. Fungal hyphae can sense these root exudates in the pre-symbiosis stages, which help to guide them to the tree fine roots (Martin et al., 2001). Another factor are mycorrhiza helper-bacteria (MHBs) around roots, whose presence elevates ergosterol levels in the soil, a metabolite promoting fungal growth (Bowen and Theodorou 1979; Garbaye 1994) Even though the fungus is invasive towards the plant and must degrade some of the plants cell walls for the symbiosis to work at **(2)**, plants are not harmed. Harmful genes for either partner likely went lost during the evolution of the symbiosis and the fungus cannot degrade plant cell walls as a carbon source (Martin et al., 2008; Martin and Nehls, 2009). Possibly, the plant can somehow suppress the gene expression of the plants pathogen defence mechanisms, bypassing plant defence mechanisms against herbivores that are otherwise provoked by low cellulose levels source (Martin et al., 2008; Martin and Nehls, 2009). The apoplast-root-cell interface in **(3)** is so densely packed that both become nearly indistinguishable, facilitating nutrient exchange in this area (Smith et al. 1994). This apoplast pathway was shown to be flexible, fast and demand orientated (Nehls et al. 2010).

It is assumed, that many pre-symbiosis steps and the differential expression of proteins that are involved in fungal attachment, plant defence and symbiosis related metabolism are influenced and coordinated by impacts of signalling pathways on regulatory elements (Martin, 2001; Frettinger et al., 2007; Martin et al., 2007). As an example, some plant genes likely code for cell wall degrading enzymes which allow the fungus to penetrate the rhizodermis tissue after first contact (Martin et al. 2008; Sally and Smith 2008; Smith and Read 2010). Further genetic modifications can influence a plants morphology in terms of increased mitotic division, the stimulation of lateral cell growth, reduction of root spreading as well as the induction of cell shape changes (Vayssières et al., 2015). This is likely accompanied by cytokinin induced morphological modulation to increase root branching and to enhance colonization rates to increase the interaction surface (Felten et al., 2009; Giron et al., 2013; Vayssières et al., 2015). Fungi are also thought to produce phytohormones to enhance plant fine root formation and suppress root hair formation to facilitate the colonization. Root hairs are then replaced with fungal hyphae to accumulate nutrients (Agerer, 2001; Schaechter, 2009; Smith and Read, 2010). In total, no ectomycorrhiza specific genes could be detected until now. All changes are made based on changes in transcription patterns of existing genes (Duplessis et al., 2005; Martin et al., 2007).

1.3 The woody plant model organism *Populus spec.*

Poplar belongs to the family of Salicaceae and is a great model organism for studies of the interactions between woody plants living in symbiosis with mycorrhiza because of its worldwide distribution and genotypic diversity (Martin and Nehls 2009; “Classification | USDA PLANTS” n.d.). *Populus tremuloides* and *P. tremula* for example are known to occur on several continents (Bradshaw et al., 2000). Worldwide, there are 40 different known poplar species, with all of them harbouring 19 chromosomes (2n = 38) that consist of about 500 million base pairs encoding for approximately 45.000 genes (Tuskan et al., 2006). Because poplar is paleopolyploid and consists of relatively large gene families, it is assumed, that its genome was duplicated several times during evolution (Brunner et al., 2004). Besides sexual reproduction, poplar is also able to reproduce asexually (Bradshaw et al., 2000). Poplar species can be hybridized, resulting in fertile diploids (Bradshaw et al., 2000). The traits of many hybrids are already compiled in large databases (Bradshaw et al., 2000). Compared to their parental types, hybrid morphology and phenology was shown to differ in *Populus trichocarpa* × *P. deltoides* hybrids, which were shown to grow faster and have larger leave sizes (Ridge et al., 1986). When comparing hybrids with each other it could be shown, that different hybrids respond differently to heavy metal stress, indicating various responses to environmental conditions (Chandra and Kang, 2016). Furthermore, a study revealed significant hybrid effects on growth traits (Pliura et al., 2014). However, a major disadvantages of hybrids could be, that they were shown to be able to disperse in a study based on molecular markers (Ziegenhagen et al., 2008). Furthermore, there might be a risk of introgressive gene flow, which might lead to a loss of species integrity (Ziegenhagen et al., 2008).

Overall, poplar hybrids are frequently used as model organisms for forest systems because **(1)** they are fast growing and easy to cultivate under sterile conditions, **(2)** their ability to regenerate *in vitro* from transformed cells (Tsai et al., 1994) and **(3)** their genome is sequenced in high quality, which can help to evaluate gene function (Brunner et al., 2004; Nanjo et al., 2004; Yang et al., 2015). Point **(3)** is so important in plant genomics research, because reverse genetic approaches are essential in relation to time when compared to the long reproduction cycles of trees. To be able to isolate full – length cDNA from the poplar genome, a well sequenced and correct gDNA template is needed (Nanjo et al. 2004). Additionally, poplar can be transformed with *Agrobacterium* to assess gene alteration, further showing its great importance as a model organism (Tsai et al., 1994; Hwang et al., 2015; Yang et al., 2015).

1.4 The ectomycorrhiza model organism *Pisolithus microcarpus*

Pisolithus microcarpus belongs to the division of Basidiomycota and family of Sclerodermataceae (Peter et al., 2003). The hyphae of Basidiomycota are vegetative growing, tubular cell structures surrounded by a cell wall. The symplast of the hyphae is continuous and is segmented by perforated septa (Bresinsky et al., 2013). Generally, the genus *Pisolithus* forms ECM with a broad woody plant host range (Martin et al., 2002). Some of its lineages are restricted to the geographical origin of the host plant, whereas others are distributed worldwide, such as *P. microcarpus*. Thereby, this fungus was associated to have dispersed with Australasian trees, such as eucalyptus (Martin et al., 2002) and basidiospores (Hitchcock et al., 2011). Studies analysing the genetic population in forests of south eastern Australia revealed little genetic diversity, indicating a high rate of gene flow (Hitchcock et al., 2011). What could be shown is a differential gene expression of several genes when comparing free mycelium and symbiotic tissues of *P. microcarpus* (Peter et al., 2003). Thereby, most transcripts in the mycelium coded for structural proteins or stress response, whereas symbiotic tissues had transcripts of cell wall proteins (Peter et al., 2003). It was however noted that transcript databases need more information and many points and questions remined unanswered yet.

As a model organism for studies in the laboratory, *P. microcarpus* was shown to form mycorrhiza under artificial conditions (Duplessis et al., 2005; Costa et al., 2010). It can be cultivated under sterile conditions and was shown to form mycorrhiza in a closed system with composite poplar (Nehls et al., unpublished).

1.5 Plant transformation methods

1.5.1 Comparing stable to transient plant transformation

Plant transformation methods are a key tool for gene analyses (Birch 1997). *Agrobacterium* mediated plant transformation is a common for both transient and stable manipulations (Tsai et al., 1994; Kapila et al., 1997; Citovsky et al., 2007; Jian et al., 2009; Hwang et al., 2015; Gelvin, 2017).

Transient transformation of plants with agrobacteria defines for a process, where the gene of interest is only temporarily but strongly expressed in a target organism for gene identification and analysis (Kapila et al., 1997). This is often combined with heterologous gene expression, where a gene is expressed in an organisms where it would not naturally occur (Gross and Hauser, 1995). Here, effects are time limited (a few days), which is why transient transformations are often conducted prior to a stable plant transformation (Fischer et al. 1999; Manavella and Chan 2009). As an example, *Agrobacterium* mediated transient expression of respective constructs in tobacco leaves can be used for subcellular protein localization (Citovsky et al. 2006). Generally, transient expression is not as reliable as stable plant transformations when evaluating root specific promoter regions. This is, because extrachromosomal transient expression in leaves of a different genus does not fully reflect all needed promoter elements, as the gene regulation is not chromatin based and some factors might not exist in a heterologous system (Hernandez-Garcia and Finer 2014).

Stable transformation means the stable integration of genes and reporter constructs into the plant genome (Birch 1997; Gelvin 2010, 2017). For this, the regeneration of organs (hybrid plants) or entire plants for single transgenics are requested. Such strategies are often based on a dominant selection marker (Valvekens et al., 1988). Because the overall process of generating and preparation of stable transformation takes month, another approach was developed particular for analyses of transgenic roots. Thereby, non – transgenic shoots are brought to form transgenic roots via *Agrobacterium* mediated plant transformation which can be evaluated within weeks. Each resulting root is a single transformation event and such plants are called "Composites" (Hansen et al., 1989; Collier et al., 2005; Neb, 2017; Neb et al., 2017; Das, 2018). Even though obtained information about gene expression are relatively robust (Hernandez-Garcia and Finer, 2014), stable transformations also have their weaknesses. It was shown that the random locus of T - DNA integration likely affects the transgene expression (position effect). T - DNA expression is also influenced by the T - DNA conformation, which can be integrated in different units, such as tandem repeats at junction sites (filler DNA) (Gelvin 2017). Additionally, the transferred amount of copy numbers may differ (Hernandez-Garcia and Finer 2014).

1.5.2 Overview of Agrobacterium mediated plant transformation

Agrobacteria are plant pathogenic, gram-negative soil bacteria belonging to the order of Rhizobiales and family of Rhizobiaceae (Moore and Chilton, 1997; Young et al., 2001; Platt et al., 2014). Some *Agrobacterium* species can sense and move to wounded plant regions, cross the destroyed plant barrier, and integrate a part of their plasmid DNA (T - DNA) into the plant's genome, causing stable transformations. Thereby, plants get diseases depending on the *Agrobacterium* strain. *A. rhizogenes* harbours a so called Ri-plasmid (Ri = root inducing) which contains *rol* – genes (root loci genes) and causes a "hairy root disease" phenotype, whereas *A. tumefaciens* transfers parts of its Ti-plasmid (Ti = Tumour inducing) and induces "crown gall disease" (Moore and Chilton 1997; Platt et al. 2014). Because they turn the bacterium into a pathogen, Ti- and Ri-plasmids belong to the group of virulence plasmids (Suzuki et al., 2009). Usually, protective gene expression is upregulated in a host once a pathogen is detected, but the agrobacteria manage to inhibit plant defence signalling (Gelvin, 2003; Anand et al., 2007; Lee and Gelvin, 2007; Hwang et al., 2015). The T - DNA regions of the plasmids consists of genes that are coding for phytohormones and opine synthesizing enzymes (McCullen and Binns 2006). While the plant is regulated by morphological changes and tumour formation, the *Agrobacterium* nourishes from the produced opines, a derivate of amino acids and sugar (Chandra 2012). Both Ti- and Ri- plasmids are classified based on the opines that the host is forced to produce (Chandra

2012; Platt et al. 2014). To be able to transfer their T - DNA, agrobacteria hijack fundamental processes of cells shared by most eukaryotic organisms, and furthermore interfere with host defence mechanisms (Tzfira and Citovsky, 2006; Anand et al., 2007). The complete process can be differentiated into seven steps: (**1) Agrobacteria chemically recognize a wounded plant** and move there chemo - tactically (Tzfira et al., 2004; Anand et al., 2007; Ma et al., 2014; Subramoni et al., 2014; Hwang et al., 2015; Gelvin, 2017) based on the excretion of the phenylpropanoid derivates, as well as by high amounts of sugars and a relatively low pH-value at the wounded plant site (Stachel et al., 1985; Joubert et al., 2002). Acetosyringone activates chromosomal *Agrobacterium* receptor genes called *vir*A and *vir*G, which are part of a two-component receptor and located on the Ti/Ri-plasmids. They activate the expression of many other *vir*-genes that are coding for virulence effector proteins (Joubert et al., 2002; Ma et al., 2014; Platt et al., 2014; Subramoni et al., 2014), **(2) Agrobacteria initiates a physical contact to the plant** (Heindl et al., 2014; Matthysse, 2014; Carlson et al., 2015), (**3) Activation of the T - DNA transfer machinery**. During this step, *vir*D1 and *vir*D2 recognize the 25 bp long left- and right border sequences that are flanking the T - DNA. *vir*D1 acts as a helicase, whereas *vir*D2 has a nuclease activity causing nicks in the double stranded Ti- and Ri plasmids at the left- and right border sequences. Thus, single stranded breaks at the border sequences are caused, cutting out the single stranded T - DNA region (ssT – DNA). The *vir*-gene *vir*D2 stays attached to the right border at the single T - DNA strand for protection against exonucleases (covalent at the 5´ end) and as a strong nucleus targeting sequence (NLS) (Tzfira et al., 2004; Gelvin, 2017), **(4) T - DNA and protein transfer into the plant cell.** The T - DNA-*vir*D2 complex is transferred into the plant cell through an infection pilus (Chandra 2012). Many involved host and bacterial proteins still need to be identified and characterized (Tzfira and Citovsky, 2006; Chandra, 2012; Gelvin, 2017), **(5) T - DNA transfer into the nucleus.** Once inside the plant cell, a “mature T - DNA complex” is formed together with plant proteins, such as importin (Tzfira and Citovsky 2006; Chandra 2012), **(6) Integration of the T - DNA into the plants genome**, a process that is still poorly understood. Newest research results support a hypothesis, in which the ssT - DNA gets copied and transformed to double stranded T - DNA (dsT - DNA) by host polymerases prior to the random occurring integration into the host DNA (Tzfira and Citovsky, 2006; Gelvin, 2017) and **(7) Gene expression of the T - DNA**.

1.5.3 Binary vector systems as a tool for Agrobacterium mediated plant transformation

Central for genetic plant engineering is that, besides its flanking regions, the T - DNA itself does not code for any genes requested for bacterial infection or DNA transfer, wherefore it can be exchanged with any gene sequence of interest (Tzfira et al. 2004; Tzfira and Citovsky

2006). Thus, the three major elements required for *Agrobacterium* mediated plant transformation T - DNA transfer are **(1)** the target construct that is supposed to be transformed into the plants **(2)** 25 bp long right and left border sequences that are flanking the T - DNA and define the regions that are later on transferred to the plants nucleus and **(3)** a marker for selection of transformants (Komori et al. 2007; Pitzschke and Hirt 2010). Because both Ti- and Ri- plasmids are quiet large (approximately 200 kbp), present in agrobacteria only in low copy and cannot be replicated in *E. coli*, so called binary vector systems were developed (Lee and Gelvin 2007; Suzuki et al. 2009). Because binary vectors are propagated in *E. coli*, transferred in agrobacteria for plant infection and T – DNA transfer into host plants, they do harbour different elements that are necessary for each purpose (Hellens et al. 2000; Komori et al. 2007; Lee and Gelvin 2007; Suzuki et al. 2009; De Rybel et al. 2011). Thereby, the T – DNA including the border sequences is transferred on a smaller shuttle vector. The rest of the necessary machinery for a successful T – DNA transfer is located on a "helper plasmid", such as the *vir*-genes, *rol* - genes or parts of the ORI that are necessary for the replication of the T – DNA shuttle vector (Alpizar et al., 2006; Komori et al., 2007; Pitzschke and Hirt, 2010). Both the shuttle vector and the helper plasmid need to be present in the same *Agrobacterium*, giving name to the binary vector system (Komori et al. 2007; Pitzschke and Hirt 2010). Thereby, the T - DNA region on the small and autonomous shuttle vector functions *in trans* to the *vir*-region on the "helper plasmid" (Tzfira and Citovsky, 2006; Signor and Nuzhdin, 2018).

1.5.4 The plant transformation vectors pGREEN and pCXUN

pGREEN is a pBluescript derived plant transformation vector that can be used for *Agrobacterium* mediated transformations. Based on pGREEN, pPLV was developed (Hellens et al., 2000; De Rybel et al., 2011). In a modified version of pPLV, the T - DNA contains a plant selection marker cassette as well as an expression cassette for fluorescence proteins (**Figure 2**) (Neb, 2017; Schnakenberg, 2020). The backbone of the binary vector contains only a part of the psa-ORI and a kanamycin resistance. To be able to replicate, the incomplete pSA ORI needs to be complemented with the "helper plasmid" pSOUP, which needs to be present in the same *Agrobacterium* cell for a successful replication (Hellens et al., 2000).

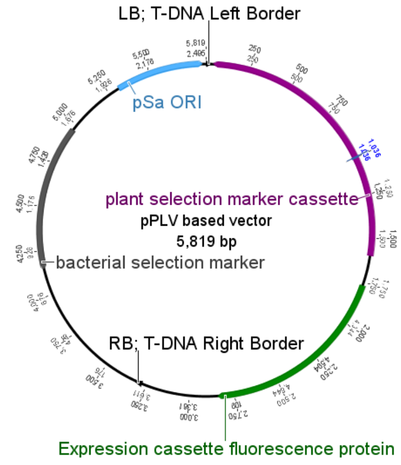
LB; T-DNA Left Border
pSa ORI
plant selection marker cassette
pPLV based vector
5,819 bp
bacterial selection marker
RB; T-DNA Right Border
Expression cassette fluorescence protein

Figure 2. Vector description of a modified pGREEN based pPLV binary vector. The T - DNA was completely exchanged via *BglII* (Neb, 2017). It contains an expression cassette for fluorescence proteins and a plant selection marker cassette. The backbone of the binary vector contains a part of the psa-ORI and a kanamycin resistance. To be able to replicate, the incomplete pSA ORI needs to be complemented with the "helper plasmid" pSOUP. For promoter and terminator descriptions see chapter 2.5.1. Figure was in silico cloned and displayed using Geneious**.**

Another plant transformation vector is the pPZP derived pCAMBIA vector named pCXUN (Hajdukiewicz et al., 1994). Its backbone contains a pBR ORI for replication in *E. coli*, a pVS1 ORI for replication in agrobacteria as well as a kanamycin resistance cassette (aadA CDS)as well as a bacterial selection marker (aadA CDS) (Vector Detail Arabidopsis Stock centre pCXUN-FLAG; Hajdukiewicz et al., 1994). In a modified version, the T – DNA is composed of a plant selection marker as well as a green- and red fluorescence protein expression cassettes (**Figure 3**).

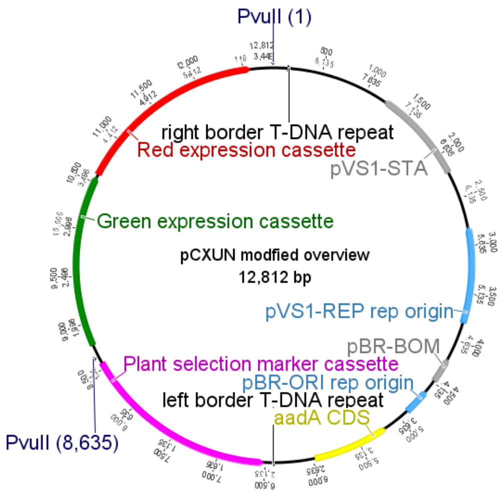
PvuII (1)
right border T-DNA repeat
Red expression cassette
pVS1-STA
Green expression cassette
pCXUN modfied overview
12,812 bp
pVS1-REP rep origin
pBR-BOM
Plant selection marker cassette
pBR-ORI rep origin
left border T-DNA repeat
aadA CDS
PvuII (8,635)

Figure 3. Visual description of a pCAMBIA derived and modified pCXUN vector. The T - DNA was composed of a variable double marker cassette (Green and Red expression cassette) and a plant selection cassette. The backbone outside of the T – DNA consisted of a pBR-ORI and a pVS1 REP ORI for plasmid stability in *Agrobacteria* as well as a kanamycin resistance cassette (aadA CDS). The Figure was in silico cloned and displayed using Geneious (further details given in M&M**).**

1.5.5 Creating plant transformation vectors using Ligase independent cloning (LIC)

Compared to cloning with restriction enzymes and DNA T4-ligase, another technique named Ligase Independent Cloning (LIC) evolved over the last years (Aslanidis and de Jong, 1990). LIC allows for a directed integration of genes into the T - DNA region of binary vector systems without restriction digestion of the target DNA. This method is especially time saving and advantageous for cloning many PCR products at a time or when no suitable restriction sites for conventional cloning strategies are available (Aslanidis and de Jong, 1990). In principle, LIC is based on the enzymatic activities of DNA polymerase 5´-3´polymerase- and 3´-5´exonuclease activity at designed "LIC adapters". These adapters are generated complementary at both the desired insert and the linearized vector backbone in using complementary dNTPs for both attempts (De Rybel et al., 2011). When linearized, double strand DNA is incubated with DNA-Polymerase and only one out of the four deoxynucleotide triphosphates (dNTP) requested for DNA synthesis. The DNA then gets degraded until the first nucleotide that corresponds to the dNTP that was added to the mixture is reached (De Rybel et al., 2011). This procedure takes place at both DNA strands, allowing for the generation of incompatible 5´overhangs to avoid re-ligation (De Rybel et al., 2011) (**Figure 4**). A possible insert is then amplified with primers that generate 5´ends compatible to the backbone DNA (De Rybel et al., 2011). In a last step, the insert and vector with the overhangs are hybridized, meaning that insert and vector LIC overhangs form phosphodiester bonds and emerge to a circular vector, which can then be used for bacteria transformation. Cell internal repair mechanisms complete the vector after the transformation (De Rybel et al., 2011).

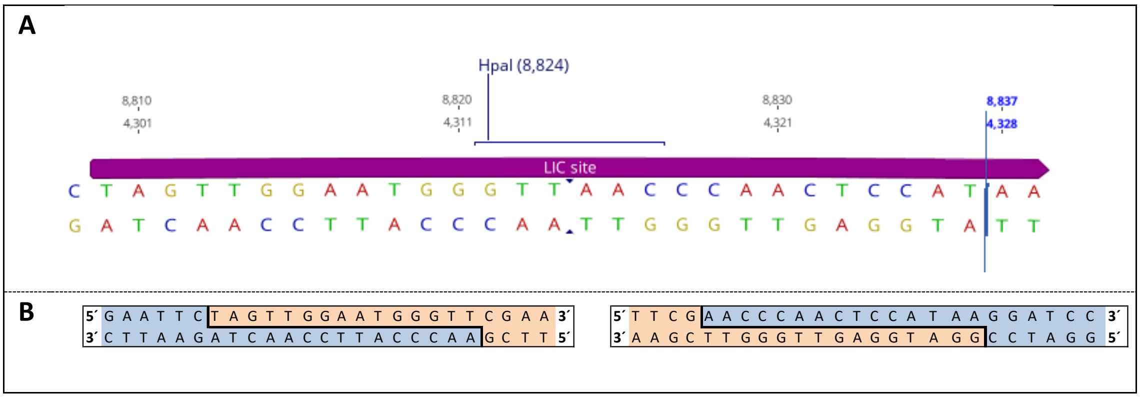
A
HpaI (8,824)
8,810
4,301
8,820
4,311
8,830
4,321
8,837
4,328
LIC site
C T A G T T G G A A T G G G T T A A C C C A A C T C C A T A A
G A T C A A C C T T A C C C A A T T G G G T T G A G G T A T T
B
5´ G A A T T C T A G T T G G A A T G G G T T C G A A 3´
3´ C T T A A G A T C A A C C T T A C C C A A G C T T 5´
5´ T T C G A A C C C A A C T C C A T A A G G A T C C 3´
3´ A A G C T T G G G T T G A G G T A G G C C T A G G 5´

Figure 4. Visualization of LIC overhangs and adapters for a LIC cloning strategy (Ligase Independent Cloning). A: LIC site in the T – DNA of binary vectors for *Agrobacterium* mediated plant transformation. The vector can be linearized with *HpaI*, the sequences. Left and right of this cutting site are so called LIC adapters. Using complementary adapters for the potential inserts in combination with respective T4-polymerase treatments allows for LIC. The image was made with Geneious. B: LIC overhangs in detail. In blue is the dCTP and T4-DNA Polymerase treated vector, in orange is the dGTP and T4-DNA Polymerase treated PCR insert, which was amplified with LIC-overhangs prior to this step. In this way the T4-DNA Polymerase treatment generates compatible overhangs that can then be annealed without a ligase.

1.6 Gene regulation in Eukaryotes: Promoter analyses

1.6.1 Overview of gene regulation in eukaryotes

Protein function, transport and localization are the result of DNA transcription, RNA splicing, translation and post-translational modifications of proteins and protein activity (Fütterer and Hohn 1996). Timing, localization and number of genes together with their expression strength help organisms to adapt to adapt to environmental changes (Sachs and Tuan-Hua, 1986; Riethoven, 2010; Hernandez-Garcia and Finer, 2014).

1.6.2 Eukaryotic promoter structure

Eukaryotic promoter regions can be divided into core- (~ 80 bp around the transcription start site (TSS)), distal-, and proximal promoter (~ – 200 to 300 bp in relation to the TSS), followed by an untranslated region (5´ UTR), the coding region consisting of introns and exons, a 3´ UTR and finally a terminator (Riethoven, 2010; Barrett et al., 2012; Porto et al., 2014; Biłas et al., 2016). A schematic overview is given in **Figure 5**. The core promoter additionally contains the TSS, which defines the transcription and accuracy of gene expression and the transcription is initiated by RNA polymerase II (Riethoven, 2010; Barrett et al., 2012; Porto et al., 2014; Biłas et al., 2016). Because of the high variability in promoter elements, eukaryotic promoters vary greatly in size (Hernandez-Garcia and Finer 2014).

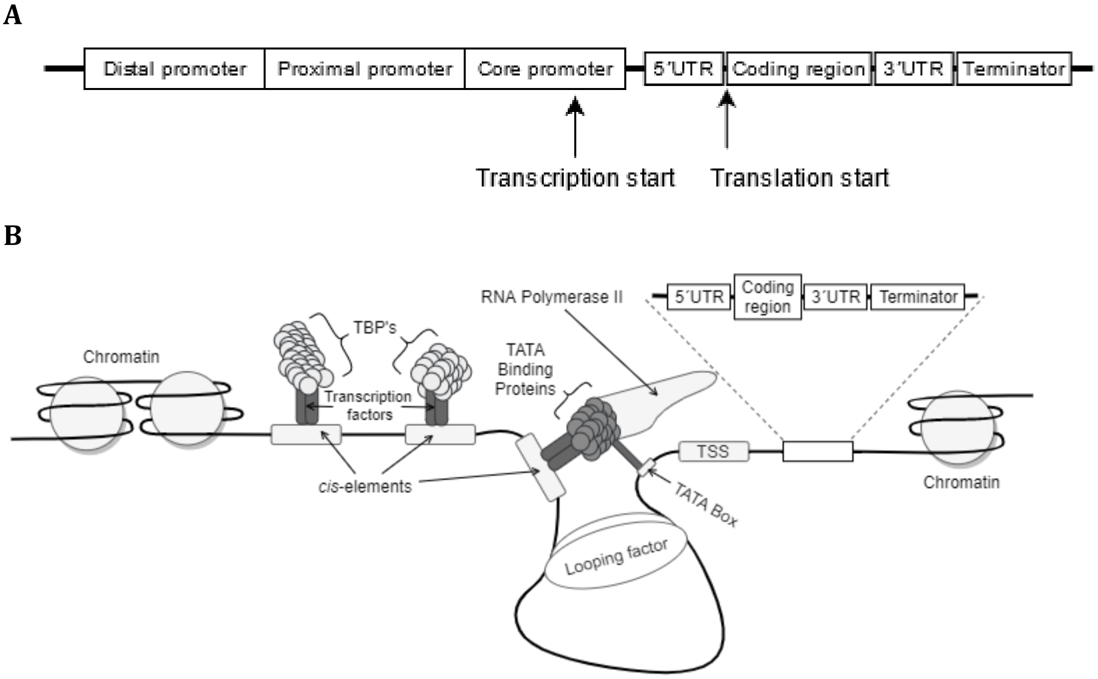
A
Distal promoter
Proximal promoter
Core promoter
5´UTR
Coding region
3´UTR
Terminator
Transcription start
Translation start
B
RNA Polymerase II
5´UTR
Coding region
3´UTR
Terminator
TBP's
Chromatin
TATA Binding Proteins
Transcription factors
cis-elements
TSS
TATA Box
Looping factor
Chromatin

Figure 5. A: Potential promoter structure of a eukaryotic gene. The transcription- and translation start are indicated. **B: Schematic display of potential locations of *cis* – elements in eucaryotic promoters.** *cis* – elements of the promoter can be bound by transcription factors, that in return can be bound by transcription factor binding proteins (TBPs) to recruit RNA polymerase II. In case of the TATA box, these are called TATA binding proteins that help position the polymerase over the transcription start (TSS). *Cis* – elements can be brought closer to the Transcription start (TSS) by looping factors that help mediate the promoter structure.

1.6.3 cis – element-based regulation of eukaryotic gene transcription

All parts of a eucaryotic promoter can contain so called *cis* – elements, which are specific DNA binding sites for transcription factors (TFs), to help regulate gene expression rates on a transcriptional level (Riethoven, 2010; Barrett et al., 2012; Porto et al., 2014; Biłas et al., 2016). Thereby, the amount of produced pre-mRNA is dependent on the amount of TFs present, which are a product of non-coding DNA translation and influence the binding capacities of RNA-polymerase II binding sites (Smale and Kadonaga, 2003; Riethoven, 2010; Zuo and Li, 2011). *cis*-elements mostly have sizes about 20 bp that can be activated independently of the distance and orientation towards the transcription start (TSS) in eukaryotes (Shahmuradov et al., 2005; Riethoven, 2010; Biłas et al., 2016). Because *cis* - elements are relatively small and likely repetitive, they are assumed to need the involvement of other bases nearby to work properly (Vollenweider et al., 1979; Kanhere and Bansal, 2005). TFs that reduce the gene expression are referred to as silencers, while TFs enhancing the probability of gene expression are called enhancer (Smale and Kadonaga, 2003; Riethoven, 2010; Zuo and Li, 2011). In eukaryotes, some enhancers were found to bind up to 1 Mbp (Mega base pair) up- or downstream from the TSS, while silencers were found to even bind within intron and exon regions of the coding sequence or target helicase sites (Porto et al., 2014; Srivastava et al., 2018). The 3´ UTR, which is not translated to protein, also stabilizes the mRNA and can contain both gene enhancers and silencers (Usadel et al., 2009; Vandepoele et al., 2009; Barrett et al., 2012; Biłas et al., 2016).

As an example for a TF binding site in the core promoter, the TATA – box can be found 5 – 30 bp upstream of the TSS in 30 – 50 % of all known promoter regions (Juven-Gershon and Kadonaga 2010; Zuo and Li 2011). Without outside influences, the TATA – box has a basal activity that can be enhanced or silenced when bound to a pre-initiation complex (PIC), which is formed of TFs, RNA polymerase II and up to 14 other polypeptides called TATA - binding proteins (TBP) – associated factors. Thereby, TBPs are highly conserved and help position RNA polymerase II over the TSS (Graw, 1962; Maniatis et al., 1987; Levine and Tjian, 2003; Juven-Gershon and Kadonaga, 2010; Akhtar and Veenstra, 2011; Zuo and Li, 2011; Biłas et al., 2016). Some plant promoters were found to be lacking a TATA-box. Instead, they often contained alternatives such as AGGA – or GC-boxes to help increase RNA - polymerase II binding, or upstream activation sites between -80 and -1800 bp of the initiation (Graw, 1962; Maniatis et al., 1987; Levine and Tjian, 2003; Porto et al., 2014; Biłas et al., 2016). Further TF binding sites are for example initiator elements (INR) close by or covering up the TSS that can influence the TATA – box, or several other TF binding sites located in upstream – and downstream promoter regions (UPE and DPE) (Barrett et al., 2012). Importantly, TATA – boxes or alternative boxes can act in both ways and mutate easily, which in return heavily effects transcription effectiveness (Biłas et al. 2016). Some genes were found to be co – expressed, likely because they share similar functions (Usadel et al., 2009; Vandepoele et al., 2009).

1.6.4 Eucaryotic promoter stability

To influence gene expression, the DNA needs to be folded and curved in a certain shape, either because of the intrinsic properties or because of external influences, such as protein binding. Therefore, many genes have sequence dependent curved DNA upstream of the TSS (Iyer and Struhl, 1995; Nagaich et al., 1997; Gabrielian et al., 1999; Kanhere and Bansal, 2005). Intrinsic properties mean, that all described elements can influence secondary loop structures for regulation and regulate each other. Based on their nucleotide composition, eukaryotic promoter regions were found to be less stable and less bendable with an enhanced curvature profile compared to non-promoter regions (downstream coding regions) (Kanhere and Bansal, 2005). Some of the mentioned features are even conserved and heavily influence the availability of *cis* – elements (Vollenweider et al., 1979; Kanhere and Bansal, 2005). The destabilized upstream region of the TSS likely leads to facilitated opening of base pairs during torsional stresses caused by RNA - polymerase movement. Additionally, nucleosome formation is destabilized in less flexible DNA regions, which is easing access to transcription factors (Vollenweider et al., 1979; Kanhere and Bansal, 2005). Chromatin based gene regulation is also influenced by some TFs, which can cause coactivator protein mediated post – translational acetylation of histones. As a result, *cis* – elements in the previously packed DNA become available (Rombauts et al., 2003; Hernandez-Garcia and Finer, 2014).

External influences on promoter stability has the so called Mediator. The earlier described PIC is mainly important for the start site selection but does not seem to respond to transcriptional activators, which is where Mediator comes into play (Karijolich and Hampsey, 2012). Mediator is a large protein complex composed of variable subunits (between 25 and 30 in plants), which acts as a binding bridge between DNA, TFs, RNA - polymerase II and the PIC. DNA is bound by transcription factors, which in turn have a binding motif for Mediator. Based on its present conformation and composition, Mediator provides a platform for co – factors as it can bind to several TFs at a time and is able to recruit RNA - polymerase II (Allen and Taatjes, 2015; Samanta and Thakur, 2015). It seems to be required for all genes as it is responsible for basal and enhanced expression but also acts as a co – repressor for down regulation of genes on RNA level. Its variable subunits allow for conformational flexibility as a reaction to different pathways (Mathur et al., 2011; Karijolich and Hampsey, 2012; Yin and Wang, 2014; Allen and Taatjes, 2015; Samanta and Thakur, 2015). Thereby it was found responsible for transcription control, chromatin architecture in terms of organising topological domains and stabilizing of loops (looping factor), RNA - polymerase II initiation as well as translation pausing (to help maintain nucleosome free regions to promote transcription activation) and elongation (in concert with PIC) (Allen and Taatjes, 2015). Possibly, Mediator adapts based on abiotic and biotic stimuli in a temporal – spatial manner (Samanta and Thakur, 2015). Thereby, Mediator secondary structures are similar between species even though their primary structures differ, which might suggest a conserved organization (Mathur et al., 2011).

1.6.5 Functional promoter analyses in Eukaryotes

One tool to align conserved regions of two or more unaligned sequences to detect probabilistic motifs based on a weight matrix is Consensus (Rombauts et al., 2003). However, eucaryotic promoters are usually hard to characterize *in silico* because regulatory sites can be present hundreds of base pairs upstream of the TSS (Iyer and Struhl, 1995; Nagaich et al., 1997; Gabrielian et al., 1999; Kanhere and Bansal, 2005). Here, *in vivo* analyses of well-established model systems might provide quantitative and qualitative data to investigate promoters (Geertz and Maerkl 2010; Hernandez-Garcia and Finer 2014). *In vivo* promoter analyses give a more biologically related context and allow for the testing of sequence specificity (Geertz and Maerkl 2010; Hernandez-Garcia and Finer 2014). The localization of potential *cis* – elements can be investigated by the generation of a series of 5´- end truncations, even though some regulatory elements might get lost because of the promoter complexity (Rombauts et al., 2003; Porto et al., 2014; Zhu et al., 2014; Sharma et al., 2017; Zhang et al., 2017). Such truncated promoter fragments drive fluorescence protein expression to reflect on the expression rate *in planta* and to get information about promoter activity (Curtis and Grossniklaus, 2003).

1.7 Fluorescence protein reporter systems

1.7.1 Fluorescence proteins

The first FP was described in 1974 and isolated from the jellyfish *Aequorea victoria* in the 1960s (Shimomura et al., 1962; Morise et al., 1974). Because it was emitting green light, the shortcut GFP for Green Fluorescence Protein was introduced (Shimomura et al., 1962). To increase the spectral properties of FPs and to help better stabilize protein structures, GFP was mutated (mostly the chromophore forming residues or at the fluorophore itself), resulting in less photo bleaching or other emission light wavelength (blue, cyan or yellow) (Kremers et al., 2006). Generally, GFP and its mutations have a unique β-sheet barrel like structure. The β-sheet forms the wall of the barrel with a diagonal α-helix running through it. A chromophore is located inside of the barrel, linked by an α-helical stretch as a tripeptide motif (Ser65-Tyr66-Gly67). It is formed in an autocatalytic cyclization of a tripeptide sequence, for which oxygen is needed. When the chromophore is formed, fluorescence occurs independently of the surrounding conditions such as other proteins, substrates or co-factors (Zimmer 2009, 2002; Odom 2011) and labels are created within the cell (Chudakov et al., 2005; Sahoo et al., 2009). Thus, this approach is independent of temperature and chemicals as a substrate. Furthermore, no drying or fixation steps are necessary. (Sahoo et al., 2009)

To expand the colour palette into orange, red and far-red, mRFP1 was obtained and mutated from *Discosoma spec* (Shaner et al., 2004). Since it was often found to be disruptive or even toxic to the target organisms because of its tetrameric structure, it was further modified to **(1)** improve its maturation time, **(2)** improve its tolerance to N-terminal fusions, **(3)** enhance its photostability and **(4)** create different colours. The first true monomer was mRFP1, which was further optimized to DsRED, finally leading to the two final products tdTomato and mCherry (Shaner et al., 2004). Both are bright and versatile in *in vivo* imaging and are engineered for brightness, stability, as well as low aggregation and can easily be fused to the N- or C-terminus of proteins (Shaner et al., 2004). tdTomato is a tandem dimer (intra-molecular) with an excitation optimum of 554 nm and an emission optimum of 581 nm. Its maturation half-life is 1 h at 37°C and shows 283 % brightness compared to GFP (Shaner et al., 2004). In comparison, mCherry has an excitation optimum of 587 nm and an emission optimum of 610 nm. Even though it has only 47% of the brightness of GFP, its maturation half time is only 15 min (Shaner et al., 2004). The autocatalytic mechanisms of chromophore formation for RFPs is more complex compared to GFP (Subach and Verkhusha, 2012). Red chromophores were shown to have a common blue intermediate or a GFP – like intermediate in the process of its maturation (Subach and Verkhusha, 2012). Further mutations of DsRED-E5 caused this GFP-like intermediate to be detectable (Terskikh et al., 2000; Mirabella et al., 2004).

1.7.2 Use for subcellular protein localization studies and promoter analysis

Because FPs can be attached to many proteins and still form the necessary chromophore, they can be used as reporters for different purposes, such as protein localization. Most proteins are not disrupted in their folding, function and localization too much when an fluorescence protein (FP) is fused to it (Shaner et al., 2004; Sahoo et al., 2009; Grefen et al., 2010). Thus, the labelling of target proteins "*in planta*" with FP´s is a common method when working with reporter gene essays in plant transformations (Nowak et al., 2004; Chudakov et al., 2005; Sahoo et al., 2009). In combination with such fusion constructs, some promoters can be used to constitutively express proteins in plants. An example is the *Arabidopsis* Ubiquitin10 promoter (P_{UBQ}), which is expressed in almost all organ tissues throughout the complete lifecycle of a plant (Hernandez-Garcia and Finer 2014). Other possible promoters are the Nopaline Synthase Promoter (P_{NOS}), or the Cauliflower Mosaic virus promoter (P_{35S}) (Odell et al., 1985; Ebert et al., 1987). The P_{NOS} is characterized by a CCAAT region 63 – 97 bp, as well as another important region 101 – 119 bp upstream of the TSS (Ebert et al., 1987). PNOS it not only constitutively expressed, but plant wound and auxin inducible (An et al., 1990). For P_{35S}, an enhancer was found to be located 434 – 46 bp upstream of the transcription start (TSS) (Odell et al., 1985). To increase the DNA transcription activity of the original promoter, the 250 bp upstream region was cloned in tandem. This obtained double P_{35S} was shown to be useful to obtain high expression levels of foreign genes in transgenic plants (Kay et al., 1987; Fang et al., 1989). Further studies showed that single subdomains can confer tissue specific gene expression via synergistic interactions among the *cis* - elements. However, such a combinatorial code was interpreted differently among species (Benfey and Chua, 1990). FPs can also be used as a reporter protein for promoter analysis with an unknown promoter (Shaner et al., 2004; Sahoo et al., 2009; Grefen et al., 2010).

The success of both stable and transient plant transformations with FPs can be detected with a laser-scanning microscope (Okumoto et al., 2004; Chudakov et al., 2005). Thereby it is possible to distinguish a combination of several FPs in the same compartment because of their different excitation and emission wavelength based on their chromophore properties (**Table 1**). Depending on the microscope and its filter settings for different fluorescence channels, it is for example possible to distinguish tdTomato from sYFP (Shaner et al., 2004).

Table 1. Fluorescence proteins with their respective size, excitation, and emission wavelength as well as their description.

Fluorescence protein	Size [kDa]	Emission wavelength in nm	Excitation wavelength in nm	Description	References
mCherry	26.2	610	587	Derived from mRFP1, monomeric	Shaner et al. 2004
tdTomato	54	581	554	Tandem dimer derived from mRFP1	Shaner et al. 2004
eGFP	54.6	509	489	Genetic fusion of two eGFP copies	Reichel et al. 1996; Takada and Jürgens 2007; Patterson et al. 1997; Heim, Cubitt, and Tsien 1995
sYFP	25.9	527	515	optimized from GFP, has an increased intrinsic brightness	Kremers et al. 2006; Day and Davidson 2009
DsRED-E5	26.5	510 for GFP and 583 for RFP	488 for GFP, 558 for RFP	Mutant of DsRED, has detectable GFP emission during maturation	Mirabella et al. 2004; Terskikh et al. 2000

1.7.3 Distinguishing autofluorescence from fluorescence protein signals

Autofluorescence defines for the natural emission of light by phenolic compounds in different plant tissues (Bright et al., 1989; Roshchina, 2012). In plants, chlorophyll, lignin, flavin, terpenes, alkaloids, flavonoids, anthocyanins, azulenes or NADPH can be the reason for autofluorescence (Bright et al., 1989; Roshchina, 2012; Donaldson, 2020). Several of these components may be located in the same area (cell wall, vacuoles, nuclei), which is why autofluorescence emission has a large range between 385 nm and 730 nm depending on the excitation wavelength (Hutzler et al., 1998; Donaldson and Radotic, 2013; Donaldson, 2020). This is relevant for fluorescence microscopy, because the excitation wavelength of a FP may lead to autofluorescence of some of the above-mentioned compounds. Lignin for example can be excited at 355 or 488 nm, which overlaps with GFP (Hutzler et al., 1998; Billinton and Knight, 2001; Donaldson, 2020). A clear differentiation of FP expression from autofluorescence is only possible when the desired FP is densely located or highly expressed. Therefore it is important to cross check every obtained result with positive and negative controls (Billinton and Knight, 2001; Donaldson, 2020).

1.8 Study background

This work is based on previous studies that were revealing a mycorrhiza dependent decrease in gene expression for the three poplar genes *Potri.9G1040*, *Potri.2G0797* and *Potri.2G2183*. The data showed an at least 50-fold difference in gene expression when comparing the expression data of mycorrhized and non-mycorrhized poplar fine roots (Nehls et al., unpublished).

1.8.1 The poplar gene Potri.2G0797

Homology analyses suggested, that *Potri.2G0797* encodes for a transmembrane transporter for basic amino acids. It is located on chromosome 2 in the poplar genome and is predicted to have one transcript five exons and four introns *Populus trichocarpa* gDNA (PhytoMine: Gene Potri.002G079700 *P. trichocarpa*; Phytozome v12.1: Gene Potri.002G079700 *P. trichocarpa*; Goodstein et al., 2012, Nehls et al., unpublished). The best homolog was found to be the Amino acid Permease 3/AAP3 in *Arabidopsis thaliana* (Wu et al. 2015; Nehls et al., unpublished). AAP3 belongs to the super family of Amino acid – Polyamine Choline (APC) transporter and, after further classification, to the Amino Acid/Auxin Permease (AAAP) family, which consists of secondary carrier proteins (Jack et al., 2000; Ortiz-Lopez et al., 2000; Okumoto et al., 2004; Su et al., 2004; Baluska et al., 2006; Wu et al., 2015). Within the AAAP family, AAP3 belongs to the sub family of Amino Acid Permeases (AAPs) (Baluska et al., 2006; Wu et al., 2015). Important features of the AAP sub family are the proton symporter activity and the unspecific symport of preferably basic or weakly charged amino acids (Baluska et al., 2006).

In *Arabidopsis*, *At*AAP3 showed a broad specificity for Gamma-Aminobutyric acid (GABA), tryptophan and basic amino acids such as arginine or lysine (Fischer et al., 1995; Baluska et al., 2006). In plants, GABA likely takes place in the stress response, development and cell signalling (Bouché and Fromm, 2004; Roberts, 2007; Ramesh et al., 2017). Thereby, GABA production is stimulated by elevated H^+ and Ca^{2+} levels in different plant tissues, which is in return regulating cytosolic pH-values. Furthermore, GABA and the other amino acids were also shown to serve as a nitrogen source for plants for long distance nitrogen transport (Breitkreuz et al., 1999; Shelp et al., 1999). In another study, most AAP3 genes were found to be almost exclusively located in plasma- and nuclear membranes of root phloem (Okumoto et al., 2004). This study also found small amounts of the protein in intracellular compartments, leading them to the assumption of protein trafficking or cycling (Okumoto et al., 2004). In terms of functionality, the location at the phloem would allow for long distance amino acid transportation and enhances the specific role required by AAP3. A localization in endodermal cells of root tips might suggest further physiological functions based on osmotic gradients (Okumoto et al., 2004). Thus, predicted functions could be **(1)** the retrieving of amino acids that leaked from the phloem, **(2)** specialized root synthesized amino acid uptake into the phloem or **(3)** moving of amino acids from the phloem through the symplast into the surrounding parenchyma, from where it can be distributed to the xylem and root tips via different strategies (Okumoto et al., 2004).

A study with rice discovered that overexpression of AAP3 leads to an increase in Lys, Arg, His, Asp, Ala, Gln, Gly, Thr and Tyr concentrations (ninhydrin and High-Performance Liquid Chromatography methods), as well as reduced bud outgrowth and rice tillering. In contrast to that, *Os*AAP3 silencing lead to significantly lower Arg, Lys, Asp and Th levels as well as more tillering and significantly higher grain yield. Additionally, the nitrogen use efficiency was enhanced in such plants (Lu et al., 2018). Furthermore, it is known, that without the symbiosis, an absence of AAP3 in plants has a negative impact on the animal community around the roots in the soil, such as root knot nematode parasitism (Marella et al., 2013).

1.8.2 The poplar gene Potri.2G2183

The poplar gene *Potri.2G2183* is predicted to be located on chromosome 2 (PhytoMine: Gene Potri.002G218300 *P. trichocarpa*; Phytozome v12.1: Gene Potri.002G218300 *P. trichocarpa*; Goodstein et al., 2012). It is predicted to have one transcript in *P. trichocarpa* gDNA (PhytoMine: Gene Potri.002G218300 *P. trichocarpa*). It was previously proposed to belong to the group of EF-hand proteins that are able to bind Ca^{2+} with a helix-loop-helix structural domain motif (Nehls et.al., unpublished). Based on the highly conserved EF-hand motifs, Calcium binding proteins can be divided into two groups: **(1)** the Calmodulin like (CML) proteins and **(2)** the Calmodulin (CAM) proteins (Mohanta et al., 2017; Zeng et al., 2017).

The majority of the CMLs have no introns (71.72 %), whereas CAMs are relatively intron rich (5.16 % have no introns). In average, plants encode more CMLs compared to CAMs. Since *Potri.2G2183* has no introns, it can be assumed to belong to the CML family. RT-qPCR analyses of poplar confirmed that it's specifically expressed in roots in this plant species (Nehls et.al., unpublished).

Calcium binding proteins act as sensors for intracellular Ca^{2+} levels (Kamano et al., 2015; Wagner et al., 2015; Verma et al., 2016). Calcium can act as a second messenger and trigger specific signal cascades, involving it in a variety of intracellular signalling pathways. Intracellular Ca^{2+} levels can be increased when the plant is exposed to adverse environmental conditions in changing the Ca^{2+} influx and efflux dynamics between cytosol, plastid stroma, the mitochondrial matrix, the endoplasmatic reticulum and the apoplast. This might be triggered mechanoreceptive by phytohormones or extracellular ATP levels, and can be mediated by Calcium-binding proteins (Kamano et al., 2015; Wagner et al., 2015; Verma et al., 2016). Once activated, the calcium-binding proteins can either bind to *cis*-elements of major stress responsive genes to influence gene expression and transcription factors, or they interact with DNA binding proteins controlling stress response genes (Miller et al., 2013; Wagner et al., 2015; Zeng et al., 2017). Also, Ca^{2+}-sensors function in concert with other second messengers and activate or suppress certain stress responses in plants or even moderate symbiotic responses with fungi (Zielinski, 1998; Miller et al., 2013; Wagner et al., 2015; Verma et al., 2016). At that, Calcium-binding proteins play a major role in the hormonal stress response of pants towards abiotic and biotic stress such as drought, heat, pathogens, bacteria, viruses, insects or nematodes (Verma et al., 2016). A number of other EF-hand proteins have already been identified, but mostly their physiological role still remains unknown (Zielinski 1998).

1.8.3 The poplar gene Potri.9G1040

According to the annotation found in the Phytozome database (PhytoMine: Gene Potri.009G104000 P. trichocarpa; Phytozome v12.1: Gene Potri.009G104000; Goodstein et al., 2012), *Potri.9G1040* likely codes for a carboxyl esterase located on chromosome 9 in poplar. Previous investigations predicted the protein to be soluble and lacking a membrane domain (Nehls, unpublished). Based on the deduced protein sequence, this enzyme was grouped to the B-type esterase class 1 α-β hydrolase superfamily, which consists of many hydrolytic enzymes sharing the same enzyme core (α-β -sheet, containing 8 strands connected by helices), generally converting carboxylic ester and water to alcohol and carboxylic acids (Gershater et al., 2007). The selective hydrolysation of mostly side chain ester linkages via carboxylesterases can modify chemical and physiological properties of metabolites, going so far as to block or activate specific pathways in altering molecule stability, localization or solubility (Gershater and Edwards, 2007; Gershater et al., 2007; Schilmiller et al., 2016). Examples for ester modifications that massively influence a plant are changes of jasmonic acid, salicylic acid or auxin, altering plant development and growth (Stuhlfelder et al., 2004; Forouhar et al., 2005; Yang et al., 2008). Members of the class I superfamily of α-β hydrolase folds are typically inhibited by organophosphates (pesticides, herbicides) (Marshall et al. 2003; Gershater and Edwards 2007). Consequently, the gene expression of CXE12 proteins is up-regulated in response to pathogenic attacks to prevent plant diseases in *Arabidopsis thaliana* (Gershater et al., 2007).

Experiments in *Arabidopsis* showed, that *At*CXE12 was present as a serine hydrolysing carboxyl esterase that uniquely hydrolysed *methyl-2,4-dichlorphenoxy acetate* (2,4-methyl) to the phytotoxic synthetic auxin *2,4-dichlorphenoxyacetic acid* (2,4-D). As an active metabolite of *2,4-dichlorophenoxbutyric acid* (2,4-DB), the degraded/beta-oxidised 2,4-D inhibits growth at the tips of stems and roots (Greene and Pohanish, 2005). Thereby, this enzyme directly takes part in bio-herbicide activation, which was predicted to take place in the intracellular space of the cytoplasm (Sánchez-Brunete et al., 1994; Gershater and Edwards, 2007; Gershater et al., 2007; Nickel et al., 2012). Furthermore, *At*CXE12 was predicted to function in lipid metabolism and degradation, thus serving as a lipolytic enzyme with hydrolase activity (Marshall et al., 2003).

1.9 Thesis aims and objectives

Main motivation to better understand ECM symbiosis is its proposed crucial role in nutrient cycling of sustainable forest ecosystems (Martin and Nehls, 2009). Many symbioses related proteins still have an unknown function. Recent research hinted, that ECM formation in beech forests can be threatened by an increased nitrogen deposition in soils, which might result from atmospheric pollution (de Witte et al., 2017). Additionally, the decomposition of ECM was shown to impact overall plant nutrition and soil carbon sequestration (Baskaran et al., 2017). Thus, ECM studies should be included when investigating their ecological effects on sustainable forest development (Zak et al., 2019).

Overall aim of this thesis was to improve and establish methods to further analyse the mycorrhiza down-regulated genes *Potri.2G0797*, *Potri.2G2183* and *Potri.9G1040* concerning their protein function, localization in plant tissues and respective promoter regions. Because the overall root transformation efficiency in composite poplar plants was below 50 %, first steps will include the optimization of the transformation system. Therefore, the plant transformation vectors pPLV and pCXUN will be compared. This includes the evaluation of transgenic root systems under the epifluorescence microscope.

Based on previous studies, parts of the promoter regions of the three mentioned genes will be PCR amplified and investigated in fluorescence marker cassettes in composite poplar plants. Aim is to investigate promoter regions concerning *cis* – elements related to ectomycorrhiza formation by determining fluorescence intensities at the epifluorescence microscope. For this purpose, a double marker system consisting of a GFP and tdTomato expression cassette was already established. Thereby, the green expression cassette will be driven by the promoters of interest and their obtained 5´truncations, and the red expression cassette is constitutively expressed as a reference cassette. It will be tested, if the GFP signals can be calibrated against the RFP signals of double marker constructs to calculate GFP: RFP ratios for comparison of different promoters of interest. Furthermore, fluorescence expression patterns will be compared between first and second order roots. It will also be tested, where the respective promoters are active and if GFP expression is impacted when the template gDNA is from a different poplar hybrid than used for the generation of composite plants. Also, the timer protein DsRED-E5 will be implemented and tested concerning its behaviour in poplar roots. This also includes the optimization of the camera settings and image processing. Subcellular localization of the three genes will be made with sYFP fusion constructs in transiently transformed tobacco leaves.

2 Material and Methods

2.1 Technical Equipment

2.1.1 Statistics

Statistics were conducted in R version 3.2.1 (R Core Team (2017), R Foundation for Statistical Computing, Vienna, Austria).

Statistical graphics were displayed with the ggplot2 and ggsignif package. Thereby, ggsignif was used to add significances to the graphs based on the "identity" method. Based on the data distribution the statistical calculation was either set to Wilcoxon rank test or t-test.

Effect sizes (d) were calculated in G*Power as described in (Faul, F., Erdfelder, E., Buchner, A., & Lang, A.-G. (2009) and describe the difference between means. Benchmarks for a small d = 0.2, a medium d = 0.5 and a large d = 0.8 (Cohen, 1988).

Statistical power analyses using G*Power 3.1: Tests for correlation and regression analyses. *Behavior Research Methods*, *41*, 1149-1160.), version 3.1.9.7. The α – error was set to 0.5.

2.1.2 Microscopy

Plant samples were analysed with a binocular (MZ10F, Leica Microsystems, Wetzlar, Germany). Sample illumination was carried out using a xenon light source (Lej LQ-HXP 120, Leistungselektronik JENA GmbH, Jena, Germany) with filter sets for sYFP (500 – 520 nm excitation and 540 – 580 nm emission window filter), GFP (450 – 490 nm excitation and 500 – 550 nm emission window filter) and dsRED (510 – 560 nm excitation and 590 – 650 nm emission window filter). Pictures were made using a Leica DFC425C camera and a Leica Application Suite software version 3.5.0 (Leica Microsystems, CH-9453, Heerbrugg). The default gamma value was set to 0.99 and the gain was set to 5.

Furthermore, fluorescence proteins in poplar roots were evaluated with a Zeiss Axioskop Microscope (Carl Zeiss, Göttingen, Germany. Serial No. 451485) in combination with an Imagingsource camera (Imagingsource DFK23UX174, 28217 Bremen, Germany with a Sony IMX174 chip with 5.64 x 5.64 µm) and an IC Capture software (IC Capture 2.5, 28217 Bremen, Germany). Sample illumination was carried out using a xenon light source (Lej LQ-

HXP 120, Leistungselektronik JENA GmbH, Jena, Germany) with filter sets for GFP (450 – 490 nm excitation and 510 – 560 nm emission window filter with a 510 nm beam splitter) and dsRED (510 – 560 nm excitation and 590 nm long pass emission filter window filter with a 580 nm beam splitter). The filter settings led to a slight underrepresentation of the RFP signals (quantum yield below 1). Because high light intensities lead to bleaching of FPs and induce flare light, the illumination times and light intensities were kept as low as possible. Default gain was set to 4.80 dB and default light intensity was 25 %. Adapted was the illumination time to accommodate visuality and ability to use the pixel information for statistics.

2.1.3 Image processing

For comparison of fluorescence intensities between root nuclei, GFP:RFP ratios were calculated with the open - source software ImageJ (version 2.1.0/1.53c). Thereby, unprocessed 8 - bit pictures were split in the three channels (RGB not weighted) and thereby converted to shades of grey. Only the green part of GFP pictures and red part of RFP pictures were used for further analyses. Areas of interests of the GFP and RFP channels were aligned and stacked before a binary mask was applied to the whole nucleus. For double marker constructs or comparisons, the mask was designed on the picture with the weaker fluorescence. As matching method, the "normalized correlation coefficient was selected in combination with a bilinear subpixel translation and Otsu (Otsu, 1979), a variant of (Zack et al., 1977) called Triangle, Intermodes (Prewitt and Mendelsohn, 1966) or Yen (Yen et al., 1995) threshold settings. Calculated was then the intensity per selected area, subtracted by the mean background fluorescence. To avoid distorted background values in cortex pictures because of their high autofluorescence levels, a mean of three cortex background areas was calculated and subtracted from the nuclei intensity values. Only nuclei within a saturation threshold of 25 to 230 (as shown in ImageJ histograms) were used for such analysis to avoid edge effects and thus distorted ratios. For the same reasons, only pictures with a background level below 50 % of the region of interest were used. These limits were based on pre – experiments (unpublished, not shown) as well as observations discussed by (Waters, 2009).

In this manner, ratios of the same areas were calculated for different roots. Because of biological variation, many nuclei were analysed for each compartment, resulting in a mean ratio per root. Thereby, each root accounted for one replicate.

Some fluorescence images were subsequently amplified with Fotos (Apple, Version 4.0) or ImageJ (version 2.1.0/1.53c) for better visualization. Each edited picture is labelled as such. To not distort ratios, corresponding pictures were edited in a montage, in which all respective pictures were treated as one. The autofluorescence background was subtracted in ImageJ with the rolling ball radius setting set to 50. Thereby, the background for each pixel is subtracted (https://imagej.net/Rolling_Ball_Background_Subtraction, accessed at 12.05.2021). The Contrast was enhanced by saturating a defined percentage of pixels. An example with the impact of changes on the histogram is given in **Figure 6**.

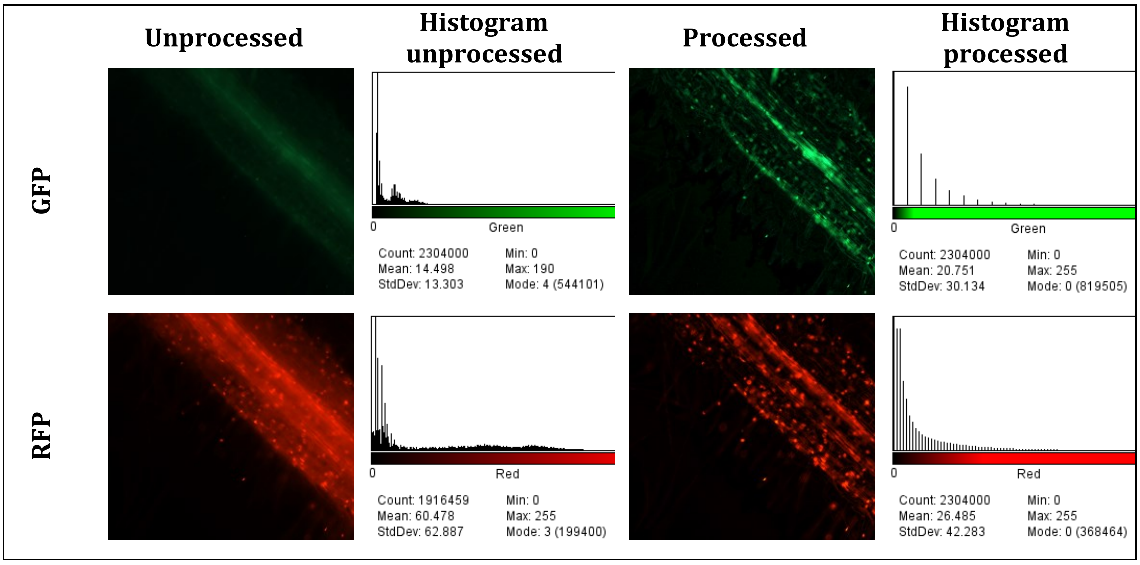
Unprocessed
Histogram unprocessed
Processed
Histogram processed
GFP
RFP
0
Green
Count: 2304000
Mean: 14.498
StdDev: 13.303
Min: 0
Max: 190
Mode: 4 (544101)
0
Green
Count: 2304000
Mean: 20.751
StdDev: 30.134
Min: 0
Max: 255
Mode: 0 (819505)
0
Red
Count: 1916459
Mean: 60.478
StdDev: 62.887
Min: 0
Max: 255
Mode: 3 (199400)
0
Red
Count: 2304000
Mean: 26.485
StdDev: 42.283
Min: 0
Max: 255
Mode: 0 (368464)

Figure 6. Visualization of impacts of picture processing on the picture and its histogram. Shown is an *Agrobacterium* transformed poplar root with GFP and RFP fluorescence proteins targeted into the nucleus. Given are the unprocessed GFP and RFP pictures with the corresponding histograms of the channels. To the processed pictures a background subtraction (rolling ball radius set to 50) was applied and the contrast was enhanced by 0.01 % in ImageJ version 2.1.0/1.53c.

Overlays were made with GIMP version 2.10.20 (GNU Image Manipulation Program) or ImageJ (version 2.1.0/1.53c).

2.1.4 Agarose gel electrophoresis

Agarose gels were observed using a DocPrint II Hood with added camera (VilberLourmat DocPrint II Hood, VilberLourmat, Eberhardzell, Germany). The exposure time was set to 22 – 60 msec.

NEB 6 x Purple Loading dye was used for gel loading with DNA fragments (New England Biolabs Inc., Frankfurt am Main, Germany).

2.1.5 Sterile working benches

Listed below are the sterile working benches that were used during this thesis:

1. Scanlaf Clean Bench Fortuna 1500 (Labogene APS, Lynge, Dänemark)
2. Clean Air CA/Rev4 (Clean Air Supplies, Voeren, Germany)

2.1.6 Centrifuges

Following centrifuges were used during this thesis:

1. Eppendorf Zentrifuge 5804R with rotors: A-2-DWP und F-34-6- 38 (Eppendorf AG, Hamburg, Germany)
2. Eppendorf Zentrifuge 5415R with rotor: F 45-24-11 (Eppendorf AG, Hamburg, Germany)

2.1.7 Thermoshaker

An Eppendorf Thermomixer 5436 (Eppendorf AG, Hamburg, Germany) was used for incubation of samples in 1.5- or 2.2-ml Reaction tubes

2.1.8 OD_{600} measurements

Optical densities (OD_{600}) were measured with a WPA biowave CO8000 cell density meter (Biochrom Ltd., Camebridge, United Kingdom)

2.1.9 Polymerase Chain Reaction (PCR) Thermocycler

Different incubation steps in small Reaction Tubes were conducted in a Peqlab primus 25 advanced machine (PEQLAB Biotechnologie GmbH, Erlangen, Germany) or a Crocodile III Thermocycler (Appligene, Illkirch, France).

Gradient PCRs were performed using a Biometra T - gradient Thermoblock (Analytic Jena GmbH, Jena, Germany).

2.1.10 Incubator

A combination of a Certomat®H, type 886342/3 incubator (B. Braun Biotech International GmbH, Mesungen, Germany) with a Infors cell shaker (Infors HT, Basel, Switzerland) was used to cultivate *E. coli* liquid cultures.

A Certomat®HK incubater in combination with a Certomat®HK 886302/4 shaker was used for different incubation steps of liquid *Agrobacteria* solutions at their given temperature optimum.

2.1.11 Sterilefiltration and autoclaving

Heat sensitive components were sterile filtrated using Merck Millipore filters with a pore size of 0.22 µm (Merck, KgaA, Darmstadt, Germany). Alternatively, a cellulose acetate membrane with a pore size of 0.2 µm was used for smaller amounts (Sartorius, Göttingen, Germany). Sterile filtrated components were stored in sterile bottles or reaction tubes and added to the respective autoclaved solutions under sterile conditions.

Autoclave conditions were 21 min at 121°C and 2 bars.

2.2 Chemicals and Enzymes

All the enzymes, antibiotics and chemicals used in the context of this dissertation are listed below in (**Table 2**, **Table 3** and **Table 4**).

Enzymes for restriction digestion were all obtained from New England Biolabs (NEB Inc, Frankfurt am Main, Germany).

Table 2. Enzymes that were used for the dissertation with their given function and the producer.

Enzyme	Function	Producer
DNA T4 ligase	Ligation of binary vector constructs	New England BioLabs Inc., Frankfurt am Main, Germany
DNA T4 polymerase	synthesis of DNA in the 5´→ 3´ direction	New England BioLabs Inc., Frankfurt am Main, Germany
Q5® High-Fidelity DNA Polymerase	Amplification of nucleic acids via PCR	New England BioLabs Inc., Frankfurt am Main, Germany. 0.02 U / µl for up to 1000 ng template DNA
RNase A	Degradation of RNA	CARL, ROTH GmbH & Co. KG, Karlsruhe, Germany
Shrimp Alkaline Phosphatase	Dephosphorylation	New England BioLabs Inc., Frankfurt am Main, Germany. 1 U / µl

Table 3. Used Chemicals and their respective producers.

Chemical	Producer
2-propanol (Isopropanol)	Sigma-Aldrich Corporation, St. Louis, USA
2-(N-morpholino) ethane sulfonic acid (MES)	CARL ROTH GmbH & Co. KG, Karlsruhe, Germany
3-(N-Morpholino) propansulfonsäure (MOPS)	Sigma-Aldrich Corporation, St. Louis, USA
Acetosyringone	Sigma-Aldrich Corporation, St. Louis, USA
Agar for bacterial agarose plates Kobe I)	CARL ROTH GmbH & Co. KG, Karlsruhe, Germany
Agar for gel electrophoresis	Biozym Scientific GmbH, Hessisch Oldendorf, Germany
Agar for plant medium	DUCHEFA Biochemie B.V., Haarlem, Netherlands
Ammonium acetate (CH_3COONH_4)	CARL ROTH GmbH & Co. KG, Karlsruhe, Germany
Ammonium molybdate (($(NH_4)_6Mo_7O_{24}$ x 4 H_2O)	CARL ROTH GmbH & Co. KG, Karlsruhe, Germany
Boric acid (H_3BO)	DUCHEFA Biochemie B.V., Haarlem, Netherlands
Bovine Serum Albumin (BSA)	CARL ROTH GmbH & Co. KG, Karlsruhe, Germany
Calcium chloride ($CaCl_2$ x 2 H_2O)	CARL ROTH GmbH & Co. KG, Karlsruhe, Germany
Cetyltrimethylammonium bromide (CTAB)	Sigma-Aldrich Corporation, St. Louis, USA
Chloroform	Sigma-Aldrich Corporation, St. Louis, USA
Copper (II) sulphate ($CuSO_4$ x 5 H_2O)	Merck KgaA, Darmstadt, Germany
Diammonium hydrogen Phosphate ($(NH_4)_2HPO_4$)	CARL ROTH GmbH & Co. KG, Karlsruhe, Germany
Diethyl pyrocarbonat (DEPC)	Sigma-Aldrich Corporation, St. Louis, USA
Dimethyl sulfoxide (DMSO)	Sigma-Aldrich Corporation, St. Louis, USA
dNTP	Thermo Fisher Scientific, Waltham, MA, USA
Dithiothreitol ($C_4H_{10}O_2S_2$)	CARL ROTH GmbH & Co. KG, Karlsruhe, Germany
Ethanol (C_2H_6O)	CARL ROTH GmbH & Co. KG, Karlsruhe, Germany
Ethidium bromide	CARL ROTH GmbH & Co. KG, Karlsruhe, Germany
Ethylenediaminetetraacetic acid (EDTA)	Merck KgaA, Darmstadt, Germany
Glacial acetic acid	Merck KgaA, Darmstadt, Germany
Glucose	DUCHEFA Biochemie B.V., Haarlem, Netherlands
Glycerol ($C_3H_8O_3$)	CARL ROTH GmbH & Co. KG, Karlsruhe, Germany
Iron (III) chloride ($FeCl_3$ x 6 H_2O)	Altmann Analytik GmbH & Co. KG, München, Germany
Isoamyl alcohol	Sigma-Aldrich Corporation, St. Louis, USA
Liciumchloride (LiCl)	CARL ROTH GmbH & Co. KG, Karlsruhe, Germany
Magnesium sulphate ($MgSO_4$ x 7 H_2O)	CARL ROTH GmbH & Co. KG, Karlsruhe, Germany

Table 3. continued: Used Chemicals and their respective producers.

Chemical	Producer
Magnesium chloride ($MgCl_2$ x $6H_2O$)	Honeywell Specialty Chemicals Seelze GmbH, New Jersey, USA
Magnesiumsulfate heptahydrate ($MgSO_4$ x 7 H_2O)	Merck KgaA, Darmstadt, Germany
Manganese chloride ($MnCl_2$)	Honeywell Specialty Chemicals Seelze GmbH, New Jersey, USA
Manganese III sulfate ($MnSO_4$ x H_2O)	Altmann Analytik GmbH & Co. KG, München, Germany
Monopotassium phosphate (KH_2PO_4)	Honeywell Specialty Chemicals Seelze GmbH, New Jersey, USA
MS salts	DUCHEFA Biochemie B.V., Haarlem, Netherlands
Myo-inositol (1,2,3,4,5,6 Hexahydroxy cyclohexane)	Sigma-Aldrich Corporation, St. Louis, USA
Nicotinic acid ($C_6H_5NO_2$)	CARL ROTH GmbH & Co. KG, Karlsruhe, Germany
Peptone	DUCHEFA Biochemie B.V., Haarlem, Netherlands
Potassium acetate (KCH_3COO)	CARL ROTH GmbH & Co. KG, Karlsruhe, Germany
Potassium chloride (KCL)	DUCHEFA Biochemie B.V., Haarlem, Netherlands
Potassium hydroxide (KOH)	Honeywell Specialty Chemicals Seelze GmbH, New Jersey, USA
Potassium phosphate dibasic trihydrate (K_2HPO_4 x 3 H_2O)	CARL ROTH GmbH & Co. KG, Karlsruhe, Germany
Pyridoxine hydrochloride (vitamin B6)	DUCHEFA Biochemie B.V., Haarlem, Netherlands
Rubidium chloride (RbCl)	CARL ROTH GmbH & Co. KG, Karlsruhe, Germany
Sodium chloride (NaCl)	Sigma-Aldrich Corporation, St. Louis, USA
Sodium dodecyl sulphate ($CH_3(CH_2)_{11}SO_4Na$)	CARL ROTH GmbH & Co. KG, Karlsruhe, Germany
Sodium hydroxide (NaOH)	Merck KgaA, Darmstadt, Germany
Sucrose	CARL ROTH GmbH & Co. KG, Karlsruhe, Germany
Thiamine hydrochloride (vitamin B1)	Merck KgaA, Darmstadt, Germany
Tris-aminomethane (TRIS base)	CARL ROTH GmbH & Co. KG, Karlsruhe, Germany
Tris(hydroxymethyl)aminomethane hydrochloride (Tris/HCL)	Sigma-Aldrich Corporation, St. Louis, USA
Yeast extract	DUCHEFA Biochemie B.V., Haarlem, Netherlands
Zinc sulphate ($ZnSO_4$ x 7 H_2O)	Altmann Analytik GmbH & Co. KG, München, Germany
β-mercaptoethanol	CARL ROTH GmbH & Co. KG, Karlsruhe, Germany

Table 4. Antibiotics that were used for selection of binary vectors with their given concentrations in liquid or solid growth medium. Antibiotics were always added freshly and the agar plates containing antibiotics were prepared a maximum of 1 – 7 days before they were used. Media containing rifampicin and tetracycline were stored in the dark because of its light sensitivity.

Antibiotics	Producer	Used for Organism	Final concentration
Ampicillin	Sigma-Aldrich Corporation, St. Louis, USA; CARL ROTH GmbH & Co. KG, Karlsruhe, Germany	*Escherichia coli*	100 mg/L
Carbenicillin	DUCHEFA Biochemie B.V., Haarlem, Netherlands	*Agrobacterium rhizogenes*	500 mg/L
Cefotaxime	DUCHEFA Biochemie B.V., Haarlem, Netherlands	*Agrobacterium rhizogenes*	252 mg/L
Kanamycin	DUCHEFA Biochemie B.V., Haarlem, Netherlands	*Escherichia coli,* *Agrobacterium tumefaciens,* *Agrobacterium rhizogenes*	50 mg/L
Tetracycline	DUCHEFA Biochemie B.V., Haarlem, Netherlands	*Agrobacterium rhizogenes*	5 mg/L

2.3 Kits

The elution of nucleic acids that were separated via gel – electrophoresis was conducted with a NucleoSpin® Gel and PCR Clean-up kit (MACHEREY-NAGEL GmbH & Co. KG, Düren, Germany).

PCR fragments were blunt end cloned in pJET1.2 with the CloneJET™ PCR Cloning Kit (Thermo Fisher Scientific, Waltham, MA, USA).

Backbone plasmid DNA for the cloning of high copy binary vector systems was obtained with a NucleoSpin® Plasmid isolation kit (Macherey & Nagel, Dueren, Germany) to ensure better cloning results. Alternatively, the Monarch Plasmid Miniprep Kit was used (T1010, New England BioLabs Inc., Frankfurt am Main, Germany).

Backbone plasmid DNA for the cloning of high copy binary vector systems was obtained with a NucleoBond Xtra Midi Kit (Macherey & Nagel, Dueren, Germany). Aliquots of the obtained vector were quantified and frozen at -80°C.

2.4 Organisms

Escherichia coli cells of the TOP^{10} F´ strain were used for gene design and plasmid-DNA amplification (Invitrogen, Groningen, Netherlands). Cells were grown in liquid LB medium (under sterile conditions, aerobe) or LB-agarose plates containing the respective selective antibiotics.

Transgenic "disarmed" (no longer carrying the tumor inducing genes) ***Agrobacterium tumefaciens*** strain C58 (Wood et al., 2001) or the armed ***Agrobacterium rhizogenes*** strain K599 (Daimon et al., 1990) were used for the transient transformation of epidermal tobacco leave cells (established in the lab by Neb, 2017).

Tobacco leave infiltration was performed on ***Nicothiana benthamiana*** leaves (Seeds originally from Prof. Dr. Hänsch, TU Braunschweig, Germany). Germination was enhanced by covering the seeds with a tall glass slide to enhance humidity. This glass was removed after germination. Seedlings were isolated in single pots after 2 weeks and used for transformation after 3 – 4 weeks. The plants were grown at 25°C with 16 h of light per day (75 µmol photons $m^{-2}s^{-1}$) and 70% humidity.

Composite plants were prepared from the plant hybrid species ***Populus tremula x tremuloides*** (T89) and ***Populus tremula x alba*** (No. 7171-B4, Institut de la Recherche Agronomique, INRA). The plants were grown in sterile preserving jars containing MS6 – medium. Each 4 – 8 weeks shoot cuttings were either used to preserve the plants, or to generate Composite plants. Plants were grown at 18°C with 16 h light per day and a light intensity of 80 µmol photons $m^{-2}s^{-1}$.

Mycorrhization was conducted with the fungal organisms ***Pisolithus microcarpus***, which was obtained from a cooperation partner (Uwe Nehls, personal communication).

2.5 Cloning strategies

2.5.1 Intermediate cloning vector pJET1.2

As intermediate vector for PCR products and the preparation of other cloning strategies, such as fusion constructs, the *Escherichia coli* high copy cloning vector **pJet1.2/blunt** (Thermo Fisher Scientific, Waltham, Massachusetts, USA) was used. A vector description is given in **Figure 7**.

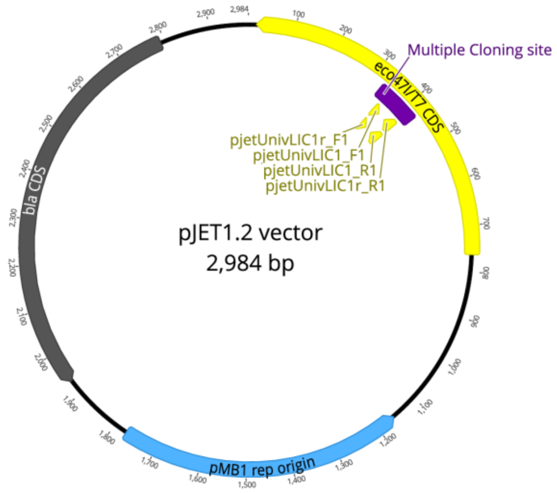
2,900
2,984
100
200
300
400
500
600
700
800
900
1,000
1,100
1,200
1,300
1,400
1,500
1,600
1,700
1,800
1,900
2,000
2,100
2,200
2,300
2,400
2,500
2,600
2,700
2,800
Multiple Cloning site
eco47I/T7 CDS
pjetUnivLIC1r_F1
pjetUnivLIC1_F1
pjetUnivLIC1_R1
pjetUnivLIC1r_R1
bla CDS
pJET1.2 vector
2,984 bp
pMB1 rep origin

Figure 7. Visualization of the pJET1.2 vector. The backbone consists of (1) a "bla" CDS that catalyses the opening and hydrolysis of the beta-lactam ring of beta-lactam antibiotics, (2) a pMB1 rep origin and (3) eco47I/T7 CDS. The mutant Eco47I has 15 additional amino acid residues encoded by the inserted T7 promoter compared to the wild type. The Eco471/T7 CDS includes a multiple cloning site (MS-site), ensuring that only plasmids with integrated DNA fragments in the MS-site to grow. Otherwise, no protective methylation leads the enzyme to recognise and cleave double-stranded DNA targets, which is ultimately leading to cell death. Annotated are Ligase independent cloning (LIC) sites. LIC is described in the introduction and the primers are further characterized in the Material and Methods of this thesis. Figure was in silico cloned and displayed using Geneious Prime® 2021.1.1**.**

2.5.2 Binary vectors pPLV and pCXUN

Intermediate LIC Binary vectors for *Agrobacterium* mediated transformation for some cloning strategies were based on **pPLV11** (a derivate of the pGREEN-II vector). This vector was obtained from the Arabidopsis Stock centre (http://arabidopsis.info/, 10.07.2021) and then modified to serve the needed characteristics (Hellens et al., 2000; De Rybel et al., 2011; Neb, 2017; Schnakenberg, 2020), furthermore referred to as modified **pPLV**. In this modified version, the T - DNA contains a kanamycin resistance (NPTII CDS) between a P_{35S} and a T_{35S} (Plant selection marker cassette) as well as an expression cassette for fluorescence proteins (**Figure 2**) (Neb, 2017; Schnakenberg, 2020). A vector description for one construct as an example is given in **Figure 8**. The needed helper plasmid pSOUP to complement the psa-ORI was also obtained from the Arabidopsis stock centre (http://arabidopsis.info/, 10.07.2021).

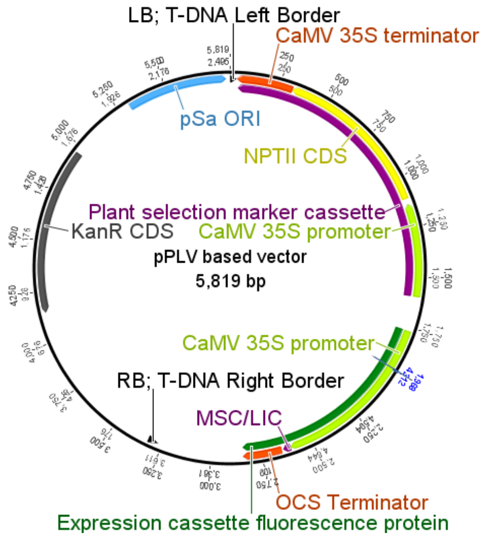
LB; T-DNA Left Border
CaMV 35S terminator
pSa ORI
NPTII CDS
Plant selection marker cassette
KanR CDS
CaMV 35S promoter
pPLV based vector
5,819 bp
CaMV 35S promoter
RB; T-DNA Right Border
MSC/LIC
OCS Terminator
Expression cassette fluorescence protein

Figure 8. Vector description of a modified pPLV binary vector. The T - DNA was completely exchanged via *BglII*, integrating a LIC site and a multiple cloning site (Neb, 2017). The expression cassette consists of a P_{35S} and T_{OCS} with a Multiple cloning site (MSC) and a LIC site in between (Expression cassette fluorescence protein) (Schnakenberg, 2020). Additionally, the T - DNA contains a kanamycin resistance (NPTII CDS) between a P_{35S} and a T_{35S} (Plant selection marker cassette). The backbone of the binary vector contains a part of the psa-ORI (origin of replication) and a kanamycin resistance (KanR CDS). To be able to replicate, the incomplete pSA ORI needs to be complemented with the "helper plasmid" pSOUP. For promoter and terminator descriptions see chapter 2.5.1. Figure was in silico cloned and displayed using Geneious.

pCXUN was used as *Agrobacterium* entry vector for all plant transformation events. As a binary vector for all strategies and cloning steps, pCXUN – FLAG was obtained from the Arabidopsis stock centre (Vector Detail Arabidopsis Stock centre pCXUN-FLAG) (based on a pCAMBIA-1300 backbone).

2.5.3 Promoters and terminators

In dependence of the construct, a Cauliflower Mosaic Virus promoter (CaMV, $\mathbf{P_{35S}}$), Nopaline Synthase Gene promoter ($\mathbf{P_{NOS}}$) Arabidopsis Ubiquitin 10 promoter ($\mathbf{P_{UBQ}}$) or an investigative promoter were combined with either a Nopaline Synthase terminator ($\mathbf{T_{NOS}}$) or an Octopine Synthase terminator ($\mathbf{T_{OCS}}$). All these promoters are constitutively expressed (Ebert et al., 1987; Holtorf et al., 1995) and obtained from PCR amplification of different vectors.

2.5.4 Fluorescence proteins

For subcellular localization, a yellow fluorescent sYFP2 (super yellow fluorescent protein) was fused in frame to the CDS of the three genes. sYFP was PCR amplified from pPLV11 and modified as needed (Neb, 2017).

Promoter activity assessments were conducted using an eGFP (enhanced Green Fluorescent Protein) in a genetic fusion of two copies and tagged with an SV40 NLS (Nehls et al., unpublished). The protein was PCR amplified and modified as needed by Jana Müller.

tdTomato-NLS was used as secondary location marker driven by a constitutive promoter to allow for the screening of positive transformants. The protein was PCR amplified and modified for the needs from pPLV06 by Jana Schnakenberg (Schnakenberg, 2020).

Furthermore, DsRED-E5 was used to detect mycorrhiza regulatory elements upon mycorrhization based on changes in the promoter activity. The protein was synthesized with restriction enzyme overhangs and an SV40 NLS by Eurofins Genomics (Eurofins Genomics GmbH, 85560 Ebersberg, Germany).

2.5.5 Used primers

All primers used in this study were obtained from Eurofins genomics (Ebersberg, Germany).

Primers were designed to amplify the coding sequence (CDS) of all three genes from cDNA of non – mycorrhized *Populus tremula x tremuloides* fine roots to generate gene fragments without introns (**Table 5**). Additionally, the CDS of *Potri.2G0797* was amplified from genomic DNA of *Populus tremula x tremuloides* to investigate whether the splicing of introns does affect gene expression. All forward primers included a Shine Dalgarno Sequence (SD) of a minimum of 10 bp upstream of the starting codon to enable the successful binding of ribosomes.

Table 5. Primers that were used to amplify the CDS with and without introns or restriction enzyme overhangs of the three genes *Potri.9G1040*, Potri.*2G2183* and *Potri.2G0797* from either gDNA or cDNA of *Populus tremula x tremuloides*. The primer sequences as well as their names and the amplified fragment length are given. Restriction site overhangs are highlighted in red.

Gene ID	**Target sequence**	**Name Forward Primer**	**Sequence Forward primer**	**Name Reverse Primer**	**Sequence Reverse Primer**
Potri.2G0797	CDS without introns	Potri,2G0797_for2	ATGAACACGACGAGCCTAAG	Potri,2G0797_rev2	TTAGTAACTGGTCTGGAAGGGT
Potri.2G0797	CDS with introns	Pt-2G0797-CDS-SD-f1	GCTATATCAGAAATATGAACACGACG	Potri,2G0797_rev2	TTAGTAACTGGTCTGGAAGGGT
Potri.2G0797	CDS with introns with *BamHI* overhangs	Pt24SLBamH1.For	CGGGATCCCTACCTCTCTGCTATATCAG	Pt24SLBamH1.Rev	CGGGATCCTTAGTAACTGGTCTGG
Potri.2G2183	CDS without introns	Potri2G218300SLF	AATTGCGAGAGACCAAAAAT	Potri2G218300SLR	AGGGTAATGGATGTGGAATTAT
Potri.2G2183	CDS without introns with *EcoRI* overhangs	P2G2183CDSEcoR1-f1	GCGAATTCATGAGTGTGGAGATTTTGGA	P2G2183CDSEcoR1-r1	GCGAATTCGGCAACCAGTTTAGCAGATTC
Potri.9G1040	CDS without introns	Potri9G104000SLR	GGGAAGAGAAAAGAAAAGCCACC	Potri9G104000SLF	AGAAAACAAGAGAACAGACAAGCA
Potri.9G1040	CDS without introns with *EcoRI* overhangs	P9G1040CDSEcoR1-f1	GCGAATTCATGTTTTCATTCAATATGGA	P9G1040CDSEcoR1-r1	GCGAATTCAGTAATGGCCATGTATGAAA

Primers for the amplification of promoter regions from genomic DNA were designed *in silico* in a consensus area of ***Populus trichocarpa*** and ***P. tremuloides*** (**Table 6**). Designed primers were then used on genomic DNA of the hybrid species *P. tremula x tremuloides* (T89) or *P. trichocarpa*. Promoter analyses were performed in T89 or *P. tremula x alba* plants.

Table 6. Primers that were used for the amplification of promoter regions from genomic DNA of *Populus tremula x tremuloides* (T89) or *P. trichocarpa* from the three genes *Potri.9G1040*, *Potri.2G0797* *Potri.2G2183*. The table contains information about the gene name, the amplified promoter length, and the names of the used primers. Forward direction is meant as from 5´to 3´and vice versa. Labelled in red are LIC overhangs for the truncation of long promoter fragments as well as restriction enzyme recognition sites.

Gene ID	Template	Name Forward Primer	Sequence Forward primer	Name Reverse Primer	Sequence Reverse Primer
Potri.9G1040	T89	Ptt-9G1040pr-f2	TCAAGCAAGTCAACTTTCCTAC	Ptt-9G1040pr-r3	TGTATGAAAACATGGTGGCTT
Potri.2G2183	*P. trichocarpa* includes ATG of CDS	Potri2G2183ProFor5	GTGAGTCCATAATCTCGTTCT	Potri2G218300PRr	AAGTTGACAATGGTGGCACC
Potri.2G2183	From pJET1.2 with 5´*KpnI* and 3´*HpaI* overhangs. No ATG of CDS	ID5_KpnI_for	GCGGTACCGTGAGTCCATAATCTCG	ID5_HpaI_rev	GCGTTAACTTTTGGTCTCTCTTAATTTAC
Potri.2G2183	From pCXUN with 5´*KpnI* and 3´*HpaI* overhangs.	ID5-2502bp-KpnI	GGGGTACCCCGACAAACCATACAC	ID5_HpaI_rev	GCGTTAACTTTTGGTCTCTCTTAATTTAC
Potri.2G2183	From pCXUN with 5´*KpnI* and 3´*HpaI* overhangs.	ID5-1289bp-KpnI	GGGGTACCCCACAGTAGAGTACAC	ID5_HpaI_rev	GCGTTAACTTTTGGTCTCTCTTAATTTAC
Potri.2G2183	From pCXUN with 5´*KpnI* and 3´*HpaI* overhangs.	ID5-516bp-KpnI	GGGGTACCCCCTTCGAGAAAGTCA	ID5_HpaI_rev	GCGTTAACTTTTGGTCTCTCTTAATTTAC
Potri.2G2183	T89	Potri02G2183ProF2	CTACAACCACCATAATATA	Ptt-2G2183pr-r3	TGGTATCTCGCAATTCACTC
Potri.2G0797	T89	Potri2G0797ProF3	TATACAGCTAATTAGTCCA	Potri2G0797ProR4	CAGAAGATTAGAAATGAGT
Potri.2G0797	From pJET1.2 with 5´*KpnI* and 3´*SmaI* overhangs	ID8_KpnI_for	GCGGTACCTATACAGCTAATTAGTCCA	ID8_SmaI_rev	GCCCCGGGCAGAAGATTAGAAATGAG
Potri.2G0797	From pCXUN with 2.892 kb promoter	ID8_KpnI_50bp	GCGGTACCAAGTTGAGAGTACTGTCCTTG	Nosp_rev_zuGFP	TTAATTCTCCGCTCATGATC

Table 6. continued

Gene ID	**Template**	**Name Forward Primer**	**Sequence Forward primer**	**Name Reverse Primer**	**Sequence Reverse Primer**
Potri.2G0797	From pCXUN with 2.892 kb promoter	ID8_KpnI_113 bp	GCGGTACCACCCAACCTCATCTTGCATTC	Nosp_rev_zuGFP	TTAATTCTCCGCTCATGATC
Potri.2G0797	From pCXUN with 2.892 kb promoter	ID8_KpnI_150 bp	GCGGTACCACCTACTGCCCCTCCCA	Nosp_rev_zuGFP	TTAATTCTCCGCTCATGATC
Potri.2G0797	From pCXUN with 2.892 kb promoter	ID8-226bp-KpnI	GGGGTACCCCAAATATTATTTTAATATATTTT	ID8_SmaI_rev	GCCCCGGGCAGAAGATTAGAAATGAG
Potri.2G0797	From pCXUN with 2.892 kb promoter	ID8-276bp-KpnI	GGGGTACCCCTAATTTTTATGTTCATATATTA	ID8_SmaI_rev	GCCCCGGGCAGAAGATTAGAAATGAG
Potri.2G0797	with LIC overhangs from pJET1.2	pjetUnivLIC1r_F1	TTATGGAGTTGGGTTTGGCTCGAGTTTTTCAGCA	ID8LIC200bp	TAGTTGGAATGGGTTAAGCTTAGGATTGTACGAGTTTGA
Potri.2G0797	From pCXUN with 2.892 kb promoter	ID8-391bp-KpnI	GGGGTACCCCGTATTGTGGGATCCTCAG	ID8_SmaI_rev	GCCCCGGGCAGAAGATTAGAAATGAG
Potri.2G0797	From pCXUN with 2.892 kb promoter	ID8-457bp-KpnI	GGGGTACCCCCCAGTTTTTATTTTAGAAAAAG	ID8_SmaI_rev	GCCCCGGGCAGAAGATTAGAAATGAG
Potri.2G0797	with LIC overhangs from pJET1.2	pjetUnivLIC1r_F1	TTATGGAGTTGGGTTTGGCTCGAGTTTTTCAGCA	ID8LIC500bp	TAGTTGGAATGGGTTTGATAGGCAAGTGGTCGTGAGAGA
Potri.2G0797	From pCXUN with 2.892 kb promoter	ID8-750bp-KpnI	GGGGTACCCCCCTCACACATCAATACATATTT	ID8_SmaI_rev	GCCCCGGGCAGAAGATTAGAAATGAG
Gene ID	Template	Name Forward Primer	Sequence Forward primer	Name Reverse Primer	Sequence Reverse Primer
Potri.2G0797	with LIC overhangs from pJET1.2	pjetUnivLIC1r_F1	TTATGGAGTTGGGTTTGGCTCGAGTTTTTCAGCA	ID8LIC1000bp	TAGTTGGAATGGGTTCTCGAACCTAAGACTATAAGATAAGCC
Potri.2G0797	with LIC overhangs from pJET1.2	pjetUnivLIC1r_F1	TTATGGAGTTGGGTTTGGCTCGAGTTTTTCAGCA	ID8LIC1500bp	TAGTTGGAATGGGTTGCTAGCGTGTGTTTGATATTATGATGG
Potri.2G0797	From pCXUN with 2.892 kb promoter	ID8-1.75kb-KpnI	GGGGTACCCCACAAGCACTGATGCCATCTA	ID8_SmaI_rev	GCCCCGGGCAGAAGATTAGAAATGAG
Potri.2G0797	with LIC overhangs from pJET1.2	pjetUnivLIC1r_F1	TTATGGAGTTGGGTTTGGCTCGAGTTTTTCAGCA	ID8LIC2000bp	TAGTTGGAATGGGTTCCATCCTGCGTCTATATATAACCTT

Used primers to amplify or construct fusion constructs are given in **Table 7**.

Table 7. Primers that were used to clone fusion constructs of *Potri.2G0797*. Furthermore, primers to amplify an existing fusion construct of *Potri.2G2183* and *Potri.2G0797* without introns are given. The table contains information about the gene name, direction of the primers, the amplified sizes as well as the names of the used primers. Forward direction is meant as from 5´to 3´and vice versa. Labelled in red are restriction enzyme recognition sites.

Gene ID	**Target sequence**	**Name Forward Primer**	**Sequence Forward primer**	**Name Reverse Primer**	**Sequence Reverse Primer**
Potri.2G0797	C-terminal fusion construct from pCXUN with *BamHI* overhangs, no introns	24SLBamHIforFus	CGGGATCCGGATCCATGAACACGACGA	24SLBamHIrevFus	CGGGATCCTTACTTGTACAGCTCGTC
Potri.2G0797	CDS with introns and 3´ *BamHI* – site, no STOP - codon	Pt-2G0797-CDS-SD-f1	GCTATATCAGAAATATGAACACGACG	Pt24SLBamH1.Rev1	CGGGATCCGTAACTGGTCTGG
sYFP	ATG – less sYFP, not targeted, with *BamHI* overhangs	YFPforBamHI fusion	CGGGATCCACTAGTAAGGGCGAGGAG	sYFP-BamHI-rev1	CGGGATCCTTACTTGTACAGCTCGTCCAT
Potri.2G2183	C-terminal fusion construct from pCXUN with *EcoRI* overhangs	P2G2183CDSEcoR1-f1	GCGAATTCATGAGTGTGGAGATTTTGGA	15-9SLfusRevEcoRI	GCGAATTCTTACTTGTACAGCTCGTC

2.5.6 Conventional cloning: Dephosphorylating and Ligation steps

The steps of conventional cloning were divided in **(1)** restriction digestion to obtain the desired fragments, **(2)** gel electrophoresis clean-up of the fragments, **(3)** optional: dephosphorylating of the vector backbone when only one restriction site is used to prevent self-ligation, **(4)** ligation of insert and vector and finally **(5)** the transformation of the newly designed construct in chemically competent *E. coli* TOP^{10} cells.

For the dephosphorylating step 500 ng of the linearized vector backbone were mixed on ice with 1 x Cutsmart buffer from NEB, 1 U of Shrimp Alkaline Phosphatase (rSAP) and 0.2 µM Magnesium chloride, all added up to a volume of 20 µl with ddH_2O in small PCR reaction tubes. The samples were thoroughly mixed and incubated at 37°C for 30 minutes, after which the enzyme was heat inactivated at 65°C for 5 min. The samples were shock frozen in liquid nitrogen and stored at -80°C for later usage due to the fast degradation of linearized DNA fragments.

For the ligation step, the linearized and dephosphorylated vector backbone was mixed with the phosphorylated insert in a molecular ratio of 1: 3 (50 ng vector and 150 ng insert) together with 0.5 mM rATP, 1 U DNA T4 - ligase and ddH_2O in a total volume of 20 µl. The ligation mixtures were incubated at 18°C over night prior to the transformation in competent *E. coli* TOP^{10} cells.

The molecular ratios were estimated via the NEBio calculator v1.9.0 (New England Biolabs, Inc).

The linearized backbone was tested for contamination with undigested plasmid DNA in transforming competent *E. coli* TOP^{10} cells with linearized backbone only. The more colonies occurred, the higher the contamination rate was and the less likely was a successful ligation process.

2.5.7 Ligase Independent Cloning (LIC) of promoter fragments

In this study, LIC was used to integrate the respective promoter fragments in the *Agrobacterium rhizogenes* entry vector pCXUN via a singular *HpaI* restriction site (**Figure 14**, page 63). In a first step the respective promoter fragments were PCR amplified from pJET1.2 with pJET-universal LIC primers (**Table 8**). The obtained promoter fragments were then cloned in the *HpaI*-opened pCXUN vector using LIC (**Figure 4**). Secondly, both insert and vector were treated with T4-DNA polymerase prior to an annealing step. To generate the mentioned compatible sticky overhangs, the "*HpaI* linearized vector backbone" mix was treated with dCTP, whereas the "insert mix" was treated with dGTP (**Table 9**). Incubation time was 2 h at 22°C, after which the T4-Polymerase was heat inactivated at 75°C for 20 min. After the T4-Polymerase treatment, vector and insert fragments were mixed for annealing in a ratio of 5:1, corresponding to 2.5 µg vector DNA and 0.5 µg insert DNA. Therefore, the samples were incubated at RT for 2 h and chilled on ice for 20 min prior to the transformation into chemically competent Top^{10} *E. coli* cells.

Table 8. Primers used to universally amplify fragments from the pJET1.2 vector with LIC overhangs. Primers were obtained from Sigma-Aldrich Corporation, St. Louis, USA. The LIC adapters in the primer sequence are highlighted in bold.

Primer name	LIC primer sequence	Tm (°C)	Used for template orientation in pJET1.2
pJetUnivLIC_rR1	**TTATGGAGTTGGGTT**--CGAACTGAGAATATTGTAGGAGATCTTCTAGA	71.2	5´- 3´
pJetUnivLic_F1	**TAGTTGGAATGGGTT**--CGAATGGCTCGAGTTTTTCAGC	70.6	5´- 3´
pJetUnivLIC_R1	**TAGTTGGAATGGGTT**--CGAATGAGAATATTGTAGGAGATCTTCTAGA	70.3	3´- 5´
pJetUnivLic_rF1	TTATGGAGTTGGGTT--CGAACTGGCTCGAGTTTTTCAGCA	71.6	3´- 5´

Table 9. LIC T4-DNA Polymerase treatment mixtures for the vector and insert. Given are the ingredients and their concentration in both the vector- and insert mixture.

Vector - Polymerase treatment mixture	Ingredient	Fragment/Insert - Polymerase treatment mixture
2.5 µg	DNA	500 ng
2 µl	NEB buffer 2	2 µl
0.5 µl dCTP	100 mM	0.5 µl dGTP
1 µl	100mM DTT	1 µl
0.2 µl	100x BSA	0.2 µl
15 U	T4-DNA-Polymerase	3 U
	H_2O_{dd} up to a total of 20 µl	

2.6 Lab protocols

2.6.1 *Extraction of genomic DNA from Populus tremula x tremuloides*

Fresh poplar leaves were harvested, wrapped in aluminium foil, and directly frozen in liquid nitrogen at -80°C. To purify the gDNA from the plant tissue, 2.5 ml 2 x CTAB isolation buffer (**Table 10**) were preheated to 60°C. Meanwhile, 0.5 g of the frozen leave tissue were grinded under liquid nitrogen using mortar and pestle to mechanically break up the cell walls. The frozen leave powder was then transferred to a new mortar, to which the preheated CTAB isolation buffer was added stepwise under stirring. The obtained solution was equally distributed in three 2.2 ml reaction tubes using a wide - bore pipette tip. To extract the gDNA, the cups containing the grinded leave powder and CTAB - buffer mix were incubated at 60°C for 30 minutes and gently swirled every 10 minutes during this incubation time. To extract nucleic acids, 0.6 ml of a mix containing chloroform and isoamyl alcohol in a ratio of 24:1 was added directly after the incubation and the samples were mixed for 5 seconds. The DNA was now located in the aqueous phase and could be separated from the rest by centrifuging the samples at 13000 rpm for 10 minutes at room temperature (RT). The aqueous phase was then slowly transferred in a new 1.5 ml Reaction tube and gently mixed with two thirds 4°C cold isopropanol to precipitate nucleic acids. After 10 minutes of incubation time on ice, the samples were centrifuged at 13000 rpm for 10 minutes at RT to pellet the precipitated DNA. The supernatant was therefore discarded carefully. The pellets were then washed with 0.6 ml wash-buffer. Therefore, the cups containing the DNA pellet and the wash-buffer were gently swirled for 20 minutes, followed by a centrifugation step at 13000 rpm for 5 minutes. After discarding the supernatant completely with a pipette, the pellets were air dried for approximately 3 minutes and then resolved in 150 µl TE-buffer (pH of 7.5), containing RNase with a concentration of 10 µg per ml. To completely solve the pellet, the samples were incubated 5 min at RT, 5 min at 50°C and again 5 min at RT, during which the cups were gently flicked in every few minutes. Next, the samples were incubated at 37°C for 30 minutes.

To further concentrate and de-salt the nucleic acids in this aqueous solution, a Lithium chloride precipitation (LiCl) was performed. The volume of the samples was mixed with 1/10 4 M LiCl and 2 volumes of 100 % Ethanol. The liquids were mixed by flicking the cups carefully and then incubated at RT for 1 hour. During this process, the salt in the samples was bound to the negatively charged DNA phosphate backbone of the DNA, causing the DNA to precipitate. The samples were then centrifuged for 10 minutes at 13000 rpm and RT and the supernatant was discarded. To remove any residual salts the pellet was washed with 500 µl 70% Ethanol, which was added to the samples. Centrifuging at 13000 rpm for 10 min, removing the supernatant and air-drying the pellets removed the Ethanol before resolving the DNA pellet in TE - buffer as described above. The samples were stored in the fridge at 4°C and backup samples were shock frozen in liquid nitrogen and stored at -80°C. The used buffers and solutions for this method are listed in **Table 10**.

Table 10. Buffers and solutions used for the extraction of genomic DNA from *Populus tremula x tremuloides* and *P. trichocarpa* leaves.

Solution	Ingredient	Final concentration	
CTAB isolation buffer	Cetyltrimethylammonium bromide (CTAB)	2 %	
	Sodium chloride (NaCl), autoclaved	1.4 M	
	0.5 M Ethylenediaminetetraacetic acid (EDTA) solution	100 mM	Autoclaved and adjusted to pH 8.0 with NaOH.
	1 M Tris(hydroxymethyl) aminomethane hydrochloride (Tris-HCl)	100 mM	Acts as a buffer to stabilize the pH, autoclaved. Adjusted to pH 8 with HCL.
	β-mercaptoethanol ($HOCH_2CH_2SH$)	0.2 %	
TE - buffer	Tris(hydroxymethyl) aminomethane hydrochloride, 2-Amino-2-(hydroxymethyl)-1, 3-propanediol solution (Tris-HCl)	10 mM	Acts as a buffer to stabilize the pH-value. Adjusted pH-value to 7.5 with HCL and autoclaved.
	EDTA	1 mM	Autoclaved and adjusted to pH 7.5 with NaOH.
	Bidestilled water (ddH_2O)		Filled up to final volume
Wash buffer	Ethanol (C_2H_6O)	76 %	
	Ammonium acetate (CH_3COONH_4)	10 mM	

2.6.2 Polymerase chain reaction (PCR)

The PCR was used to amplify promoter fragments and CDS from gDNA of the respective genes from the poplar hybrids *Populus tremula x tremuloides* and *P. trichocarpa*. Furthermore, the CDS of the three genes was PCR amplified from RNA obtained cDNA of non – mycorrhized fine roots. PCR was also used to amplify certain fragments with restriction site overhangs from pJET1.2 to allow sticky end cloning of the desired constructs.

PCR - primers were designed *in silico* using the Geneious version 7.1.19 software. Oligonucleotide primers generally had a length of 20 – 40 nucleotides and a G-C content of 40 – 60%. Fitting annealing temperatures were calculated online with the NEB Tm calculator v1.9.12 (New England Biolabs Inc). To ascertain the annealing temperature where the polymerase worked best, temperature gradients were performed for each of the approaches.

The PCRs was executed with Biometra TGradient Thermoblock (Biometra GmbH, Göttingen, Germany) using the Q5 Polymerase (**Table 11**).

Each experimental approach was performed in a total volume 25 µl, containing 10 ng of gDNA, 1 x concentrated Q5 buffer solution, 200 µM of each dNTP, 0.5 µm of each Primer and 0.6 U Q5 DNA Polymerase, filled up to the final volume with ddH_2O. The ingredients were mixed on ice in small PCR - reaction tubes. The PCR machine was preheated before usage to increase the efficiency of the polymerase with a "hot-start". For each approach, a negative control containing no template was made. The obtained PCR products were blunt ended and dephosphorylated. Based on their purity they could either be cleaned up directly with a column or had to be gel-purified beforehand.

Table 11. Steps of a Polymerase Chain Reaction (PCR). Steps 2 to 4 were repeated for 35 times in each case.

Step		**Temperature (°C)**	**Time (seconds)**
1	Initialization	98	30
2	Denaturation	98	10
3	Annealing	Sample dependent	30
4	Extension/elongation	72	90
5	Final elongation	72	600
6	Final hold	4	Indefinite time
7	Storage	-20	Indefinite time

Table 12. Ingredients of a PCR reaction sample with the given final concentrations.

Ingredient	**Concentration in final volume**
Nuclease free water	Added up to a final volume of 25 µl
Q5 buffer	1x
dNTP Mix	200 µM of each dNTP
Forward Primer	0.5 µM
Reverse Primer	0.5 µM
Template DNA	50 – 250 ng genomic DNA or 1 pg – 10 ng plasmid DNA
DMSO (optional)	3 %
Q5 DNA Polymerase	0.6 U

2.6.3 Agarose gel electrophoresis (Sambrook et al., 1989)

Analytical agarose electrophoresis gels were prepared with a 1 % agarose gel in 0.5 x TAE buffer (**Table 13**). The agar was completely solved in a microwave at maximum power for approximately 2 minutes. When cooled down at RT to about 75°C, 30 – 60 ml of the liquid agar were poured into a gel chamber and a comb was added.

After loading, the gel was run at 80 V for approximately 40 min. Preparative gels were run at 60 V to avoid the degradation of sticky ends for further cloning steps.

DNA bands were visualized by incubating the gels for 20 minutes in a 4.23 µM Ethidium-bromide (EtBr) bath, a fluorescent protein that intercalates into double stranded DNA and shows an orange colour when exposed to UV light. The more DNA is present in a band, the higher is the given intensity of the fluorescence, allowing a densitometric quantification of DNA amounts in comparison to the intensity of the loaded marker (marker description in chapter 2.6.4).

Pictures of the stained gels were made on a documentation desk with a camera system and a UV light source and optimized in adjusting the zoom and UV light exposure time (UV desk 312 nm, Pharmacia LKB Biotechnology AB, Uppsala, Sweden combined with a Doc Print II PEQLAB Biotechnologie GmbH, Erlangen, Germany).

DNA bands for clean – up and further cloning were cut out mechanically with a scalpel under a weak UV lamp (312 nm; HL-6-KM; H. Saur, 72770 Reutlingen, Germany). The obtained agarose gel slices containing the correct fragments were transferred to 2.2 ml Reaction tubes and re-extracted using a gel clean-up kit (kit description see page 33). Obtained DNA fragments were stored at -80°C until further usage.

Table 13. Receipt for a 50x TAE stock solution, which is diluted 0.5 x prior to agarose gel electrophoresis and used as liquid conductor in the gel chambers.

Ingredient	Final Concentration	Properties
Tris-aminomethane (TRIS base)	2 M	
Glacial acetic acid	1 M	
Ethylenediaminetetraacetic acid (EDTA)	0.1 M	pH was adjusted to 8 with 10 M NaOH, autoclaved.

2.6.4 DNA quantification methods

The amount of DNA in each sample was either estimated **(1)** photometrically (Nano DropTM DN1000, PEQLAB Biotechnologie GmbH, Erlangen, Germany) or **(2)** densitometrically with ImageJ 1.50i and per eye, using different dilution series of both the sample and the corresponding marker bands in a gel electrophoresis.

To densitometrically estimate the amount of DNA in the loaded samples, 0.5, 1 and 1.5 µl of each plasmid sample or PCR product were loaded on the gel in a total volume of 6 µl with loading dye and ddH_2O. Additionally, three different concentrations (1.5, 3 and 6 µl) of marker DNA. Based on their characteristics three different markers were used: Phage Lambda DNA/Eco130I (StyI) DNA ladder (421- 19329 bp, Bioron, Ludwigshafen am Rhein, Germany), a Gene Ruler 100 bp plus DNA ladder (Thermo Fisher Scientific, Waltham, MA, USA) or the Quick – Load 1 kb plus DNA ladder (New England BioLabs Inc., Frankfurt am Main, Germany) were loaded next to the DNA samples. DNA amounts were estimated in comparing band fluorescence intensities from the defined marker and the unknown DNA sample.

2.6.5 Cloning of PCR fragments in the pJET 1.2 vector

PCR products were either directly cloned in pJet1.2 or cleaned up prior to the cloning step with a kit based on the PCR quality and purity.

Since the generated PCR fragments had dephosphorylated blunt ends, the pJET1.2 cloning kit could be used for easy integration in the pJET1.2 vector. The vector of this kit selected for successful transformation events via a lethal gene fragment that is only active in empty vectors. Furthermore, inserts could easily be verified using two multiple cloning sites to the right and the left of an integrated insert. The different ligation and transformation steps in chemically competent *Escherichia coli* Top^{10} cells were executed according to the recipe in the cloning kit.

2.6.6 Chemical competent Escherichia coli cells

Chemically competent *E. coli* TOP^{10} cells were obtained with an adjusted version of the Rubidium chloride ($RbCl_2$) method (Hanahan, 1983).

In a first step, 3 ml of liquid LB medium (**Table 16**) were inoculated with *E. coli* TOP^{10} cells overnight under agitation at 37°C (160 rpm). 500 µl of this pre-culture were used to inoculate 50 ml of fresh LB medium in a 100 ml flask to synchronize the growth rate of individual cells. This culture was incubated at 37°C under agitation until an optical density (OD_{600}) of 0.4 was reached, corresponding to an optimal growth phase of the cells. At this point the cells were put on ice for 15 min before spinning them down at 2000 xg and 4°C for 15 min. The obtained bacterial pellet was re-suspended in 18 ml of cold RF1 (**Table 14**) and incubated on ice for 30 minutes before again spinning down the cells as before. The supernatant was discarded and the chemically treated bacterial pellet resolved in 4 ml of RF2 (**Table 15**). In a final step, 100 µl aliquots of the new competent cells were prepared, shock frozen in liquid nitrogen and stored at -80°C for later usage. The cells were stored for a maximum time of 3 month before replacement due to loss of transformation efficiency.

Table 14. Ingredients of RF1 for plasmid isolation of *Escherichia coli* using the Rubidium chloride method following Hanahan, 1938. After mixing the ingredients the pH-value was adjusted to 5.8 with glacial acetic acid and the solution was autoclaved and stored at 4°C.

Ingredient	Concentration
Potassium acetate (KCH_3COO)	0.03 M
Rubidium chloride ($RbCl_2$)	0.01 M
Calcium chloride ($CaCl_2$)	0.01 M
Manganese chloride ($MnCl_2$)	0.05 M
Glycerol ($C_3H_8O_3$)	15 %

Table 15. Ingredients of RF2 for plasmid isolation of *Escherichia coli* using the Rubidium chloride method following (Hanahan, 1983). The pH of RF2 was adjusted to 6.5 with KOH after mixing the ingredients. The final solution was autoclaved and stored at 4°C.

Ingredient	Concentration
3-(*N*-morpholino) propane sulfonic acid (MOPS)	0.01 M
Rubidium chloride ($RbCl_2$)	0.01 M
Calcium chloride ($CaCl_2$)	0.075 M
Glycerol ($C_3H_8O_3$)	15 %

Table 16. Ingredients and their final concentrations in LB-Medium (Luria – Bertani; Sambrook, Fritsch, and Maniatis 1989). After mixing the ingredients the Medium was autoclaved. For agar plates 1.8 % agarose were added prior to autoclaving. Media were made selective in adding 100 µg/L Ampicillin or 50 µg/L Kanamycin (final concentrations). Medium purity was equal "pro analysi".

Ingredient	Final concentration
Sodium chloride (NaCl)	5 g/L
Peptone	15 g/L
Yeast extract	5 g/L

2.6.7 Transformation of chemically competent E. coli

For the transformation of chemically competent *E. coli* TOP^{10} cells, 100 µl of the competent cells were defrosted on ice and mixed with a pre-mixture composed of 1 x KCM (**Table 17**) and the desired plasmid or ligation mixture (1 - 20 µl), filled up to a volume of 100 µl with ddH_2O. After adding together, this sample was well mixed and incubated on ice for 20 minutes, followed by a heat shock at 42°C for 2 minutes. Immediately afterwards, 700 µl of non-selective LB medium were added, followed by an incubation step at 37°C for 60 minutes under agitation. The cells were then carefully spun down (2 minutes at 5000 x g). 600 µl of the supernatant were removed and the bacterial pellet resolved in the remaining 100 µl for plating on selective agar plates, allowing only transformed cells to grow. The plates were then incubated over night at 37°C and stored in the fridge at 4°C when colonies were formed.

The competence of the obtained cells varied between 2 x 10^7 and 1 x 10^8 CFU/µg.

Table 17. Ingredients and their concentrations used for a 5 - fold concentrated KCM solution.

Ingredient	Final concentration
Potassium chloride (KCL)	500 mM
Calcium chloride ($CaCl_2$)	150 mM
Magnesium chloride ($MgCl_2$)	250 mM

2.6.8 Plasmid isolation from E. coli using the Alkaline Lysis Method

Plasmids were isolated from saturated 3 ml selective LB-medium overnight cultures (18 h at 37°C, agitation at 140 rpm, single colony per culture). The following steps describe the treatment of one individual sample. The cells of the overnight culture were harvested in transferring 1.8 ml to a 2.2 ml Reaction tube and spinning the cells down with a centrifuge for 5 minutes at 8000 xg and RT. The bacterial pellet was then resolved in adding 300 µl Solution 1 and mixing the sample thoroughly for 20 seconds (**Table 18**). This step helped destabilizing the cell wall, prevented DNases from damaging the cell wall, degraded cellular RNA and maintained the osmotic pressure for the cells not to burst yet. In a next step, 300 µl of Solution 2 (**Table 19**) were added and the sample was inverted for 8 times. Solution 2 is a lysis buffer that solubized and broke down the cell wall and disrupted hydrogen bonding between the DNA bases and many proteins to denaturize in the cell and converted all double-stranded DNA to single-stranded DNA. After an incubation time of 5 min at RT, 200 µl of ice-cold Solution 3 (**Table 20**) were added and the sample was again inverted for 5 - 6 times, followed by a 30 min incubation time on ice. During the incubation, the alkalinity of the mixture decreased, and the plasmid DNA could form double bands again, whereas genomic DNA, SDS and denaturised cellular proteins stacked together in large particles because of hydrophobic interactions.

The plasmid DNA could therefore be separated from the rest with a centrifugation step at 16000 xg for 20 min and 4°C, allowing to transfer the supernatant containing the desired plasmid DNA to a new 1.5 ml Reaction tube. The plasmid DNA was precipitated in adding 500 µl of 100 % isopropanol, mixing thoroughly and incubating on ice or 10 minutes. Centrifuging the sample 30 min at 16000 x g and RT pelleted the precipitated DNA, which was then washed in adding 500 µl of 70 % EtOH, inverting 5-6 times and again centrifuging at 16000 xg for 10 min at RT. The supernatant was completely removed with a pipette and the pellet air dried to remove the remaining alcohol. Alternatively, the pellet was dried for 5 min in a heating block of 50°C with an open lid. In a last step, the pellet was resolved in 20 µl of 5 mM Tris-HCL, which was adjusted to a pH-value of 8. The resolving steps included a 5 min incubation time at RT with mixing, 15 minutes of incubation at 50°C and a short spin down step with a centrifuge for 30 sec. The obtained plasmid DNA was long-term stored at -20°C.

In most cases a LiCl precipitation was performed to further concentrate and de-salt the nucleic acids in the aqueous solution. Therefore, the volume of the samples was mixed with 1/10 volume LiCl. Immediately 2 volumes of 100 % Ethanol were added, and the sample again was mixed by flicking the cup and incubated at RT for 1 hour. During this process, the DNA precipitated because the salt bound to the negatively charged DNA phosphate backbone. The samples were then centrifuged for 10 min at 13000 rpm and RT and the supernatant was discarded. To remove any residual salts the pellet was washed with 500 µl 70 % Ethanol. After the 70 % Ethanol was added, the samples were again centrifuged at 13000 rpm for 5 min. In a last step, the supernatant was completely removed, air-dried, and again resolved in 20 µl 5 mM Tris-HCL with a pH of 8 as described before. The samples were long-time stored at -20°C.

Table 18. Ingredients and their final concentrations of Solution 1 for plasmid isolation from bacterial *E. coli* cells via alkaline lysis. The solution was stored at 4°C.

Ingredient	Final concentration
Tris-aminomethane hydrochloride (Tris-HCL), adjusted to pH 7.5, autoclaved	0.1 M
Ethylenediaminetetraacetic acid (EDTA), adjusted to pH 8 with NaOH and autoclaved	0.05 M
RNase A	100 mg/L
ddH$_2$O	Filled up to final volume

Table 19. Ingredients and their final concentrations of Solution 2 for plasmid isolation from *E. coli* cells via alkaline lysis.

Ingredient	Concentration in total volume
Sodium hydroxide (NaOH)	0.2 M
Sodium dodecyl sulphate (SDS)	1 %
ddH_2O	Fill up to final volume

Table 20. Ingredients and their final concentrations of Solution 3 for plasmid isolation from *E. coli* cells via alkaline lysis. The pH was adjusted to 4.8 using acetic acid. The solution was stored at 4°C. Final concentration = 375 mM)

Ingredient	Concentration in total volume
Potassium acetate	1.5 M
ddH_2O	Filled up to final volume

1.1.12 Restriction digestion

Restriction digestion was used to verify cloned plasmids. The recipe for the individual restriction digestions varied regarding different enzyme and DNA concentrations of the respective samples. Generally, 1 µg plasmid DNA, 1 x enzyme dependent buffer, 10 U endonuclease enzyme and ddH_2O were mixed in a total volume of 20 µl and incubated for 3 h at the enzyme dependent temperature. If possible, the enzymes were heat inactivated in a heating block prior to further steps. Mostly the digestions were followed by an analytical gel electrophoresis or a preparative gel electrophoresis, followed by a densitometrical quantification of DNA amounts.

2.6.9 Sanger Sequencing

500 ng of plasmid DNA, 50 pm primer and ddH_2O in a total volume of 10 µl were sent to the sequencing company Macrogen Europe (Meibergdreef 31, 1105 AZ Amsterdam-Zuidoost, Niederlande) for Sanger Sequencing. Used primers for sequencing are listed in **Table 21**.

In dependence of the direction of sequencing, the sequencing results get worse towards the end because of the distance to the start.

Table 21. Description of primers that were used for Sanger sequencing. Given are the primer name, Primer sequence, Orientation of sequencing and the vector backbone it could be used for.

Primer name	Primer sequence	Sequencing orientation	Used for vector
M13 rev	GGAAACAGCTATGACCATG	3´ to 5´	pPLV and pCXUN
M13 seq	GTAAAACGACGGCCAGTG	5´ to 3´	pPLV and pCXUN
sYFP seq	GGTGCAGATCAGCTTCAGG	3´ to 5´	pPLV and pCXUN
pJET1.2 for	GCCTGAACACCATATCCATCC	5´ to 3´	pJET1.2
pJET1.2 rev	GCAGCTGAGAATATTGTAGGAGATC	3´ to 5´	pJET1.2

2.6.10 Glycerol stocks

Glycerol stocks were prepared in mixing 600 µl of a saturated bacterial overnight culture containing the desired construct with the appropriate selective antibiotics and 600 µl of 100 % glycerol in small plastic tubes under sterile conditions. The cups were well mixed, shock frozen in liquid nitrogen and long-term stored at -80°C.

2.6.11 In silico cloning

In silico cloning was performed prior to actual cloning steps. All the constructs were created, verified, and proofed with Geneious 7.1.19, a tool to edit and wok with gene fragments and nucleic acids. For further visualizations, Geneious Prime® 2021.1.1. was used.

2.6.12 Transformation of Agrobacterium rhizogenes modified from (Holsters et al., 1978)

Finished binary vectors were transformed into chemically competent *Agrobacterium* cells for *in planta* analyses.

Competent cells were stored at -80°C and defrosted on ice prior to the transformation. Then about 1 µg of plasmid DNA was added, and the mixture was incubated on ice for 20 minutes. This step was followed by a 5 - minute incubation in liquid nitrogen and a 5-minute incubation at 37°C to make the cell wall permeable. Immediately after the heat shock, 800 µl of CPY medium (**Table 22**) were added for cell regeneration. The samples were incubated at 28°C under agitation for 4 h to allow for phenotypic expression before harvesting the cells with a centrifuge (4 min at 3000 xg). In a final step, 700 µl of the supernatant were discarded and the pellet was resolved in the remaining 100 µl. The cells were then plated on plasmid selective CPY agar plates and stored at 28°C for 2 - 4 days. One of the transformed colonies was further used for the plant transformation steps.

Table 22. Ingredients and their final concentrations of CPY medium used for Agrobacteria cultivation. Cells containing the desired plasmids were selected in adding 0.1 mM kanamycin and in some cases tetracycline after autoclaving the ingredients. For CPY plates 1.5 % agar was added prior to autoclaving. Rifampicin was added additionally to kanamycin to minimize contamination with other bacteria when cells were reactivated from glycerol stocks. The purity of the components was equal “pro analysi”.

Ingredient	Final concentration
Peptone	0.5 % (w/v)
Saccharose	14.6 mM
Yeast extract	0.1 % (w/v)
Magnesium sulphate heptahydrate ($MgSO_4$ x $7H_2O$)	2.03 mM

2.6.13 Chemical competent Agrobacteria

Agrobacterium cells were made chemically competent in pelleting a 10 ml saturated overnight culture (in selective medium at 140 rpm and 28°C under aerobe conditions) of the empty strain in CPY medium for 5 minutes at 4000 rpm (**Table 22**). This pre-culture contained tetracycline in the presence of the pSOUP plasmid and was used to inoculate 500 ml of fresh CPY medium up to a starting OD_{600} of 0.1. The obtained cell suspension was incubated at 28°C and 140 rpm until an OD_{600} of 0.8 was reached. Cells were then harvested in spinning them down at 5000 rpm (3210 xg) and 4°C for 5 min. The supernatant was discarded, and the bacterial pellet resolved in 10 ml 0.15 M NaCl, followed by another centrifugation step at 5000 rpm for 5 min at 4°C. Afterwards, the supernatant was again discarded, and the bacterial pellet resolved in 1 ml of 20 mM $CaCl_2$ and aliquoted in 100 µl volumes. The tubes containing the cells were always kept on ice In between the centrifugation steps. In a last step the cells were shock-frozen in liquid nitrogen and kept at -80°C for up to six months for storage.

2.6.14 Subcellular localization of proteins in Nicotiana benthamiana leaves

Subcellular localization was performed via tobacco leave infiltration with *A. tumefaciens* strain C58. Therefore, one overnight culture of each to be tested construct as well as a plasma membrane marker (PM) were prepared in 10 ml kanamycin selective CPY medium (24 h, 28°C 140 rpm, aerobe conditions). Strains containing the helper plasmid pSOUP were additionally treated with tetracycline. All cultures were prepared from fresh glycerol stocks to avoid recombination of the cells on the plates. After 24 h the cells were spun down at 4.000 rpm for 20 min at RT. The supernatant was discarded whereas cell pellet was re-suspended in 2 ml of activation medium (**Table 23**) The OD_{600} of the re-suspended cells was measured and it was calculated, how much of the construct had to be added to a final volume of 9 ml activation medium to be present in an OD_{600} of 0.3, 0,03 or 0,003.

After an activation of the bacteria for 2 h at 28°C under agitation (140 rpm), the cell suspension was transferred into a syringe to pressure infiltrate the complete bottom side of *N. benthamiana* leaves through the stomata. Furthermore, each leave contained a control spot, where an empty construct was infiltrated as a reference for the transformation efficiency.

After three days of incubation time (22°C and 12 h light per day) the infiltrated leaves were reviewed with a stereomicroscope to identify tissue regions showing DsRED and/or sYFP signals. Such identified leave sections were cut out with a scalpel and viewed under a confocal laser-scanning microscope.

Table 23. Ingredients and their final concentration of Activation medium for tobacco leave infiltration with *Agrobacterium tumefaciens*.

Ingredient	Final concentration
2-(*N*-morpholino) ethane sulfonic acid (MES), adjusted to a pH of 6 with KOH, sterile filtrated and stored in the dark.	10 mM
Magnesium chloride, autoclaved	10 mM
Acetosyringone, sterile filtrated	150 µM
ddH₂O, autoclaved	Added up to total volume

2.6.15 Transformation of Populus alba and P. tremula x tremuloides: Composite plants

Poplar shoots of *Populus tremula x alba* or *Populus tremula x tremuloides* were transformed via infection with a transgenic *Agrobacterium rhizogenes* strain K599.

Therefore, shoots containing two or three leaves were removed from a sterile culture plant under sterile conditions with a heat-sterilized scalpel. The size of the shoot tips had to be relatively small to avoid high transpiration rates and lignification of the shoot-stems. The cutting site of the shoot tips was then “dipped” in the previously transformed *A. rhizogenes* culture. Bacterial *Agrobacterium* cultures were grown on a selective CPY plate (**Table 22**). Furthermore, the empty *Agrobacterium* strain was used as a negative control concerning autofluorescence.

The infected shoots were then cultivated in petri dishes containing MS6 medium (**Table 24**) and incubated for 3 days at 22°C and a day and night rhythm of 16 h (48 µmol photons m^2s_{-1}) in an upright position. To be able to place the shoots in the petri dishes, the MS6 agar plates were cut in half beforehand and half of the agar was removed. The shoots were placed in the medium in such a manner, that the stem was in the agar and the leaves were in the space where half of the agar was removed.

After three days the poplar shoots were transferred to another set of petri dished containing MS6 medium with a mixture of Cefotaxime (0.52 mM) and Carbenicillin (1.18 mM) to kill any remaining living agrobacteria. The shoots were grown under these conditions until the first fine roots became visible for observation under the epifluorescence microscope.

Plants that were selected for the preparation of root sections (see chapter below) were later placed on medium plates with a thin foil between the agarose and the formed roots to facilitate the process of separating the roots.

Table 24. Ingredients and their final concentrations of MS6 medium (Murashige and Skoog, 1962) . The purity of the components was equal “pro analysi”. The pH – value was adjusted to 5.6 with KOH prior to autoclaving.

Ingredient	Final concentration
***MS salts* including vitamins**	0.22 % (w/v)
Sucrose	29.2 mM
Agar	8 % (w/v)

2.6.16 Mycorrhization of transformed poplar fine roots

The mycorrhization process combines **(1)** pre – grown three-week-old composite plants with **(2)** pre – grown fungal tissue.

In step **(1)** the composite plants are prepared as described in chapter 2.6.15, except that only 6.7 % of agarose concentration in the growth medium.

(2) Fungal stocks were grown on modified Melin Norkrans Medium (MMN) plates containing 50 mM glucose. Fungal tissue for mycorrhization was prepared in square petri dishes containing MMN medium with 10 mM glucose. The medium was then covered with a thin layer of foil, which was washed in a solution containing 2 % $NaHCO_3$ and 1mM EDTA prior to autoclaving. Small square parts of the fungal mycelium were harvested from a stock plate and spotted on the foil. Thus prepared, the fungal parts were pre – grown on the foil for two to three weeks.

For mycorrhization, square MMN plates containing 10 mM glucose and 1/5 N were prepared (**Table 25**). Half of the plate was removed under sterile conditions. The remaining agar was completely covered with a foil spotted with pre – grown fungal tissue. In a next step, three to four plants were added in such a way, that the root system was placed on the agarose with the foil and the shoot had space to grow in the empty half of the plate. The agarose – foil – fungus – root part was then covered with a mixture of sterile, pre – soaked (with liquid MMN medium) vermiculite, clay, and coconut fibre as an artificial substrate. Excess water was prevented by adding sterile cotton rolls before closing the system with adhesive tape. The mycorrhization event was observed after approximately three months (22°C, 16 h of light a day with 48 µmol photons $m^{-2} s^{-1}$). Mycorrhiza were then harvested by Uwe Nehls under a binocular using forceps. The material was then directly cut and prepared for the cLSM as described above.

Table 25. Ingredients of MMN medium (Kottke and Oberwinkler, 1987). Given are the ingredients and final concentration of 10 mM/50 mM glucose MMN medium as used for the pre – culturing of fungi for mycorrhization as well as the MMN 1/5 N for the mycorrhization plates. The purity of the components was equal "pro analysi".

Ingredient	**Final concentration (mg/L)**	**Final concentration (mg/L) with 1/5 N**
Potassium chloride (KCl)	12.28	12.28
Boric acid (H_3BO_3)	15.46	15.46
Manganese(II) sulfate ($MnSO_4$ x H_2O)	8.45	8.45
Zinc sufate ($ZnSO_4$ x 7 H_2O)	5.75	5.75
Copper (II) sulphate ($CuSO_4$ x 5 H_2O)	1.25	1.25
Ammonium molybdate ($(NH_4)_6Mo_7O_{24}$ x 4 H_2O)	0.18	0.18
Sodium chloride (NaCl)	25	25
Monopotassium phosphate (KH_2PO_4)	500	500
Diammonium phosphate ($(NH_4)_2HPO_4$)	250	50
Calcium chloride ($CaCl_2$ x 2 H_2O)	50	50
Magnesium sulphate ($MgSO_4$ x 7 H_2O)	150	150
Iron (III) chloride ($FeCl_3$ x 6 H_2O)	1	1
Potassium phosphate dibasic trihydrate (K_2HPO_4 x 3 H_2O)	0	344.62
For plates: 2% agar		
Added sterile – filtrated after autoclaving		
Glucose	10 mM or 50 mM	10 mM
Thiamine hydrochloride (vitamin B1)	0.1	0.1
Pyridoxin hydrochloride (vitamin B6)	1	1
Myoinositol (1,2,3,4,5,6 Hexahydroxy cyclohexane)	100	100
$C_6H_5NO_2$ (Nicotinic acid)	1	1

3 Results

3.1 Optimizing composite Poplar root transformation efficiencies

3.1.1 Establishing pCXUN as standard plant transformation vector for Composite plants

pBIN19 and pPLV based vectors were used in the lab for the generation of transgenic hybrid plants (Neb, 2017). However, pBIN19 vectors are quite large and only have low copy numbers in *E. coli*, making them overall difficult to handle in terms of cloning and multiplication. pPLV vectors are relatively small and have high copy numbers in *E. coli*, but the number of transgenic roots at hybrid poplars was relatively low. Therefore, a modified pCXUN vector backbone was tested as an alternative for T – DNA integration into the plants. For comparison reasons, different FP cassettes were introduced into both pPLV and pCXUN.

The FP cassettes in pPLV were introduced in collaboration with other members of the working group, except for a tmTomato - SNL construct, which was implemented in this thesis (**Supplementary figure 1**). Some cassettes consisted of two fluorescence expression cassettes in tandem and all were integrated into pCXUN using *PvuII* restriction sites, which exchanged a large part of the T – DNA next to a kanamycin selection cassette (**Figure 9**). In this first approach, the orientation of the integrated cassettes was random (verifications via restriction digestion in **Supplementary figure 2**, Backbone description see **Figure 14** at page 63). An overview of the cloning strategy is given in **Figure 10**.

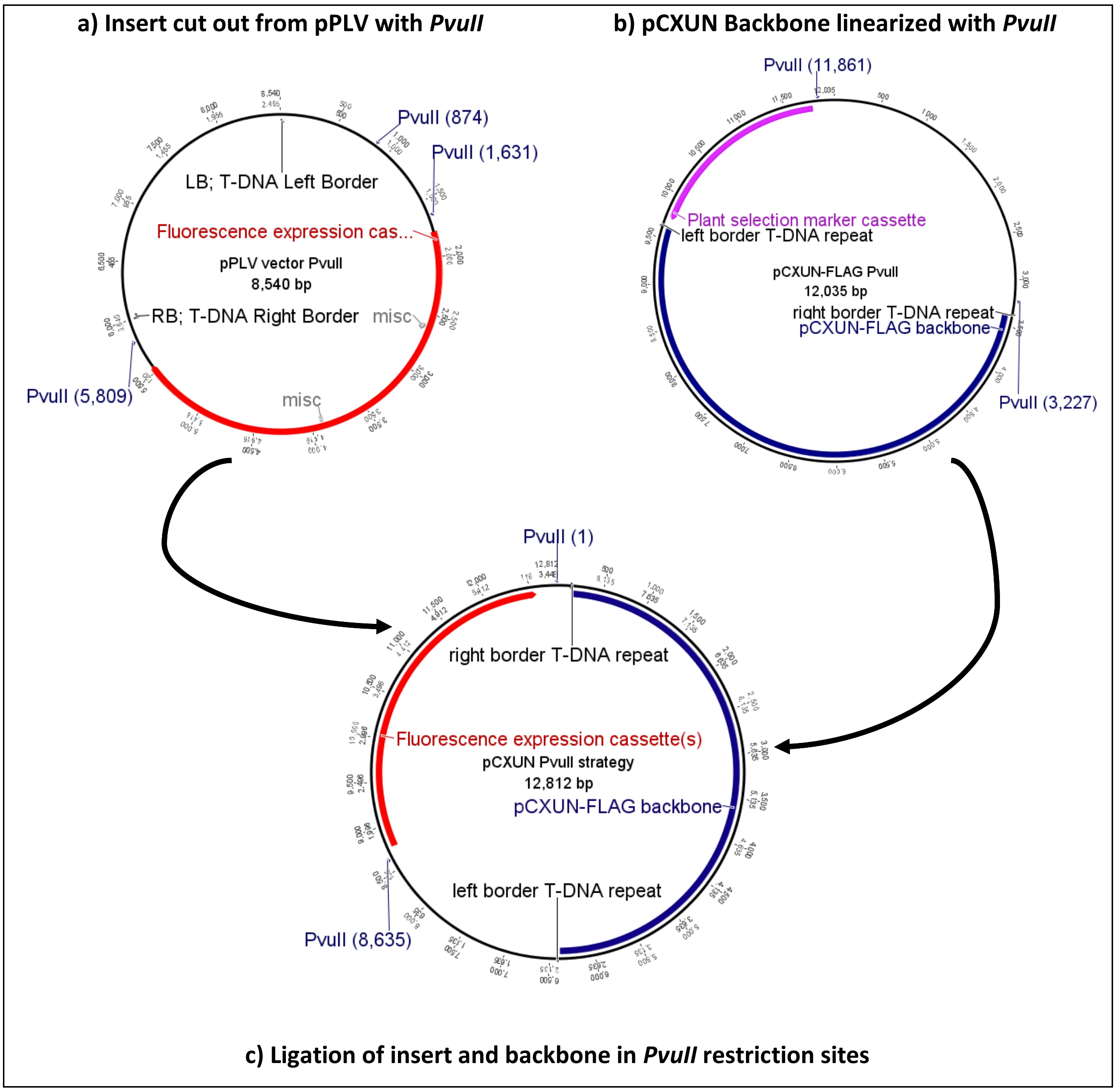

a) Insert cut out from pPLV with *PvuII*

b) pCXUN Backbone linearized with *PvuII*

c) Ligation of insert and backbone in *PvuII* restriction sites

PvuII (874)
PvuII (1,631)
LB; T-DNA Left Border
Fluorescence expression cas...
pPLV vector PvuII
8,540 bp
RB; T-DNA Right Border
misc
misc
PvuII (5,809)
PvuII (11,861)
Plant selection marker cassette
left border T-DNA repeat
pCXUN-FLAG PvuII
12,035 bp
right border T-DNA repeat
pCXUN-FLAG backbone
PvuII (3,227)
PvuII (1)
right border T-DNA repeat
Fluorescence expression cassette(s)
pCXUN PvuII strategy
12,812 bp
pCXUN-FLAG backbone
left border T-DNA repeat
PvuII (8,635)

Figure 9. Schematic display of pCXUN modifications by integrating a large part of a pPLV T – DNA into *PvuII* sites of pCXUN-FLAG. a) Fluorescence expression cassettes were cut out from pPLV with the restriction enzyme *PvuII*. b) The pCXUN-FLAG vector was linearized with PvuII, which cut out a large part of the T – DNA. c) The pCXUN backbone was ligated with the insert from pPLV.

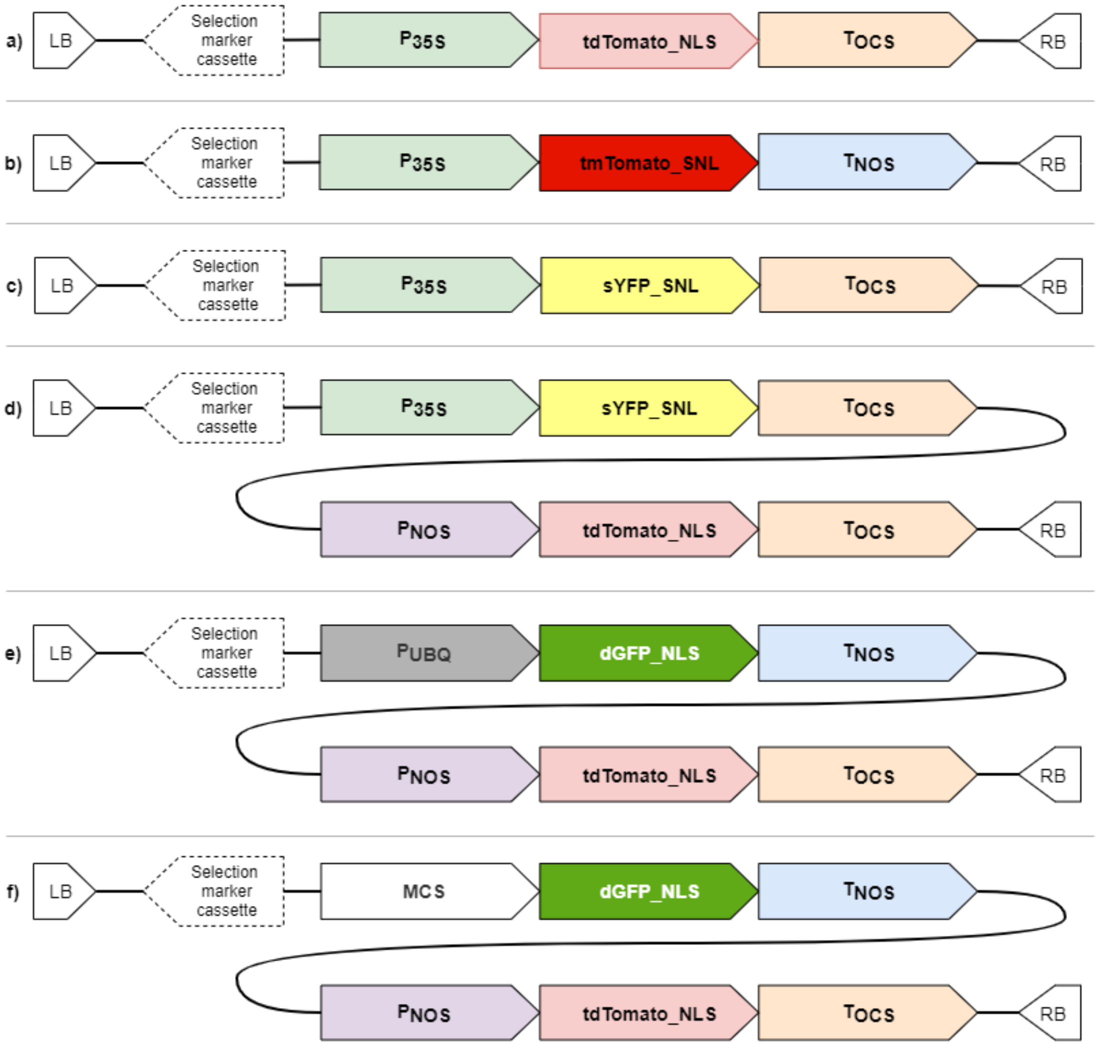
a)
LB
Selection marker cassette
P35S
tdTomato_NLS
TOCS
RB
b)
LB
Selection marker cassette
P35S
tmTomato_SNL
TNOS
RB
c)
LB
Selection marker cassette
P35S
sYFP_SNL
TOCS
RB
d)
LB
Selection marker cassette
P35S
sYFP_SNL
TOCS
PNOS
tdTomato_NLS
TOCS
RB
e)
LB
Selection marker cassette
PUBQ
dGFP_NLS
TNOS
PNOS
tdTomato_NLS
TOCS
RB
f)
LB
Selection marker cassette
MCS
dGFP_NLS
TNOS
PNOS
tdTomato_NLS
TOCS
RB

Figure 10. T – DNA with marker cassettes that were created and cloned into either a pPLV based vector or a pCXUN binary vector to compare transformation efficiencies in composite poplar roots. NLS means the protein has a nuclear targeting signal, SNL means the protein has a peroxisome targeting signal. LB = left border and RB = right border sequence of the T-DNA. Selection marker = a kanamycin resistance cassette for selection of stable plant transformants. n = number of transgenic root systems observed: a) n for pCXUN = 32. b) n for pPLV = 15; n for pCXUN = 19. c) n for pCXUN = 12. d) n for pPLV = 13; n for pCXUN = 42. e) n for pCXUN = 7. f) n for pCXUN = 3. The used promoters and terminators as well as fluorescence proteins are described in the Material and Methods. MSC means Multiple Cloning Site, meaning that the cassette has no promoter. The cassettes point in their orientation in relation to LB and RB.

In addition to such implemented testing cassettes, further constructs were cloned and included in this test as shown in **Figure 11**. The implementation of the *Potri.2G0797* and *Potri.2G2183* promoters is described in the respective chapters.

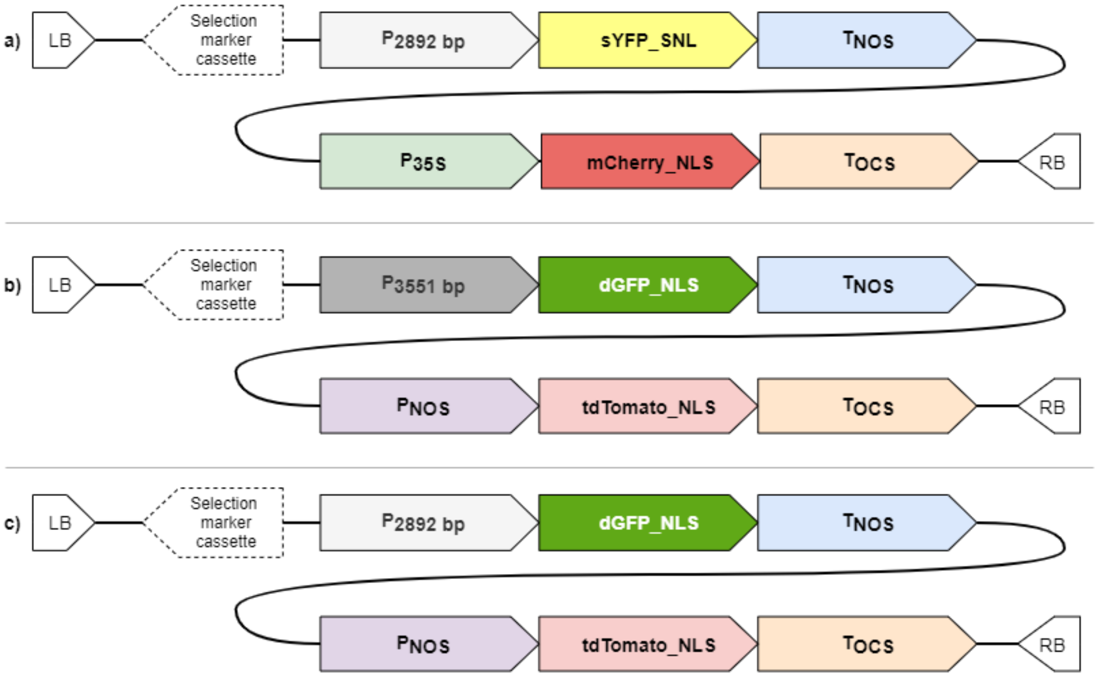
a)
LB
Selection marker cassette
P2892 bp
sYFP_SNL
TNOS
P35S
mCherry_NLS
TOCS
RB
b)
LB
Selection marker cassette
P3551 bp
dGFP_NLS
TNOS
PNOS
tdTomato_NLS
TOCS
RB
c)
LB
Selection marker cassette
P2892 bp
dGFP_NLS
TNOS
PNOS
tdTomato_NLS
TOCS
RB

Figure 11. T-DNA with fluorescence cassettes that were created and cloned into either a pPLV based vector or a pCXUN binary vector to compare transformation efficiencies in composite poplar roots. NLS means the protein has a nuclear targeting signal, SNL means the protein has a peroxisome targeting signal. LB = left border and RB = right border sequence of the T-DNA. Selection marker = a kanamycin resistance cassette for selection of stable plant transformants. n = number of transgenic root systems observed: a) n for pPLV = 11. b) n for pCXUN = 24. c) n for pCXUN = 16. The used promoters and terminators as well as fluorescence proteins are described in the Material and Methods. The $P_{2892\ bp}$ refers to a 2892 bp long promoter region of *Potri.2G0797*. $P_{3551\ bp}$ refers to a 3551 bp long promoter region of *Potri.2G2183*. The cassettes point in their orientation in relation to LB and RB.

Observed and compared were the number of transgenic roots per root system, which is furthermore defined as root transformation efficiency. Depending on the comparisons, obtained transformation efficiencies of all constructs were averaged for different grouping factors. Each construct was investigated in at least two independent transformation experiments.

For comparisons of transformation efficiencies between pPLV and pCXUN, all shown constructs were grouped according to the vector backbone. As a result, pCXUN constructs showed an overall transformation efficiency of 76 % (SE = 2.6; n = 155 plants). Transformation efficiencies with pPLV were significantly lower at 6.2 % (SE = 2.1; n = 39 plants) ($p < 0.001$, Wilcoxon - test, Effect size = 2.8) (**Figure 12**). An example for such a completely transgenic root system is given in **Figure 13**.

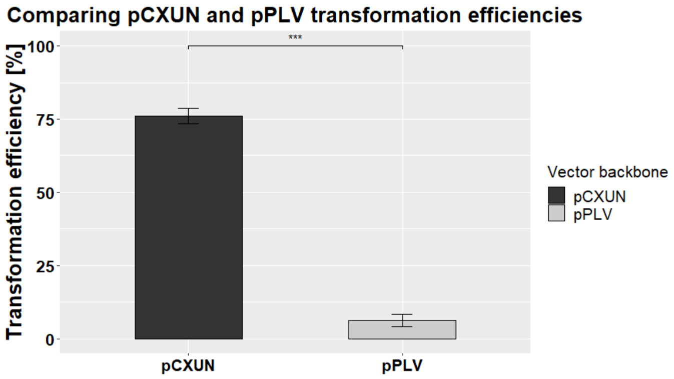

Figure 12. Percentage of transgenic roots formed by poplar cuttings after incubation with transgenic agrobacteria harbouring pPLV or pCXUN based binary vectors with fluorescence protein cassettes. *Populus tremula x alba* cuttings were incubated with *Agrobacterium rhizogenes* strain K599 containing pPLV (n = 39 plants) or pCXUN (n = 155 plants). Thereby, the plants contained different fluorescence cassettes that consisted of either one or two expression cassettes in both orientations on the T – DNA. After four to eight weeks the percentage of fluorescent roots in relation to the total number of roots was determined. Statistics were conducted in R as specified in the M&M.

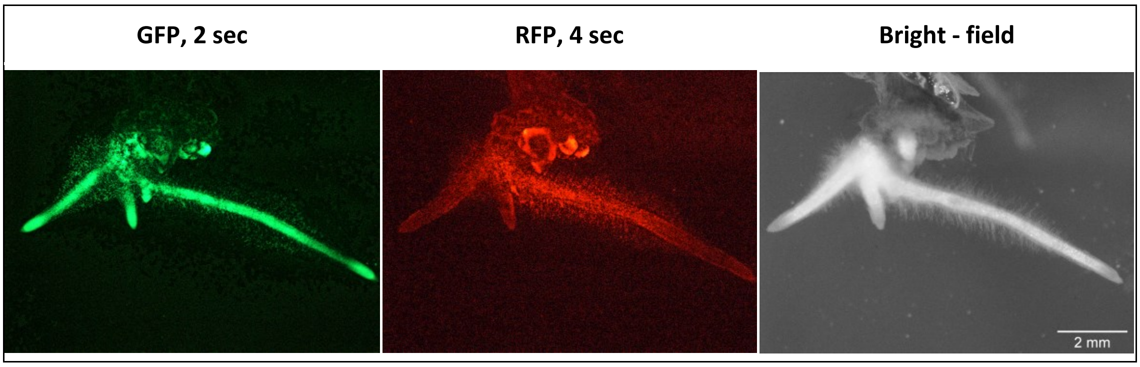

Figure 13. Example for a transgenic poplar root system containing two fluorescence marker constructs. *Populus tremula x tremuloides* composite plants were transformed with a pCXUN binary vector using *Agrobacterium rhizogenes* strain K599. The T – DNA contained two fluorescence marker cassettes which were composed of a 2892 bp promoter fragment of *Potri.2G0797*, GFP-NLS and an NOS terminator as well as a NOS promoter, tdTomato-NLS and an OCS terminator. The 2892 bp promoter was established in this thesis and described in the respective chapters. NLS means the proteins are targeted to the nucleus. Images were taken at a Leica binocular MZ10F with 2 sec illumination time (Leica DFC425C camera, dsRED filters with 510 – 560 nm excitation and 590 – 650 nm emission window filter; GFP filters with 450 – 490 nm excitation and 500 – 550 nm emission window filter). Pictures in different filter settings were taken using the same settings, such as with a gamma correction of 0.99, a colour saturation factor of 1 and a 5x increase in optical power (gain). Additionally, the roots are shown under bright - field conditions. The roots were 3 weeks old. Pictures were processed for better visualization of the fluorescence (contrast enhanced by 0.01 % and background subtracted with ImageJ). Further details about the used devices and image processing are given in the M&M.

Experiments were performed with agrobacteria containing pBIN19/pBI121 plasmids. Similarly, they showed transformation efficiencies between 10 % for pBIN19 (n = 24 plants) and 24 % for pBI121(n = 20 plants) (further data not shown).

Based on these findings, pCXUN was chosen as a base for all further plant transformation vectors. In collaboration with other group members, two vectors were constructed for all further gene analysis. Both contain a green and red expression cassette in tandem on their

T – DNA. One vector contains a P$_{\mathrm{UBQ}}$, which can be exchanged with *KpnI* and *HpaI* restriction sites to integrate promoters for investigation. Alternatively, both expression cassettes can be cut out with *KpnI* and *SacI* restriction sites to integrate cassettes for subcellular localization or overexpression of the genes (**Figure 14**). The second vector has the same construction but misses the P$_{\mathrm{UBQ}}$. This allows for the integration of promoter regions using LIC (**Figure 15**).

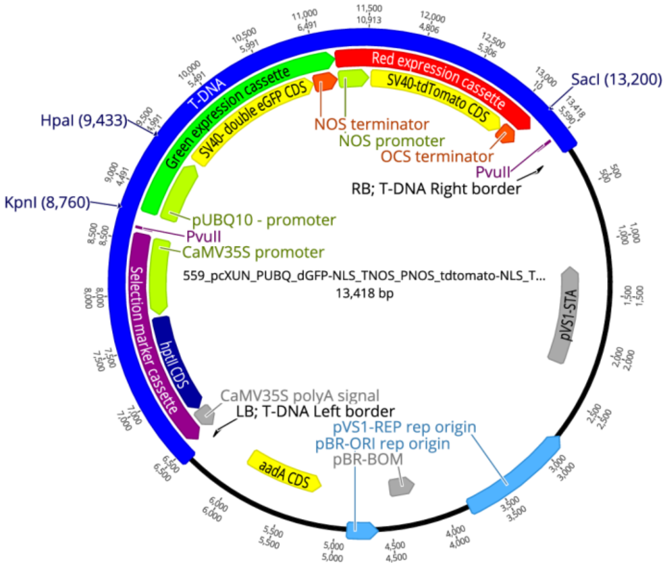
11,000
6,491
11,500
10,913
12,000
4,806
10,500
5,991
12,500
5,306
10,000
5,491
13,000
10
SacI (13,200)
13,418
5,590
T-DNA
Red expression cassette
Green expression cassette
SV40-tdTomato CDS
SV40- double eGFP CDS
HpaI (9,433)
9,500
4,991
NOS terminator
NOS promoter
OCS terminator
PvuII
RB; T-DNA Right border
9,000
4,491
500
500
KpnI (8,760)
pUBQ10 - promoter
PvuII
CaMV35S promoter
8,500
8,500
1,000
1,000
559_pcXUN_PUBQ_dGFP-NLS_TNOS_PNOS_tdtomato-NLS_T...
13,418 bp
8,000
8,000
1,500
1,500
pVS1-STA
Selection marker cassette
hptII CDS
7,500
7,500
2,000
2,000
CaMV35S polyA signal
LB; T-DNA Left border
7,000
7,000
2,500
2,500
pVS1-REP rep origin
pBR-ORI rep origin
pBR-BOM
6,500
6,500
aadA CDS
3,000
3,000
6,000
6,000
3,500
3,500
5,500
5,500
5,000
5,000
4,500
4,500
4,000
4,000

Figure 14. Visual description of the pCXUN vector used for promoter integration based on the *KpnI/HpaI* strategy for promoter analyses, or the exchange of the complete cassette via *KpnI/SacI* from pPLV for subcellular localization studies. The T - DNA was composed of a variable double marker cassette (Green and Red expression cassette) and a hptII CDS Selection marker cassette (kanamycin resistance). The backbone outside of the T – DNA consisted of a pBR-ORI and a pVS1 REP ORI for plasmid stability in *Agrobacteria* as well as a kanamycin resistance cassette (aadA CDS). SV40 codes for a nucleus targeting signal (NLS). For promoter and terminator descriptions see chapter 2.5.1. The red expression cassette was constitutively expressed. Figure was in silico cloned and displayed using Geneious Prime® 2021.1.1**.**

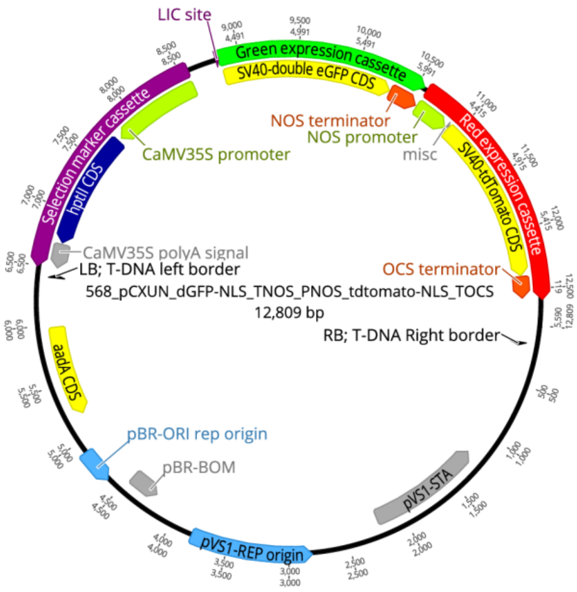
LIC site
Green expression cassette
SV40-double eGFP CDS
NOS terminator
NOS promoter
misc
Red expression cassette
SV40-tdTomato CDS
OCS terminator
RB; T-DNA Right border
CaMV35S promoter
Selection marker cassette
hptII CDS
CaMV35S polyA signal
LB; T-DNA left border
568_pCXUN_dGFP-NLS_TNOS_PNOS_tdtomato-NLS_TOCS
12,809 bp
aadA CDS
pBR-ORI rep origin
pBR-BOM
pVS1-STA
pVS1-REP origin

Figure 15. Visual description of the pCXUN vector used for promoter integration based on LIC. The T - DNA was composed of a green and red expression cassette, a ccdB CDS (for the selection of positive clones) and a hptII CDS selection marker cassette (kanamycin resistance). The backbone outside of the T – DNA consisted of a pBR-ORI and a pVS1 REP ORI for plasmid stability in *Agrobacteria* as well as a kanamycin resistance cassette (aadA CDS). SV40 codes for a nucleus targeting signal (NLS). For promoter and terminator descriptions see chapter 2.5.1. The red expression cassette was constitutively expressed. Promoter fragments were inserted in the green expression cassette using Ligase Independent Cloning (LIC). Figure was in silico cloned and displayed using Geneious Prime® 2021.1.1**.**

3.1.2 Does the orientation of the marker cassettes in the T – DNA impact the transformation efficiency of poplar roots?

First tests with pCXUN as an *Agrobacterium* transformation vector focused on transformation efficiencies. In a second step, impacts of the marker cassette orientation in relation to the right- and left borders on the T - DNA on transformation efficiencies were observed. A schematic overview of the orientations is given in **Figure 16.**

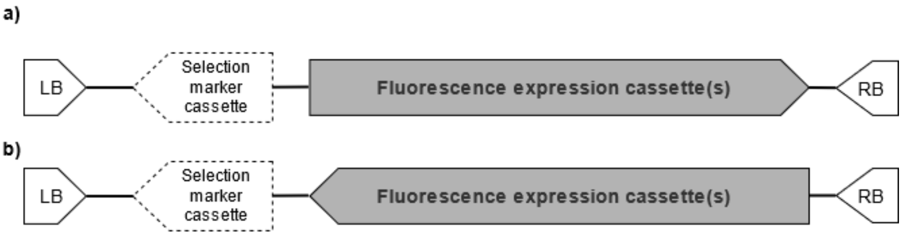
a)
LB
Selection marker cassette
Fluorescence expression cassette(s)
RB
b)
LB
Selection marker cassette
Fluorescence expression cassette(s)
RB

Figure 16. Schematic display of the orientation of fluorescence expression cassettes in relation to left- and right border sequences (LB and RB) and a plant selection marker cassette on the T – DNA in a pCXUN binary vector. a) The fluorescence expression cassette is introduced from LB to RB and b) from RB to LB.

Different pCXUN constructs were grouped according to their orientation on the T – DNA (**Table 26**) and overall average transformation efficiencies of the groups were compared. Thereby, both single and double marker constructs were included. No differences were observed between the different constructs. Such tests were important to evaluate if the different protections of the T – DNA left – and right border impact the plant transformation events. The implementation of the *Potri.2G0797* and *Potri.2G2183* promoters is described in the respective chapters.

Table 26. Composition of fluorescence expression cassettes in pCXUN binary vector T-DNA to test for impacts of their orientation on poplar transformation efficiencies. Given is the composition of the first expression cassette with its promoter, fluorescence protein and terminator. Some constructs contained a second expression cassette in tandem, which was composed of a NOS promoter. tdTomato-NLS and OCS terminator. NLS means the protein has a nuclear targeting signal, SNL means the protein is targeted to the peroxisomes. LB = left border and RB = right border sequence of the T-DNA (see schematic display in **Figure 16**). Additionally, the number of observed plants per construct is given. The $P_{2892\ bp}$ refers to a 2892 bp long promoter region of *Potri.2G0797*. $P_{3551\ bp}$ refers to a 3551 bp long promoter region of *Potri.2G2183*.

Promoter	Fluorescence Protein	Terminator	tdTomato-NLS cassette	Orientation on T - DNA	Plant No.
35S	tdTomato-NLS	OCS	No	RB to LB	32
35S	tmTomato-SNL	NOS	No	LB to RB	19
35S	sYFP-SNL	OCS	No	LB to RB	12
35S	sYFP-SNL	OCS	Yes	RB to LB	26
35S	sYFP-SNL	OCS	Yes	LB to RB	16
UBQ	GFP	NOS	Yes	LB to RB	7
No promoter	GFP	NOS	Yes	LB to RB	3
***Potri.2G2183* 3551 bp**	GFP	NOS	Yes	LB to RB	24
***Potri.2G0797* 2892 bp**	GFP	NOS	Yes	LB to RB	16

Differences in the transformation efficiency between the two orientations on the T-DNA of pCXUN were observed. For single marker cassettes, an orientation from right border (RB) to left border (LB) gave higher transformation efficiencies compared to LB – RB orientation (**Figure 17**, LB-RB: mean = 70 %, SE = 5.2; RB-LB: mean = 85 %, SE = 3.8; Wilcoxon rank test: p<0.05, effect size = 3.3).

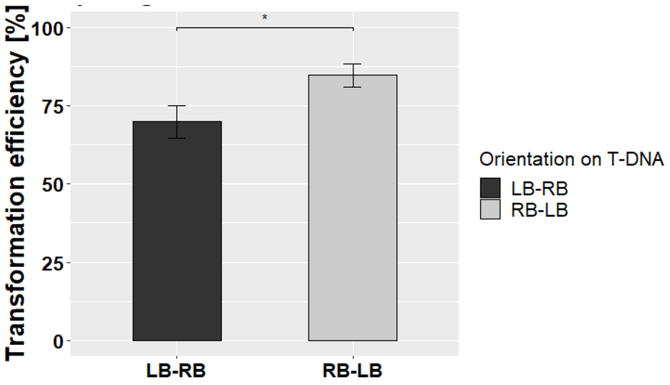

Figure 17. Poplar root transformation efficiencies in dependence on the orientation of fluorescence marker cassettes on the T – DNA of pCXUN. LB means left border and RB means right border in the T – DNA. A schematic overview of the orientations is given in Figure 16. Only single fluorescence protein cassettes were observed. *Populus tremula x alba* was transformed with *Agrobacterium rhizogenes* strain K599. pCXUN LB-RB: n = 31 plants, mean transformation efficiency = 70 %, SE = 5.2; pCXUN RB-LB: n = 32 plants, mean transformation efficiency = 85%, SE = 3.8. The root system was observed eight weeks after the transformation event. Significances are based on a Wilcoxon test (see M&M), * = p < 0.05. The standard error is given. Statistics were conducted in R as specified in the M&M.

When observing double constructs with two fluorescence expression cassettes in tandem on the pCXUN T – DNA, the left- to right border orientation gave higher transformation efficiencies compared to right-to left orientation (**Figure 18**, LB-RB: mean = 81 %, SE = 3.7; RB-LB: mean = 59 %, SE = 8.3; Wilcoxon test: p<0.01, effect size = 3.4).

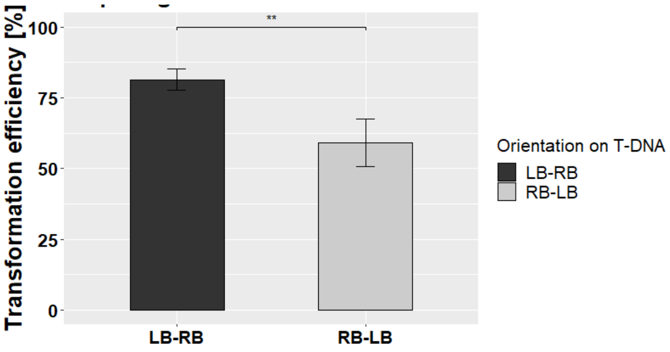

Figure 18. Poplar root transformation efficiencies in dependence on the orientation of fluorescence marker cassettes on the T – DNA of pCXUN. LB means left border and RB means right border in the T – DNA. A schematic overview of the orientations is given in **Figure 16**. Only double fluorescence protein cassettes were observed. *Populus tremula x alba* was transformed with *Agrobacterium rhizogenes* strain K599. pCXUN LB-RB: n = 67 plants, mean transformation efficiency = 81 %, SE = 3.7; pCXUN RB-LB: n = 26 plants, mean transformation efficiency = 59 %, SE = 8.3. The root system was observed eight weeks after the transformation event. Significances are based on a Wilcoxon test (see M&M), ** = p < 0.01. The standard error is given. Statistics were conducted in R as specified in the M&M.

When comparing both single and double marker cassettes together to increase the dataset, no significant differences could be detected between the two orientations on the T-DNA of pCXUN (**Figure 19,** LB-RB: mean = 78.6 %, SE = 3; RB-LB: mean = 73.3 %, SE = 4.5; Wilcoxon test: p>0.05, Effect size = 0.16). Overall, it was decided to keep the orientation that was already established in the pPLV-based vector systems, namely from LB to RB (5´ - 3´orientation). This means, that the kanamycin resistance on the T - DNA is facing opposite to the T - DNA and the marker cassette reads from the right to the left border.

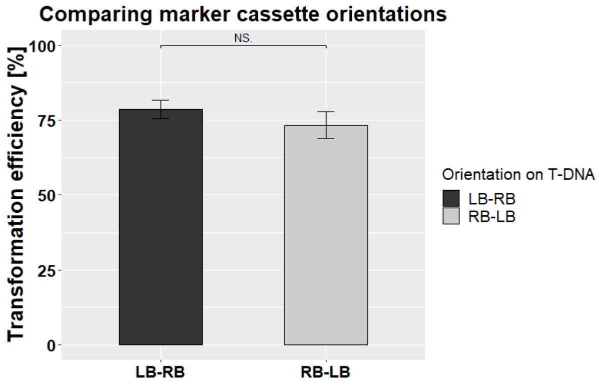

Figure 19. Poplar root transformation efficiencies in dependence on the orientation of fluorescence marker cassettes on the T – DNA of pCXUN. LB means left border and RB means right border in the T – DNA. A schematic overview of the orientations is given in Figure 16. Both single and double fluorescence protein cassettes were observed. *Populus tremula x alba* was transformed with *Agrobacterium rhizogenes* strain K599. pCXUN RB-LB: n = 58 plants; pCXUN LB-RB: n = 97 plants. The root system was observed eight weeks after the transformation event. Significances are based on a Wilcoxon test (see M&M). NS = not significant. The standard error is given. Statistics were conducted in R as specified in the M&M.

Additionally, no significant differences in transformation efficiency between single and double marker constructs were found (Mean Double = 75.1%, SE = 3.7; Mean Single = 77.5%, SE = 3.3; Wilcoxon test: p>0.05, Effect size d = 0.07) (**Figure 20**).

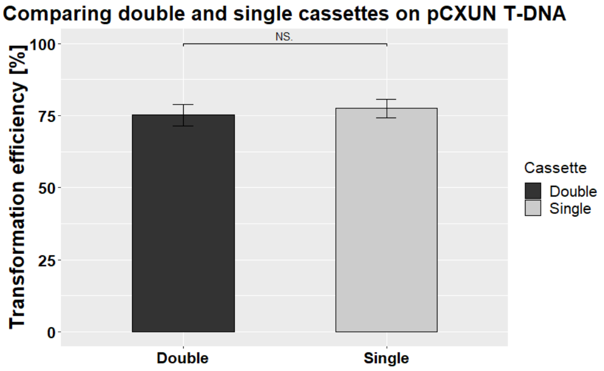

Figure 20. Poplar root transformation efficiency based on the introduced cassette size. Compared were single cassettes consisting of a Promoter, gene, and terminator, against double constructs in which second fluorescence cassette was introduced. The orientation of the T-DNA is described in Table 26. *Populus tremula x alba* was transformed with *Agrobacterium rhizogenes* strain K599. single cassette plants: n = 63; double cassette plants: n= 92. The root system was observed eight weeks after the transformation event. Significances are based on a Wilcoxon test (see Material and Methods). NS = not significant. The standard error is given. Statistics were conducted in R as specified in the M&M.

3.2 Establishing DsRED-E5 as potential marker gene for *in planta* investigation of gene regulation in poplar

Double marker systems are based on two different fluorescence reporter proteins that have different maturation and degradation times. Therefore, a timer protein (DsRED-E5) was tested as a potential marker for *in planta* investigation of gene regulation in poplar. As a timer protein, DsRED-E5 shows detectable GFP signals upon its maturation, resulting in a steady state of green to red fluorescence over time based on one single protein. The synthetic gene was targeted to the nucleus and had added 5´*HpaI* and 3´*BamHI* restriction site overhangs, which allowed for easy integration into the modified pCXUN as described in **Figure 14**. In this process, a large part of the pCXUN T – DNA was exchanged, resulting in a single cassette with DsRED-E5-NLS between a UBQ promoter and OCS terminator (**Figure 21**). The correct integration into pCXUN was verified with restriction digestion (**Figure 22**).

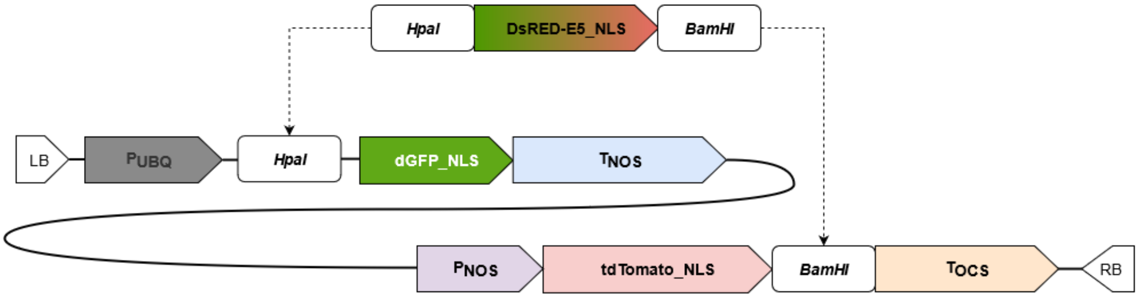
HpaI
DsRED-E5_NLS
BamHI
LB
PUBQ
HpaI
dGFP_NLS
TNOS
PNOS
tdTomato_NLS
BamHI
TOCS
RB

Figure 21. Schematic overview of the integration of the nucleus targeted timer protein DsRED-E5 in *HpaI* and *BamHI* restriction sites in pCXUN T – DNA. The vector is described in Figure 14. LB is the left border and RB the right border of the T – DNA. NLS means the protein is targeted to the nucleus. The used promoters, terminators and FPs are further described in the M&M.

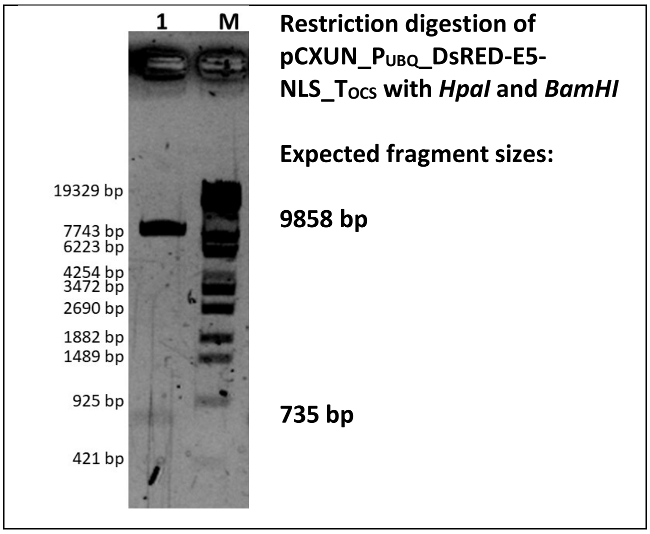
1
M
19329 bp
7743 bp
6223 bp
4254 bp
3472 bp
2690 bp
1882 bp
1489 bp
925 bp
421 bp
Restriction digestion of pCXUN_P$_{UBQ}$_DsRED-E5-NLS_T$_{OCS}$ with HpaI and BamHI
Expected fragment sizes:
9858 bp
735 bp

Figure 22. A: Verification of DsRED-E5 in pCXUN driven by a UBQ promoter by restriction digestion. The pCXUN_P$_{UBQ}$_DsRED-E5-NLS_T$_{OCS}$ plasmid was verified with *HpaI/BamHI* restriction digestion. Expected fragment sizes were 735 bp + 9858 bp. As marker (Lane M, 6 µl) the Phage Lambda DNA/Eco130I (StyI) DNA ladder was used. Further details are given in the M&M.

Expected was a detectable shift from green to red fluorescence over time (Mirabella et al., 2004) that could indeed be observed after transient expression of the construct in *Nicotiana benthamiana* leaves (**Figure 23**).

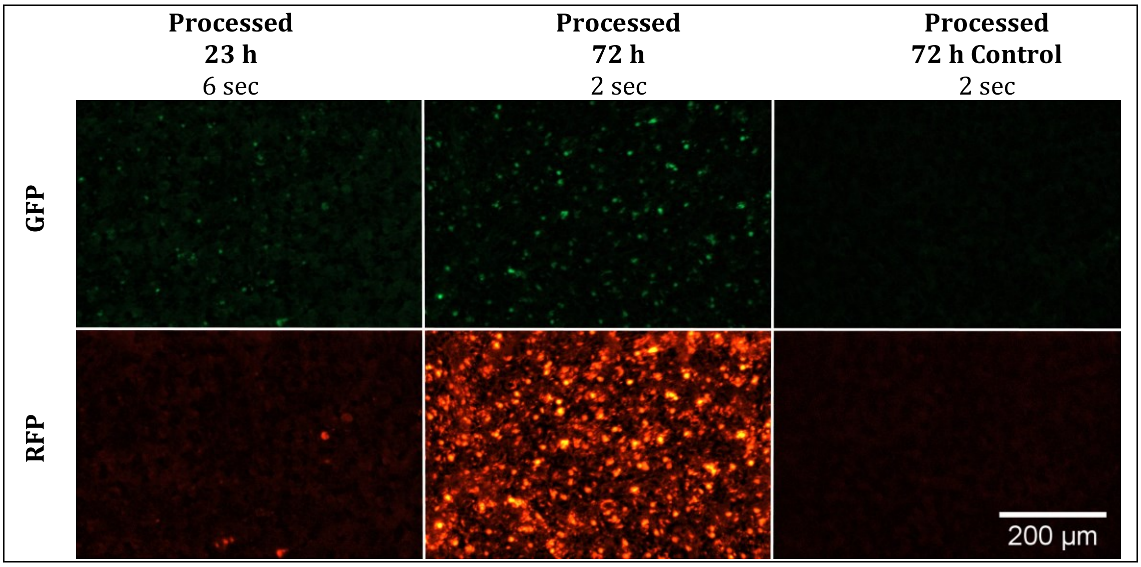

Figure 23. Visualization of nuclear targeted DsRED-E5 driven by a P_{UBQ} or without a promoter (neg. control). Transgenic *Agrobacterium rhizogenes* (strain K599) were used to transform tobacco leaves with an OD_{600} of 0.3. Fluorescence was observed after 23 h and 72 h. All pictures were taken under the exact same conditions and were compiled in a montage, where the background was subtracted, and contrast enhanced by 0.3 % in ImageJ. Used filter settings and further specifications are listed in the M&M.

After successfully establishing the "Timer" system in tobacco leaves, further constructs with a NOS promoter and a 2892 bp promoter fragment of *Potri.2G0797* driving the DsRED-E5 expression were cloned, verified with restriction digestion (**Supplementary figure 3** for P_{NOS} and **Supplementary figure 19** for a 2892 bp promoter of *Potri.2G0797*) and tested in *Populus tremula x alba* roots. All constructs showed green as well as red fluorescence in the respective transgenic poplar roots in root hairs (**Figure 24**) as well as the cortex (**Figure 25**).

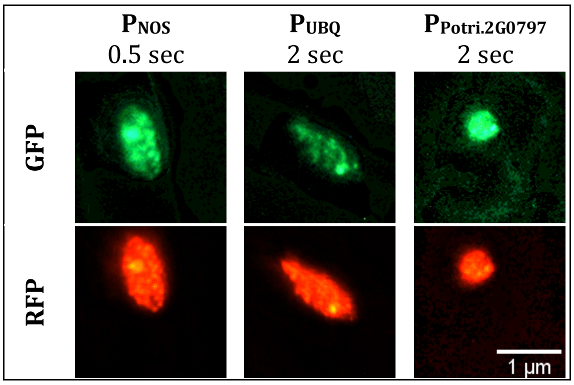
PNOS
0.5 sec
PUBQ
2 sec
PPotri.2G0797
2 sec
GFP
RFP
1 µm

Figure 24. Visualization of nuclear targeted DsRED-E5 fluorescence in composite poplar plants. Gene expression was driven by the three different promoters P_{UBQ}, P_{NOS} and $P_{2892\ of\ Potri.2G0797}$ in root hairs of *Populus tremula x alba* plants. Composite plants were generated via *Agrobacterium rhizogenes* mediated transformation. Fluorescence was observed two to six weeks after root formation with a Zeiss microscope (as described in the M&M). All pictures were taken (gain = 4.8 dB) and processed under the same conditions in ImageJ (background subtraction and contrast enhancement by 0.001 % of individual pictures).

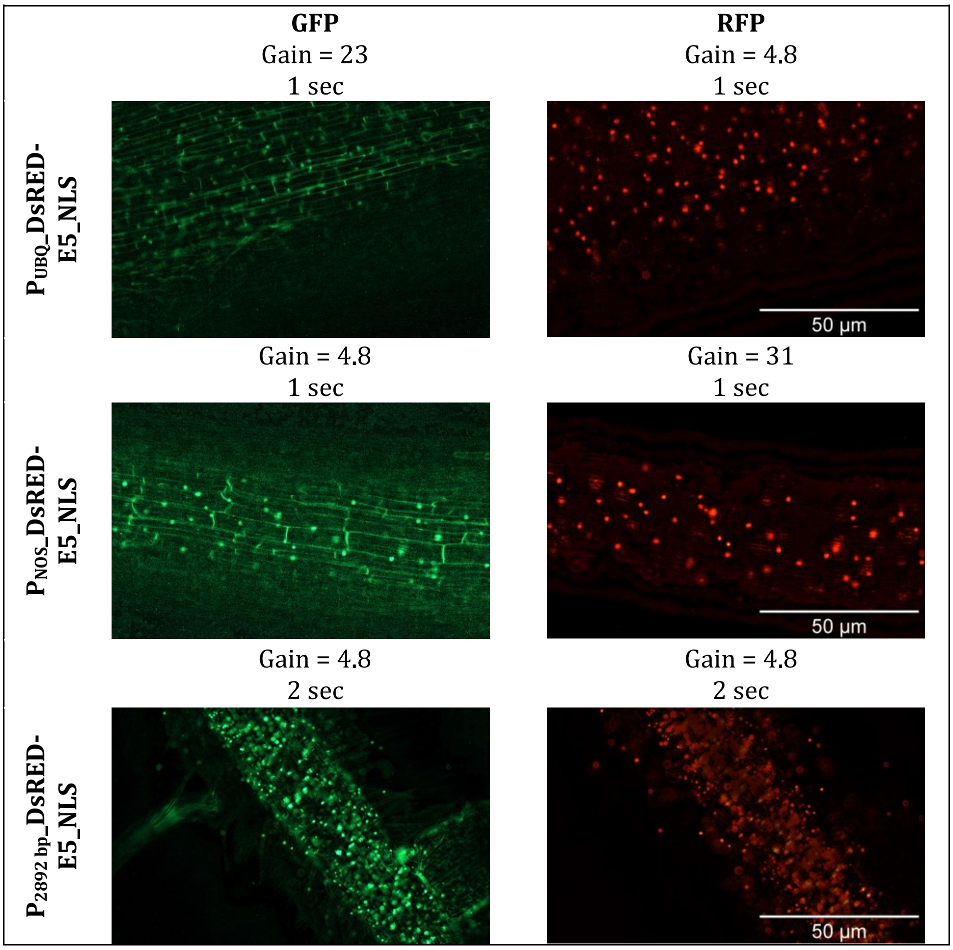
GFP
Gain = 23
1 sec
RFP
Gain = 4.8
1 sec
PUBQ_DsRED-E5_NLS
50 µm
Gain = 4.8
1 sec
Gain = 31
1 sec
PNOS_DsRED-E5_NLS
50 µm
Gain = 4.8
2 sec
Gain = 4.8
2 sec
P2892 bp_DsRED-E5_NLS
50 µm

Figure 25. Visualization of nucleus targeted DsRED-E5 fluorescence in composite poplar plants. Gene expression was driven by the three different promoters P_{UBQ}, P_{NOS} and $P_{2892\ of\ Potri.2G0797}$ in cortex cells of *Populus tremula x alba* roots**.** Composite plants were generated via *Agrobacterium rhizogenes* mediated transformation with a pCXUN vector backbone. Fluorescence was observed two to seven weeks after root formation with a Zeiss microscope (as described in the M&M). All pictures were taken and processed under the same conditions in ImageJ (background subtraction and contrast enhancement by 0.1 - 0.001 % of the individual pictures). The gain is given in dB.

3.3 Determining promoter activity based on fluorescence intensities

Fluorescence intensities of GFP and RFP signals from the same nuclei were determined with ImageJ and correlated by calculating GFP: RFP ratios. This was done for both the double marker constructs (GFP and tdTomato) as well as the timer protein (DsRED-E5). Main aim was to compare ratios of promoter fragments and its 5´ truncations concerning their activity to localize possible *cis* – elements.

3.3.1 Establishing camera settings for the analysis of promoter intensities based on images

The calculation of fluorescence intensities from microscopic images included the definition of optimal camera settings. The optimal light intensity and illumination times as well as the definition of a histogram range were determined in collaboration with other members of the working group and are described in the M&M.

A short pre – experiment to test these camera settings for possible bleaching effects showed, that the GFP:RFP ratios of one single root hair nucleus shifted from 1.28 after 2 sec illumination time to 1.3 after 60 sec and 1.45 after 120 sec in a double marker construct (**Figure 26**).

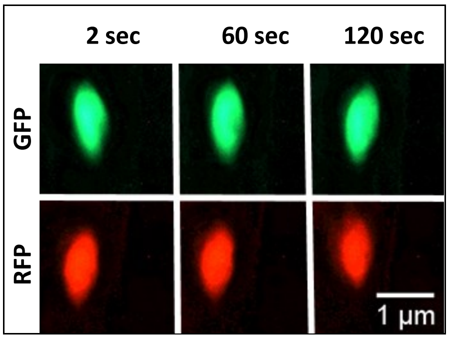

Figure 26. Bleaching experiment of GFP-NLS and tdTomato-NLS in root hair nuclei of transgenic composite poplar. The same nucleus of a pCXUN double marker construct was illuminated for 2 sec, 60 sec and 120 sec respectively under 2 sec exposure time. The total illumination time including adjustments was approximately 4 min. Fluorescence intensities were determined with ImageJ to calculate GFP: RFP intensity ratios. For better visualization, all pictures were processed with the same conditions (Background subtracted and contrast enhanced by 0.0001 % in ImageJ). n = 1 nucleus. Further details about the used devices and software are given in the M&M.

It was tested whether images in GFP and RFP channels of the same nucleus could be taken with different gain values without distorting the obtained GFP: RFP fluorescence ratios. This was sometimes necessary to be able to take images that were neither oversaturated, nor under a detection limit. Therefore, Pictures of the same nuclei were made in both GFP and RFP channels with increasing gain. All other parameters remained unchanged. Ratios of GFP: RFP were calculated from the obtained fluorescence intensities of both before and after normalizing against the corresponding gain factor. No differences could be seen for two tested cortex nuclei and two tested root hair nuclei of a DsRED-E5_NLS construct driven by a 2892 bp promoter of *Potri.2G0797*. A visual example for such a series given in **Figure 27**.

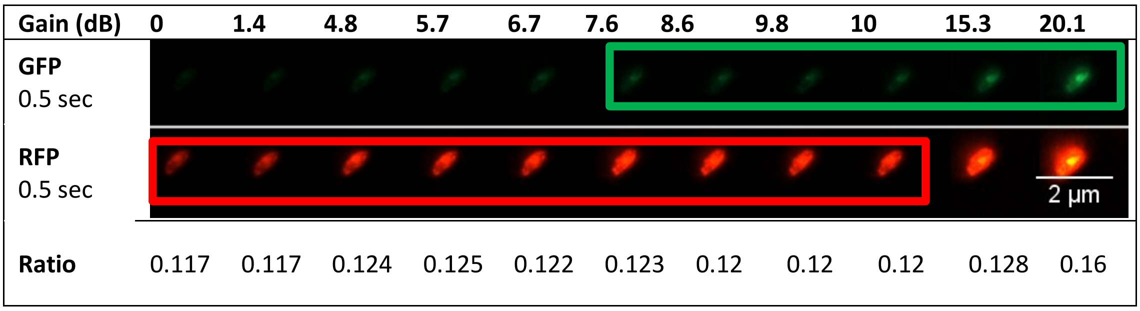

Figure 27. Gain series of a *Populus tremula x alba* root hair nuclei containing a nucleus targeted DsRED-E5. Pictures were made with a Zeiss microscope and details about the camera setting and used filter sets can be found in the M&M. All pictures were taken under the same conditions, only the gain value differed. Because the GFP was hard to detect, the pictures are visualized with an enhanced contrast (0.3 %) and subtracted background (ImageJ, further specifications in the M&M). To avoid distortion of ratios, the alterations were made after compiling the pictures in a montage. The red and green box indicate, which gain levels gave fluorescence intensities that were neither under- nor over saturated. The GFP: RFP fluorescence ratio is given, also for pictures in which one or the other channel is over/undersaturated.

3.3.2 Determining impacts on the comparability of fluorescence ratios

It was noted that the root growth differed in dependence of the root replicate (**Figure 28**). When transformed with the same construct (pCXUN_P_{NOS}_DsRED-E5_T_{OCS}), one root grew 0.9 mm per day when observed over a timescale of 15 days, whereas another root from the same plant batch grew 1.7 mm per day. It was not determined, if the root growth impacts fluorescence ratios in a detectable manner. Because it was aimed to compare fluorescence ratios between different constructs it needed to be tested, if and how much root growth impacts GFP: RFP ratios along a gradient in a root.

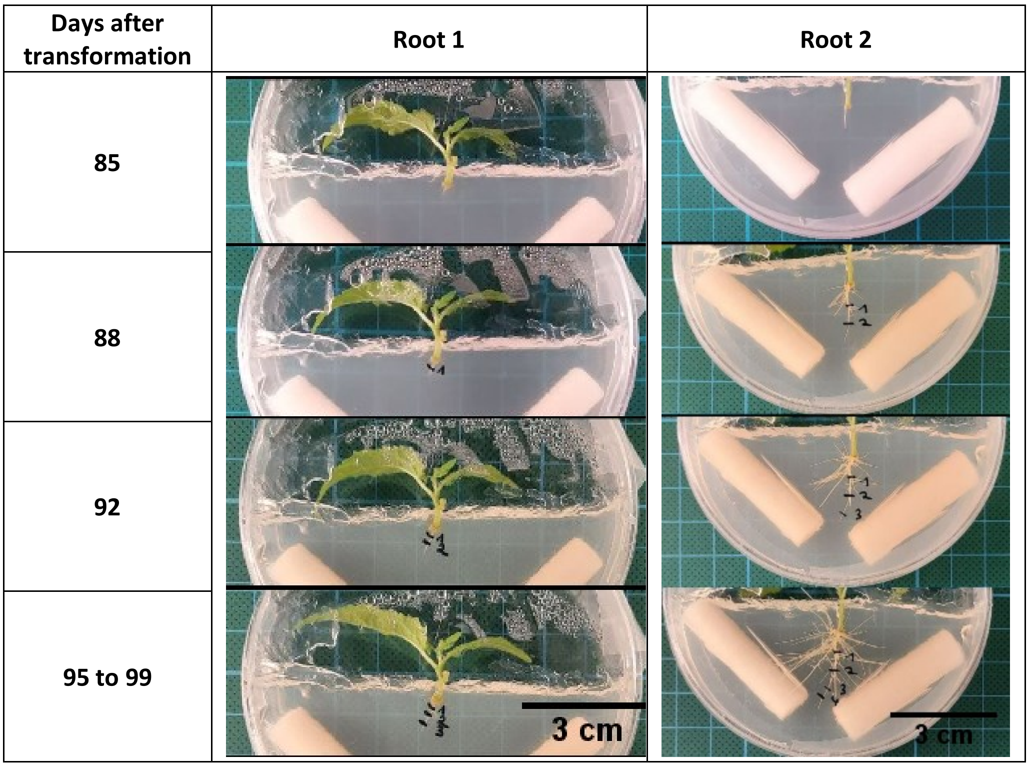

Figure 28. Root growth of two roots from transgenic composite poplar root systems. The root growth over a time scale of 15 days was observed, starting 85 days after the transformation event. *Populus tremula x alba* plants were transformed with *Agrobacterium* rhizogenes strain K599 harboring a pCXUN binary vector. The T – DNA consists of a NOS promoter, nuclear targeted DsRED-E5 and an OCS terminator. Both root systems were treated identically

A ratio gradient occurred when comparing cortex nuclei of one plant containing a P$_{2892\text{ bp Potri.2G0797}}$_DsRED-E5-NLS_T$_{OCS}$ construct at different parts of a second order root (**Figure 29**). The GFP: RFP ratio 1 mm above the root tip was 0.05 (n = 4 nuclei, SE = 0.003), 0.03 at 2 mm above the root tip (n = 9 nuclei, SE = 0.002) and 0.33 close to the main root (n = 10 nuclei, SE = 0.001).

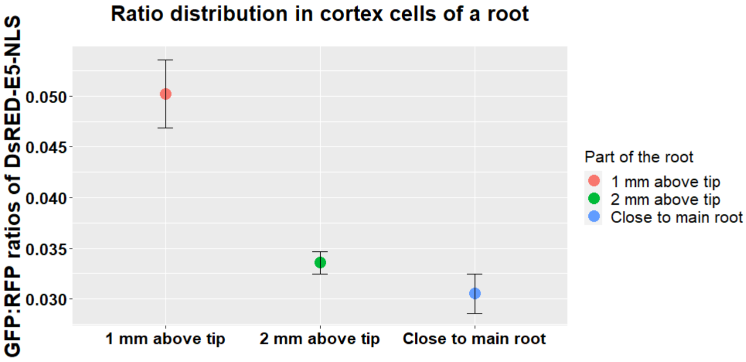

Figure 29. GFP: RFP fluorescence ratios of DsRED-E5-NLS in one second order root at the three different areas 1 mm above the root tip, 2 mm above the root tip and close to its origin at the main root. Composite *Populus tremula x alba* plants were generated with *Agrobacterium rhizogenes* strain K599 harboring a pCXUN binary vector. The T – DNA was composed of a NOS promoter, DsRED-E5 targeted to the nucleus and an OCS terminator. The root was observed three weeks after root formation. Statistics were conducted in R as specified in the M&M. The standard error for each site is given. From left to right: n = 4, 9 and 10 nuclei per area.

3.4 Comparing fluorescence ratios between first and second order root hair nuclei

At a first glance, both first and second order roots of transgenic composite poplar look morphologically similar (**Figure 30**).

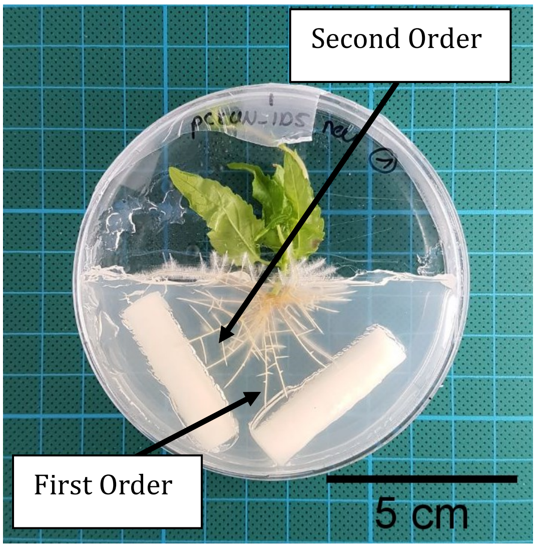

Figure 30. Example for a transgenic composite poplar plant. The plant transformation was mediated by *Agroacterium rhizogenes* (strain K599). First and second order roots are indicated. The root system was six weeks old and shows the "hairy root" phenotype.

No obvious differences in expression strength and the FP location for 176 bp and 3551 bp promoter fragments of *Potri.2G0797* and *Potri.2G2183* could be seen when comparing first and second order roots concerning their root tips, elongation zones and root hair nuclei. (**Figure 31** and **Figure 32**). Further details about both promoters can be found in the following chapters.

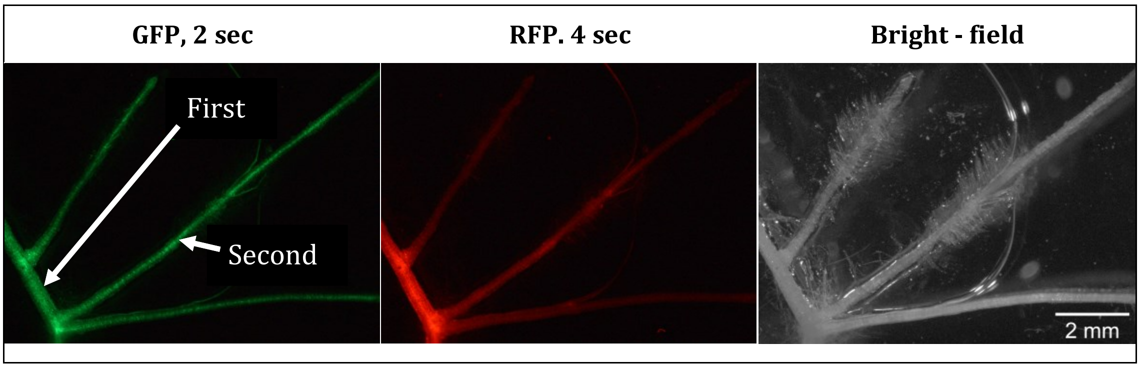

Figure 31. Visualization of the promoter activity of a 176 bp promoter region from *Potri.2G0797* in a first order root compared to a second order root. Pictures were obtained from a binocular (specifications in the M&M). All pictures were made under the same conditions. The promoter was amplified from *Populus tremula x tremuloides* gDNA and visualized in *P. tremula x alba* plants. The roots were 5 to 8 weeks old. For visualization, the pictures were processed in the same manner.

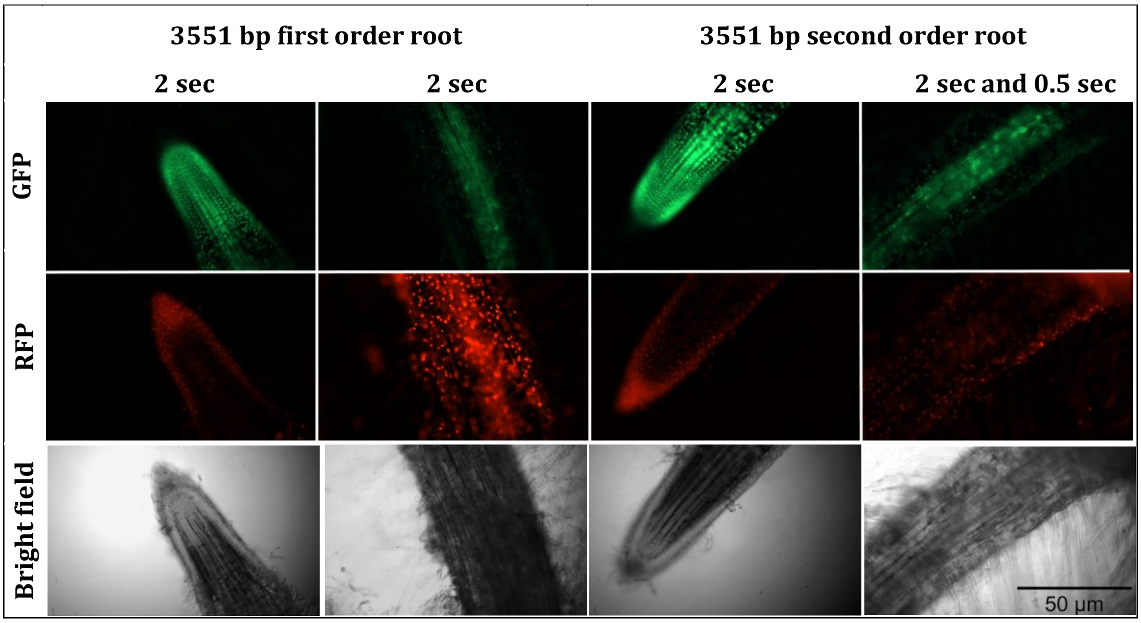

Figure 32. Visualization of the promoter activity of a 3551 bp promoter region from *Potri.2G2183,* amplified from *Populus trichocarpa* gDNA and visualized in *P. tremula x alba* plants, in a first order root compared to a second order root. Pictures were obtained from a Zeiss microscope (specifications in the M&M). All pictures were made under the same conditions. The root system was 8 weeks old. For visualization, the corresponding RFP and GFP pictures were processed in the same manner.

Calculated GFP: RFP fluorescence intensity ratio of root hairs did not significantly differ between first and second order roots in three different constructs in both double marker constructs and DsRED-E5 constructs (**Figure 33**). Thereby, root hair nuclei of approximately the same age were analysed (*Potri.2G0797* 2892 bp in DsRED-E5 expression cassette: first order root hair nuclei n = 2, mean GFP: RFP ratio = 0.14 with SE = 0.1, second order root n = 2, mean ratio = 0.2 with SE = 0.18; 2892 bp promoter fragment in double marker construct: first order root n = 4, mean = 1 with SE = 0.6, second order root n = 0.4, mean = 0.4 with SE = 0.06; 176 bp promoter fragment of *Potri.2G0797* in double marker construct: first order root n = 4, mean = 3.5 with SE = 0.4, second order root n = 3, mean = 3.5 with SE = 0.8).

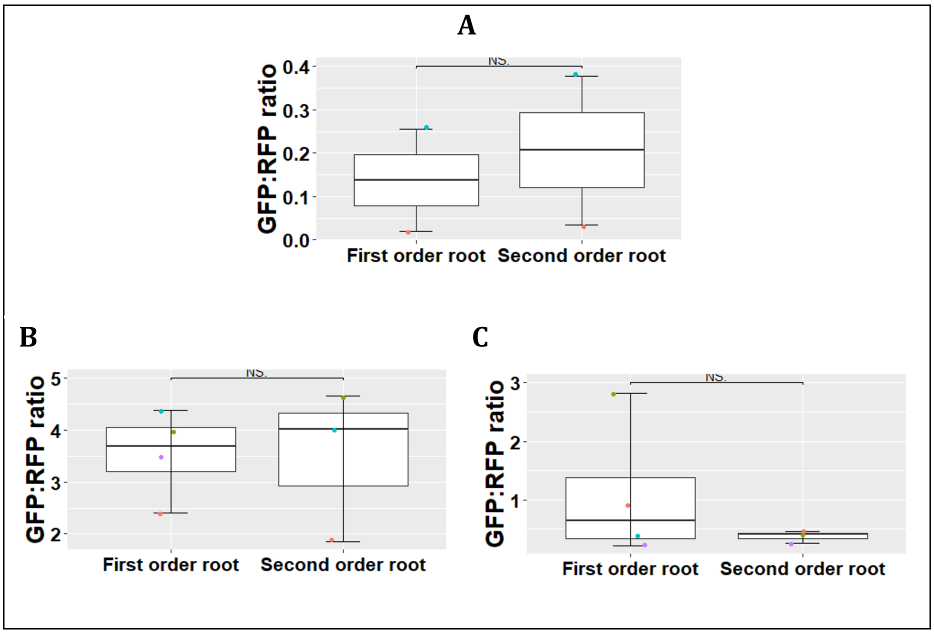

Figure 33. Boxplot comparing root hair nuclei GFP:RFP ratios between first and second order roots. Transgenic composite *Populus tremula x alba* plants were transformed with *Agrobacterium rhizogenes* (strain K599). The root systems were two to seven weeks old. A: DsRED-E5-NLS driven by a 2892 bp promoter fragment of *Potri.2G0797* in pCXUN (d = 0.33). B: A 176 bp promoter fragment of *Potri.2G0797* in a double marker system (d = 0.04) and C: a 2892 bp promoter of *Potri.2G0797* in a double marker system (d = 0.83). Each root replicate represents a mean of two to four single nuclei. Statistics were performed in R. Comparisons were calculated based on a Wilcoxon rank test. Effect sizes were calculated in GPower 3.1. The standard error is given. Statistics were conducted in R as specified in the M&M.

3.5 Consistency of fluorescence expression levels in one transgenic root system

It was observed that fluorescence intensities differed at roots formed by the same plant. This was independently of the orientation of the fluorescence cassette on the T - DNA. In two independent experiments using a **P_{35S}_td-tomato-NLS_T_{OCS}** construct (orientation from RB to LB, in tandem with the plant selection marker cassette), approximately 32.7 % showed strong red fluorescence, 40.2 % had intermediate fluorescence and 27 % of the roots had only very weak red fluorescence (n = 30 plants) (**Figure 34**). Such findings were also obtained with other fluorescence proteins (data not shown). qPCR data revealed a positive correlation between the observed fluorescence intensities and gene expression of tdTomato (**Figure 35**). Weak expressing roots had a relative expression rate of ~6 (SD = 0.1), intermediate expressing roots of ~12 (SD = 0.26) and strong expressing roots of ~18 (SD = 0.28). Thus, expression was found to be 3.16 - fold higher in strong fluorescent roots compared to roots with weak expressions.

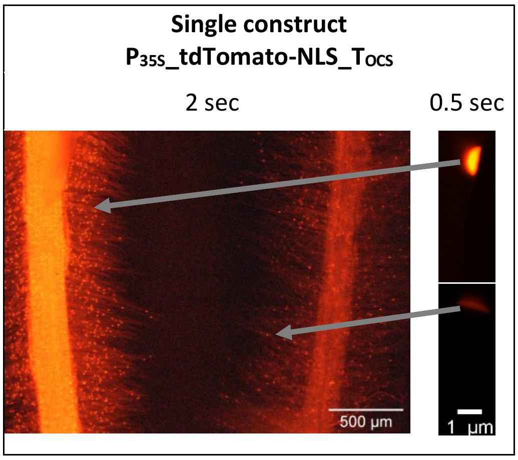

Figure 34 Visualization of the fluorescence of a tdTomato construct in independent poplar roots of the same transgenic root system. Overview images were taken at a Leica binocular MZ10F with 2 sec illumination time (Leica DFC425C camera, dsRED filters with 510 – 560 nm excitation and 590 – 650 nm emission window filter). Detailed pictures of root hair nuclei were taken using an epifluorescence microscope with 0.5 sec illumination time (Zeiss Axioskop Microscope, Imagingsource DFK23UX174 camera, dsRED filter with 510 – 560 nm excitation and 590 nm long pass emission window filter with a 580 nm beam splitter). Thereby, images of different roots were taken under the same conditions. Pictures were made three to four weeks after the transformation event. The binocular picture was processed for better visualization (contrast enhanced by 0.01 % in ImageJ), whereas unprocessed microscope pictures are shown. Further details about the used devices and image processing are given in the M&M.

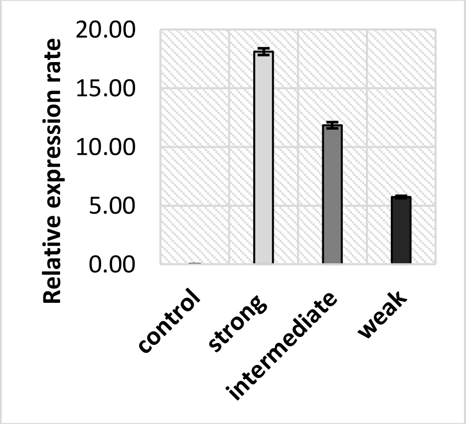

Figure 35. Comparison of the relative transcription rate of tdTomato driven by a 35S-promoter in roots of three fluorescence intensity categories. The expression cassette consisted of a nucleus targeted tdTomato between a P_{35S} and a T_{OCS}. Given is the relative expression rate in roots revealing strong, intermediate, and weak fluorescing roots. The control did not contain tdTomato. Ten root systems were dissected, pooled according to their fluorescence, and used for RNA extraction three weeks after root formation. The qPCR analysis was conducted by Annette Hintelmann with a primer targeted to tdTomato. The data were normalized against a constitutively expressed reference gene driven by a P_{UBQ} (Neb, 2017). The standard deviation is given (SD strong = 0.28, SD intermediate = 0.26 and SD weak = 0.1).

3.6 Characterization of *Potri.2G0797*

3.6.1 Subcellular protein localization of Potri.2G0797: Do introns matter?

To elucidate the impacts of introns on fluorescence signal intensities, C – terminal fusions of *Potri.2G0797* and sYFP were constructed with and without introns. The CDS was either amplified from cDNA (1443 bp) or gDNA (1932 bp).

C-terminal Fusion constructs without introns

A fusion construct without introns was already created by Lucas Lansing (Lansing 2015, Master thesis) in such a way, that the CDS of *Potri.2G0797* was STOP-codon less and sYFP was cloned ATG-less in frame. This fusion construct was PCR amplified with added *BamHI* restriction sites overhangs (Forward primer 24SLBamHIforFus and revers primer 24SLBamHIrevFus, see **Table 7**). The obtained PCR product was initially verified in pJET1.2 by restriction analysis and partial sequencing (**Supplementary figure 4**). The *Potri.2G0797*-sYFP construct was released by *BamHI* digestion, gel purified and cloned into the *BamHI* site between P_{35S} and T_{OCS} in pPLV (vector description see **Figure 8**). The construct was verified via restriction digestion analysis and partial sequencing (**Supplementary figure 5**). Finally, the P_{35S}_ *Potri.2G0797*-sYFP_T_{OCS} cassette was released by *KpnI/SacI* digestion and introduced into pCXUN *KpnI/SacI* restriction sites (pCXUN_P_{35S}_ *Potri.2G0797*_sYFP_T_{OCS}, vector description in **Figure 14**). A schematic overview of this strategy is given in **Figure 36**. Verification of successful integration was performed by restriction digestion (**Supplementary figure 6**).

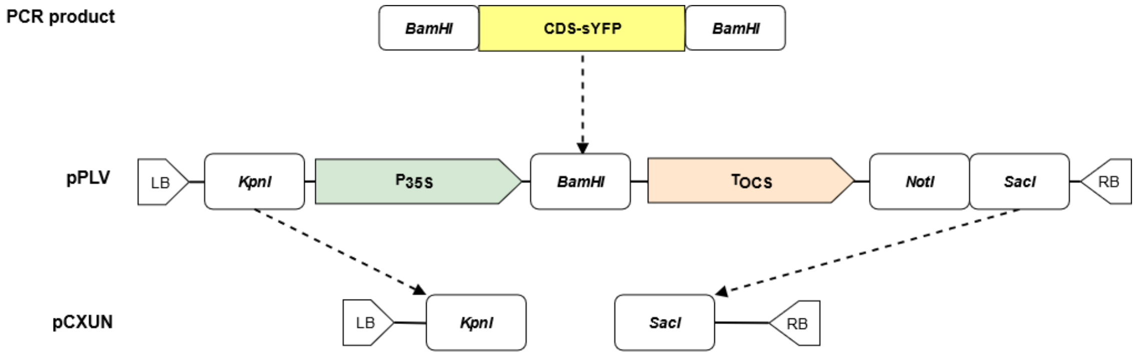

Figure 36. Relevant part of the T – DNA in pCXUN to localize *Potri.2G0797* on a subcellular level. A fusion construct with sYFP was PCR amplified with added BamHI restriction sites at the 5´and 3´end. This fusion construct was cloned between a 35S promoter and OCS terminator in a pPLV vector. The 35S promoter. fusion construct and OCS terminator cassette was the released with KpnI and SacI for integration in the T – DNA of pCXUN. The pPLV and pCXUN vectors are described in Figure 8 and Figure 14.The fluorescent protein, promoter and terminator are described in the M&M.

A second marker cassette (P_{NOS}_tdTomato-NLS_T_{OCS}) was introduced in tandem into the *NotI/SacI* restriction sites in pPLV in a directed manner before the double cassette was released by *KpnI/SacI* digestion and introduced into pCXUN *KpnI/SacI* restriction sites (pCXUN_ P_{35S}_ *Potri.2G0797*_sYFP_T_{OCS}_ P_{NOS}_tdTomato-NLS_T_{OCS}) (**Supplementary figure 7**). This second marker cassette could not be directly introduced into pCXUN because of the different availability of restriction sites in pPLV and pCXUN.

C-terminal Fusion constructs with introns

A fusion construct of *Potri.2G0797* with introns and sYFP was constructed in pJET1.2. Accordingly, a STOP-codon less CDS with a newly introduced 3´*BamHI* restriction site was PCR – amplified (Forward primer Pt-2G0797-CDS-SD-f1 and revers primer Pt24SLBamH1.Rev1 (**Table 7**)). At the same time, an ATG less and non-targeted sYFP was PCR amplified with *BamHI* overhangs (Forward primer YFPforBamHIfusion and revers primer sYFP-BamHI-rev1(**Table 7**)), which allowed for the *in-frame* integration of sYFP in the 3´*BamHI* site of *Potri.2G0797*. Both PCR products showed the expected fragment sizes and were verified after cloning to pJET1.2 via restriction digestion (not shown).

As a next step, both PCR fragments were combined by introducing sYFP in the 3´*BamHI* restriction site of pJET1.2_*Potri.2G0797*. The correct *in frame* combination of CDS and sYFP was verified via restriction digestion (**Supplementary figure 8**) as well as partial sequencing (**Supplementary figure 9**). The fusion construct was then introduced in pPLV in the *BglII* site between P_{35S} and T_{OCS}, (vector description in **Figure 8)** which was verified via restriction digestion and partial sequencing (**Supplementary figure 10**).

As a final step the P_{35S}_ Potri.2G0797_sYFP_T_{OCS} cassette was released by *KpnI/SacI* digestion and introduced into pCXUN *KpnI/SacI* restriction sites (Vector description in **Figure 14**, schematic display of the T – DNA in **Figure 36**). Verification of successful integration was performed with restriction digestion (**Supplementary figure 11**). A second marker cassette (P_{NOS}_tdTomato-NLS_T_{OCS}) was added as described above (schematic display in **Figure 37**).

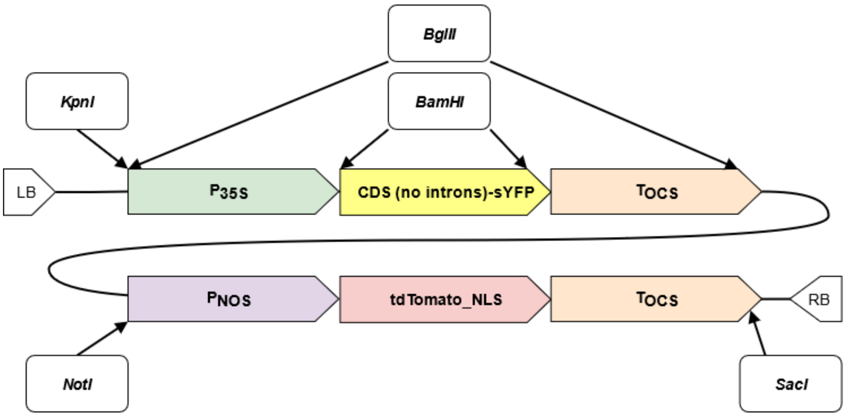

Figure 37. Relevant part of the T – DNA in pCXUN for subcellular localization studies including a second marker for screening of positive transformants of *Potri.2G0797*. The different fluorescent proteins, promoter and terminators are described in the Material and Methods.

However, after transient transformation into tobacco leaves, no sYFP fluorescence signals were obtained at the epifluorescence microscope. As expected, constructs with the second marker cassette showed red signals in the nuclei. An example for the intron less double marker construct is given in **Figure 38**.

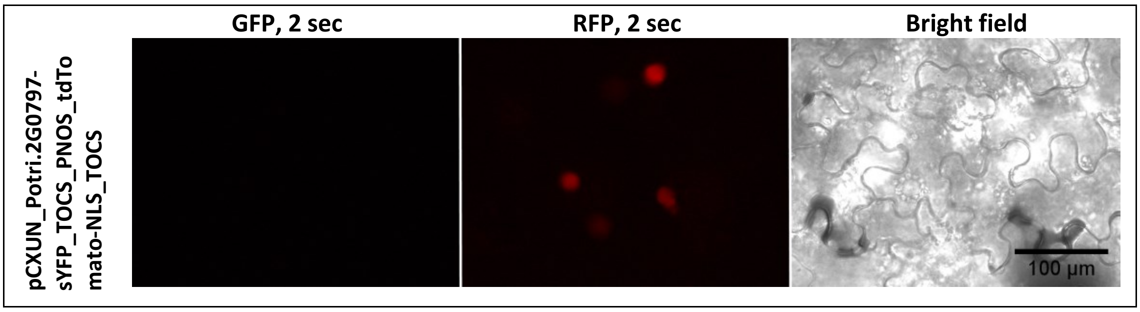

Figure 38. Visualization of the fluorescence of a sYFP fusion-tdTomato-NLS construct in transiently transformed tobacco leave cells. Images were taken using an epifluorescence microscope with 2 sec illumination time (Zeiss Axioskop Microscope, Imagingsource DFK23UX174 camera, filter settings are described in the Material and Methods). Pictures were made five days after the transformation event. The contrast of the pictures was enhanced by 0.5 % in ImageJ. Further details about the used devices and image processing are given in the M&M.

3.6.2 Promoter analyses of Potri.2G0797 in a pCXUN backbone double marker system

A 2892 bp promoter fragment of *Potri.2G0797* was successfully PCR amplified from gDNA of *Populus tremula x tremuloides*, ranging from -2922 bp to -30 bp in relation to the ATG (all primers used primers are available and listed in **Table 6**). The PCR fragment was initially cloned into pJET1.2 and verified via restriction digestion (**Supplementary figure 13)** as well as partial sequencing (**Supplementary figure 14**). The promoter fragment was then amplified with additional *KpnI/SmaI* overhangs from pJET1.2 DNA and introduced in the *KpnI/HpaI* site of pCXUN as described in **Figure 14** (schematic overview in **Figure 39**). The obtained construct was verified with restriction digestion (**Supplementary figure 15**).

Using a second (RFP) marker cassette allowed for easy identification of transgenic plant material due to the constitutive promoter driving the tdTomato-NLS.

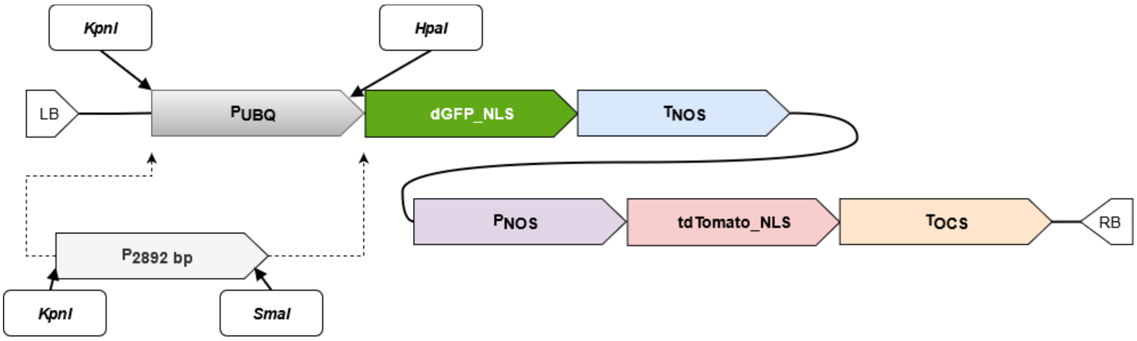

Figure 39. Double marker cassette as part of the T - DNA of a pCXUN binary vector for *Agrobacterium* mediated plant transformation for promoter analysis. LB is the left border- and RB the right border of the T – DNA. The used vector is described in Figure 14. The P_{UBQ} of the green expression cassette can be exchanged with a promoter of interest using *KpnI* and *HpaI* restriction sites. Because *HpaI* cuts blunt-end, the blunt-end cutting *SmaI* can be used for a directed cloning of promoter regions into pCXUN. NLS means the protein is targeted to the nucleus. $P_{2892\ bp}$ corresponds to a promoter region from *Potri.2G0797* amplified from *Populus tremula x tremuloides*.

Even with several independent attempts with different 5´primers it was not possible to amplify larger promoter fragments from either *P. tremula x tremuloides* or *P. trichocarpa* gDNA. However, the 2892 bp promoter fragment was furthermore truncated with three different strategies **(1)** LIC (based on pCXUN as described in **Figure 15**), **(2)** *KpnI/SmaI* (based on pCXUN as described in **Figure 14**) and **(3)** *KpnI/XhoI* (based on pCXUN as described in **Figure 14**). An overview of the obtained promoter fragments and an indication of their cloning strategy is given in **Figure 40**.

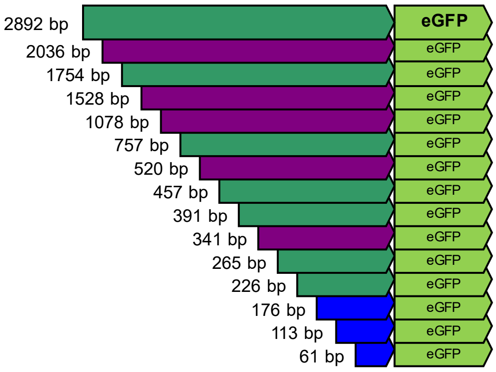

Figure 40. Promoter – reporter constructs of *Potri.2G0797* fragments from *Populus tremula x tremuloides* and eGFP-NLS to identify regulatory elements in this gene upon ectomycorrhiza formation. Transgenic poplar roots were generated with *Agrobacterium* mediated plant transformation, during which Composite plants were generated. The GFP expression was compared between the constructs visually at a microscope (eGFP = enhanced green fluorescent protein). Dark green: constructs were cloned with the *KpnI/SmaI* strategy. Magenta: Constructs were cloned using LIC. Blue: Constructs were cloned with the *KpnI/XhoI* strategy.

Displayed in magenta are promoter fragments that were PCR amplified with LIC adapters and cloned into the respective pCXUN vector. This strategy was used for the 341 bp, 520 bp, 1078 bp, 1528 bp and 2036 bp fragments. The verification of the amplicons via gel electrophoresis is shown in **Supplementary figure 16**. Colour coded in dark green are the promoter fragments that were PCR amplified with artificial 5´ *KpnI* and 3´*SmaI* restriction site overhangs. Those fragments could be introduced into pCXUN in the same manner as the longest amplified fragment of 2892 bp (**Figure 39**). Namely, these fragments had sizes of 1754 bp, 757 bp, 475 bp, 391 bp, 265 bp, and 226 bp. The three shortest fragments of 61 bp, 113 bp and 176 bp (coloured in blue) were too small to be able to verify PCR products with gel electrophoresis with the used Material and Methods. Therefore, the pCXUN vector containing the 2892 bp region was used as a template to amplify the fragments with 5´*KpnI* overhangs together with the rest of the green expression cassette, which included a *XbaI* restriction site at the 3´end of the PCR product (**Figure 41**). The obtained PCR fragments were then cloned into the *KpnI* and *XbaI* linearized pCXUN backbone as described in **Figure 14**. All used primers are listed in **Table 6** and **Table 8** in the M&M.

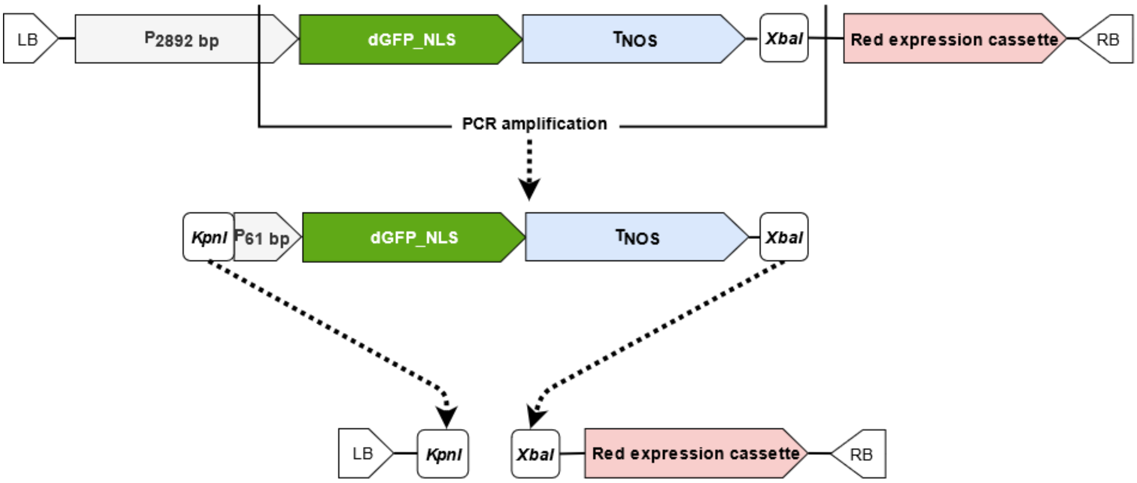

Figure 41. PCR based cloning strategy for the generation of promoter truncations based on restriction digestion for the poplar gene *Potri.2G0797* exemplarily for the 61 bp promoter fragment. Template plasmid for the PCR was a double marker construct with a green and red expression cassette on pCXUN binary vector T – DNA. The green expression cassette was driven by a 2892 bp promoter fragment of the investigated gene. The truncated promoter fragment was 61 bp long and was amplified along with the rest of the green expression cassette. An artificial 5´*KpnI* restriction site was added to the promoter, whereas a native 3´located *XbaI* site was used for further steps. The obtained PCR fragment was then cloned into a KnpI and XbaI linearized pCXUN vector as described in Figure 14. LB is the left border- and RB the right border of the T – DNA. NLS means the protein is targeted to the nucleus. $P_{2892\ bp}$ corresponds to a promoter region from *Potri.2G0797* amplified from *Populus tremula x tremuloides*.

Most obtained constructs were verified with restriction digestion (**Supplementary figure 17**). The three smallest fragments could only be verified via sequencing (**Supplementary figure 18**). It can likely be excluded that this change in promoter activity is caused by differences in the cloning strategies, because the 176 bp promoter was cloned in the same manner as the 113 bp fragment and all constructs were verified via sanger sequencing. Additionally, the only difference that was caused by the three different cloning strategies were three base pairs that were missing at the 3´end of the promoter. *In silico* analyses showed, that integration via *KpnI/SmaI* generated a 24 bp gap to the ATG of GFP, whereas both and *KpnI/XbaI* and LIC generated a 21 bp gap.

First tests *in Populus tremula x alba* showed both GFP and RFP signals the root tip, root hairs as well as the cortex (**Figure 42**) of infected fine roots. No clear results could be obtained for the endodermis and central cylinder because it was not possible to clearly separate FP signals from autofluorescence with the used cameras.

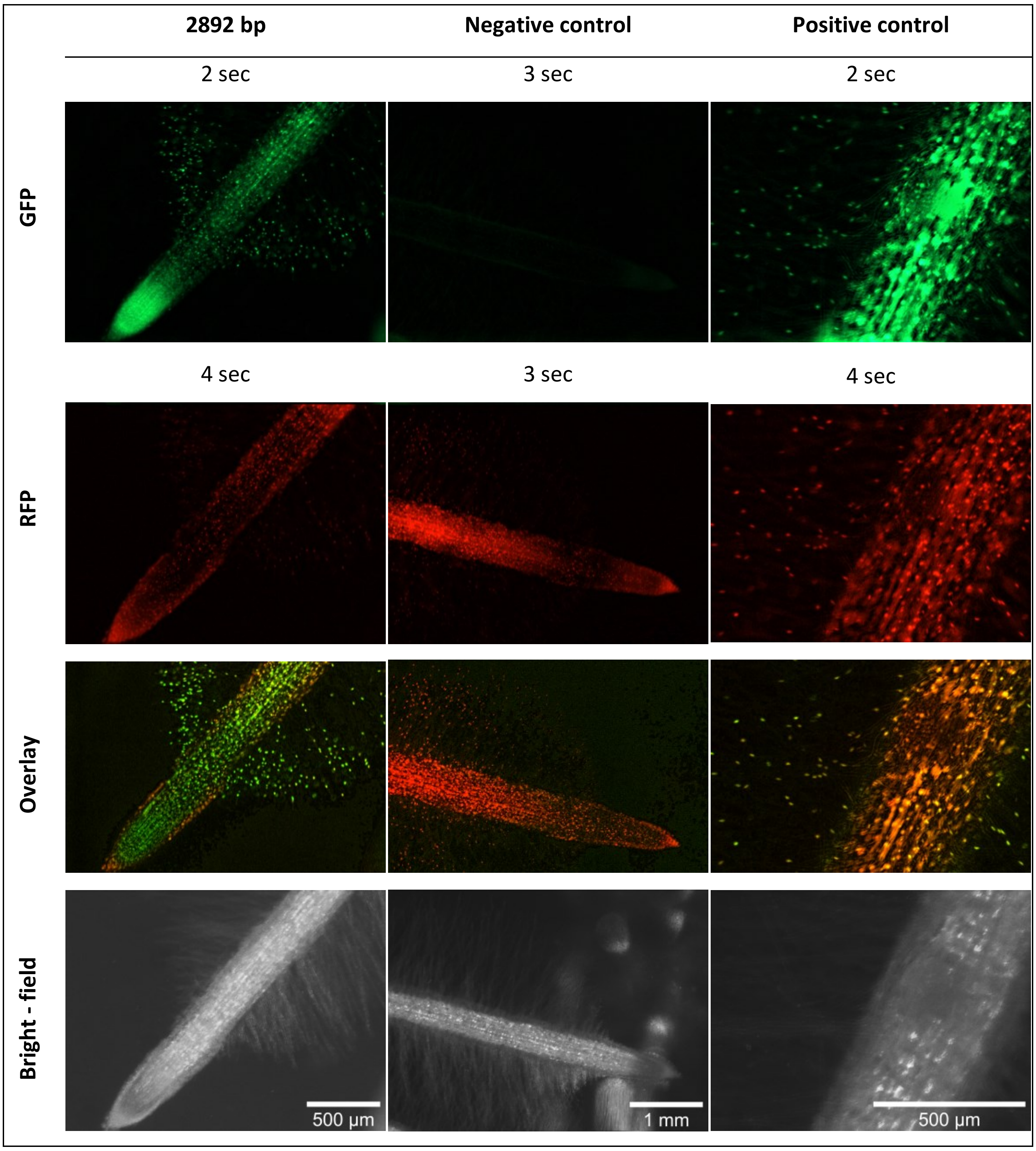

Figure 42. Visualization of the promoter activity of a 2892 bp promoter fragment from *Potri.2G0797* driving nuclear targeted GFP expression *in planta* (*Populus tremula x alba*). As a positive control the GFP expression was driven by P_{UBQ}, as negative control a promoter was GFP less. For a detailed description of the construct see Figure 39. All pictures were taken by a MZ10F Leica binocular with a Leica DFC425C camera using a Leica Application Suite software. Filter sets for GFP had 450 – 490 nm excitation and 500 – 550 nm emission window, RFP filter sets had a 510 – 560 nm excitation and 590 – 650 nm emission window. As light source a Lej LQ-HXP 120, Leistungselektronik JENA GmbH, Jena, Germany was used. All pictures were made with a gamma value of 0.99 and a gain of 5 dB. All devices and further details are given in the M&M. The overlay was made with the RFP and GFP picture. The roots all were 5 to 8 weeks old. For visualization, the pictures were processed in ImageJ (montage of the three corresponding pictures, then background subtracted, and contrast enhanced by 1 %). Further details concerning image processing are given in the M&M.

In planta tests of the promoter truncations in poplar main roots of *Populus tremula x alba* showed a GFP signal in nuclei of randomly picked root hairs of approximately the same age from 2892 bp to 176 bp. As a visual impression, these signals varied slightly in intensity but were clearly present. To determine fluorescence intensity between the longest and shortest promoter fragments showing GFP fluorescence (2892 bp and 176 bp), those were further analysed in **(1)** root tip, **(2)** elongation zone and **(3)** root hair zone (**Figure 43**). Green and red fluorescence were observed in root tip, calyptra, cortex, and root hairs for both promoter fragments, indicating active transcription enabled by promoter fragments of *Potri.2G0797* and the NOS promoter (in the reference red expression cassette). Next to the nucleus, fluorescence signals were observed also in the plant cell wall, particularly in the stele. Lowest background fluorescence was found in the elongation zone. The pictures are always made from single roots of one plant.

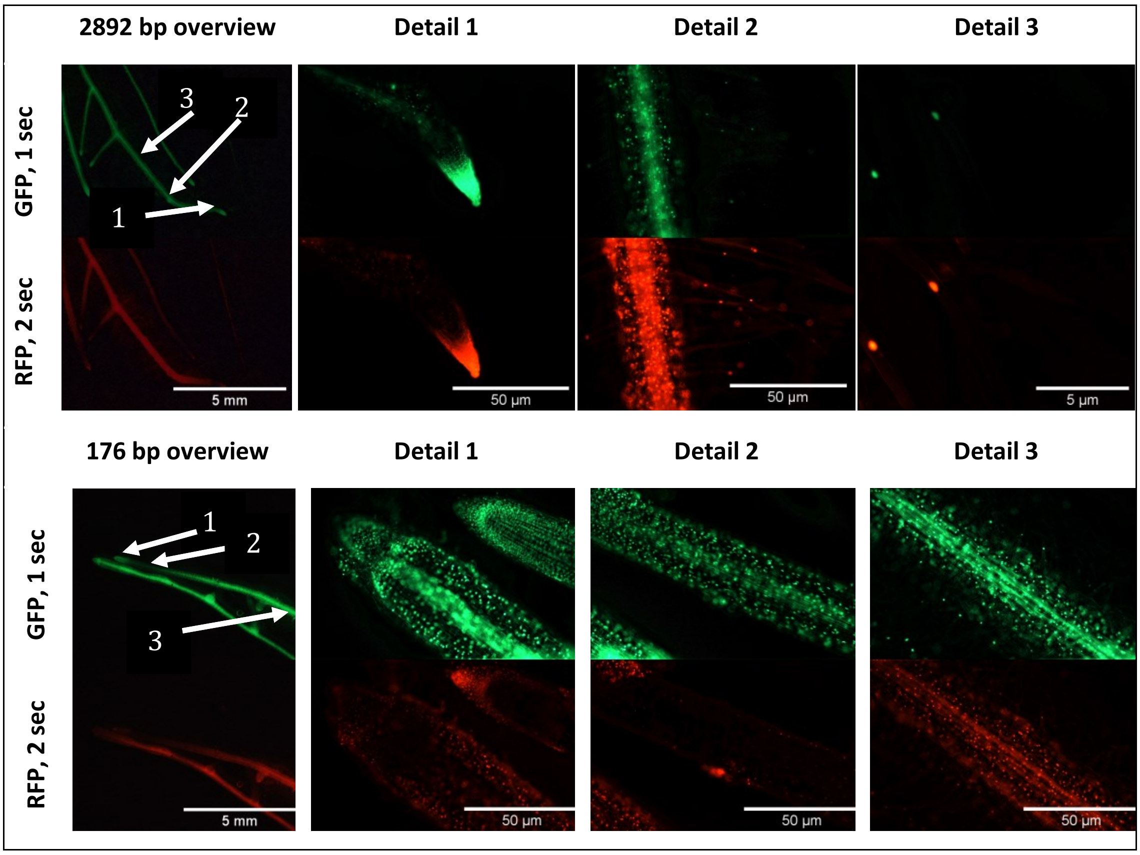

Figure 43. Visualization of the promoter activity of a 2892 bp and 176 bp promoter region from *Potri.2G0797* in first order roots. The promoters were amplified from *Populus tremula x tremuloides* gDNA and its activity is visualized in nuclei of *P. tremula x alba* plants. Composite plants were generated via *Agrobacterium rhizogenes* strain K599 mediated plant transformation. The T-DNA of the used pCXUN vector backbone contained a Promoter_dGFP-NLS_T_{NOS}_P_{NOS}_tdTomato-NLS_T_{OCS} cassette. Overview pictures were made with a Leica binocular and detailed pictures were obtained from a Zeiss microscope (specifications in the M&M). All pictures were made under the same conditions. Additionally, the roots are shown under bright - field conditions. The roots all were 5 to 8 weeks old. For visualization, corresponding pictures were processed in the same manner in a montage (background subtraction and contrast enhanced by 0.1 % in ImageJ).

To confirm similar expression patterns of the 2892 bp and 176 bp promoter fragments, GFP:RFP ratios of the fluorescence intensities obtained from ImageJ were calculated for root hair nuclei of the same age. No significant differences were found when comparing ratios of five roots from independent transformation events (2892 bp: n = 4 roots, mean = 1, SE = 0.6; 176 bp: n = 4 roots, mean = 3.5, SE = 0.4; Effect size = 0.2, **Figure 44**). Thereby, each root replicate was a mean value obtained from three to ten single root hair nuclei.

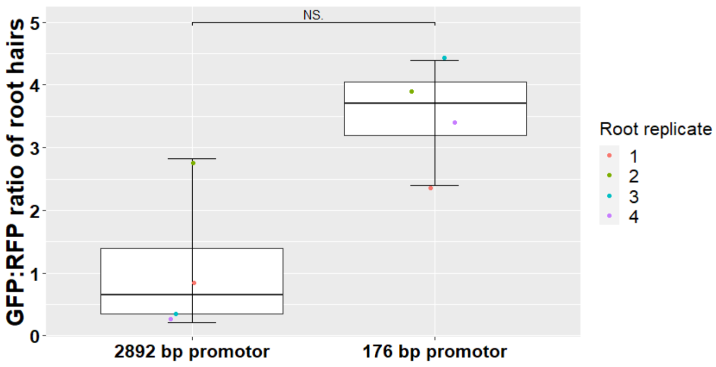

Figure 44. Boxplot with jitter dots comparing GFP:RFP ratios of the 2892 bp promoter fragment of *Pori.2G0797* against the 176 bp fragment in transgene *Populus tremula x alba* root hairs. The GFP-NLS is driven by the respective promoter, whereas tdTomato-NLS is driven by the constitutively expressed NOS promoter (Promoter_dGFP NLS_T_{NOS}_P_{NOS}_tdTomato-NLS_T_{OCS}) NLS means the protein was targeted to the nucleus. For each construct four root replicates were analyzed. The value given for the roots are a mean value of three to ten single nuclei each. The standard error and significances calculated based on a Wilcoxon test are given. NS = not significant. Statistics were conducted in R as specified in the M&M.

No obvious GFP signal was detected in the range of 113 bp to 61 bp. The findings are shown in **Figure 45**. For each construct at least five technical replicates from two independent plant experiments were taken. Shown are representative images. To avoid bleaching, the average total illumination time per channel was not longer than two minutes.

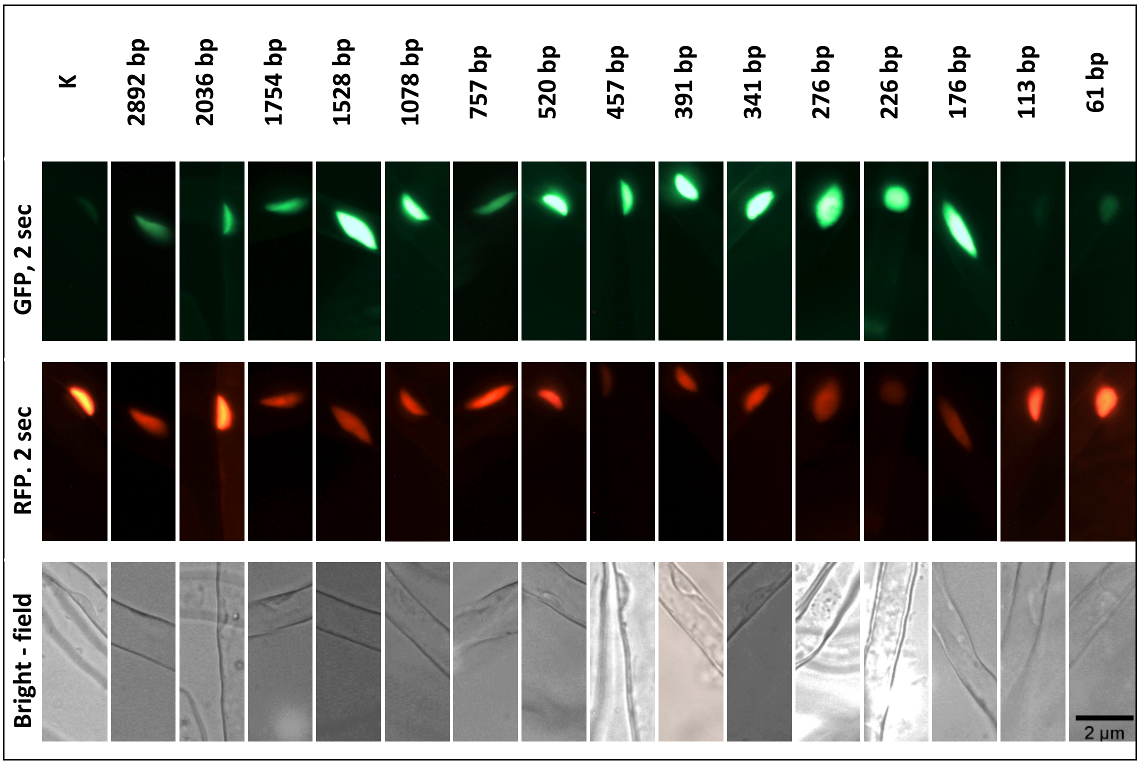

Figure 45. Single nuclei in transgenic root hairs containing promoter truncations of *Potri.2G0797* in a double marker construct (Promoter_dGFP-NLS_T_{NOS}_P_{NOS}_tdTomato-NLS_T_{OCS}). The truncations range from -61 bp to -2892 bp. K is the negative control harbouring a promoter less GFP. The 2892 bp promoter fragment was amplified from *Populus tremula x tremuloides* gDNA, truncated with 5´deletion and visualized in transgenic *P. tremula x alba* plants. Shown are randomly picked nuclei of main roots that were illuminated for 2 sec in both the GFP and RFP channel at the lowest possible light intensity (25 %) with xenon light source at a Zeiss Axioskop Microscope. Pictures were made with a Imagingsource camera in an IC Capture software. Filter sets for GFP were in a 450 – 490 nm excitation and 510 – 560 nm emission window and for RFP in a 510 – 560 nm excitation and 590 nm long pass emission filter window filter with a 580 nm beam splitter. Further details are given in the M&M. Additionally, root hairs are shown under bright - field conditions. The roots were 4 to 7 weeks old and in approximately the same growth state. For better visualization, the illumination time and contrast were edited. All pictures were processed under the same conditions to avoid distortions inf Apple Fotos. Thereby, the contrast was enhanced by 1. Each picture is representative for at least five nuclei from different plants.

The 2892 bp and 113 bp promoter fragments were also analysed in transient tobacco leaves to determine if the same results can be obtained in a different system. It could be shown that the promoter activity behaved the same in composite poplar plants and transient transformed tobacco leaves (**Figure 46**).

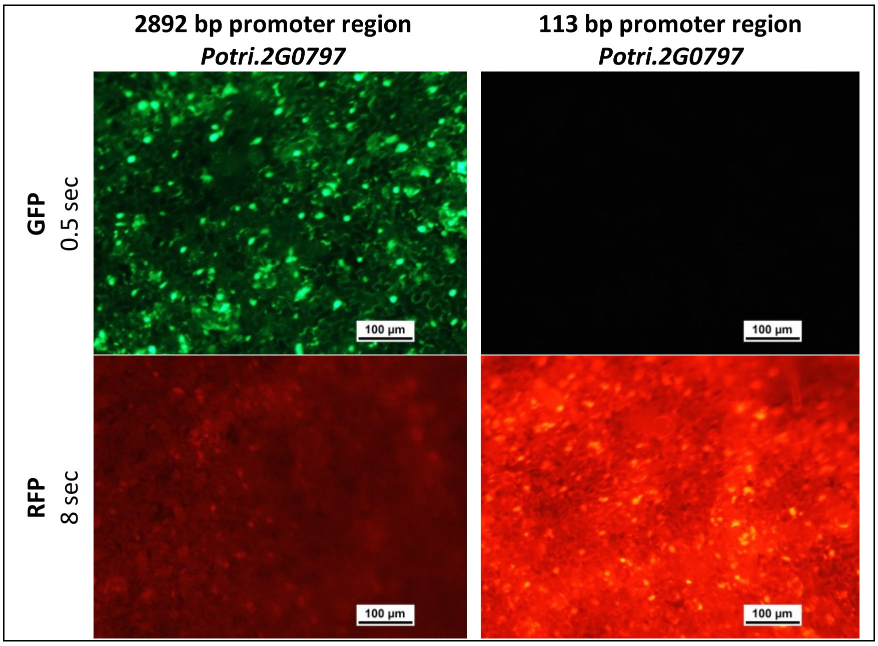

Figure 46. Promoter activity of 2892 bp and 113 bp promoter fragments from *Potri.2G0797* in a promoter reporter double cassette approach in *Nicotiana benthamiana* leaves. Tobacco leaves were transiently transformed with *Agrobacterium rhizogenes* strain K599 in an OD_{600} of 0.3. The binary vector was pCXUN and the T-DNA was composed of the respective promoter fragment, dGFP-NLS and a NOS terminator as well as a second constitutively expressed NOS promoter, tdTomato-NLS and OCS terminator cassettes. NLS means the protein was targeted to the nucleus. Pictures were obtained with a Leica binocular with a gain of 4.7 dB three days after the infiltration. All pictures were processed in the same manner. Further details about the devices and settings can be found in the M&M.

3.6.3 Using different poplar hybrids for promoter analysis?

Because *Potri.2G0797* was amplified from *P. tremula x tremuloides* but observed in *P. tremula x alba* for handling reasons it was tested whether this had impacts on the FP expression. However, in hybrid plants of *P. tremula x tremuloides* containing identical constructs compared to *P. tremula x alba* hybrids no obvious differences were found (**Figure 47**). For a further comparison, GFP:RFP ratios of root hair nuclei of the same age from different roots of independent transformation events were compared (**Figure 48**). No significant differences were found (*P. tremula x alba*: n = 4 roots, mean = 1.08, SE = 0.6; *P. tremula x tremuloides* n = 2 roots, mean = 0.66, SE = 0.26; Wilcoxon-Mann-Whitney-U test, Effect size = 0.45). Thereby, the ratios per root were calculated based on means of three to ten single nuclei each.

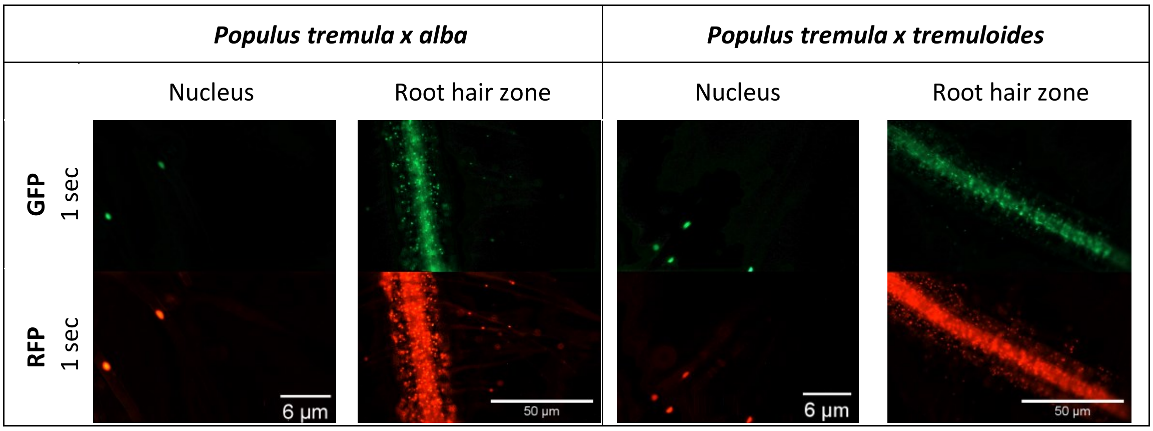

Figure 47. Comparing GFP fluorescence intensities driven by the 2892 bp promoter fragment of *Potri.2G0797* in first order roots between *Populus tremula x alba* and *Populus tremula x tremuloides* plants. Composite plants were generated via *Agrobacterium rhizogenes* strain K599 mediated plant transformation using a Promoter_dGFP NLS_T_{NOS}_P_{NOS}_tdTomato-NLS_T_{OCS}. Pictures were obtained from a Zeiss microscope (specifications in the M&M). All pictures were made under the same conditions. The roots all were 3 to 5 weeks old. For visualization, the pictures were processed in the same manner in ImageJ (In merged pictures of both corresponding channel pictures: Contrast of root hairs increased by 0.01 % and of cortex regions by 0.1 %, background subtracted). All pictures were taken with the same parameters (gain = 4.8 dB, light intensity = 25 %) as further described in the M&M.

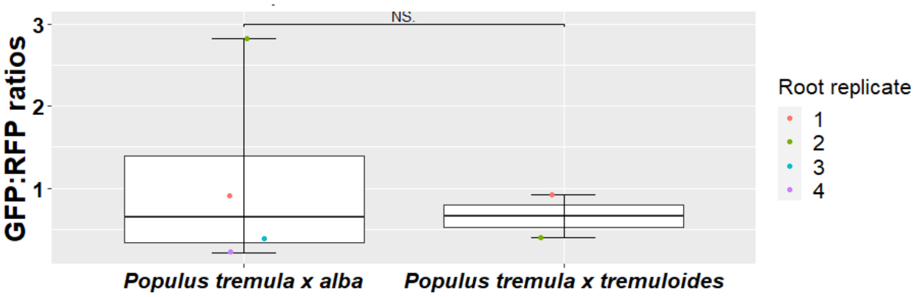

Figure 48. Boxplot with jitter dots comparing GFP:RFP ratios of the 2892 bp promoter fragment of *Pori.2G0797* in *Populus tremula x alba* and *P. tremula x tremuloides* hybrids. The GFP-NLS is driven by the respective promoter, whereas tdTomato-NLS is driven by the constitutively expressed NOS promoter (Promoter_dGFP-NLS_T_{NOS}_P_{NOS}_tdTomato-NLS_T_{OCS}) NLS means the protein was targeted to the nucleus. *P. tremula x alba*: n = 4 roots. *P. tremula x tremuloides*: n = 2 roots. The value given for each root is a mean value of three to ten single nuclei to compensate for biological fluctuations. The standard error and significances calculated based on a Wilcoxon test are given. NS = not significant. Statistics were conducted in R as specified in the M&M.

3.6.4 Fluorescence intensities in mycorrhized and non – mycorrhized fine - roots

A change in the fluorescence expression pattern was observed in relation to root age. Younger fine-roots (four to eight weeks old) showed detectable GFP and tdTomato signals of the double marker cassette in root hair nuclei and the outer cortex, whereas older roots (three- to four-month-old) obtained from mycorrhized root systems only had detectable FP signals in the inner cortex regions (**Figure 49**). This observation was important when observing mycorrhized root systems because they were at least three-month-old when investigated.

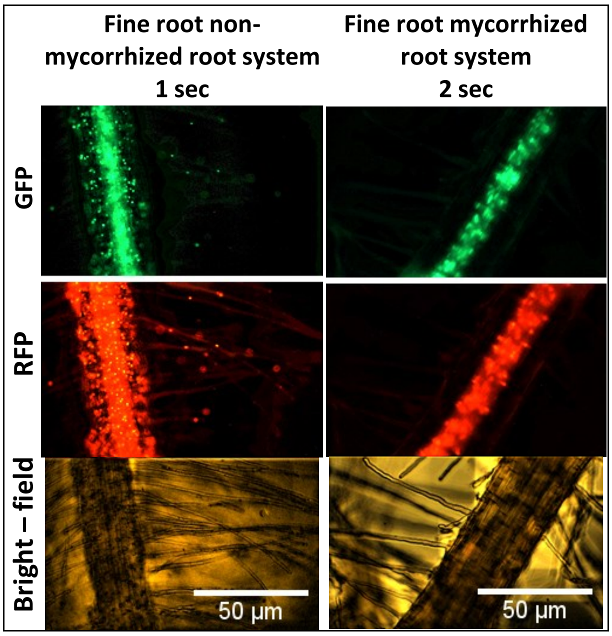
Fine root non-mycorrhized root system
1 sec
Fine root mycorrhized root system
2 sec
GFP
RFP
Bright – field
50 µm
50 µm

Figure 49. Comparison of GFP and RFP signals in non – mycorrhized fine roots of transgenic poplar hybrids shown in absence or presence of the mycorrhiza fungus *Pisolithus microcarpus*. Observed were GFP fluorescence intensities driven by the longest 2892 bp promoter fragment of *Potri.2G0797* in first order roots of *Populus tremula x tremuloides* plants. Composite plants were generated via *Agrobacterium rhizogenes* strain K599 mediated plant transformation using a Promoter_dGFP-NLS_T_{NOS}_P_{NOS}_tdTomato-NLS_T_{OCS}. Non-mycorrhized fine-roots were observed after three to four weeks, fine-roots from a mycorrhized root system after ~12 weeks. Pictures were taken at the epifluorescence microscope. All details including the filter settings, used camera and camera settings are given in the M&M. Fluorescence signals were enhanced similarly for both GFP and RFP in each sample (ImageJ: Contrast enhanced by 0.1 % and background subtracted in montages).

To find out if the amplified promoter fragment could confer gene regulation in the observed mycorrhiza dependent manner, transgenic hybrid plants harbouring the construct with the 2892 bp promoter fragment of *Potri.2G0797* were mycorrhized with *Pisolithus microcarpus* in four independent replicates. An example for a mycorrhized poplar fine root is given in **Figure 50**.

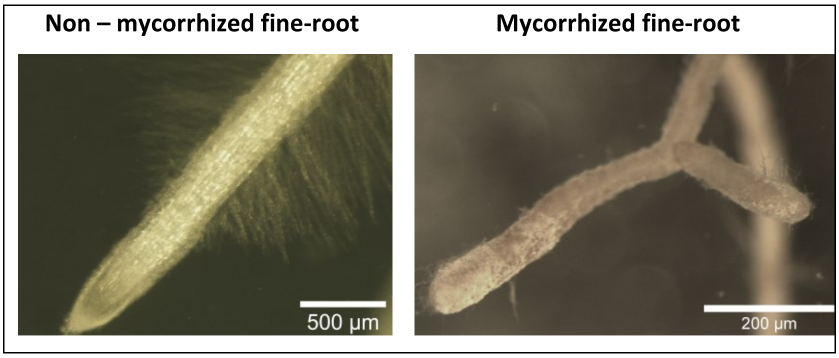
Non – mycorrhized fine-root
Mycorrhized fine-root
500 µm
200 µm

Figure 50. Example for a non-mycorrhized and mycorrhized *Populus tremula x alba* fine root. The fungal partner was *Pisolithus microcarpus*. The picture was taken with a binocular under bright field (as described in the M&M).

In further analyses of the mycorrhized fine roots at the epifluorescence microscope it was not possible to clearly distinguish FP signals from autofluorescence of the fungal mantle (**Figure 51**). Therefore, no predictions about a down-regulation of Potri.2G0797 can be made.

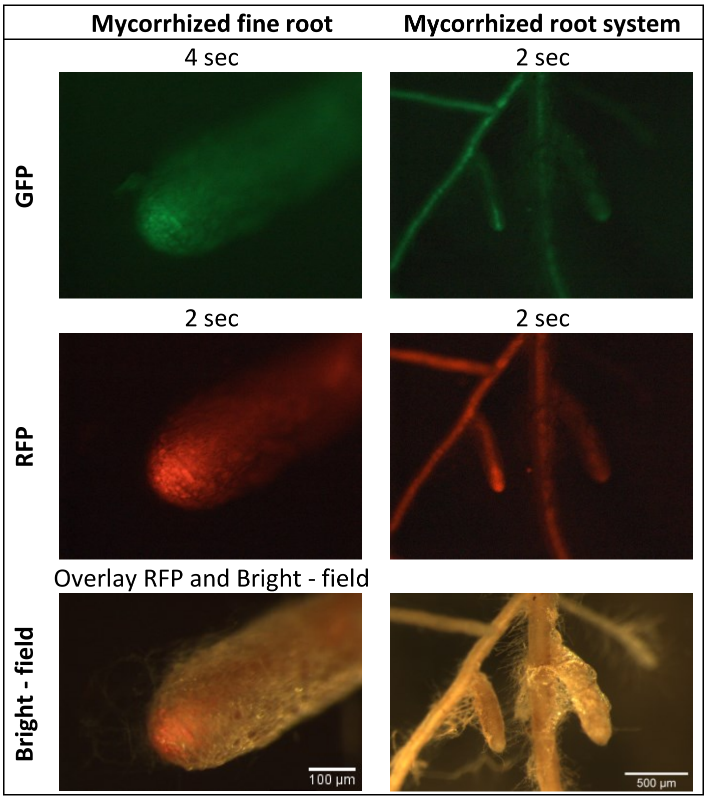
Mycorrhized fine root
Mycorrhized root system
4 sec
2 sec
GFP
2 sec
2 sec
RFP
Overlay RFP and Bright - field
Bright - field
100 µm
500 µm

Figure 51. GFP and RFP signals in a mycorrhized fine - root. *Populus tremula x alba* was mycorrhized with *Pisolithus microcarpus*. The GFP signal was driven by a 2982 bp promoter fragment of *Potri.2G0797*, whereas the tdTomato signal was driven by a NOS promoter. Both FPS were part of a double marker cassette and targeted to the nucleus. Images were taken using a binocular and filter sets are described in the M&M. Fluorescence signals were enhanced similarly for both GFP and RFP channels by increasing the contrast by 0.3 % in ImageJ.

3.7 Characterization of *Potri.2G2183*

3.7.1 Subcellular protein localization of Potri.2G2183

As for *Potri.2G0797*, a C-terminal fusion construct of *Potri.2G2183* (411 bp) and sYFP was designed and cloned by Lucas Lansing (Lansing 2015, Master thesis). The same cloning strategy as for *Potri.2G0797* was applied with the only difference, that the fusion construct was PCR amplified with added *EcoRI* restriction sites for cloning into pPLV (**Figure 36**). The initial PCR fragment (Forward primer P2G2183CDSEcoR1-f1 and revers primer 15-9SLfusRevEcoRI, see Table 7) was verified in pJET1.2 by restriction digestion (**Supplementary figure 20**) and partial sequencing (**Supplementary figure 21**). The correct integration in pPLV was verified with restriction digestion and sequencing (**Supplementary figure 21**). In a last step, the P_{35S}_ *Potri.2G2183*_sYFP_T_{OCS} was released by *KpnI* and *SacI* restriction sites and cloned into the above described modified pCXUN vector *KpnI/SacI* restriction sites (**Supplementary figure 22**).

For *Potri.2G2183*, no additional red expression cassette was cloned in tandem to the fusion cassette on the pCXUN T – DNA. As for *Potri.2G0797*, no sYFP fluorescence signals were obtained at the epifluorescence microscope after transient transformation into tobacco leaves.

3.7.2 Promoter analyses of Potri.2G2183

A 3551 bp promoter fragment of *Potri.2G2183* was successfully PCR amplified from *P. trichocarpa* gDNA, ranging from -3551 bp and 0 bp in relation to the ATG (**Supplementary figure 23**). The PCR fragment was initially cloned into pJET1.2 and verified via restriction digestion (not shown). A further PCR amplification with added 5´ *KpnI* and 3´*HpaI* restriction sites was performed (Forward primer ID5_KpnI_for and revers primer ID5_HpaI_rev, see Table 6) and the obtained fragment introduced into pCXUN as described for the 2892 bp promoter fragment of *Potri.2G0797* (**Figure 39**). The obtained plasmid was verified with restriction digestion (**Supplementary figure 24**) and sequencing (**Supplementary figure 25**).

The 3551 bp promoter fragment was further truncated based on PCR amplifications with added 5´ *KpnI* and 3´ *HpaI* restriction site overhangs. Template for the PCR was the pCXUN double marker construct with the 3551 bp promoter fragment and the 5´primer was used to generate the 5´deletions. Overall, 2502 bp (Forward primer ID5-2502bp-KpnI and revers primer ID5_HpaI_rev), 1289 bp (Forward primer ID5-1289bp-KpnI and revers primer ID5_HpaI_rev) and 516 bp (Forward primer ID5-516bp-KpnI and revers primer ID5_HpaI_rev) fragments were generated (**Figure 52**). The primer details are given in the M&M **Table 6**. Further cloning steps to integrate the amplicons into pCXUN (**Figure 14**) were conducted as described above. The obtained constructs were verified with restriction digestion (**Supplementary figure 26**).

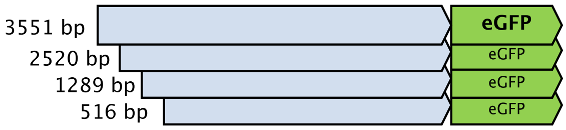

Figure 52. Promoter fragments of *Potri.2G2183*from *Populus trichocarpa* that were coupled to a reporter (eGFP) to identify regulatory elements in this gene upon ectomycorrhiza formation. The eGFP was targeted to the nucleus. Transgenic poplar roots were generated with Agrobacterium mediated plant transformation, during which Composite plants were generated. The eGFP expression was compared between the constructs visually at a microscope and determined by qPCR.

First tests of the 3551 bp promoter fragment in transiently transformed *Nicotiana benthamiana* leaves showed both GFP and RFP signals in the nucleus compared against a negative control with a promoter less GFP (**Figure 53**).

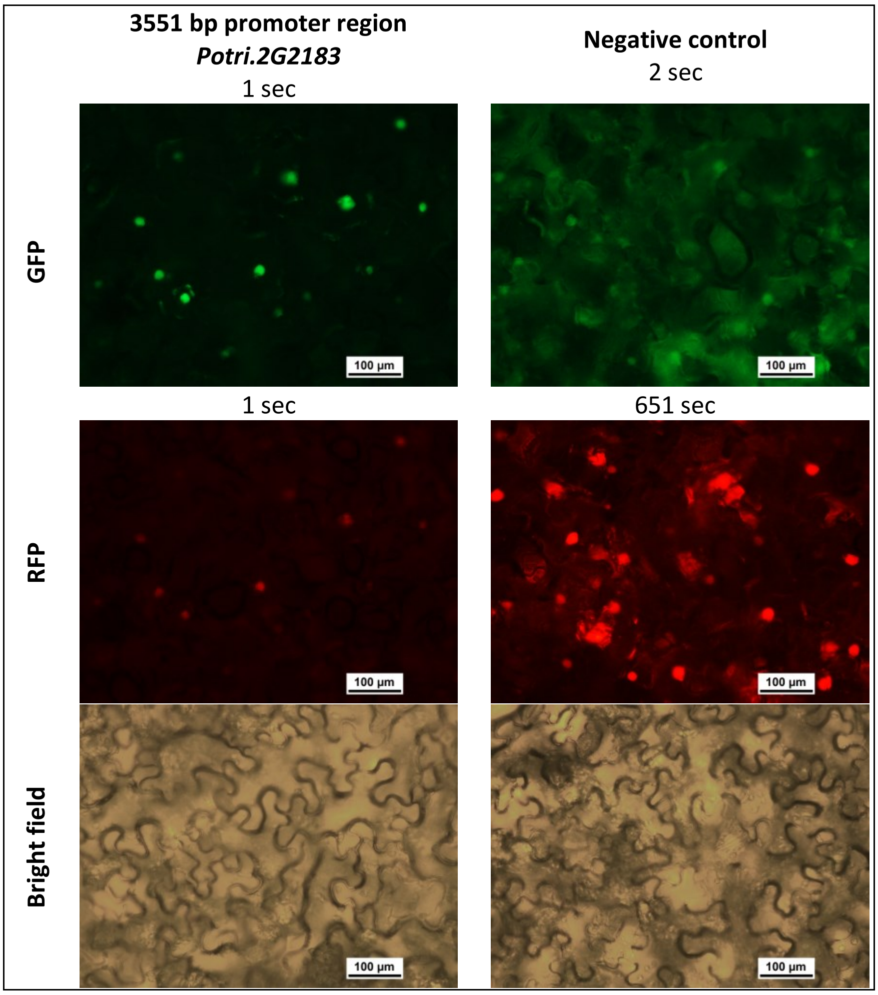

Figure 53. Visualization of the promoter activity of a 3551 bp promoter fragment from *Potri.2G2183* driving nuclear targeted GFP expression in transiently transformed tobacco leaves in a double marker construct. As negative control a promoter was GFP less. Tobacco leaves were transiently transformed with *Agrobacterium rhizogenes* strain K599 in an OD_{600} of 0.3. The binary vector was pCXUN and the T-DNA was composed of the respective promoter fragment, dGFP-NLS and a NOS terminator as well as a second constitutively expressed NOS promoter, tdTomato-NLS and OCS terminator cassettes. NLS means the protein was targeted to the nucleus. Pictures were obtained with a Leica binocular with a gain of 4.7 dB three days after the infiltration. All pictures were processed in the same manner. Further details about the devices and filter settings can be found in the M&M.

In planta tests of the 3551 bp promoter fragment and its truncations in transgenic *Populus tremula x alba* first order roots showed very weak overall GFP signals in the range of 3551 bp to 1289 bp (**Figure 54**). Only the 516 bp truncation showed detectable GFP signals in root hair and cortex nuclei when compared against a positive (GFP with UBQ promoter) and negative control (GFP promoter less)

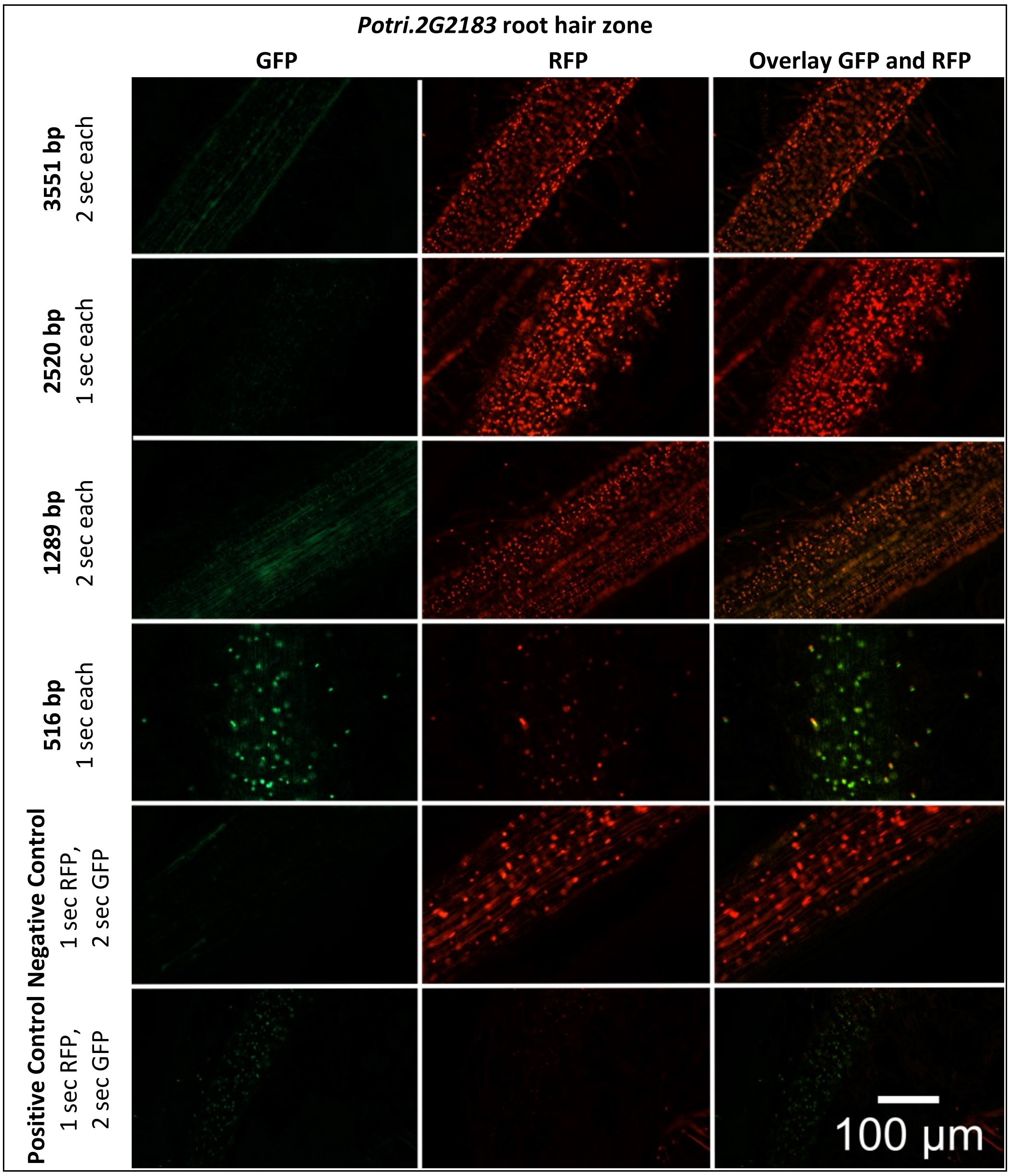
Potri.2G2183 root hair zone
GFP
RFP
Overlay GFP and RFP
3551 bp
2 sec each
2520 bp
1 sec each
1289 bp
2 sec each
516 bp
1 sec each
Negative Control
1 sec RFP,
2 sec GFP
Positive Control
1 sec RFP,
2 sec GFP
100 µm

Figure 54. Promoter activity of *Potri.2G2183* promoter truncations in a double marker construct (Promoter_dGFP-NLS_T$_{NOS}$_P$_{NOS}$_tdTomato-NLS_T$_{OCS}$). The truncations range from -516 bp to -3551 bp. The negative control harbouring a promoter less GFP and the positive control harbours GFP driven by a NOS promoter. The 3551 bp promoter fragment was amplified from *Populus trichocarpa* gDNA, truncated with 5´deletion and visualized in transgenic *P. tremula x alba* plants. Shown are root hair areas 1 cm above the root tip. Roots were illuminated at the lowest possible light intensity (25 %) with xenon light source at a Zeiss Axioskop Microscope. Pictures were made with a Imagingsource camera in an IC Capture software. Filter sets for GFP were in a 450 – 490 nm excitation and 510 – 560 nm emission window and for RFP in a 510 – 560 nm excitation and 590 nm long pass emission filter window filter with a 580 nm beam splitter. Further details are given in the M&M. The roots were 5 to 8 weeks old and in approximately the same growth state. For visualization the contrast enhanced by 0.01 % and background subtracted in ImageJ (further details in the M&M). Representative pictures are given for n = 10 plants per construct from two independent transformation events.

Because of their different expression patterns, the 3551 bp and 516 bp promoter fragments were further compared concerning their GFP levels. Green and red fluorescence in nuclei were observed in the root tip, root hairs and the stele for both promoter fragments, indicating active transcription in those areas (**Figure 55**). However, comparisons of root hair nuclei indicate a higher GFP expression under the 516 bp truncation (**Figure 56**). Furthermore, the 516 bp fragment induced high levels of autofluorescence particularly in the stele. Because the plane of focus of epifluorescence microscope and binocular did not reach further then the first cortex layers, no predictions can be made concerning promoter activity in the endodermis and central cylinder.

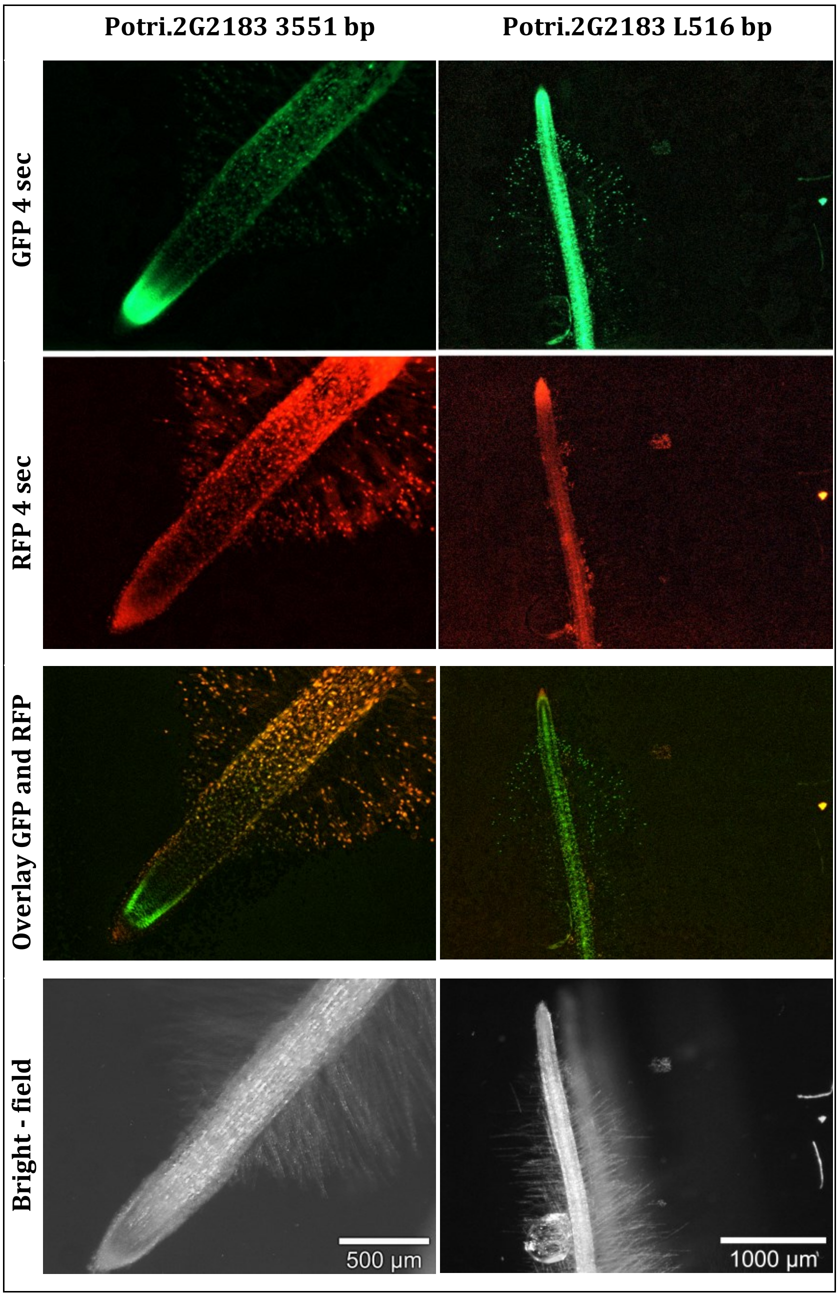

Figure 55. Comparing GFP fluorescence intensities driven by 3551 bp and 516 bp promoter fragments of *Potri.2G2183* in first order roots. Composite plants were generated via *Agrobacterium rhizogenes* strain K599 mediated plant transformation using a Promoter_dGFP-NLS_T_{NOS}_P_{NOS}_tdTomato-NLS_T_{OCS}. Pictures were obtained from a Leica binocular (specifications in the M&M). All pictures were made under the same conditions. The roots all were 5 to 8 weeks old. For visualization, the pictures were processed in the same manner in ImageJ (In merged pictures of both corresponding channel pictures: Contrast of root hairs increased by 0.1 %, background subtracted). All pictures were taken with the same parameters (gain = 4.8 dB, light intensity = 25 %) as further described in the M&M.

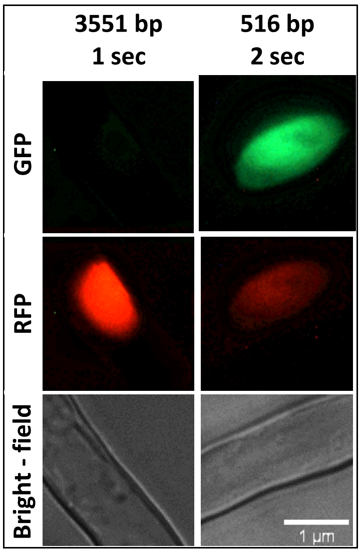

Figure 56. Comparing GFP fluorescence intensities driven by 3551 bp and 516 bp promoter fragments of *Potri.2G2183* root hair nuclei of first order roots. Composite plants were generated via *Agrobacterium rhizogenes* strain K599 mediated plant transformation using a Promoter_dGFP-NLS_T_{NOS}_P_{NOS}_tdTomato-NLS_T_{OCS}. Pictures were obtained from a Zeiss microscope (specifications in the M&M). All pictures were made under the same conditions. The roots all were 5 to 8 weeks old and root hairs of approximately the same age were compared. For visualization, the pictures were processed in the same manner in ImageJ (In merged pictures of both corresponding channel pictures: Contrast of root hairs increased by 0.1 %, background subtracted). All pictures were taken with the same parameters (gain = 4.8 dB, light intensity = 25 %) as further described in the M&M.

3.8 Characterization of *Potri.9G1040*

3.8.1 Promoter analyses and the identification of transcription factors of Potri.9G1040

The longest promoter fragment that could be PCR amplified for *Potri.9G1040* had a size of 1183 bp and ranged from -1185 bp to -2 bp in relation to the ATG. In a first step, this 1183 bp promoter fragment was successfully amplified from *Populus tremula x tremuloides* gDNA (Forward primer pJetUnivLIC_R1 and revers primer pJetUnivLic_rF1, see **Table 6**). The PCR fragment was initially cloned into pJET1.2 and verified via restriction digestion (**Supplementary figure 27** and **Supplementary figure 28**) and partial sequencing (**Supplementary figure 29**). In a further cloning step, the promoter fragment was PCR amplified with LIC adapters (Forward primer pJetUnivLIC_R1 and revers primer pJetUnivLic_rF1, see **Table 8**) and integrated into a pCXUN double marker cassette using LIC (vector description **Figure 15**). The correct integration was verified with restriction digestion (**Supplementary figure 30**) and sequencing (**Supplementary figure 31**).

In planta tests of this 1181 bp promoter gave no detectable GFP signals when using the epifluorescence microscope (**Figure 57**). Attempts to amplify a larger promoter fragment from either *Populus tremula x tremuloides* or *P. trichocarpa* failed.

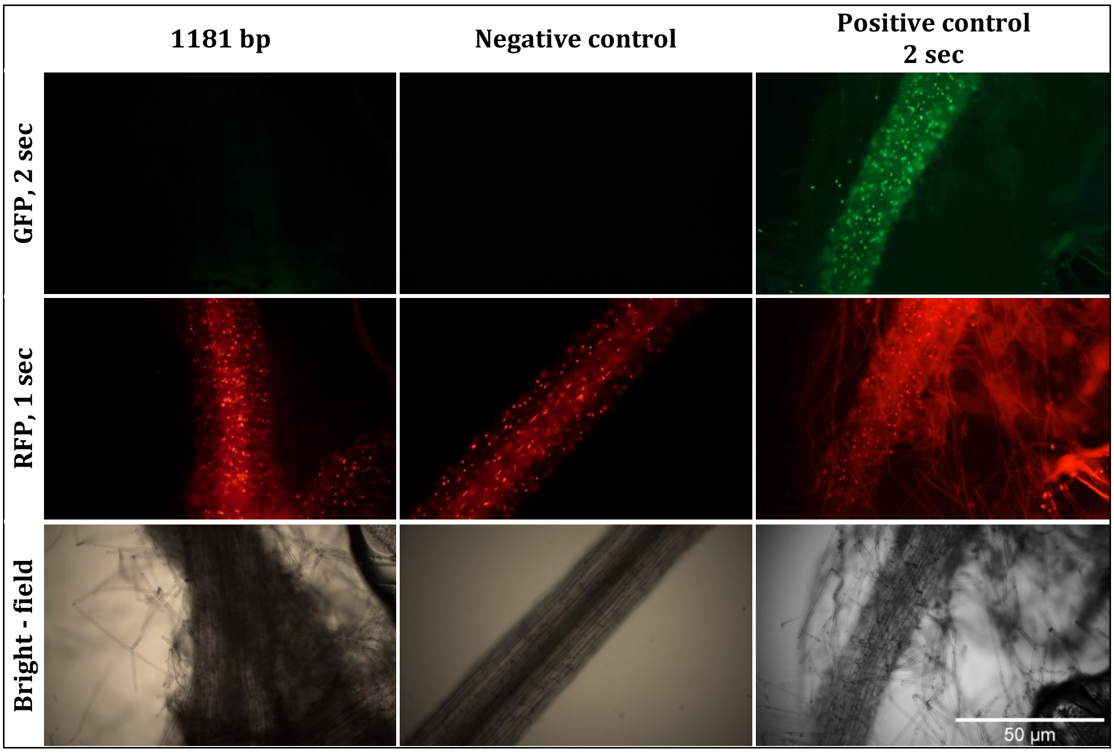

Figure 57. Promoter activity of a *Potri.9G1040* 1181 bp promoter fragment in a double marker construct (Promoter_dGFP-NLS_T_{NOS}_P_{NOS}_tdTomato-NLS_T_{OCS}). The negative control harbours a promoter less GFP and the positive control harbours GFP driven by a NOS promoter. The promoter fragment was amplified from *Populus tremula x tremuloides* gDNA and visualized in transgenic *P. tremula x alba* plants. Roots were illuminated at the lowest possible light intensity (25 %) with xenon light source at a Zeiss Axioskop Microscope. Pictures were made with a Imagingsource camera in an IC Capture software. Filter sets for GFP were in a 450 – 490 nm excitation and 510 – 560 nm emission window and for RFP in a 510 – 560 nm excitation and 590 nm long pass emission filter window filter with a 580 nm beam splitter. Further details are given in the M&M. The roots were 5 to 8 weeks old and in approximately the same growth state. For visualization the contrast enhanced by 0.1 % (further details in the M&M). Representative pictures are given for n = 10 plants per construct from two independent transformation events.

4 Discussion

4.1 Establishing pCXUN as poplar root transformation vector

4.1.1 Plant transformation efficiencies of the binary vectors pPLV and pCXUN

In composite poplar plants, transgenic roots originate from microcalli of transgenic cells from non – transgenic shoots. This method was established to generate fast transgenic roots compared to entirely transgenic plants and can be used for *in vivo* promoter analysis (Neb et al., 2017). However, next to the T – DNA of interest, a second T – DNA from an Ri – plasmid is transferred to the infected plant cell and drives efficient transformation of transgenic roots (Suzuki et al., 2009; Chandra, 2012; Xiang et al., 2016). Both T – DNAs are transferred into plant cells, but not always at the same time and in the same frequency. Therefore, transgenic roots that are formed by composite plants must be checked for the presence of the binary vector derived T – DNA, which are further called “fully transgenic roots”. The approach for their detection that was followed in this thesis was a second marker cassette on the binary T – DNA, leading to the accumulation of a red fluorescence protein in the nuclei of fully transgenic roots. In this context, the two binary vectors “pPLV and pCXUN” were tested in this work concerning the frequency of *Agrobacterium rhizogenes* (strain K599) formation of fully transgenic roots. This further called “transformation efficiency” was thereby defined as the percentage of fluorescent roots of one transgenic composite poplar. For different approaches, either single or double fluorescence marker cassettes were used as reporters. pPLV vectors that were used for comparative analysis were implemented by Jana Schnakenberg and Jana Müller (AG Nehls).

Initially, different marker cassettes (single and double cassettes) were transferred from pPLV to pCXUN in this thesis. The obtained constructs were then transformed together with the pPLV ancestors into different batches of *Populus tremula x alba* plants. It turned out, that the overall transformation efficiency was 69.8 % higher when modified pCXUN vectors were used compared to pPLV based vectors (**Figure 12**). A transformation efficiency as obtained with different pCXUN derivates of 76 % (SE = 2.6) is suitable for the intended promoter analyses and was like results from other studies (Porter and Flores 1991, Neb et al. 2017). No low copy number vectors were used because they were less suitable for cloning purposes. Also, In other plant systems pCXUN was successfully used, e.g. in *Arabidopsis thaliana* transformation using floral dip (Kempinski and Chappell, 2019), *Nicotiana benthamiana* leaves (Das, 2018; Schnakenberg, 2020) or studies in rice (Meng et al., 2021). pCXUN works also for plant transformations using different *Agrobacterium tumefaciens* strains (such as GV3101, data not shown). This allows to use pCXUN constructs for transformation of different plant species but also for the generation of transient or stable transgenics.

In addition to its lower root transformation efficiencies, pPLV needs an additional “helper plasmid” (pSOUP) for successful replication, whereas pCXUN does not. Furthermore, two different antibiotics are needed for the cultivation of agrobacteria containing pPLV and pSOUP (Schnakenberg, 2020). This might reduce the fitness of *Agrobacterium* in plant infection and might thus explain the observed lower root transformation efficiency in composite poplar plants. As a consequence of differing ORIs in pPLV and pCXUN, pCXUN might also achieve a higher plasmid copy number in the used *Agrobacterium rhizogenes* (strain K599) resulting in a higher root transformation efficiency, even though more data are needed for validation (Gelvin, 2003; Schnakenberg, 2020).

4.1.2 Impacts of the orientation of the expression cassette in the pCXUN T-DNA

Location and orientation of expression cassettes in the T – DNA of binary vectors might influence fluorescence protein (FP) expression. One reason is, that the right- and left border sequences resist different to endo- and exonucleases during T - DNA transport into the nucleus of the host plant. While the right border is better protected because of virD2, which is attached to the respective end of the T-DNA, the left border sequence remains unprotected and only 25% stay intact (Tzfira et al., 2004; Gelvin, 2017). Thus, deletions extending from the LB junction were found to be larger compared to deletions extending from the RB (Gelvin, 2017).

To investigate the impact of marker cassette orientation on FP expression in composite poplar plants (**Figure 16**), both orientations were tested concerning their root transformation efficiency. For single expression cassettes, an orientation from RB to LB gave a slightly better transformation efficiency, whereas double fluorescence cassettes had a better transformation efficiency when the cassettes were orientated from LB to RB on the T – DNA. However, this might be related to the constructs that were observed. All single marker cassettes in LB-RB orientation on the T – DNA were targeted to the peroxisomes (tmTomato and sYFP), which were harder to locate with the binocular and might have led to an underestimation of transformation efficiency in this orientation. Additionally, only one of the compared double marker constructs had an RB-LB orientation on the T – DNA (**Table**

26), which might lead to a skewed comparison. For this reason, both datasets with single and double marker constructs were combined for a pooled analysis. Thereby, no overall differences were observed when comparing both double and single marker cassettes together, indicating that the root transformation efficiency is possibly independent on the marker cassette orientation on the T – DNA of the plant transformation vector. The most likely explanation for this observation is a kanamycin resistance cassette that is present at the left border of the pCXUN T – DNA (**Figure 58**). It can be assumed, that this cassette serves as a buffer concerning exonuclease activity and thus no obvious difference in fluorescence expression levels was observed for both orientations of the marker cassette(s). No other combinations of possible orientations of the individual parts of the T – DNA were tested.

Based on these findings it was decided to use a LB to RB orientation of the fluorescence expression cassettes for all further constructs. For double marker constructs, both expressions were in tandem on the T – DNA (**Figure 58** and **Figure 16**). A set of two pCXUN based binary vectors was designed for the easy integration of promoter fragments in a double marker cassette in collaboration with other group members of AG Nehls. Thereby, GFP was used as a reporter for investigated promoters and tdTomato was used as a constitutively expressed reference reporter protein. The only difference between the two vectors was, that one contained a UBQ promoter driving the GFP expression cassette (**Figure 58**), whereas the other vector had a LIC site at this location. This allowed for a directed integration of promoter fragments either by exchanging the UBQ promoter using a conventional restriction site-based strategy or implementing them by using LIC.

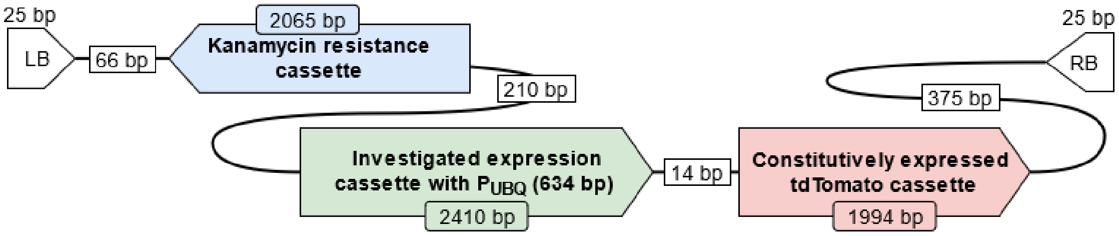
25 bp
LB
66 bp
2065 bp
Kanamycin resistance cassette
210 bp
Investigated expression cassette with P_{UBQ} (634 bp)
2410 bp
14 bp
Constitutively expressed tdTomato cassette
1994 bp
375 bp
25 bp
RB

Figure 58. Schematic display of a pCXUN T – DNA harbouring two fluorescence marker cassettes. Shown are the components of the T – DNA and their respective size in bp. A kanamycin resistance cassette serves as plant selection marker. LB: left border- and RB: right border sequence. The investigated expression cassette was composed of a UBQ promoter or the promoter of a gene of interest (Investigated expression cassette), a nucleus targeted eGFP and a NOS terminator. The constitutively expressed a constitutively expressed tdTomato cassette consisted of a NOS promoter, a nuclear targeted tdTomato and an OCS terminator. The total T – DNA size was 7.2 kb. The numbers between the elements indicate the number of spacer base pairs between the elements.

4.1.3 Plant transformation efficiencies of single and double marker cassettes

The complete T – DNA as shown in (**Figure 58**) had size of 7.2 kb when containing the relatively small UBQ promoter (634 bp) in the investigated expression cassette of a double marker construct. This size drastically increases when integrating a promoter fragment of a gene of interest (3- to 4 kb). Therefore, it was tested whether differences in composite poplar plant transformation efficiency eventually differ between single and double marker cassettes because of the T – DNA sizes. However, a comparison of several single and double cassette construct revealed no such differences. Thereby, the smallest tested expression cassette had 1.5 kb and the longest double cassette was composed of 7.3 kb. Thus, it can be hypothesized, that the T – DNA transfer is not impacted by the tested sizes. Main reason for this might be, that the T – DNA of wild type plasmids can be larger than 20.000 bp, which was at least reported for *Agrobacterium tumefaciens* strains pTiC58 and pTi15955 (Barker et al., 1983; Gielen et al., 1999). This is approximately 2.7 times larger compared to the T – DNA of a double cassette with the green expression cassette driven by P_{UBQ}.

Not evaluated was, if fluorescence expression patterns or the overall expression strength of double marker cassettes differs when compared to the respective single cassettes. This could be tested by determining fluorescence intensities of transgenic composite poplar plants containing the constitutively expressed tdTomato cassette once as a single cassette and once as part of a double cassette. This analysis might be complemented by additional qPCR data investigating the FP expression strength in single and double marker constructs. Such investigations might reveal a possible overloading of the transcription machinery, which might result in gene silencing of one or both FPs and thus impact predictions concerning promoter activity (Hernandez-Garcia and Finer, 2014).

4.2 Fluorescence reporters for the investigation of promoter activity

To characterize three genes that are down – regulated upon ECM symbiosis formation, promoter analysis was performed in composite poplar plants. The promoters of interest were integrated into the T – DNA of pCXUN, driving nuclear targeted double GFP as reporter for the visualization of gene expression strength. Thereby, it was aimed to quantify gene expression levels on a visual scale *in vivo* to **(1)** find *cis* – regulatory elements within the promoter region using 5´truncations and **(2)** determine, whether qPCR-based expression profiles of the genes in mycorrhized- compared to non-mycorrhized fine-roots can be confirmed with fluorescence marker cassettes.

4.2.1 Calibration of double fluorescence marker cassettes for promoter analysis

To be able to detect transgenic plants in composite poplar plants, a second constitutively expressed marker cassette was added in tandem to the GFP expression cassette. T – DNA of pCXUN always consisted of a nuclear targeted double eGFP driven by the promoter of interest and a constitutively expressed nuclear targeted fluorescence cassette with tdTomato as a transformation marker with a dual function: **(1)** for the detection of transgenic roots in composite poplar plants and **(2)** as a reference to calibrate GFP fluorescence intensity. GFP and tdTomato were used as reporters, because their emission wavelength could be well distinguished by epifluorescence microscopy (Shaner et al., 2004; Chudakov et al., 2005; Morris et al., 2010) and cLSM microscopy (Sahoo et al., 2009).

The constitutively expressed RFP fluorescence cassette consisted of a NOS promoter, tdTomato and OCS terminator and was implemented in collaboration with Jana Schnakenberg (Schnakenberg, 2020). *In planta* analysis showed, that the NOS promoter is functional in both transiently transformed tobacco leaves and roots of composite poplar plants (Schnakenberg, 2020). Its expression strength and fluorescence distribution in different tissues for both stable and transient expression analyses was also supported by Ebert et al. (1987). Thereby, NOS promoter driven fluorescence proteins were evenly distributed in both root hairs and cortex cells and did not cause overly much autofluorescence in the stele. When driving tdTomato targeted to the nucleus, these properties resulted in nicely detectable nuclei (Schnakenberg, 2020), what made this construct ideal as a transformation selection marker in composite poplar plants.

Besides its function as a transformation selection marker, the RFP fluorescence cassette was used to calibrate GFP fluorescence expression, which was driven by a promoter of interest. Thereby, the fluorescence intensity of nuclear targeted GFP was related to the constitutively expressed and nuclear targeted tdTomato by calculating GFP: RFP fluorescence intensity ratios. This calibration allowed for a comparison of promoter expression levels between different constructs or promoter truncations independently of overall expression levels and root transformation efficiencies. Thereby, obtained fluorescence ratios were dependent on the GFP expression levels induced by the promoters of interest as well as the FP maturation and degradation times. eGFP matures with a $t\frac{1}{2}$ of 27 min and tdTomato of 60 min at 37°C in *E. coli* (Shaner et al., 2004; Iizuka et al., 2011; Trauth et al., 2020). Degradation times were at $t\frac{1}{2}$ of 1 day for eGFP and of 4.6 days for DsRED2 in *Drosophila* S2 cells (Verkhusha et al., 2003). Because tdTomato derived from DsRED it can be assumed, that the degradation time of both proteins might be similar. Corresponding analyses were conducted in collaboration with Jonas Lucht (AG Nehls).

First tests in composite poplar plants revealed, that it can be determined if GFP signals are higher or lower compared to RFP expression in double marker cassettes and with the timer protein. However, the calibration of this system is not finished yet. Thus far, *in planta* analysis of transgenic poplar roots was only partially possible, because most obtained images were oversaturated in the GFP channel for double marker constructs. Therefore, it was only possible to compare root hair nuclei. Root hairs are known to enlarge their vacuole and the nucleus shows basipetal movement at the cytoskeleton with age (Sato et al., 1995; Ketelaar et al., 2002; Esseling et al., 2004). The aging of root hairs was calculated to be 20 – to 24 h in *Medicago truncatula* (Mirabella et al., 2004), which might be slightly different for poplar but was not evaluated. In this time, the nucleus changes shape from roundish to elliptic, until it is moved to the base. The nuclei get compressed by the vacuole, which might impact the observed fluorescence intensities of GFP and RFP and could cause problems when comparing nuclei of root hairs with varying ages. For cortex nuclei, the high autofluorescence especially of cell walls was shown be a problem and most images could not be properly analysed. As described above and observed for a DsRED-E5 root, fluorescence gradients are possible along the root in dependence of the tissue age, because both GFP and RFP fluorescence intensities depend on the protein maturation and degradation ratio. Therefore, root tips often have higher amounts of GFP because not much GFP is degraded yet, whereas tdTomato accumulates in cells and is therefore more present in older tissues. Furthermore, protein expression was shown to be higher in young plant material compared to older transient transformed tobacco leaves (Wroblewski et al., 2005), which might likely lead to a fluorescence gradient in the root cortex.

Further studies need to investigate the extent of biological variance that occurs when calculating GFP: RFP ratios. This might be possible when implementing a double marker cassette with both GFP and tdTomato driven by the same promoter, which would allow for the comparison of FP reporters driven with the same promoter strength. Because homologous sequences in close proximity might affect gene expression stability as well as gene activity in plants (Meyer and Saedler, 1996), it might be necessary to implement functionally equivalent synthetic promoters in which the homologies are reduced (Bhullar et al., 2003). Further problems of a calibration against the used RFP cassette for calibration might be caused by the used NOS promoter. This promoter was used, because it caused visible fluorescence signals when compared to P_{35S} and P_{UBQ} (distribution in root hairs, root cortex and the central cylinder) (Schnakenberg, 2020). However, the expression strength of P_{NOS} was shown to be induced in wounded plant regions or under high auxin conditions (An et al., 1990). Because *in planta* analysis of this thesis were conducted in composite poplar, it cannot be excluded that auxin levels impact expression rates of tdTomato because of the altered root morphology (Veena and Taylor 2007).

4.2.2 The timer protein DsRED-E5

GFP and RFP ratios are supposed to reveal differences in promoter activity of promotors of interest upon ECM formation. The obtained relation of GFP and tdTomato of such double marker cassettes are dependent on different FP reporter maturation and degradation times, which might lead to problems concerning signal consistency in different root areas and the comparison of root systems with different ages. To take this into account, the timer protein DsRED-E5 was established in this work as a potential reporter for promoter analysis in composite poplar plants. This protein has a detectable GFP signal upon early stages of maturation, but the emission maximum changes to red fluorescence at later maturation stages. This allows for the detection of both GFP- and RFP signals induced by one single protein, which is solely dependent on DsRED-E5 maturation time from green to red (18 h) and its degradation time (4.6 days) and independent of transgene expression levels (Mirabella et al., 2004). Therefore, GFP and RFP fluorescence intensities were determined simultaneously to calculate GFP: RFP ratios.

In this thesis, a nuclear targeted DsRED-E5 driven by an UBQ promoter signal showed detectable GFP signals in transiently transformed tobacco leaves after 24 h. 72 h after infiltration, a red shift of the fluorescence window was clearly visible, and the signal intensity was much stronger in the red compared to the green fluorescence window (not quantified). In a next step, the functionality of nuclear targeted DsRED-E5 was analysed. Different promoters (P_{NOS} and P_{UBQ} constitutively expressed) as well as a 2892 bp promoter region of *Potri.2G0797* (mycorrhiza repressed) were used. First impressions of cortex regions of one root with the 2892 bp promoter fragment showed a GFP: RFP ratio of 0.03 (close to the root tip) to 0.05 (close to the first order root) in cortex nuclei of second order roots, which was very low compared to initial experiments conducted by Mirabella et al. (2004). They observed a steady fluorescence ratio of 0.17 in cowpea protoplasts and 2.8 in young root hairs of *Medicago truncatula* (with a constitutively expressed *ACTIN2* (*MtACT2*) promoter). This allowed them to detect up- or down regulation of genes when comparing their promoter induced DsRED-E5 ratios against the steady state of the constitutive promoter (Mirabella et al., 2004).

It was not possible to determine steady state ratios for all three promoters and obtain more overall data in this thesis, because the obtained DsRED-E5 GFP signals were often much weaker and already only barely distinguishable from background fluorescence in the investigated transgenic poplar roots. Only for one root hair a ratio of 0.22 could be observed thus far. It is unsure if DsRED-E5 is suitable for the intended purpose to detect down-regulation of promoters of interest upon ECM formation, because GFP levels in mycorrhized fine-roots would be expected to be even lower compared to protein expression in non-mycorrhized fine roots.

4.3 Epifluorescence microscopy-based quantification of fluorescence intensities

4.3.1 Defining camera settings to obtain reliable fluorescence intensities

To not distort fluorescence intensity ratios between GFP and RFP, corresponding pictures were taken with the same camera settings (light intensity, illumination time, gain factor). However, sometimes it was not possible to find camera settings for both channels because one of the two would be just over- or undersaturated. This was true for both DsRED-E5 and GFP-tdTomato double constructs.

The parameters to detect over- and undersaturation as well as impacts of light intensity and illumination time settings on fluorescence intensity were determined in collaboration with Jonas Lucht (AG Nehls). As a short summary, an exposure time above 4 sec or increase of light intensity over 25 % turned out to be problematic. This was especially true for increased light intensity, which might result in bleaching effects (Mamontova et al., 2017).

Bleaching is a common problem of fluorescence proteins (Zimmer, 2002; Waters, 2009; Mamontova et al., 2017). To avoid strong impacts of photobleaching on fluorescence protein ratios, a short pre – experiment with the defined camera settings was performed for one root hair nucleus. It turned out, that GFP and RFP behaved differently because the GFP:RFP ratios of one single root hair nucleus increased from 1.28 at 2 sec exposure time to 1.3 sec after 60 sec and to 1.45 at 120 sec exposure time (25 % light intensity, xenon light source). This increase in the GFP: RFP ratio occurred because RFP signal intensity was reduced by 19.9 % after 120 sec exposure time, while reduction of GFP signal intensity was only 3.7 %, indicating different photostability of eGFP and tdTomato. The eGFP variant has an enhanced photostability compared to the original GFP (Zajac et al., 2018). tdTomato as part of the mFruits series (Day and Davidson, 2009) has accelerated bleaching properties because the molecular chromophore structure allows an easy access of oxygen to the chromophores due to a gap in the beta barrel structure (Chapagain et al., 2011; Mamontova et al., 2017).

Because of these results, an illumination time maximum of four seconds was chosen for all other experiments for both GFP and RFP channels in this thesis. It can thus be supposed, that bleaching effects have a relatively weak impact on the results and were neglected. If the different behaviour of FPs becomes problematic in further analyses, it could be considered to apply a 2,2'-thiodiethanol (TDE) clearing prior to microscopy, as this was shown to reduce tdTomato bleaching in *Arabidopsis* tissues by influencing the refractive index of the sample (Musielak et al., 2016). Alternative strategies are the use of different RFP with altered oxygen sensitivity (Chapagain et al., 2011).

Part of this thesis was the modulation of the gain value in the camera system to evaluate, whether **(1)** this factor has impacts on the measured fluorescence intensities and **(2)** if it can be adapted for both GFP and RFP channels of corresponding pictures separately without distorting obtained fluorescence ratios. The gain amplifies the received signals from the camera sensor. The question was whether obtained fluorescence intensities can be normalized against the used gain factor. The corresponding experiment with DsRED-E5 in root hair nuclei of transgenic composite poplar plants revealed, that the measured fluorescence intensity had a relatively linear relationship to the gain value. This was evaluated by measuring fluorescence intensities of one single root hair nucleus in both GFP and RFP channels with increasing gain values. Thus, when normalizing the fluorescence intensities, obtained GFP: RFP ratios were nearly identical for all corresponding pictures of this gain series. Based on these findings it was decided to keep all factors equal and only adapt the gain value if necessary to compare FP fluorescence intensity values.

4.3.2 Autofluorescence in fluorescence microscopy

Autofluorescence of cell walls (mainly lignin), vacuole content (phenolic compounds) or chloroplasts (chlorophyll) is common in plant research. A large problem for analyses of FP light emission was background fluorescence of the cell walls, mainly in the root cortex. The problem is, that the emission light spectrum partly overlaps with GFP signals (340 – 560 nm) (Timonen, 1995; Donaldson, 2020), resulting in less autofluorescence in the RFP channel compared to the GFP channel except for chlorophyll autofluorescence (Chapagain et al., 2011). In most samples the background fluorescence was more than 50 %

of the FP (data not shown), which makes it essential to find a way to overcome this problem. This is especially true for older roots and mycorrhiza (Agerer, 1991; Timonen, 1995; Neb et al., 2017).

One way to proof whether the formed fluorescence originates from autofluorescence is a spectral analysis of the emission light by cLSM (Lambda Scan). The obtained Lambda Scan of infiltrated tobacco leaves and transformed composite poplar leaves clearly showed expected fluorescence for both eGFP and tdTomato targeted to the nuclei (Schnakenberg, 2020, Nehls unpublished). This could be determined thanks to pinholes in the filter channel, (Sahoo et al. 2009; Review: Chudakov, Lukyanov, and Lukyanov 2005) and indicates that fluorescence emission observed by epifluorescence microscopy were reliable for both GFP and RFP in plant nuclei.

However, only the upper cell layers can be analysed when observing whole roots even at the cLSM (Nehls, unpublished), leading to high amounts of autofluorescence from the cell layers beneath. This makes it impossible to investigate promoter activity in the inner cortex layers. Therefore, it was tested if fine-root cuttings can reduce a part of this background noise. Unfortunately, non-fixed agarose embedded semi-thin sections turned out to be not suitable because most cells are longitudinal expanded and burst when damaged by cutting devices because of their turgor and many root cells of such cuttings were missing nuclei. Embedding however often leads to a massive loss in fluorescence intensity of FPs (Ganguly et al., 2011). In further investigations it was tried to remove autofluorescence in both tobacco leaves and poplar roots by applying a clearing protocol (Kurihara et al., 2015). After the ClearSee treatment the samples not only lost their color, but also the FP signals. Nevertheless, since then different versions of this protocol evolved and could be adapted for the given systems in the future (Nagaki et al., 2017; Imoto et al., 2021). Since none of the above-mentioned protocols worked, one could try to remove autofluorescence by manipulating images prior to the determination of fluorescence levels in future steps. As an example, ImageJ allows for a background subtraction (Rolling Ball Background Subtraction, Michael Castle and Janice Keller, Mental Health Research Institute, University of Michigan).

4.3.3 Impact of root orders on gene expression in poplar

Upon ectomycorrhiza formation, only freshly emerging roots become mycorrhized. Therefore, initial investigations concerning root order and FP based fluorescence emission were performed because potential differences in the root physiology between root orders might impact gene expression (Wells and Eissenstat, 2002).

Epifluorescence microscopy revealed that poplar first and second order roots seem to be similar concerning their fluoresce emission. This was observed for double marker constructs with GFP driven by a 176 bp promoter fragment of *Potri.2G0797* and GFP driven by a 3551 bp promoter fragment of *Potri.2G2183*. Concerning GFP: RFP ratios, statistic comparisons between GFP:RFP ratios of root hair nuclei of first and second order roots from three different constructs were made. None of the constructs showed differences concerning fluorescence intensities in dependence on the observed root orders. Unfortunately, cortex nuclei could not be compared because of high autofluorescence levels. This would have been a better indicator for the comparison of root orders because other tree species such as *Cunninghamia lanceolata, Acacia auriculiformis* and *Gordonia axillaries* showed a reduced cortex thickness with increasing root orders (Long et al., 2013) and the root diameter decreased and nitrogen levels increased with higher branching orders in *Acer saccharum* and *Fraxinus americana* (Pregitzer et al., 1997). This indicates a need to further investigate FP expression patterns of cortex cells in different root orders to be able to compare mycorrhized and non-mycorrhized poplar fine-roots.

4.3.4 Gene expression patterns in roots of composite poplar plants

When analysing root systems of composite poplar plants, it was observed, that plants of the same root system showed different fluorescence protein expression patterns when stemming from different calluses. This is because each root is a single transformation event (Neb et al., 2017). To investigate differences in expression patterns with qPCR, a total of ten root systems containing a pCXUN binary vector with a tdTomato-NLS driven by a 35S promoter were separated into weak, intermediate, and strong fluorescence intensity signals. As a result, weak expressing roots had a relative expression rate of ~6 and strong expressing roots of ~18, which is a 3.16 - fold difference, indicating that differences in fluorescence intensity are not because of autofluorescence. Main reason for this observation is probably the copy numbers, which was not determined in this study. Collier et al., (2005) evaluated for *A. rhizogenes* (strain NCPPB 2659) based transformation copy numbers in *Nicotiana tabacum ex vitro* composite plants using a Southern blot approach. They found that some roots contained only a single T – DNA insertion, whereas others had four to more insertions, which is likely to affect gene expression rates. Furthermore, the T – DNA is likely integrated at different locations in the plant´s genome, which might be differently active at a transcriptional level, causing a position effect (Gelvin, 2017). However, there are supposedly preferred T - DNA integration sites in *Arabidopsis thaliana*, which have high CG-skew ratios and are in the 5′ and 3′ UTR of protein coding sequences as well as the promoter region of RNA polymerase transcribed rRNA gene repeats (Schneeberger et al., 2005). This was also confirmed by Shilo et al., (2017), who detected a bias towards AT – rich motifs as well as towards sequences with a microhomology to T – DNA border sequences based on a modified adapter-ligation mediated PCR method. Therefore, the expression strength is likely related to the integrated copy numbers.

However, because both GFP and RFP are integrated at the same location into the gDNA, no impacts on fluorescence intensity ratios are expected. Because this experiment was only conducted with a single marker construct, potential impacts of expression strength on GFP: RFP fluorescence intensity ratios in nuclei of transgenic poplar was not determined.

4.4 Promoter analysis of mycorrhiza regulated genes

4.4.1 Promoter truncations as a step to find potential cis - elements

Eucaryotic promoters are very large and hard to predict *in silico*, because regulative elements can be in a wide area around the transcription start and *cis* – elements often need chromatin folding to be in a proximity to influence gene expression. Thus, there is a high chance that promoter elements are missing when taking it from its native environment for further analysis (Hernandez-Garcia and Finer 2014). Taking a promoter from its native environment for analysis by random integration into gDNA might also disable chromatin based promoter regulation (Hernandez-Garcia and Finer 2014). To reduce the possibility to miss important regulative elements, large upstream areas need to be amplified for promoter analysis.

The promoter region of the three genes *Potri.2G0797*, *Potri.2G2183* and *Potri.9G1040* that are found to be down – regulated in ectomycorrhizas (Nehls et al., unpublished) were investigated in this thesis. In this context, the largest possible promoter fragments (depending on PCR primers) were PCR amplified and cloned in front of a fluorescence expression cassettes in a binary vector. Thereby, the promoters were expected to be active non – mycorrhized fine-roots, resulting in detectable GFP expression in the double marker constructs. In a second step to locate potential *cis* – elements 5´deletion analysis was performed. Thereby, *cis* – elements are only approximately eight to ten base pairs long, even though the transcription complex might cover around 50 bp (Odom, 2011). Lastly, hybrid poplars were generated and applied to mycorrhization to investigate whether fluorescence reporter expression changes during symbiosis as observed for the original gene. Such an *in vivo* analysis allows the localization of *cis* - elements in a biological context. Generally, it was possible to clearly see 8 - fold differences for RFP- and 11.4 - fold differences for GFP fluorescence levels at an epifluorescence microscope (**Figure 59**).

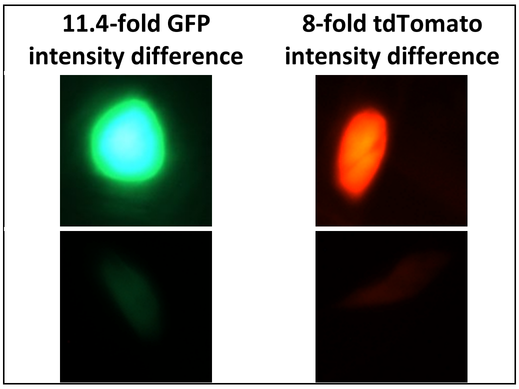
11.4-fold GFP intensity difference
8-fold tdTomato intensity difference

Figure 59. Visualizing an 8 – fold TdTomato-NLS- and 11.4 – fold GFP-NLS expression difference in root hair nuclei of *Populus tremula x alba* plants. Shown are composite poplar plants, which were transformed with a pCXUN binary vector via *Agrobacterium rhizogenes* strain K599. To determine the differences, fluorescence intensities of raw images were obtained from ImageJ. Based on the obtained intensities of weak and strong expressing nuclei the above-mentioned ratios were calculated. The nuclei did not belong to the same construct or the same plant. The sole purpose of this comparison was to see, if and how differences in expression strength can be visualized.

4.4.2 Promoter analyses of Potri.2G0797

The longest promoter fragment of *Potri.2G0797* that could be amplified from *Populus tremula x tremuloides* gDNA was 2.892 kb in length. In total, 14 truncations were made from the 5´ end of the fragment and analyzed for promoter activity in a FP reporter system. This analysis was based on the double marker system in composite *Populus tremula x alba* plant roots. No GFP:RFP ratios were calculated for most truncations as the number of replicates was too low for statistical analysis. However, promoter activity was visible from 2892 bp to 176 bp in root hair nuclei when compared to the promoter-less GFP control. For the 2892 bp and the 176 bp promoter fragment sufficient nuclei were observed showing reliable fluorescence for the green and red channel to allow for a statistical analysis. No significant difference in the expression strength was found, indicating similar expression levels of both promoter fragments.

The promoter analysis of double marker cassettes in composite poplar roots revealed, that a 2892 bp promoter fragment is active in root hairs, root cortex and the root tip in young root systems in poplar. Because of high levels of autofluorescence it was not possible to make assumptions about the central cylinder and the tip meristem. However, this indicates that the amino acid transporter is likely expressed in all root regions, presumably up to the endodermis. In older root systems with non – mycorrhized fine roots, the only visible fluorescence was close to the central cylinder (**Figure 49**). This is probably due to the fact, that root hair nuclei change their location towards the cortex upon maturation, which was also observed for older roots harbouring a double marker cassette with GFP driven by the 2892 bp promoter fragment.

Because no GFP fluorescence was obtained for the two smallest promoter fragments, an essential element might be located between bp 176 and 113 upstream of the translation start. Many core promoter regions are in an 80 bp upstream area of the transcription start (TSS) and many control elements are located up to 300 bp above the TSS (Barrett et al., 2012). For the integrated poplar genes, the TSS was not determined experimentally as the aim of this thesis was the identification of *cis* - elements involved in ECM based regulation. It was decided to include part of the non-translated but transcribed region of the gene prior to the translation start in the amplified promoter fragments.

Due to time constraints, only very few mycorrhizas could be analyzed. One reason for insufficient numbers of many mycorrhizas was that mycorrhization was set up in wintertime. Even when plant and fungi are cultivated exclusively in growth chambers, worse mycorrhization is a parameter that regularly occurs (Nehls, personal communication). Furthermore, even when the initial percentage of roots harboring the T – DNA of the binary vector was high (>70 %), this number decreased over time and was much lower when mycorrhiza plates were opened (> 4 months after transformation, Nehls et al., unpublished). This means, that after transferring plants to mycorrhiza plates further roots emerged that were mostly non – transgenic. This observation clearly demonstrates the demand for a visual selection system for binary vector T – DNA roots after ectomycorrhiza formation. This selection process is not possible with an antibiotic selection marker, because composite plants have non – transgenic shoots that could not grow on a selective medium.

These mycorrhizas harboring the 2892 bp promoter driven GFP cassette still showed GFP fluorescence, indicating at least some promoter activity upon ECM formation. Because no promoter of a mycorrhiza repressed gene has ever been characterized, different explanations can be given for this result: **(1)** Because eucaryotic promoters can be quiet large also for plants (Pumplin et al., 2012; Liu et al., 2014; Nanjareddy et al., 2017), the investigated 2892 bp long promoter fragment could be too short and thus misses important regulatory elements. A solution could be the amplification of longer upstream regions by designing a revers primer that is located at the 3´end of the amplified 2892 bp promoter to reduce the size of the amplicon. **(2)** In eucaryotic promoters regulatory elements could be found also in the coding sequence (introns) and 3´UTR (Usadel et al., 2009; Vandepoele et al., 2009; Barrett et al., 2012; Biłas et al., 2016). This could be investigated by amplifying the promoter together with a part of the gene and perform both 3´and 5´deletions in a double marker cassette system, Such 3´truncations were successfully performed by (Nishiyama et al., 2003; Rose, 2019). It was decided to perform in silico analysis based on databases, because most databases are suitable for few species such as *Arabidopsis* (Khan et al., 2018) but not poplar in general. Particularly, because no *cis* – elements responsible for mycorrhiza regulation were yet identified.

4.4.3 Promoter analyses of Potri.2G2183

The longest promoter fragment of *Potri.2G2183* that could be amplified from *Populus trichocarpa* gDNA was 3551 bp in length. In total three truncations were made from the 5´ end of the fragment and analyzed for promoter activity in a FP reporter system as described above.

Comparisons based on the epifluorescence microscopy revealed an increase of detectable GFP fluorescence in the 516 bp truncation compared to the longer promoter fragments. This was especially visible in root hairs, where the 516 bp promoter fragment induced clearly visible GFP signals whereas the 3551 bp fragment showed less fluorescence intensity, indicating that the overall expression pattern of the reporter protein changed. This leads to the assumption, that a repressing element was removed by the 5´deletion. A review on deletion analyses of multiple genes found, that in 55 % of the analyzed promoter regions repressing elements were located between 516 – and 1000 bp above the TSS (Barrett et al., 2012), which would correspond to the observed findings. However, further truncation steps are needed to identify the exact location of the potential element and possibly find further elements closer to the translation start. Possible strategies are described for *Potri.2G0797* and could be applied here as well.

Promoter analysis of a 3551 bp promoter revealed, that the promoter is mainly active in the root tip and weakly expressed in cortex cells. This indicates, that *Potri.2G2183* seems to be involved in certain developmental stages in highly specific regions. In concert with this, a study analysing differential gene expression showed, that genes of this calcium binding protein family are not only expressed tissue – specific, but also in a spatial-temporal manner (Mohanta et al., 2017).

A down-regulation of the gene was expected upon ECM formation, wherefore no mycorrhization attempts were made thus far. This is, because the overall low observed fluorescence intensities were very likely not suitable to detect a further down-regulation. The 516 bp truncation was generated at a time-point where no further mycorrhization events were attempted due to time restraints.

4.4.4 Promoter analyses of Potri.9G1040

A 1138 bp promoter fragment was successfully PCR amplified from *P. tremula x tremuloides* gDNA and cloned into a double fluorescence marker cassette on pCXUN T – DNA for *in planta* analysis. As a result, the promoter, gave no detectable eGFP signals in the observed *P. tremula x alba* hybrid roots. Because it was not possible to amplify a larger promoter region and no truncations were cloned, no predictions can be made. It remains unknown, where the promoter is active and how this promoter is regulated. Only assumptions can be made based on the predicted protein function of the correlated protein. Because the activity of most CXE12 proteins is pH dependent, they are soluble and lack a membrane domain (Kaschani et al., 2009, 2012) it could be concluded, that the promoter needs a certain environment to be active. Furthermore, the promoter might be repressed at its current length, which could be tested by generating 5´ truncations.

4.4.5 Using different poplar hybrids for promoter analyses

Best *in silico* sequences are available for *Populus trichocarpa* thus far. Because this poplar hybrid was difficult to handle under sterile conditions, all *in planta* analysis were conducted in *P. tremula x alba* hybrids. However, because primers for PCR amplification were designed on the better *in silico* consensus sequences of *P. trichocarpa* and *P. tremula x tremuloides* it was tested whether this change of hybrids impacted fluorescence expression patterns in composite poplar plants. Therefore, the 2892 bp promoter fragment of *Potri.2G0797* and the 3551 bp promoter fragment of *Potri.2G2183* were both transformed in *P. tremula x alba* and *P. tremula x tremuloides* hybrids. No differences in fluorescence expression could be detected in both cases when comparing GFP fluorescence in different root areas. It can be concluded that the poplar hybrids are extremely compatible concerning gene expression of the given genes and that the use of different poplar hybrids for different steps of promoter analysis likely has no impact on the promoter activity and thus FP expression.

4.5 Subcellular protein localization in tobacco leaves

4.5.1 Heterologous expression in tobacco leaves

Subcellular localization of proteins *in planta* can be performed by heterologous transient transformation of tobacco leaves with agrobacteria. Thereby, the proteins of interest are fused *in frame* with a reporter gene, e.g., a fluorescence protein. This fusion construct is then expressed *in planta* under the control of a constitutive promoter. The fusion proteins can then be tracked in the cells by epifluorescence microscopy. In this thesis, all generated fusion constructs were based on a sYFP that was fused to the C – terminus of the protein of interest.

Subcellular localization of proteins *in planta* can be performed by heterologous transient transformation of tobacco leaves with agrobacteria. Thereby, the proteins of interest are fused *in frame* with a reporter gene, e.g., a fluorescence protein. This fusion construct is then expressed *in planta* under the control of a constitutive promoter. The fusion proteins can then be tracked in the cells by epifluorescence microscopy. In this thesis, all generated fusion constructs were based on a sYFP that was fused to the C – terminus of the protein of interest. A 35S promoter was chosen to drive the expression cassettes for subcellular protein localisation in transiently transformed tobacco leaves. This promoter shows constitutive gene expression in tobacco leave cells and a model plant promoter (Odell et al., 1985; Biłas et al., 2016). Previous tests and other studies successfully showed subcellular localizations with P_{35S} in *Nicotiana benthamiana, Lotus japonicus* and *Arabidopsis thaliana* (Nehls et al., unpublished, Binder et al. 2014). Its combination with a T_{OCS} was previously also shown to work well together with P_{35S} in *Arabidopsis* (Halfter et al., 1992; Regierer et al., 2002).

4.5.2 Subcellular localization of Potri.2G0797, Potri.2G2183 and Potri.9G1040

Previous analysis of the proteins of the three investigated genes located Potri.9G1040 and Potri.2G2183 in the cytoplasm in transient tobacco leaves and Potri.2G0797 eventually in the plasma membrane (Nehls, personal communication). In the context of this thesis, this experiment was repeated. However, none of the constructs showed detectable sYFP signals. Therefore, the expression cassettes were party re-constructed and, in some cases, a constitutively expressed second red expression cassette was added to the respective T – DNA (P_{NOS}_tdTomato-NLS_T_{OCS}). However, even though red fluorescence was detected in tobacco leave cells, no sYFP signals could be obtained, avoiding successful localizations of the target proteins. To exclude a frame-shift event at the junction sites of the fusion constructs, all constructs were partially sequenced.

Because the red expression cassette was functional, these findings hint towards a problem with the sYFP fusion cassette. One reason for these results might be an only very weak sYFP signal in cytoplasm, because later experiments showed a rather weak sYFP signal in tobacco leaves compared to GFP as a reporter (Schnakenberg, 2020). However, this is no explanation for expected but missing signals at the plasma membrane for Potri.2G0797. Therefore, there might be a possibility that the C – terminal fusion of sYFP somehow disrupts or blocks the gene expression in a way, that **(1)** no genes are expressed, or **(2)** the chromophore of the sYFP does not mature.

In case of the transmembrane protein *Potri.2G0797* it might be possible to add a fusion tag in one of its transmembrane regions. Based on predictions in Geneious (Krogh et al., 2001), the cDNA of the amino acid transporter has a total of nine transmembrane regions with the N – terminus located in the cytoplasm and the C – terminus in the extracellular matrix (**Figure 60**). Based on these findings, it might be possible to add FP tags in frame in one of the four loops located in the cytoplasm.

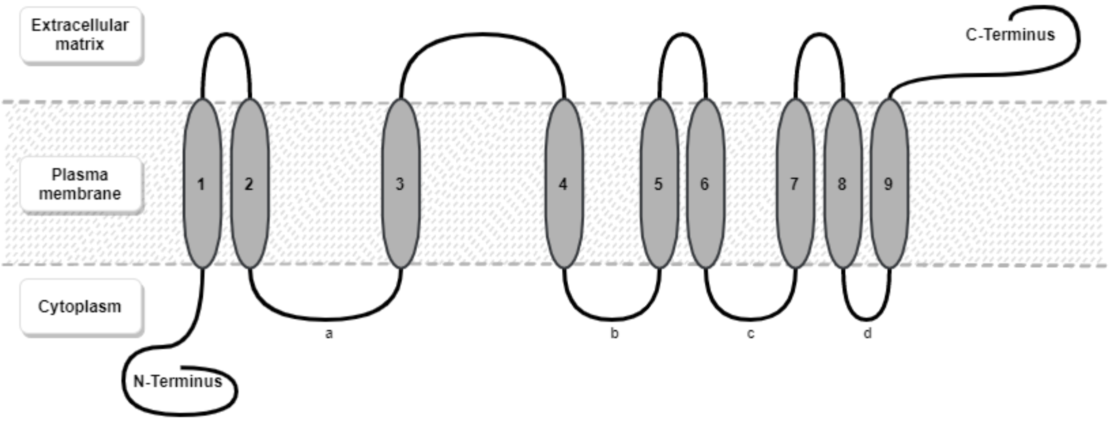

Figure 60. Predicted topology of *Potri.2G0797* as a membrane protein. *Potri.2G0797* likely codes for an amino acid transporter located at the plasma membrane with nine transmembrane regions. The N – terminus is in the cytoplasm and the C – terminus in the extracellular matrix. Loops in the cytoplasm are numbered from a to d. Predictions were made with Geneious Prime version 2021.

To improve the overall subcellular localization efficiency, several other possibilities would be available. Firstly, one could try to add a linker between the protein and the fusion tag, which was shown to improve the localization efficiency for membrane proteins (Xie et al., 2009). Secondly, it could also help to add a silencing inhibitor, such as the p19 protein of tomato bushy stunt virus to prevent post – transcriptional gene silencing in a transient expression system (Voinnet et al., 2003). In a different approach, the reporter protein could be changed from sYFP to eGFP, which was shown to work as a reporter for localization studies (Palmer and Freeman, 2004). Additionally, a study was able to show 2 – fold enhanced transient protein expression when using a double terminator (Yamamoto et al., 2018), which could also be tried in this case

5 Outlook

The improvement of the transformation efficiency of composite poplar plants was successful. This included a switch to pCXUN as a transformation vector to enhance the root transformation efficiencies.

The promoter analysis of promoters from down-regulated genes upon ECM formation still needs to be refined. Some potential *cis* – elements were detected, these sites need to be further narrowed down. For all amplified promoter regions of the genes, it is recommended to amplify longer regions and include downstream sequences in relation to the translation start. Next steps would also include mycorrhization to hopefully detect down – regulation of the investigated genes.

Promoter analyses were conducted in a double fluorescence marker construct in composite poplar plants. In the future, RFP needs to be further established as a calibration marker against GFP driven by promoters of interests to generate reliable comparisons between different promoters and their 5´ truncations. Not considered thus far is a consistent underestimation of RFP because of different quantum yields between GFP and RFP. Furthermore, bleed through of fluorescence between the GFP and RFP channels at the epifluorescence microscope was not considered yet.

Furthermore, subcellular localization studies need to be optimized to be able correlate the area of promoter activity with the location of the respective proteins and deduce why they are downregulated upon ECM formation.

To determine a possible function for the amino acid transporter, yeast spotting essays based on amino acid availability could reveal what exactly is transported (Dreyer et al., 1999; Görgens et al., 2005). To further analyse protein function in poplar, it might be useful to overexpress or silence the respective genes prior to ECM formation and investigate differences compared to the wild type.

6 Appendix and supplementary data

6.1 List of Tables

Table 1. Fluorescence proteins with their respective size, excitation, and emission wavelength as well as their description. **20**

Table 2. Enzymes that were used for the dissertation with their given function and the producer. **30**

Table 3. Used Chemicals and their respective producers. **31**

Table 4. Antibiotics that were used for selection of binary vectors with their given concentrations in liquid or solid growth medium. Antibiotics were always added freshly and the agar plates containing antibiotics were prepared a maximum of 1 – 7 days before they were used. Media containing rifampicin and tetracycline were stored in the dark because of its light sensitivity. **33**

Table 5. Primers that were used to amplify the CDS with and without introns or restriction enzyme overhangs of the three genes *Potri.9G1040*, Potri*.2G2183* and *Potri.2G0797* from either gDNA or cDNA of *Populus tremula x tremuloides*. The primer sequences as well as their names and the amplified fragment length are given. Restriction site overhangs are highlighted in red. **38**

Table 6. Primers that were used for the amplification of promoter regions from genomic DNA of *Populus tremula x tremuloides* (T89) or *P. trichocarpa* from the three genes *Potri.9G1040*, *Potri.2G0797 Potri.2G2183*. The table contains information about the gene name, the amplified promoter length, and the names of the used primers. Forward direction is meant as from 5´to 3´and vice versa. Labelled in red are LIC overhangs for the truncation of long promoter fragments as well as restriction enzyme recognition sites. **39**

Table 7. Primers that were used to clone fusion constructs of *Potri.2G0797*. Furthermore, primers to amplify an existing fusion construct of *Potri.2G2183* and *Potri.2G0797* without introns are given. The table contains information about the gene name, direction of the primers, the amplified sizes as well as the names of the used primers. Forward direction is meant as from 5´to 3´and vice versa. Labelled in red are restriction enzyme recognition sites. **41**

Table 8. Primers used to universally amplify fragments from the pJET1.2 vector with LIC overhangs. Primers were obtained from Sigma-Aldrich Corporation, St. Louis, USA. The LIC adapters in the primer sequence are highlighted in bold. **43**

Table 9. LIC T4-DNA Polymerase treatment mixtures for the vector and insert. Given are the ingredients and their concentration in both the vector- and insert mixture. **43**

Table 10. Buffers and solutions used for the extraction of genomic DNA from *Populus tremula x tremuloides* and *P. trichocarpa* leaves. **45**

Table 11. Steps of a Polymerase Chain Reaction (PCR). Steps 2 to 4 were repeated for 35 times in each case. **46**

Table 12. Ingredients of a PCR reaction sample with the given final concentrations. **46**

Table 13. Receipt for a 50x TAE stock solution, which is diluted 0.5 x prior to agarose gel electrophoresis and used as liquid conductor in the gel chambers. **47**

Table 14. Ingredients of RF1 for plasmid isolation of *Escherichia coli* using the Rubidium chloride method following Hanahan, 1938. After mixing the ingredients the pH-value was adjusted to 5.8 with glacial acetic acid and the solution was autoclaved and stored at 4°C. **49**

Table 15. Ingredients of RF2 for plasmid isolation of *Escherichia coli* using the Rubidium chloride method following (Hanahan, 1983). The pH of RF2 was adjusted to 6.5 with KOH after mixing the ingredients. The final solution was autoclaved and stored at 4°C. **49**

Table 16. Ingredients and their final concentrations in LB-Medium (Luria – Bertani; Sambrook, Fritsch, and Maniatis 1989). After mixing the ingredients the Medium was autoclaved. For agar plates 1.8 % agarose were added prior to autoclaving. Media were made selective in adding 100 µg/L Ampicillin or 50 µg/L Kanamycin (final concentrations). Medium purity was equal “pro analysi”. **49**

Table 17. Ingredients and their concentrations used for a 5 - fold concentrated KCM solution. **50**

Table 18. Ingredients and their final concentrations of Solution 1 for plasmid isolation from bacterial *E. coli* cells via alkaline lysis. The solution was stored at 4°C. **51**

Table 19. Ingredients and their final concentrations of Solution 2 for plasmid isolation from *E. coli* cells via alkaline lysis. **52**

Table 20. Ingredients and their final concentrations of Solution 3 for plasmid isolation from *E. coli* cells via alkaline lysis. The pH was adjusted to 4.8 using acetic acid. The solution was stored at 4°C. Final concentration = 375 mM) **52**

Table 21. Description of primers that were used for Sanger sequencing. Given are the primer name, Primer sequence, Orientation of sequencing and the vector backbone it could be used for. **52**

Table 22. Ingredients and their final concentrations of CPY medium used for Agrobacteria cultivation. Cells containing the desired plasmids were selected in adding 0.1 mM kanamycin and in some cases tetracycline after autoclaving the ingredients. For CPY plates 1.5 % agar was added prior to autoclaving. Rifampicin was added additionally to kanamycin to minimize contamination with other bacteria when cells were reactivated from glycerol stocks. The purity of the components was equal “pro analysi”. **53**

Table 23. Ingredients and their final concentration of Activation medium for tobacco leave infiltration with *Agrobacterium tumefaciens*. **55**

Table 24. Ingredients and their final concentrations of MS6 medium (Murashige and Skoog, 1962) . The purity of the components was equal “pro analysi”. The pH – value was adjusted to 5.6 with KOH prior to autoclaving. **56**

Table 25. Ingredients of MMN medium (Kottke and Oberwinkler, 1987). Given are the ingredients and final concentration of 10 mM/50 mM glucose MMN medium as used for the pre – culturing of fungi for mycorrhization as well as the MMN 1/5 N for the mycorrhization plates. The purity of the components was equal “pro analysi”. **57**

Table 26. Composition of fluorescence expression cassettes in pCXUN binary vector T-DNA to test for impacts of their orientation on poplar transformation efficiencies. Given is the composition of the first expression cassette with its promoter, fluorescence protein and terminator. Some constructs contained a second expression cassette in tandem, which was composed of a NOS promoter. tdTomato-NLS and OCS terminator. NLS means the protein has a nuclear targeting signal, SNL means the protein is targeted to the peroxisomes. LB = left border and RB = right border sequence of the T-DNA (see schematic display in **Figure 16**). Additionally, the number of observed plants per construct is given. The $P_{2892\ bp}$ refers to a 2892 bp long promoter region of *Potri.2G0797*. $P_{3551\ bp}$ refers to a 3551 bp long promoter region of *Potri.2G2183*. **65**

6.2 List of Figures

Figure 1. Overview of where the symbiosis of trees and ectomycorrhiza takes place. Atrebe10: “Basic morphology of a common ectomycorrhizal association”, (https://commons.wikimedia.org/wiki/File:Ectomycorrhiza _illustration.jpg). Published at Wikimedia commons, 19.07.2021, Licensed under Attribution Share Alike 3.0 Unported license (https://creativecommons.org/licenses/by-sa/3.0/deed.en). SEM = Scanning Electron Microscope. **2**

Figure 2. Vector description of a modified pGREEN based pPLV binary vector. The T - DNA was completely exchanged via *BglII* (Neb, 2017). It contains an expression cassette for fluorescence proteins and a plant selection marker cassette. The backbone of the binary vector contains a part of the psa-ORI and a kanamycin resistance. To be able to replicate, the incomplete pSA ORI needs to be complemented with the “helper plasmid” pSOUP. For promoter and terminator descriptions see chapter 2.5.1. Figure was in silico cloned and displayed using Geneious**.** **12**

Figure 3. Visual description of a pCAMBIA derived and modified pCXUN vector. The T - DNA was composed of a variable double marker cassette (Green and Red expression cassette) and a plant selection cassette. The backbone outside of the T – DNA consisted of a pBR-ORI and a pVS1 REP ORI for plasmid stability in *Agrobacteria* as well as a kanamycin resistance cassette (aadA CDS). The Figure was in silico cloned and displayed using Geneious (further details given in M&M**).** **12**

Figure 4. Visualization of LIC overhangs and adapters for a LIC cloning strategy (Ligase Independent Cloning). A: LIC site in the T – DNA of binary vectors for *Agrobacterium* mediated plant transformation. The vector can be linearized with *HpaI*, the sequences. Left and right of this cutting site are so called LIC adapters. Using complementary adapters for the potential inserts in combination with respective T4-polymerase treatments allows for LIC. The image was made with Geneious. B: LIC overhangs in detail. In blue is the dCTP and T4-DNA Polymerase treated vector, in orange is the dGTP and T4-DNA Polymerase treated PCR insert, which was amplified with LIC-overhangs prior to this step. In this way the T4-DNA Polymerase treatment generates compatible overhangs that can then be annealed without a ligase. **13**

Figure 5. A: Potential promoter structure of a eukaryotic gene. The transcription- and translation start are indicated. **B: Schematic display of potential locations of *cis* – elements in eucaryotic promoters.** *cis* – elements of the promoter can be bound by transcription factors, that in return can be bound by transcription factor binding proteins (TBPs) to recruit RNA polymerase II. In case of the TATA box, these are called TATA binding proteins that help position the polymerase over the transcription start (TSS). *Cis* – elements can be brought closer to the Transcription start (TSS) by looping factors that help mediate the promoter structure. **15**

Figure 6. Visualization of impacts of picture processing on the picture and its histogram. Shown is an *Agrobacterium* transformed poplar root with GFP and RFP fluorescence proteins targeted into the nucleus. Given are the unprocessed GFP and RFP pictures with the corresponding histograms of the channels. To the processed pictures a background subtraction (rolling ball radius set to 50) was applied and the contrast was enhanced by 0.01 % in ImageJ version 2.1.0/1.53c. **28**

Figure 7. Visualization of the pJET1.2 vector. The backbone consists of (1) a "bla" CDS that catalyses the opening and hydrolysis of the beta-lactam ring of beta-lactam antibiotics, (2) a pMB1 rep origin and (3) eco47I/T7 CDS. The mutant Eco47I has 15 additional amino acid residues encoded by the inserted T7 promoter compared to the wild type. The Eco471/T7 CDS includes a multiple cloning site (MS-site), ensuring that only plasmids with integrated DNA fragments in the MS-site to grow. Otherwise, no protective methylation leads the enzyme to recognise and cleave double-stranded DNA targets, which is ultimately leading to cell death. Annotated are Ligase independent cloning (LIC) sites. LIC is described in the introduction and the primers are further characterized in the Material and Methods of this thesis. Figure was in silico cloned and displayed using Geneious Prime® 2021.1.1. **35**

Figure 8. Vector description of a modified pPLV binary vector. The T - DNA was completely exchanged via *BglII*, integrating a LIC site and a multiple cloning site (Neb, 2017). The expression cassette consists of a P_{35S} and T_{OCS} with a Multiple cloning site (MSC) and a LIC site in between (Expression cassette fluorescence protein) (Schnakenberg, 2020). Additionally, the T - DNA contains a kanamycin resistance (NPTII CDS) between a P_{35S} and a T_{35S} (Plant selection marker cassette). The backbone of the binary vector contains a part of the psa-ORI (origin of replication) and a kanamycin resistance (KanR CDS). To be able to replicate, the incomplete pSA ORI needs to be complemented with the "helper plasmid" pSOUP. For promoter and terminator descriptions see chapter 2.5.1. Figure was in silico cloned and displayed using Geneious. **36**

Figure 9. Schematic display of pCXUN modifications by integrating a large part of a pPLV T – DNA into *PvuII* sites of pCXUN-FLAG. a) Fluorescence expression cassettes were cut out from pPLV with the restriction enzyme *PvuII*. b) The pCXUN-FLAG vector was linearized with PvuII, which cut out a large part of the T – DNA. c) The pCXUN backbone was ligated with the insert from pPLV. **59**

Figure 10. T – DNA with marker cassettes that were created and cloned into either a pPLV based vector or a pCXUN binary vector to compare transformation efficiencies in composite poplar roots. NLS means the protein has a nuclear targeting signal, SNL means the protein has a peroxisome targeting signal. LB = left border and RB = right border sequence of the T-DNA. Selection marker = a kanamycin resistance cassette for selection of stable plant transformants. n = number of transgenic root systems observed: a) n for pCXUN = 32. b) n for pPLV = 15; n for pCXUN = 19. c) n for pCXUN = 12. d) n for pPLV = 13; n for pCXUN = 42. e) n for pCXUN = 7. f) n for pCXUN = 3. The used promoters and terminators as well as fluorescence proteins are described in the Material and Methods. MSC means Multiple Cloning Site, meaning that the cassette has no promoter. The cassettes point in their orientation in relation to LB and RB. **60**

Figure 11. T-DNA with fluorescence cassettes that were created and cloned into either a pPLV based vector or a pCXUN binary vector to compare transformation efficiencies in composite poplar roots. NLS means the protein has a nuclear targeting signal, SNL means the protein has a peroxisome targeting signal. LB = left border and RB = right border sequence of the T-DNA. Selection marker = a kanamycin resistance cassette for selection of stable plant transformants. n = number of transgenic root systems observed: a) n for pPLV = 11. b) n for pCXUN = 24. c) n for pCXUN = 16. The used promoters and terminators as well as fluorescence proteins are described in the Material and Methods. The $P_{2892\ bp}$ refers to a 2892 bp long promoter region of *Potri.2G0797*. $P_{3551\ bp}$ refers to a 3551 bp long promoter region of *Potri.2G2183*. The cassettes point in their orientation in relation to LB and RB. **61**

Figure 12. Percentage of transgenic roots formed by poplar cuttings after incubation with transgenic agrobacteria harbouring pPLV or pCXUN based binary vectors with fluorescence protein cassettes. *Populus tremula x alba* cuttings were incubated with *Agrobacterium rhizogenes* strain K599 containing pPLV (n = 39 plants) or pCXUN (n = 155 plants). Thereby, the plants contained different fluorescence cassettes that consisted of either one or two expression cassettes in both orientations on the T – DNA. After four to eight weeks the percentage of fluorescent roots in relation to the total number of roots was determined. Statistics were conducted in R as specified in the M&M. **62**

Figure 13. Example for a transgenic poplar root system containing two fluorescence marker constructs. *Populus tremula x tremuloides* composite plants were transformed with a pCXUN binary vector using *Agrobacterium rhizogenes* strain K599. The T – DNA contained two fluorescence marker cassettes which were composed of a 2892 bp promoter fragment of *Potri.2G0797*, GFP-NLS and an NOS terminator as well as a NOS promoter, tdTomato-NLS and an OCS terminator. The 2892 bp promoter was established in this thesis and described in the respective chapters. NLS means the proteins are targeted to the nucleus. Images were taken at a Leica binocular MZ10F with 2 sec illumination time (Leica DFC425C camera, dsRED filters with 510 – 560 nm excitation and 590 – 650 nm emission window filter; GFP filters with 450 – 490 nm excitation and 500 – 550 nm emission window filter). Pictures in different filter settings were taken using the same settings, such as with a gamma correction of 0.99, a colour saturation factor of 1 and a 5x increase in optical power (gain). Additionally, the roots are shown under bright - field conditions. The roots were 3 weeks old. Pictures were processed for better visualization of the fluorescence (contrast enhanced by 0.01 % and background subtracted with ImageJ). Further details about the used devices and image processing are given in the M&M. **62**

Figure 14. Visual description of the pCXUN vector used for promoter integration based on the *KpnI/HpaI* strategy for promoter analyses, or the exchange of the complete cassette

via *KpnI/SacI* from pPLV for subcellular localization studies. The T - DNA was composed of a variable double marker cassette (Green and Red expression cassette) and a hptII CDS Selection marker cassette (kanamycin resistance). The backbone outside of the T – DNA consisted of a pBR-ORI and a pVS1 REP ORI for plasmid stability in *Agrobacteria* as well as a kanamycin resistance cassette (aadA CDS). SV40 codes for a nucleus targeting signal (NLS). For promoter and terminator descriptions see chapter 2.5.1. The red expression cassette was constitutively expressed. Figure was in silico cloned and displayed using Geneious Prime® 2021.1.1. **63**

Figure 15. Visual description of the pCXUN vector used for promoter integration based on LIC. The T - DNA was composed of a green and red expression cassette, a ccdB CDS (for the selection of positive clones) and a hptII CDS selection marker cassette (kanamycin resistance). The backbone outside of the T – DNA consisted of a pBR-ORI and a pVS1 REP ORI for plasmid stability in *Agrobacteria* as well as a kanamycin resistance cassette (aadA CDS). SV40 codes for a nucleus targeting signal (NLS). For promoter and terminator descriptions see chapter 2.5.1. The red expression cassette was constitutively expressed. Promoter fragments were inserted in the green expression cassette using Ligase Independent Cloning (LIC). Figure was in silico cloned and displayed using Geneious Prime® 2021.1.1. **64**

Figure 16. Schematic display of the orientation of fluorescence expression cassettes in relation to left- and right border sequences (LB and RB) and a plant selection marker cassette on the T – DNA in a pCXUN binary vector. a) The fluorescence expression cassette is introduced from LB to RB and b) from RB to LB. **64**

Figure 17. Poplar root transformation efficiencies in dependence on the orientation of fluorescence marker cassettes on the T – DNA of pCXUN. LB means left border and RB means right border in the T – DNA. A schematic overview of the orientations is given in Figure 16. Only single fluorescence protein cassettes were observed. *Populus tremula x alba* was transformed with *Agrobacterium rhizogenes* strain K599. pCXUN LB-RB: n = 31 plants, mean transformation efficiency = 70 %, SE = 5.2; pCXUN RB-LB: n = 32 plants, mean transformation efficiency = 85%, SE = 3.8. The root system was observed eight weeks after the transformation event. Significances are based on a Wilcoxon test (see M&M), * = $p < 0.05$. The standard error is given. Statistics were conducted in R as specified in the M&M. **66**

Figure 18. Poplar root transformation efficiencies in dependence on the orientation of fluorescence marker cassettes on the T – DNA of pCXUN. LB means left border and RB means right border in the T – DNA. A schematic overview of the orientations is given in **Figure 16**. Only double fluorescence protein cassettes were observed. *Populus tremula x alba* was transformed with *Agrobacterium rhizogenes* strain K599. pCXUN LB-RB: n = 67 plants, mean transformation efficiency = 81 %, SE = 3.7; pCXUN RB-LB: n = 26 plants, mean transformation efficiency = 59 %, SE = 8.3. The root system was observed eight weeks after the transformation event. Significances are based on a Wilcoxon test (see M&M), ** = $p < 0.01$. The standard error is given. Statistics were conducted in R as specified in the M&M. **66**

Figure 19. Poplar root transformation efficiencies in dependence on the orientation of fluorescence marker cassettes on the T – DNA of pCXUN. LB means left border and RB means right border in the T – DNA. A schematic overview of the orientations is given in Figure 16. Both single and double fluorescence protein cassettes were observed. *Populus tremula x alba* was transformed with *Agrobacterium rhizogenes* strain K599. pCXUN RB-LB: n = 58 plants; pCXUN LB-RB: n = 97 plants. The root system was observed eight weeks after the transformation event. Significances are based on a Wilcoxon test (see M&M). NS = not significant. The standard error is given. Statistics were conducted in R as specified in the M&M. **67**

Figure 20. Poplar root transformation efficiency based on the introduced cassette size. Compared were single cassettes consisting of a Promoter, gene, and terminator, against double constructs in which second fluorescence cassette was introduced. The orientation of the T-DNA is described in Table 26. *Populus tremula x alba* was transformed with *Agrobacterium rhizogenes* strain K599. single cassette plants: n = 63; double cassette plants: n= 92. The root system was observed eight weeks after the transformation event. Significances are based on a Wilcoxon test (see Material and Methods). NS = not significant. The standard error is given. Statistics were conducted in R as specified in the M&M. **67**

Figure 21. Schematic overview of the integration of the nucleus targeted timer protein DsRED-E5 in *HpaI* and *BamHI* restriction sites in pCXUN T – DNA. The vector is described in Figure 14. LB is the left border and RB the right border of the T – DNA. NLS means the protein is targeted to the nucleus. The used promoters, terminators and FPs are further described in the M&M. **68**

Figure 22. A: Verification of DsRED-E5 in pCXUN driven by a UBQ promoter by restriction digestion. The pCXUN_P_{UBQ}_DsRED-E5-NLS_T_{OCS} plasmid was verified with *HpaI/BamHI* restriction digestion. Expected fragment sizes were 735 bp + 9858 bp. As marker (Lane M, 6 µl) the Phage Lambda DNA/Eco130I (StyI) DNA ladder was used. Further details are given in the M&M. **68**

Figure 23. Visualization of nuclear targeted DsRED-E5 driven by a P_{UBQ} or without a promoter (neg. control). Transgenic *Agrobacterium rhizogenes* (strain K599) were used to transform tobacco leaves with an OD_{600} of 0.3. Fluorescence was observed after 23 h and 72 h. All pictures were taken under the exact same conditions and were compiled in a montage, where the background was subtracted, and contrast enhanced by 0.3 % in ImageJ. Used filter settings and further specifications are listed in the M&M. **69**

Figure 24. Visualization of nuclear targeted DsRED-E5 fluorescence in composite poplar plants. Gene expression was driven by the three different promoters P_{UBQ}, P_{NOS} and $P_{2892\ of\ Potri.2G0797}$ in root hairs of *Populus tremula x alba* plants. Composite plants were generated via *Agrobacterium rhizogenes* mediated transformation. Fluorescence was observed two to six weeks after root formation with a Zeiss microscope (as described in the M&M). All pictures were taken (gain = 4.8 dB) and processed under the same conditions in ImageJ (background subtraction and contrast enhancement by 0.001 % of individual pictures). 70

Figure 25. Visualization of nucleus targeted DsRED-E5 fluorescence in composite poplar plants. Gene expression was driven by the three different promoters P_{UBQ}, P_{NOS} and $P_{2892 \text{ of } Potri.2G0797}$ in cortex cells of *Populus tremula x alba* roots**.** Composite plants were generated via *Agrobacterium rhizogenes* mediated transformation with a pCXUN vector backbone. Fluorescence was observed two to seven weeks after root formation with a Zeiss microscope (as described in the M&M). All pictures were taken and processed under the same conditions in ImageJ (background subtraction and contrast enhancement by 0.1 - 0.001 % of the individual pictures). The gain is given in dB. 70

Figure 26. Bleaching experiment of GFP-NLS and tdTomato-NLS in root hair nuclei of transgenic composite poplar. The same nucleus of a pCXUN double marker construct was illuminated for 2 sec, 60 sec and 120 sec respectively under 2 sec exposure time. The total illumination time including adjustments was approximately 4 min. Fluorescence intensities were determined with ImageJ to calculate GFP: RFP intensity ratios. For better visualization, all pictures were processed with the same conditions (Background subtracted and contrast enhanced by 0.0001 % in ImageJ). n = 1 nucleus. Further details about the used devices and software are given in the M&M. 71

Figure 27. Gain series of a *Populus tremula x alba* root hair nuclei containing a nucleus targeted DsRED-E5. Pictures were made with a Zeiss microscope and details about the camera setting and used filter sets can be found in the M&M. All pictures were taken under the same conditions, only the gain value differed. Because the GFP was hard to detect, the pictures are visualized with an enhanced contrast (0.3 %) and subtracted background (ImageJ, further specifications in the M&M). To avoid distortion of ratios, the alterations were made after compiling the pictures in a montage. The red and green box indicate, which gain levels gave fluorescence intensities that were neither under- nor over saturated. The GFP: RFP fluorescence ratio is given, also for pictures in which one or the other channel is over/undersaturated. 72

Figure 28. Root growth of two roots from transgenic composite poplar root systems. The root growth over a time scale of 15 days was observed, starting 85 days after the transformation event. *Populus tremula x alba* plants were transformed with *Agrobacterium* rhizogenes strain K599 harboring a pCXUN binary vector. The T – DNA consists of a NOS promoter, nuclear targeted DsRED-E5 and an OCS terminator. Both root systems were treated identically 73

Figure 29. GFP: RFP fluorescence ratios of DsRED-E5-NLS in one second order root at the three different areas 1 mm above the root tip, 2 mm above the root tip and close to its origin at the main root. Composite *Populus tremula x alba* plants were generated with *Agrobacterium rhizogenes* strain K599 harboring a pCXUN binary vector. The T – DNA was composed of a NOS promoter, DsRED-E5 targeted to the nucleus and an OCS terminator. The root was observed

three weeks after root formation. Statistics were conducted in R as specified in the M&M. The standard error for each site is given. From left to right: n = 4, 9 and 10 nuclei per area. **73**

Figure 30. Example for a transgenic composite poplar plant. The plant transformation was mediated by *Agroacterium rhizogenes* (strain K599). First and second order roots are indicated. The root system was six weeks old and shows the "hairy root" phenotype. **74**

Figure 31. Visualization of the promoter activity of a 176 bp promoter region from *Potri.2G0797* in a first order root compared to a second order root. Pictures were obtained from a binocular (specifications in the M&M). All pictures were made under the same conditions. The promoter was amplified from *Populus tremula x tremuloides* gDNA and visualized in *P. tremula x alba* plants. The roots were 5 to 8 weeks old. For visualization, the pictures were processed in the same manner. **74**

Figure 32. Visualization of the promoter activity of a 3551 bp promoter region from *Potri.2G2183,* amplified from *Populus trichocarpa* gDNA and visualized in *P. tremula x alba* plants, in a first order root compared to a second order root. Pictures were obtained from a Zeiss microscope (specifications in the M&M). All pictures were made under the same conditions. The root system was 8 weeks old. For visualization, the corresponding RFP and GFP pictures were processed in the same manner. **75**

Figure 33. Boxplot comparing root hair nuclei GFP:RFP ratios between first and second order roots. Transgenic composite *Populus tremula x alba* plants were transformed with *Agrobacterium rhizogenes* (strain K599). The root systems were two to seven weeks old. A: DsRED-E5-NLS driven by a 2892 bp promoter fragment of *Potri.2G0797* in pCXUN (d = 0.33). B: A 176 bp promoter fragment of *Potri.2G0797* in a double marker system (d = 0.04) and C: a 2892 bp promoter of *Potri.2G0797* in a double marker system (d = 0.83). Each root replicate represents a mean of two to four single nuclei. Statistics were performed in R. Comparisons were calculated based on a Wilcoxon rank test. Effect sizes were calculated in GPower 3.1. The standard error is given. Statistics were conducted in R as specified in the M&M. **76**

Figure 34 Visualization of the fluorescence of a tdTomato construct in independent poplar roots of the same transgenic root system. Overview images were taken at a Leica binocular MZ10F with 2 sec illumination time (Leica DFC425C camera, dsRED filters with 510 – 560 nm excitation and 590 – 650 nm emission window filter). Detailed pictures of root hair nuclei were taken using an epifluorescence microscope with 0.5 sec illumination time (Zeiss Axioskop Microscope, Imagingsource DFK23UX174 camera, dsRED filter with 510 – 560 nm excitation and 590 nm long pass emission window filter with a 580 nm beam splitter). Thereby, images of different roots were taken under the same conditions. Pictures were made three to four weeks after the transformation event. The binocular picture was processed for better visualization (contrast enhanced by 0.01 % in ImageJ), whereas unprocessed microscope pictures are shown. Further details about the used devices and image processing are given in the M&M. **77**

Figure 35. Comparison of the relative transcription rate of tdTomato driven by a 35S-promoter in roots of three fluorescence intensity categories. The expression cassette consisted of a nucleus targeted tdTomato between a P_{35S} and a T_{OCS}. Given is the relative expression rate in roots revealing strong, intermediate, and weak fluorescing roots. The control did not contain tdTomato. Ten root systems were dissected, pooled according to their fluorescence, and used for RNA extraction three weeks after root formation. The qPCR analysis was conducted by Annette Hintelmann with a primer targeted to tdTomato. The data were normalized against a constitutively expressed reference gene driven by a P_{UBQ} (Neb, 2017). The standard deviation is given (SD strong = 0.28, SD intermediate = 0.26 and SD weak = 0.1). **77**

Figure 36. Relevant part of the T – DNA in pCXUN to localize *Potri.2G0797* on a subcellular level. A fusion construct with sYFP was PCR amplified with added BamHI restriction sites at the 5´and 3´end. This fusion construct was cloned between a 35S promoter and OCS terminator in a pPLV vector. The 35S promoter. fusion construct and OCS terminator cassette was the released with KpnI and SacI for integration in the T – DNA of pCXUN. The pPLV and pCXUN vectors are described in Figure 8 and Figure 14.The fluorescent protein, promoter and terminator are described in the M&M. **78**

Figure 37. Relevant part of the T – DNA in pCXUN for subcellular localization studies including a second marker for screening of positive transformants of *Potri.2G0797*. The different fluorescent proteins, promoter and terminators are described in the Material and Methods. **80**

Figure 38. Visualization of the fluorescence of a sYFP fusion-tdTomato-NLS construct in transiently transformed tobacco leave cells. Images were taken using an epifluorescence microscope with 2 sec illumination time (Zeiss Axioskop Microscope, Imagingsource DFK23UX174 camera, filter settings are described in the Material and Methods). Pictures were made five days after the transformation event. The contrast of the pictures was enhanced by 0.5 % in ImageJ. Further details about the used devices and image processing are given in the M&M. **80**

Figure 39. Double marker cassette as part of the T - DNA of a pCXUN binary vector for *Agrobacterium* mediated plant transformation for promoter analysis. LB is the left border- and RB the right border of the T – DNA. The used vector is described in Figure 14. The P_{UBQ} of the green expression cassette can be exchanged with a promoter of interest using *KpnI* and *HpaI* restriction sites. Because *HpaI* cuts blunt-end, the blunt-end cutting *SmaI* can be used for a directed cloning of promoter regions into pCXUN. NLS means the protein is targeted to the nucleus. $P_{2892\ bp}$ corresponds to a promoter region from *Potri.2G0797* amplified from *Populus tremula x tremuloides*. **81**

Figure 40. Promoter – reporter constructs of *Potri.2G0797* fragments from *Populus tremula x tremuloides* and eGFP-NLS to identify regulatory elements in this gene upon ectomycorrhiza formation. Transgenic poplar roots were generated with *Agrobacterium* mediated plant transformation, during which Composite plants were generated. The GFP expression was compared between the constructs visually at a microscope (eGFP = enhanced green fluorescent protein). Dark green: constructs were cloned with the *KpnI/SmaI* strategy. Magenta: Constructs were cloned using LIC. Blue: Constructs were cloned with the *KpnI/XhoI* strategy. **81**

Figure 41. PCR based cloning strategy for the generation of promoter truncations based on restriction digestion for the poplar gene *Potri.2G0797* exemplarily for the 61 bp promoter fragment. Template plasmid for the PCR was a double marker construct with a green and red expression cassette on pCXUN binary vector T – DNA. The green expression cassette was driven by a 2892 bp promoter fragment of the investigated gene. The truncated promoter fragment was 61 bp long and was amplified along with the rest of the green expression cassette. An artificial 5´*KpnI* restriction site was added to the promoter, whereas a native 3´located *XbaI* site was used for further steps. The obtained PCR fragment was then cloned into a KnpI and XbaI linearized pCXUN vector as described in Figure 14. LB is the left border- and RB the right border of the T – DNA. NLS means the protein is targeted to the nucleus. $P_{2892\ bp}$ corresponds to a promoter region from *Potri.2G0797* amplified from *Populus tremula x tremuloides*. **82**

Figure 42. Visualization of the promoter activity of a 2892 bp promoter fragment from *Potri.2G0797* driving nuclear targeted GFP expression *in planta* (*Populus tremula x alba*). As a positive control the GFP expression was driven by P_{UBQ}, as negative control a promoter was GFP less. For a detailed description of the construct see Figure 39. All pictures were taken by a MZ10F Leica binocular with a Leica DFC425C camera using a Leica Application Suite software. Filter sets for GFP had 450 – 490 nm excitation and 500 – 550 nm emission window, RFP filter sets had a 510 – 560 nm excitation and 590 – 650 nm emission window. As light source a Lej LQ-HXP 120, Leistungselektronik JENA GmbH, Jena, Germany was used. All pictures were made with a gamma value of 0.99 and a gain of 5 dB. All devices and further details are given in the M&M. The overlay was made with the RFP and GFP picture. The roots all were 5 to 8 weeks old. For visualization, the pictures were processed in ImageJ (montage of the three corresponding pictures, then background subtracted, and contrast enhanced by 1 %). Further details concerning image processing are given in the M&M. **84**

Figure 43. Visualization of the promoter activity of a 2892 bp and 176 bp promoter region from *Potri.2G0797* in first order roots. The promoters were amplified from *Populus tremula x tremuloides* gDNA and its activity is visualized in nuclei of *P. tremula x alba* plants. Composite plants were generated via *Agrobacterium rhizogenes* strain K599 mediated plant transformation. The T-DNA of the used pCXUN vector backbone contained a Promoter_dGFP-NLS_T_{NOS}_P_{NOS}_tdTomato-NLS_T_{OCS} cassette. Overview pictures were made with a Leica binocular and detailed pictures were obtained from a Zeiss microscope (specifications in the M&M). All pictures were made under the same conditions. Additionally, the roots are shown under bright - field conditions. The roots all were 5 to 8 weeks old. For visualization, corresponding pictures were processed in the same manner in a montage (background subtraction and contrast enhanced by 0.1 % in ImageJ). **85**

Figure 44. Boxplot with jitter dots comparing GFP:RFP ratios of the 2892 bp promoter fragment of *Pori.2G0797* against the 176 bp fragment in transgene *Populus tremula x alba* root hairs. The GFP-NLS is driven by the respective promoter, whereas tdTomato-NLS is driven by the constitutively expressed NOS promoter (Promoter_dGFP NLS_T_{NOS}_P_{NOS}_tdTomato-NLS_T_{OCS}) NLS means the protein was targeted to the nucleus. For each construct four root replicates were analyzed. The value given for the roots are a mean value of three to ten single nuclei each. The standard error and significances calculated based on a Wilcoxon test are given. NS = not significant. Statistics were conducted in R as specified in the M&M. **86**

Figure 45. Single nuclei in transgenic root hairs containing promoter truncations of *Potri.2G0797* in a double marker construct (Promoter_dGFP-NLS_T_{NOS}_P_{NOS}_tdTomato-NLS_T_{OCS}). The truncations range from -61 bp to -2892 bp. K is the negative control harbouring a promoter less GFP. The 2892 bp promoter fragment was amplified from *Populus tremula x tremuloides* gDNA, truncated with 5´deletion and visualized in transgenic *P. tremula x alba* plants. Shown are randomly picked nuclei of main roots that were illuminated for 2 sec in both the GFP and RFP channel at the lowest possible light intensity (25 %) with xenon light source at a Zeiss Axioskop Microscope. Pictures were made with a Imagingsource camera in an IC Capture software. Filter sets for GFP were in a 450 – 490 nm excitation and 510 – 560 nm emission window and for RFP in a 510 – 560 nm excitation and 590 nm long pass emission filter window filter with a 580 nm beam splitter. Further details are given in the M&M. Additionally, root hairs are shown under bright - field conditions. The roots were 4 to 7 weeks old and in approximately the same growth state. For better visualization, the illumination time and contrast were edited. All pictures were processed under the same conditions to avoid distortions inf Apple Fotos. Thereby, the contrast was enhanced by 1. Each picture is representative for at least five nuclei from different plants. **87**

Figure 46. Promoter activity of 2892 bp and 113 bp promoter fragments from *Potri.2G0797* in a promoter reporter double cassette approach in *Nicotiana benthamiana* leaves. Tobacco leaves were transiently transformed with *Agrobacterium rhizogenes* strain K599 in an OD_{600} of 0.3. The binary vector was pCXUN and the T-DNA was composed of the respective promoter fragment, dGFP-NLS and a NOS terminator as well as a second constitutively expressed NOS promoter, tdTomato-NLS and OCS terminator cassettes. NLS means the protein was targeted to the nucleus. Pictures were obtained with a Leica binocular with a gain of 4.7 dB three days after the infiltration. All pictures were processed in the same manner. Further details about the devices and settings can be found in the M&M. **88**

Figure 47. Comparing GFP fluorescence intensities driven by the 2892 bp promoter fragment of *Potri.2G0797* in first order roots between *Populus tremula x alba* and

***Populus tremula x tremuloides* plants.** Composite plants were generated via *Agrobacterium rhizogenes* strain K599 mediated plant transformation using a Promoter_dGFP NLS_T_{NOS}_P_{NOS}_tdTomato-NLS_T_{OCS}. Pictures were obtained from a Zeiss microscope (specifications in the M&M). All pictures were made under the same conditions. The roots all were 3 to 5 weeks old. For visualization, the pictures were processed in the same manner in ImageJ (In merged pictures of both corresponding channel pictures: Contrast of root hairs increased by 0.01 % and of cortex regions by 0.1 %, background subtracted). All pictures were taken with the same parameters (gain = 4.8 dB, light intensity = 25 %) as further described in the M&M. **89**

Figure 48. Boxplot with jitter dots comparing GFP:RFP ratios of the 2892 bp promoter fragment of *Pori.2G0797* in *Populus tremula x alba* and *P. tremula x tremuloides* hybrids. The GFP-NLS is driven by the respective promoter, whereas tdTomato-NLS is driven by the constitutively expressed NOS promoter (Promoter_dGFP-NLS_T_{NOS}_P_{NOS}_tdTomato-NLS_T_{OCS}) NLS means the protein was targeted to the nucleus. *P. tremula x alba*: n = 4 roots. *P. tremula x tremuloides*: n = 2 roots. The value given for each root is a mean value of three to ten single nuclei to compensate for biological fluctuations. The standard error and significances calculated based on a Wilcoxon test are given. NS = not significant. Statistics were conducted in R as specified in the M&M. **89**

Figure 49. Comparison of GFP and RFP signals in non – mycorrhized fine roots of transgenic poplar hybrids shown in absence or presence of the mycorrhiza fungus *Pisolithus microcarpus*. Observed were GFP fluorescence intensities driven by the longest 2892 bp promoter fragment of *Potri.2G0797* in first order roots of *Populus tremula x tremuloides* plants. Composite plants were generated via *Agrobacterium rhizogenes* strain K599 mediated plant transformation using a Promoter_dGFP-NLS_T_{NOS}_P_{NOS}_tdTomato-NLS_T_{OCS}. Non-mycorrhized fine-roots were observed after three to four weeks, fine-roots from a mycorrhized root system after ~12 weeks. Pictures were taken at the epifluorescence microscope. All details including the filter settings, used camera and camera settings are given in the M&M. Fluorescence signals were enhanced similarly for both GFP and RFP in each sample (ImageJ: Contrast enhanced by 0.1 % and background subtracted in montages). **90**

Figure 50. Example for a non-mycorrhized and mycorrhized *Populus tremula x alba* fine root. The fungal partner was *Pisolithus microcarpus*. The picture was taken with a binocular under bright field (as described in the M&M). **90**

Figure 51. GFP and RFP signals in a mycorrhized fine - root. *Populus tremula x alba* was mycorrhized with *Pisolithus microcarpus*. The GFP signal was driven by a 2982 bp promoter fragment of *Potri.2G0797*, whereas the tdTomato signal was driven by a NOS promoter. Both FPS were part of a double marker cassette and targeted to the nucleus. Images were taken using a binocular and filter sets are described in the M&M. Fluorescence signals were enhanced similarly for both GFP and RFP channels by increasing the contrast by 0.3 % in ImageJ. **91**

Figure 52. Promoter fragments of *Potri.2G2183*from *Populus trichocarpa* that were coupled to a reporter (eGFP) to identify regulatory elements in this gene upon ectomycorrhiza formation. The eGFP was targeted to the nucleus. Transgenic poplar roots were generated with Agrobacterium mediated plant transformation, during which Composite plants were generated. The eGFP expression was compared between the constructs visually at a microscope and determined by qPCR. **93**

Figure 53. Visualization of the promoter activity of a 3551 bp promoter fragment from *Potri.2G2183* driving nuclear targeted GFP expression in transiently transformed tobacco leaves in a double marker construct. As negative control a promoter was GFP less. Tobacco leaves were transiently transformed with *Agrobacterium rhizogenes* strain K599 in an OD_{600} of 0.3. The binary vector was pCXUN and the T-DNA was composed of the respective promoter fragment, dGFP-NLS and a NOS terminator as well as a second constitutively expressed NOS promoter, tdTomato-NLS and OCS terminator cassettes. NLS means the protein was targeted to the nucleus. Pictures were obtained with a Leica binocular with a gain of 4.7 dB three days after the infiltration. All pictures were processed in the same manner. Further details about the devices and filter settings can be found in the M&M. **94**

Figure 54. Promoter activity of *Potri.2G2183* promoter truncations in a double marker construct (Promoter_dGFP-NLS_T_{NOS}_P_{NOS}_tdTomato-NLS_T_{OCS}). The truncations range from -516 bp to -3551 bp. The negative control harbouring a promoter less GFP and the positive control harbours GFP driven by a NOS promoter. The 3551 bp promoter fragment was amplified from *Populus trichocarpa* gDNA, truncated with 5´deletion and visualized in transgenic *P. tremula x alba* plants. Shown are root hair areas 1 cm above the root tip. Roots were illuminated at the lowest possible light intensity (25 %) with xenon light source at a Zeiss Axioskop Microscope. Pictures were made with a Imagingsource camera in an IC Capture software. Filter sets for GFP were in a 450 – 490 nm excitation and 510 – 560 nm emission window and for RFP in a 510 – 560 nm excitation and 590 nm long pass emission filter window filter with a 580 nm beam splitter. Further details are given in the M&M. The roots were 5 to 8 weeks old and in approximately the same growth state. For visualization the contrast enhanced by 0.01 % and background subtracted in ImageJ (further details in the M&M). Representative pictures are given for n = 10 plants per construct from two independent transformation events. **95**

Figure 55. Comparing GFP fluorescence intensities driven by 3551 bp and 516 bp promoter fragments of *Potri.2G2183* in first order roots. Composite plants were generated via *Agrobacterium rhizogenes* strain K599 mediated plant transformation using a Promoter_dGFP-NLS_T_{NOS}_P_{NOS}_tdTomato-NLS_T_{OCS}. Pictures were obtained from a Leica binocula (specifications in the M&M). All pictures were made under the same conditions. The roots all were 5 to 8 weeks old. For visualization, the pictures were processed in the same manner in ImageJ (In merged pictures of both corresponding channel pictures: Contrast of root hairs increased by 0.1 %, background subtracted). All pictures were taken with the same parameters (gain = 4.8 dB, light intensity = 25 %) as further described in the M&M. **96**

Figure 56. Comparing GFP fluorescence intensities driven by 3551 bp and 516 bp promoter fragments of *Potri.2G2183* root hair nuclei of first order roots. Composite plants were generated via *Agrobacterium rhizogenes* strain K599 mediated plant transformation using a Promoter_dGFP-NLS_T_{NOS}_P_{NOS}_tdTomato-NLS_T_{OCS}. Pictures were obtained from a Zeiss microscope (specifications in the M&M). All pictures were made under the same conditions. The roots all were 5 to 8 weeks old and root hairs of approximately the same age were compared. For visualization, the pictures were processed in the same manner in ImageJ (In merged pictures of both corresponding channel pictures: Contrast of root hairs increased by 0.1 %, background subtracted). All pictures were taken with the same parameters (gain = 4.8 dB, light intensity = 25 %) as further described in the M&M. **97**

Figure 57. Promoter activity of a *Potri.9G1040* 1181 bp promoter fragment in a double marker construct (Promoter_dGFP-NLS_T_{NOS}_P_{NOS}_tdTomato-NLS_T_{OCS}). The negative control harbours a promoter less GFP and the positive control harbours GFP driven by a NOS promoter. The promoter fragment was amplified from *Populus tremula x tremuloides* gDNA and visualized in transgenic *P. tremula x alba* plants. Roots were illuminated at the lowest possible light intensity (25 %) with xenon light source at a Zeiss Axioskop Microscope. Pictures were made with a Imagingsource camera in an IC Capture software. Filter sets for GFP were in a 450 – 490 nm excitation and 510 – 560 nm emission window and for RFP in a 510 – 560 nm excitation and 590 nm long pass emission filter window filter with a 580 nm beam splitter. Further details are given in the M&M. The roots were 5 to 8 weeks old and in approximately the same growth state. For visualization the contrast enhanced by 0.1 % (further details in the M&M). Representative pictures are given for n = 10 plants per construct from two independent transformation events. **98**

Figure 58. Schematic display of a pCXUN T – DNA harbouring two fluorescence marker cassettes. Shown are the components of the T – DNA and their respective size in bp. A kanamycin resistance cassette serves as plant selection marker. LB: left border- and RB: right border sequence. The investigated expression cassette was composed of a UBQ promoter or the promoter of a gene of interest (Investigated expression cassette), a nucleus targeted eGFP and a NOS terminator. The constitutively expressed a constitutively expressed tdTomato cassette consisted of a NOS promoter, a nuclear targeted tdTomato and an OCS terminator. The total T – DNA size was 7.2 kb. The numbers between the elements indicate the number of spacer base pairs between the elements. **101**

Figure 59. Visualizing an 8 – fold TdTomato-NLS- and 11.4 – fold GFP-NLS expression difference in root hair nuclei of *Populus tremula x alba* plants. Shown are composite poplar plants, which were transformed with a pCXUN binary vector via *Agrobacterium rhizogenes* strain K599. To determine the differences, fluorescence intensities of raw images were obtained from ImageJ. Based on the obtained intensities of weak and strong expressing nuclei the above-mentioned ratios were calculated. The nuclei did not belong to the same construct or the same plant. The sole purpose of this comparison was to see, if and how differences in expression strength can be visualized. **111**

Figure 60. Predicted topology of *Potri.2G0797* as a membrane protein. *Potri.2G0797* likely codes for an amino acid transporter located at the plasma membrane with nine transmembrane regions. The N – terminus is in the cytoplasm and the C – terminus in the extracellular matrix. Loops in the cytoplasm are numbered from a to d. Predictions were made with Geneious Prime version 2021. **116**

6.3 Construct verifications

6.3.1 Verification of marker constructs in pCXUN for establishing experiments

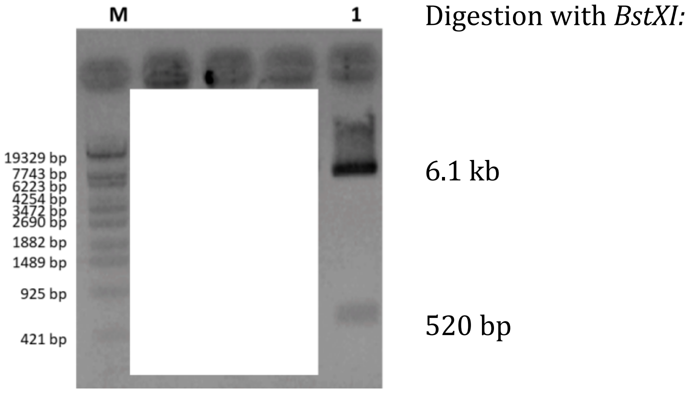
M
1
Digestion with *BstXI:*
19329 bp
7743 bp
6223 bp
4254 bp
3472 bp
2690 bp
1882 bp
1489 bp
925 bp
421 bp
6.1 kb
520 bp

Supplementary figure 1. Restriction digestion of a pPLV binary vector containing a P$_{35S}$_tmTomato-SNL_T$_{OCS}$ marker cassette on its T – DNA. The construct was verified by restriction digestion with *BstxI* (Lane 1). Expected were 6.1 kb and 520 bp. As marker (Lane M, 6 µl) the Phage Lambda DNA/Eco130I (StyI) DNA was used (see M&M). SNL means the protein was targeted to the peroxisomes.

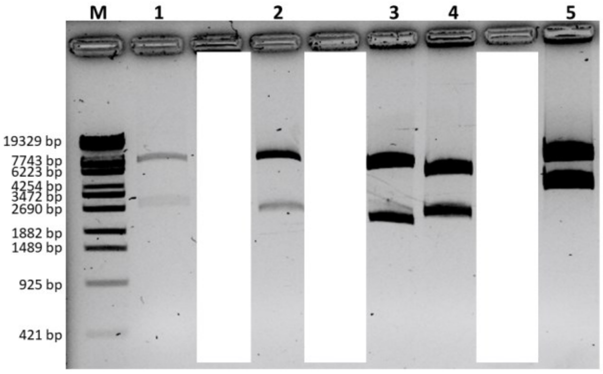
M
1
2
3
4
5
19329 bp
7743 bp
6223 bp
4254 bp
3472 bp
2690 bp
1882 bp
1489 bp
925 bp
421 bp

Supplementary figure 2. Verification of different marker cassettes in the pCXUN binary vector T - DNA by restriction digestion. All constructs were verified with *PvuII* restriction digestion. Lane 1: P$_{35S}$_tdTomato-NLS_T$_{OCS}$, expected were 2899 bp and 8634 bp. Lane 2: P$_{35S}$_tmTomato-SNL_T$_{NOS}$, expected were 2285 bp and 8634 bp. Lane 3: P$_{35S}$_sYFP-SNL_T$_{OCS}$, expected were 2203 bp and 8634 bp. Lane 4: P$_{NOS}$_tdTomato-NLS_T$_{OCS}$, expected were 2300 bp and 8634 bp. Lane 5: P$_{35S}$_sYFP-SNL_T$_{OCS}$_ P$_{NOS}$_tdTomato-NLS_T$_{OCS}$, expected were 4230 bp and 8634 bp. As marker (Lane M, 6 µl) the Phage Lambda DNA/Eco130I (StyI) DNA ladder was used. Further details are given in the M&M.

6.3.2 Establishing DsRED-E5

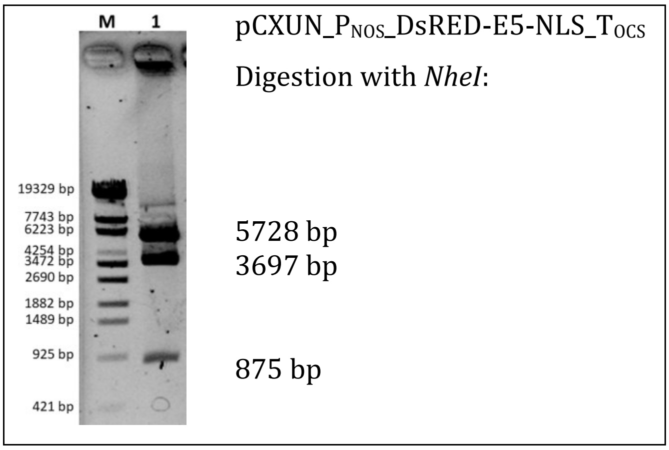
M
1
19329 bp
7743 bp
6223 bp
4254 bp
3472 bp
2690 bp
1882 bp
1489 bp
925 bp
421 bp
pCXUN_P$_{NOS}$_DsRED-E5-NLS_T$_{OCS}$
Digestion with *NheI*:
5728 bp
3697 bp
875 bp

Supplementary figure 3. Verification of a nuclear targeted DsRED-E5 expression cassette in the pCXUN binary vector T - DNA by restriction digestion. The pCXUN_P$_{NOS}$_DsRed-E5-T$_{OCS}$ construct was verified with *NheI* restriction digestion (Lane 1). Expected were 875 bp + 3697 bp + 5728 bp. As marker (Lane M, 6 µl) the Phage Lambda DNA/Eco130I (StyI) DNA ladder was used. Further details are given in the M&M.

6.3.3 Verifications of Potri.2G0797 subcellular localization constructs

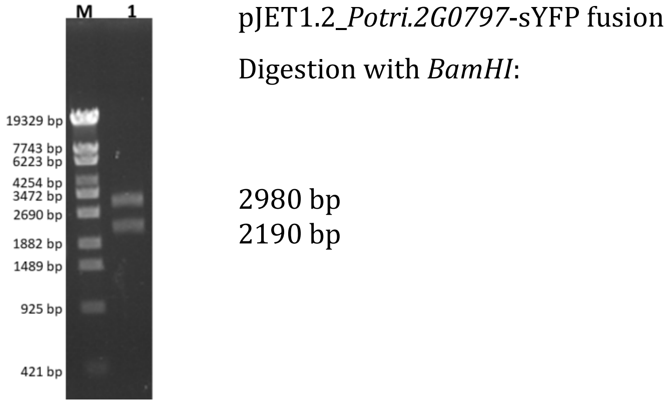
M
1
19329 bp
7743 bp
6223 bp
4254 bp
3472 bp
2690 bp
1882 bp
1489 bp
925 bp
421 bp
pJET1.2_*Potri.2G0797*-sYFP fusion
Digestion with *BamHI*:
2980 bp
2190 bp

Supplementary figure 4. Verification of the C-terminal fusion of *Potri.2G0797* without introns with sYFP in pJET1.2. The construct was verified with *BamHI* digestion, and the results of the gel electrophoresis are shown in Lane 1. Expected were 2.190 kb and 2.980 kb. As marker (Lane M, 6 µl) the Phage Lambda DNA/Eco130I (StyI) DNA ladder was used. Further details are given in the M&M.

Sequencing of *Potri.2G0797*-sYFP without introns in pPLV between P_{35S} and T_{OCS}

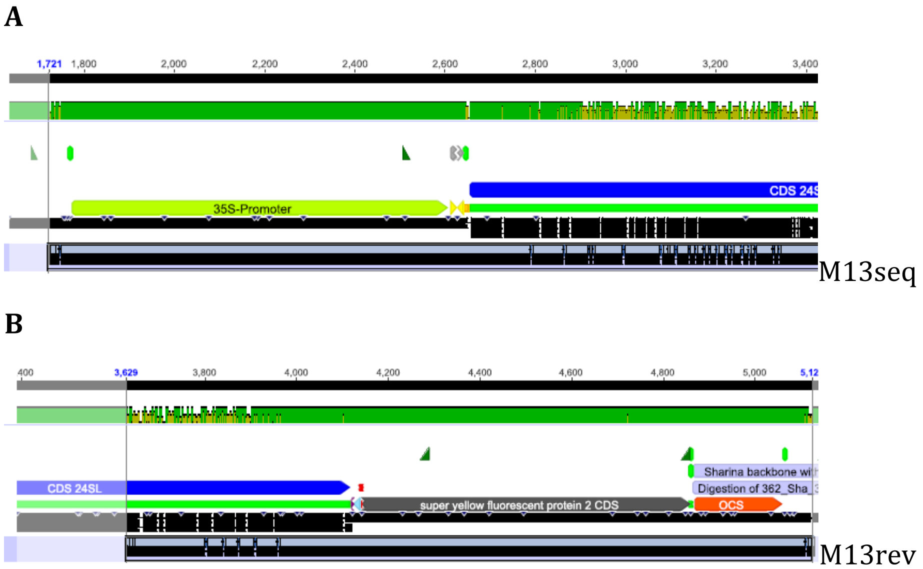
A
1,721
1,800
2,000
2,200
2,400
2,600
2,800
3,000
3,200
3,400
35S-Promoter
CDS 24S
M13seq
B
400
3,629
3,800
4,000
4,200
4,400
4,600
4,800
5,000
5,12
CDS 24SL
Sharina backbone wi
Digestion of 362_Sha
super yellow fluorescent protein 2 CDS
OCS
M13rev

Supplementary figure 5. Verification of *Potri.2G0797*-sYFP (24SL) without introns in pPLV between P_{35S} and T_{OCS} via partial Sanger sequencing. Sequenced was with M13seq (A) and M13rev (B) (see Table 21, page 52). The alignments against a reference plasmid were performed with Geneious (described in chapter 2.6.11). Further details are given in the M&M.

pCXUN_P_{35S}_CDS-sYFP_T_{OCS}

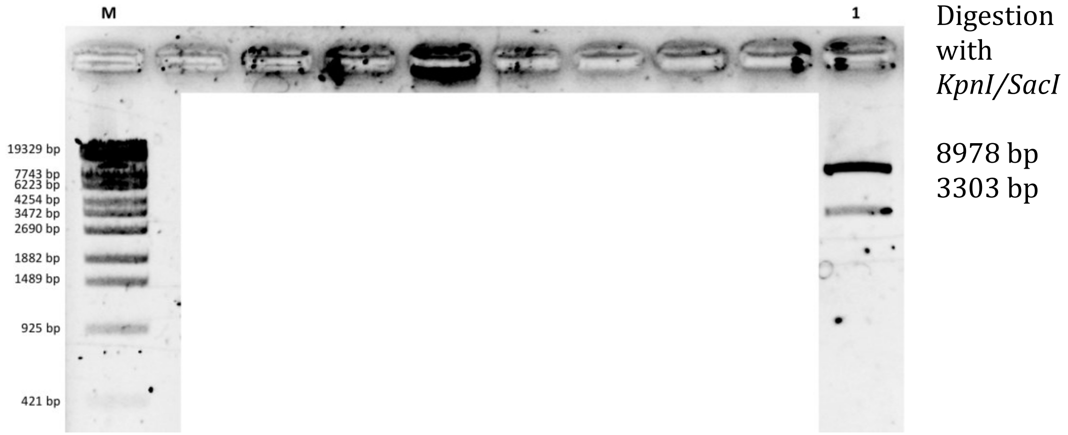
M
1
19329 bp
7743 bp
6223 bp
4254 bp
3472 bp
2690 bp
1882 bp
1489 bp
925 bp
421 bp
Digestion with *KpnI/SacI*
8978 bp
3303 bp

Supplementary figure 6. Verification of a C-terminal fusion of *Potri.2G0797* without introns with sYFP in a pCXUN binary vector T – DNA between a 35S promoter and OCS terminator. The construct was verified with *KpnI/SacI* restriction digestion. Lane 1: expected were 3303 bp and 8978 bp. As marker (Lane M, 6 µl) the Phage Lambda DNA/Eco130I (StyI) DNA ladder was used. Further details are given in the M&M.

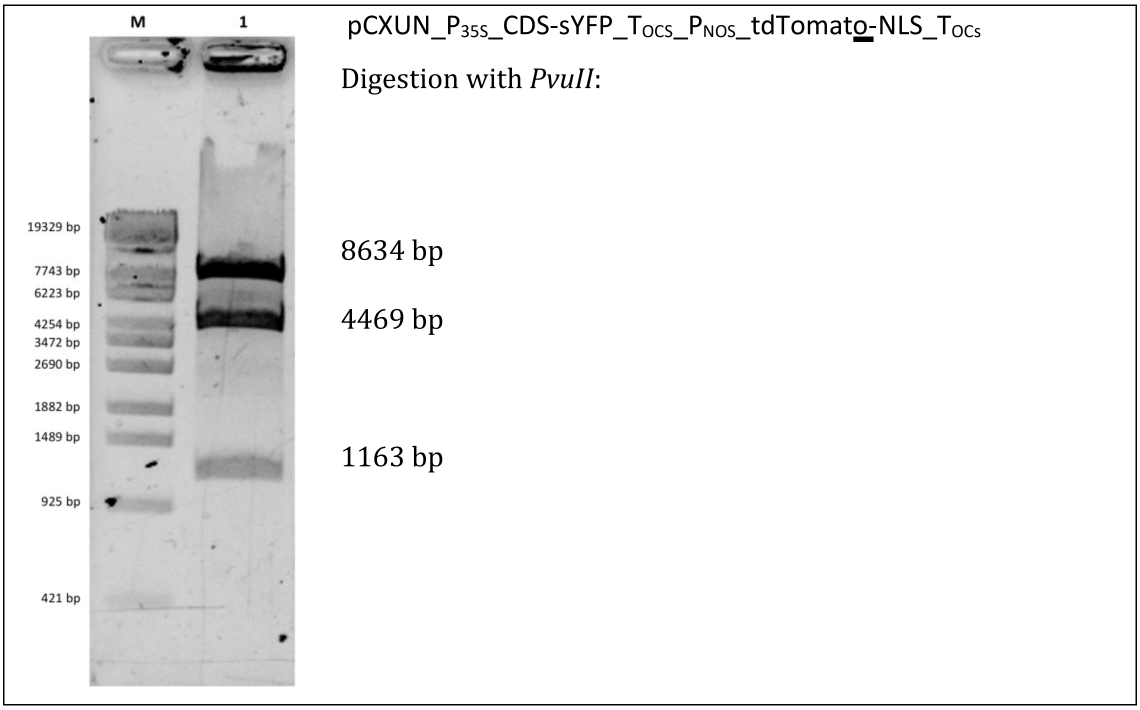
M
1
pCXUN_P_{35S}_CDS-sYFP_T_{OCS}_P_{NOS}_tdTomato-NLS_T_{OCs}
Digestion with *PvuII*:
19329 bp
7743 bp
6223 bp
4254 bp
3472 bp
2690 bp
1882 bp
1489 bp
925 bp
421 bp
8634 bp
4469 bp
1163 bp

Supplementary figure 7. Verification of the subcellular localization construct for *Potri.2G0797* with a second marker cassette *without introns* in pCXUN (P_{35S}_CDS *Potri.2G0797*– secYFP_T_{OCS}_P_{NOS}_tdTomato-NLS_T_{OCS}) with *PvuII* restriction digestion. Lane 1: expected were 1163 bp, 4469 bp and 8634 bp. As marker (Lane M, 6 µl) the Phage Lambda DNA/Eco130I (StyI) DNA ladder was used. Further details are given in the M&M.

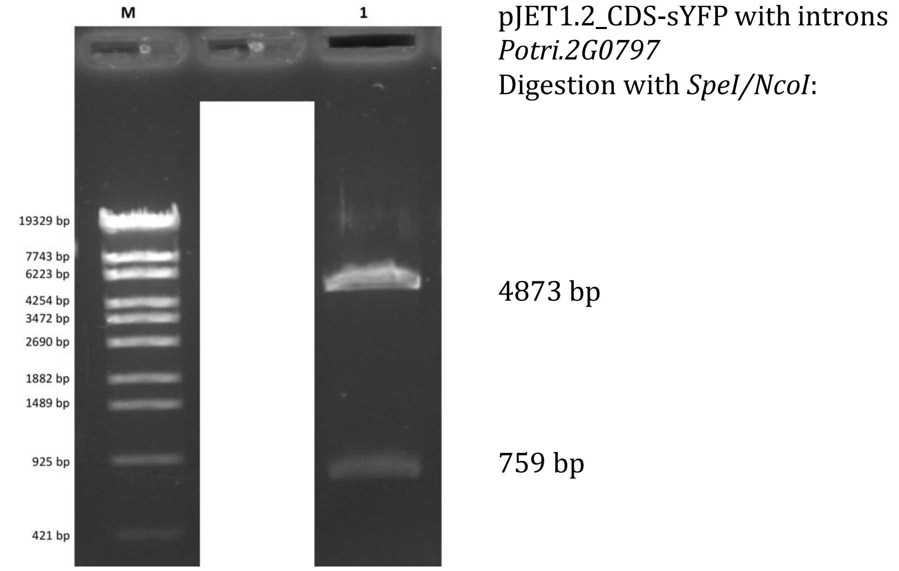
M
1
pJET1.2_CDS-sYFP with introns
Potri.2G0797
Digestion with *SpeI/NcoI*:
19329 bp
7743 bp
6223 bp
4254 bp
3472 bp
2690 bp
1882 bp
1489 bp
925 bp
421 bp
4873 bp
759 bp

Supplementary figure 8. Verification of the C-terminal fusion of *Potri.2G0797* from *Populus tremula x tremuloides* gDNA with sYFP in pJET1.2. The construct was verified with *SpeI/NcoI* restriction digestion (Lane 1). Expected were 759 bp and 4873 bp. As marker (Lane M, 6 µl) the Phage Lambda DNA/Eco130I (StyI) DNA ladder was used. Further details are given in the M&M.

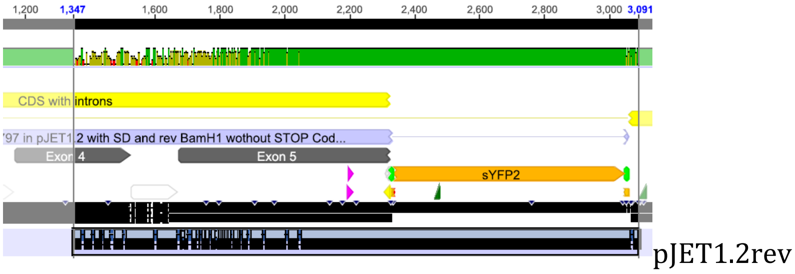
1,200
1,347
1,600
1,800
2,000
2,200
2,400
2,600
2,800
3,000
3,091
CDS with introns
'97 in pJET1.2 with SD and rev BamH1 wothout STOP Cod...
Exon 4
Exon 5
sYFP2
pJET1.2rev

Supplementary figure 9. Verification of *Potri.2G0797*-sYFP with introns in pJET1.2 via partial Sanger sequencing (as described in chapter 2.6.9). Sequenced was with pJET1.2rev (see Table 21, page 52). The alignment against a reference plasmid was performed with Geneious (described in chapter 2.6.11).

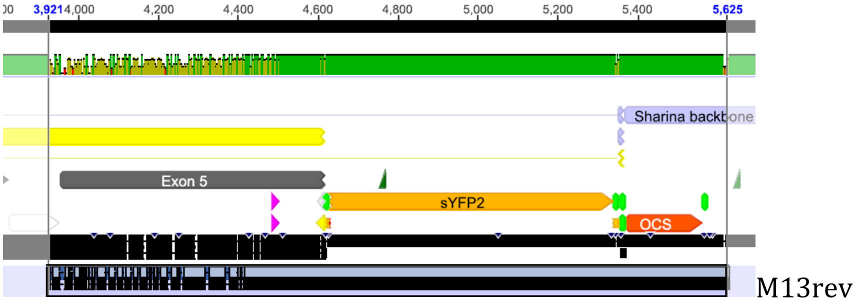
3,921
4,000
4,200
4,400
4,600
4,800
5,000
5,200
5,400
5,625
Sharina backbone
Exon 5
sYFP2
OCS
M13rev

Supplementary figure 10 Verification of *Potri.2G0797*-sYFP with introns in pPLV between P_{35S} and T_{OCS} via partial Sanger sequencing (as described in chapter 2.6.9). Sequenced was with M13rev (see Table 21, page 52). The alignment against a reference plasmid was performed with Geneious (described in chapter 2.6.11). pPLV is referred to as Sharina.

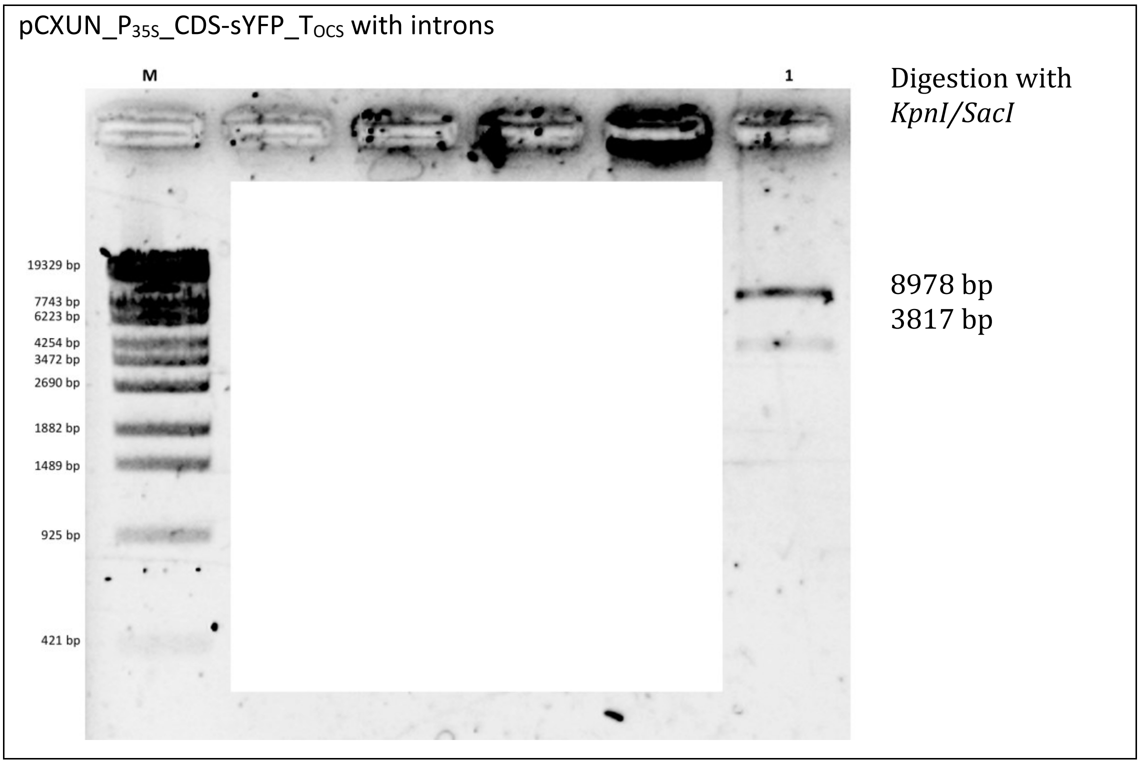
pCXUN_P35S_CDS-sYFP_TOCS with introns
M
1
Digestion with
KpnI/SacI
19329 bp
7743 bp
6223 bp
4254 bp
3472 bp
2690 bp
1882 bp
1489 bp
925 bp
421 bp
8978 bp
3817 bp

Supplementary figure 11. Verification of a C-terminal fusion of *Potri.2G0797* with introns with sYFP in a pCXUN binary vector T – DNA between a 35S promoter and OCS terminator. The construct was verified with *KpnI* and *SacI* digestion (Lane 1). Expected were 3817 bp and 8978 bp. As marker (Lane M, 6 µl) the Phage Lambda DNA/Eco130I (StyI) DNA ladder was used. Further details are given in the M&M.

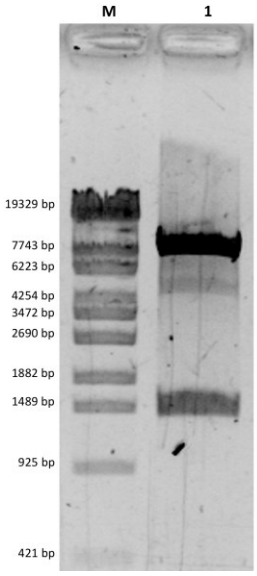
M
1
19329 bp
7743 bp
6223 bp
4254 bp
3472 bp
2690 bp
1882 bp
1489 bp
925 bp
421 bp

pCXUN_P$_{35S}$_CDS-sYFP_T$_{OCS}$_P$_{NOS}$_tdTomato-NLS_T$_{OCs}$

Potri.2G0797 with introns
Digestion with *PvuII*:

8634 bp
4836 bp

1310 bp

Supplementary figure 12. Verification of a C-terminal fusion of *Potri.2G0797* with introns with sYFP and a second marker cassette in a pCXUN binary vector T – DNA between a 35S promoter and OCS terminator. The construct (P$_{35S}$_CDS *Potri.2G0797*– sYFP_T$_{OCS}$_P$_{NOS}$_tdTomato-NLS_T$_{OCS}$) was verified with *PvuII* restriction digestion (Lane 1). Expected were 1310 bp, 4836 bp and 8634 bp. As marker (Lane M, 6 µl) the Phage Lambda DNA/Eco130I (StyI) DNA ladder was used. Further details are given in the M&M.

6.3.4 *Verifications of Potri.2G0797 promoter constructs*

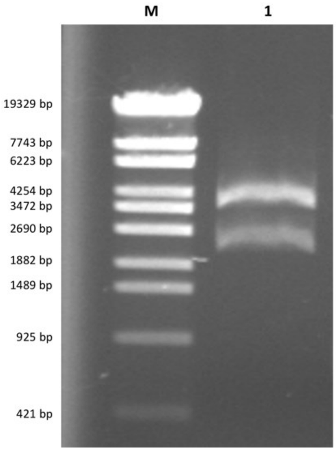
M
1
19329 bp
7743 bp
6223 bp
4254 bp
3472 bp
2690 bp
1882 bp
1489 bp
925 bp
421 bp

Potri.2G0797
pJET1.2_2892 bp promoter

Digestion with *XhoI*:

3597 bp
2269 bp

Supplementary figure 13. Verification of a 2.892 bp promoter fragment of *Potri.2G0797* in pJET1.2. The fragment was amplified from *Populus tremula x tremuloides* gDNA and was verified with *XhoI* restriction digestion (Lane 1). Expected were 2269 bp and 3597 bp for 3´ -5´orientation. As marker (Lane M, 6 µl) the Phage Lambda DNA/Eco130I (StyI) DNA ladder was used. Further details are given in the M&M.

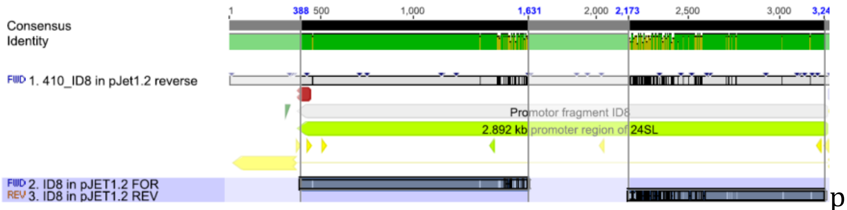
1
388
500
1,000
1,631
2,000
2,173
2,500
3,000
3,24
Consensus
Identity
FWD 1. 410_ID8 in pJet1.2 reverse
Promotor fragment ID8
2.892 kb promoter region of 24SL
FWD 2. ID8 in pJET1.2 FOR
REV 3. ID8 in pJET1.2 REV

pJET1.2for and rev

Supplementary figure 14. Verification of a 2.892 kb promoter region (ID8) of *Potri.2G0797* (24SL) in 3´- 5´orientation in pJET1.2, with partial Sanger sequencing (as described in chapter 2.6.9). Sequenced was with pJET1.2for and pJET1.2rev (see Table 21, page 52). The multiple alignment was performed with Geneious (described in chapter 2.6.11) against an *in-silico* consensus of *Populus tremuloides* and *P. trichocarpa*.

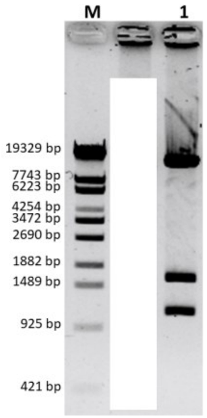
M
1
19329 bp
7743 bp
6223 bp
4254 bp
3472 bp
2690 bp
1882 bp
1489 bp
925 bp
421 bp

Potri.2G0797
pCXUN_2892 bp_dGFP-NLS_T_{NOS}_P_{NOS}_tdTomato-NLS_T_{OCS}
Digestion with *XhoI*:

12930 bp

1618 bp

1093 bp

Supplementary figure 15. Verification of a 2892 bp promoter fragment of *Potri.2G0797* in a pCXUN double marker cassette. The complete cassette consisted of 2892 bp Promoter_eGFP-NLS_T_{NOS}_P_{NOS}_tdTomato-NLS_T_{OCS}. The construct was verified with *XhoI* restriction digestion (Lane 1). Expected were 1093 bp + 1618 bp and 12930 bp. As marker (Lane M, 3 µl) the Phage Lambda DNA/Eco130I (StyI) DNA ladder was used. Further details are given in the M&M.

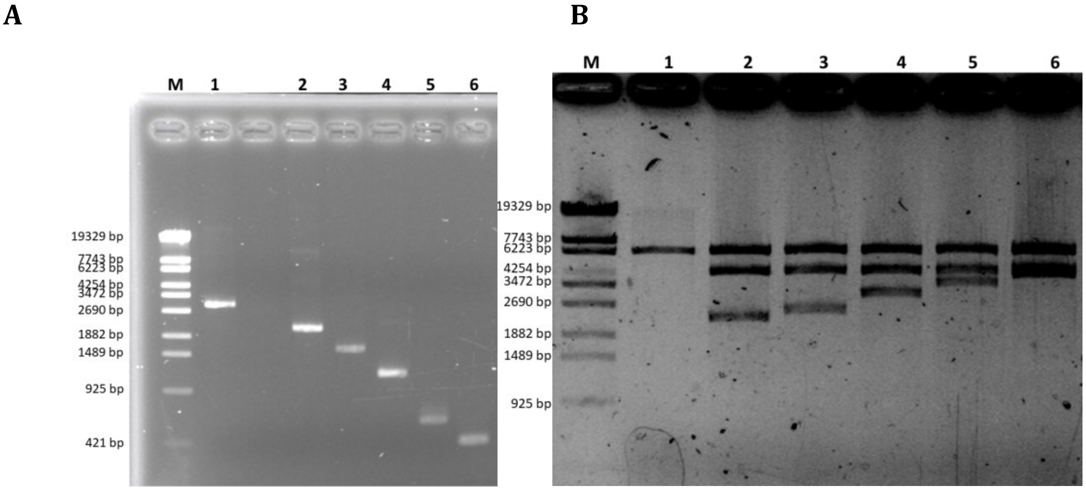
A
M
1
2
3
4
5
6
19329 bp
7743 bp
6223 bp
4254 bp
3472 bp
2690 bp
1882 bp
1489 bp
925 bp
421 bp
B
M
1
2
3
4
5
6
19329 bp
7743 bp
6223 bp
4254 bp
3472 bp
2690 bp
1882 bp
1489 bp
925 bp

Supplementary figure 16. A: PCR amplification of different 5´deletions from a 2892 bp promoter fragment of *Potri.2G0797* with LIC overhangs. Lane 1 = 2892 bp, Lane 2 = 2036 bp, Lane 3 = 1528, Lane 4 = 1078, Lane 5 = 520, Lane 6 = 341. The lowest bands run slightly higher than expected because of the large LIC adapters. Tm = 60°C. As marker (Lane M, 6 µl) the Phage Lambda DNA/Eco130I (StyI) DNA ladder was used. Further details are given in the M&M. **B: Verification of *Potri.2G0797* promoter LIC truncations in pCXUN with restriction digestion.** The complete cassette consisted of the respective truncation_eGFP_T_{NOS}_P_{NOS}_tdTomato-NLS_T_{OCS}. The constructs were verified with *ScaI* restriction digestions. Lane 1: vector control consisting of the LIC entry vector. Expected were 6253 bp + 254 bp + 6302 bp. Lane 2: 341 bp promoter in pCXUN. Expected were 6253 bp + 254 bp + 4309 bp + 2333 bp. Lane 3: 520 bp promoter in pCXUN. Expected were 6253 bp + 254 bp + 4309 bp + 2512 bp. Lane 4: 1078 bp promoter in pCXUN. Expected were 6253 bp + 254 bp + 4309 bp + 3068 bp. Lane 5: 1528 bp promoter in pCXUN. Expected were 6253 bp + 254 bp + 4309 bp + 3522 bp. Lane 6: 2032 bp promoter in pCXUN. Expected were 6253 bp + 254 bp + 4309 bp + 4029 bp. As marker (Lane M, 6 µl) the Phage Lambda DNA/Eco130I (StyI) DNA ladder was used. Further details are given in the M&M.

Potri.2G0797

pCXUN_2892 bp truncations_dGFP-NLS_T_{NOS}_P_{NOS}_tdTomato-NLS_T_{OCS}

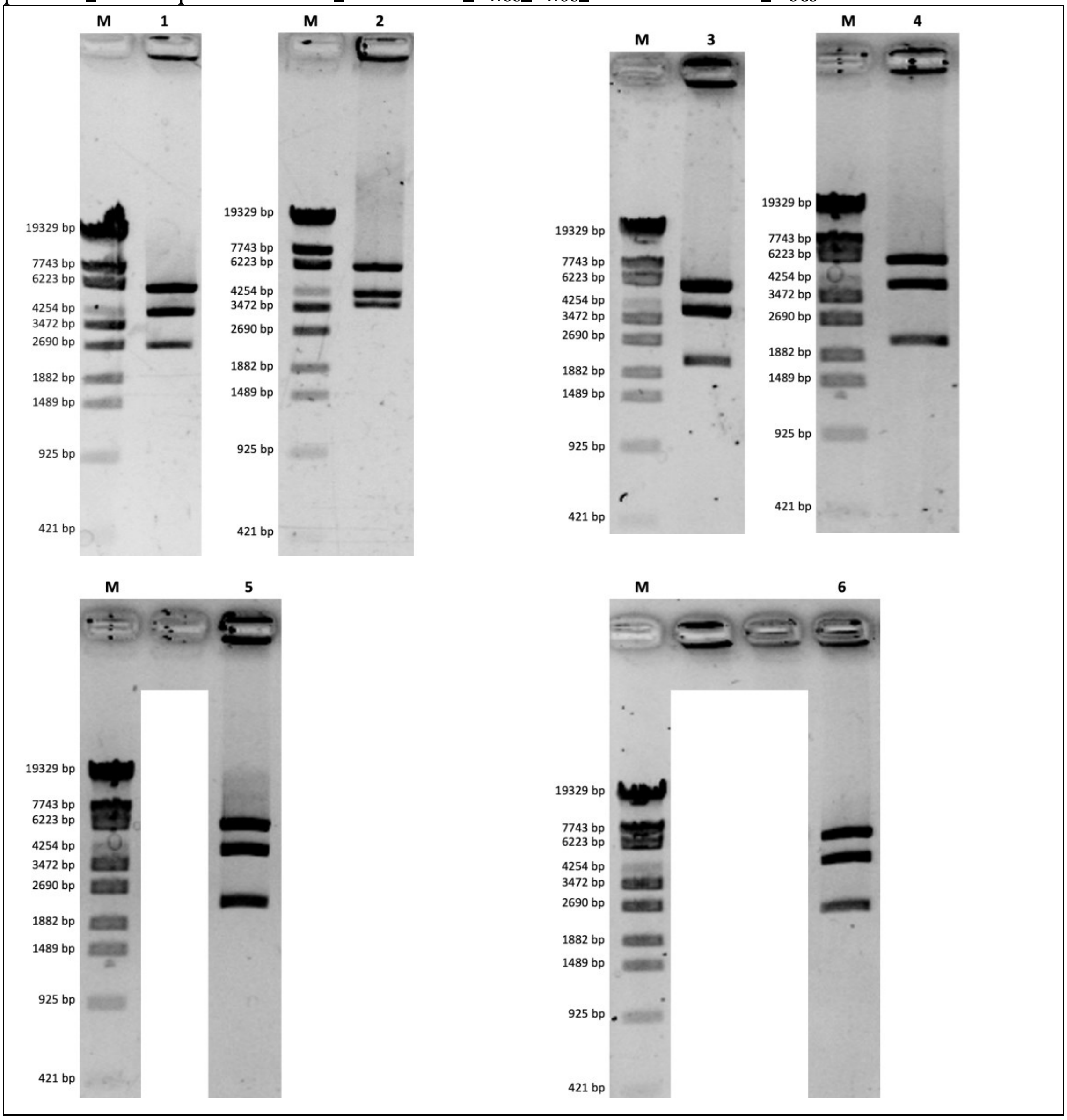
M
1
19329 bp
7743 bp
6223 bp
4254 bp
3472 bp
2690 bp
1882 bp
1489 bp
925 bp
421 bp
M
2
19329 bp
7743 bp
6223 bp
4254 bp
3472 bp
2690 bp
1882 bp
1489 bp
925 bp
421 bp
M
3
19329 bp
7743 bp
6223 bp
4254 bp
3472 bp
2690 bp
1882 bp
1489 bp
925 bp
421 bp
M
4
19329 bp
7743 bp
6223 bp
4254 bp
3472 bp
2690 bp
1882 bp
1489 bp
925 bp
421 bp
M
5
19329 bp
7743 bp
6223 bp
4254 bp
3472 bp
2690 bp
1882 bp
1489 bp
925 bp
421 bp
M
6
19329 bp
7743 bp
6223 bp
4254 bp
3472 bp
2690 bp
1882 bp
1489 bp
925 bp
421 bp

Supplementary figure 17. Verification of *Potri.2G0797* promoter truncations in pCXUN with restriction digestion and gel electrophoresis. The complete cassette consisted of the respective truncation_eGFP_T_{NOS}_P_{NOS}_tdTomato-NLS_T_{OCS}. The constructs were verified with *ScaI* restriction digestions. Lane 1: a 757 bp promoter in pCXUN. Expected were 251 bp + 4312 bp + 2691 bp + 6253 bp. Lane 2: a 1754 bp promoter in pCXUN. Expected were 251 bp + 4312 bp + 3688 bp + 6253 bp. Lane 3: a 226 bp promoter in pCXUN. Expected were 251 bp + 4312 bp + 2160 bp + 6253 bp. Lane 4: a 276 bp promoter in pCXUN. Expected were 251 bp + 4312 bp + 2210 bp + 6253 bp. Lane 5: a 391 bp promoter in pCXUN. Expected were 251 bp + 4312 bp + 2352 bp + 6253 bp. Lane 6: a 475 bp promoter in pCXUN. Expected were 251 bp + 4312 bp + 2391 bp + 6253 bp. As marker (Lane M, 6 µl) the Phage Lambda DNA/Eco130I (StyI) DNA ladder was used. Further details are given in the M&M.

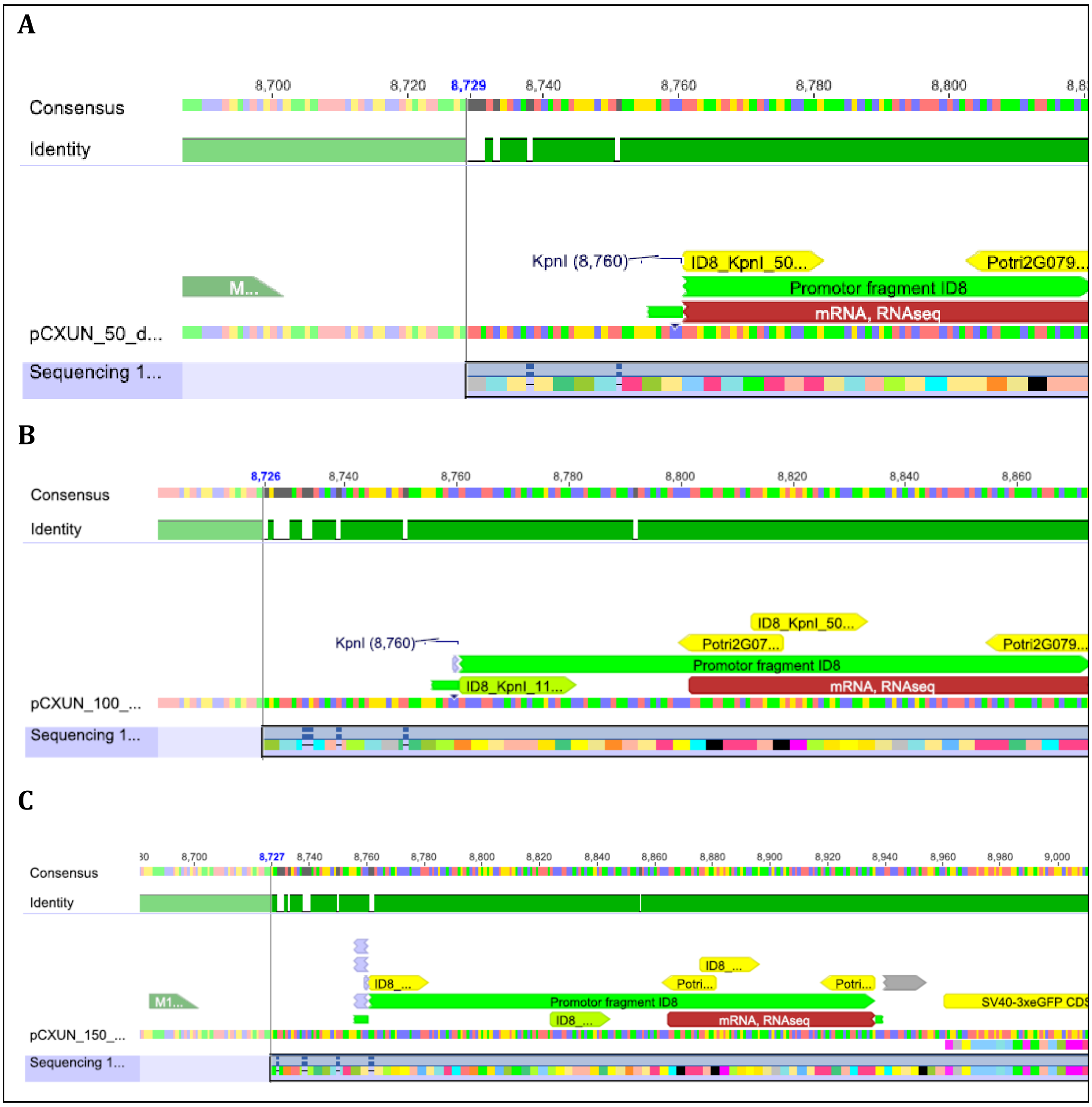
A
8,700
8,720
8,729
8,740
8,760
8,780
8,800
Consensus
Identity
KpnI (8,760)
ID8_KpnI_50...
Potri2G079...
M...
Promotor fragment ID8
mRNA, RNAseq
pCXUN_50_d...
Sequencing 1...
B
8,726
8,740
8,760
8,780
8,800
8,820
8,840
8,860
Consensus
Identity
ID8_KpnI_50...
KpnI (8,760)
Potri2G07...
Potri2G079...
Promotor fragment ID8
ID8_KpnI_11...
mRNA, RNAseq
pCXUN_100_...
Sequencing 1...
C
8,700
8,727
8,740
8,760
8,780
8,800
8,820
8,840
8,860
8,880
8,900
8,920
8,940
8,960
8,980
9,000
Consensus
Identity
ID8_...
ID8_...
Potri...
Potri...
M1...
Promotor fragment ID8
SV40-3xeGFP CDS
ID8_...
mRNA, RNAseq
pCXUN_150_...
Sequencing 1...

Supplementary figure 18. Verification of a 61 bp (A), 113 bp (B) and 176 bp (C) promoter fragment of *Potri.2G0797* (ID8) in pCXUN via partial Sanger sequencing (described in chapter 2.6.9). Sequenced was with the primer M13seq (see Table 21, page 52). The alignment was performed with Geneious (described in chapter 2.6.11). The sequencing result was aligned against an *in silico* consensus sequence of *P. tremuloides* and *P. trichocarpa.*

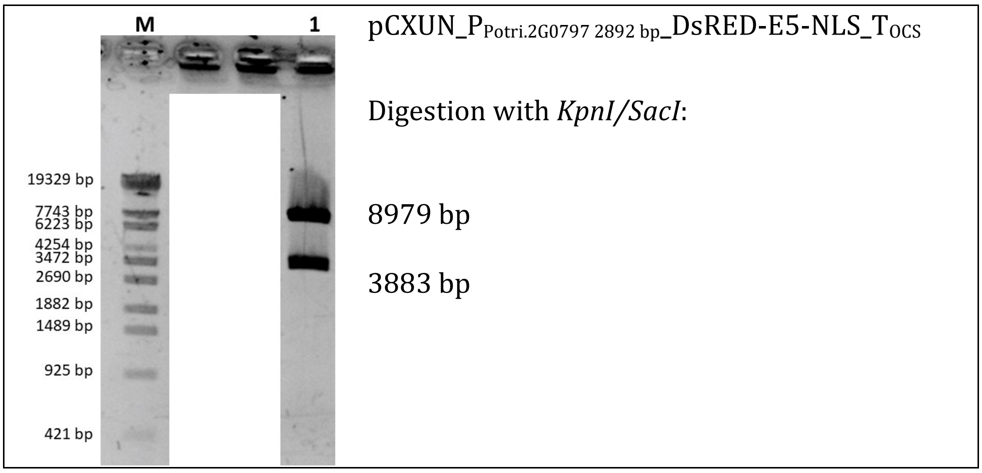
M
1
pCXUN_P$_{Potri.2G0797\ 2892\ bp}$_DsRED-E5-NLS_T$_{OCS}$
Digestion with *KpnI/SacI*:
8979 bp
3883 bp
19329 bp
7743 bp
6223 bp
4254 bp
3472 bp
2690 bp
1882 bp
1489 bp
925 bp
421 bp

Supplementary figure 19 Verification of pCXUN_P$_{2892\ bp\ Potri.2G0797}$_DsRed-E5-T$_{OCS}$ with restriction digestion. Lane 1: digested was with *KpnI/SacI*, expected were 3883 bp and 8979 bp. As marker (Lane M, 3 µl) the Phage Lambda DNA/Eco130I (StyI) DNA ladder (421- 19329 bp, Bioron, Ludwigshafen am Rhein, Germany) was used.

6.3.5 Verifications of Potri.2G2183 subcellular localization

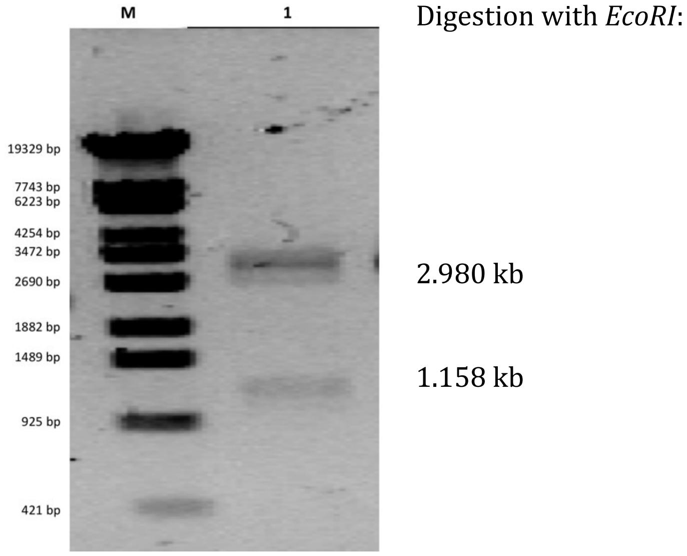
M
1
Digestion with *EcoRI*:
2.980 kb
1.158 kb
19329 bp
7743 bp
6223 bp
4254 bp
3472 bp
2690 bp
1882 bp
1489 bp
925 bp
421 bp

Supplementary figure 20. Verification of the C-terminal fusion construct of *Potri.2G2183* with sYFP in pJET1.2. The construct was verified with *EcoRII* digestion (Lane 1). Expected were 1.158 kb and 2.980 kb. As marker (Lane M, 6 µl) the Phage Lambda DNA/Eco130I (StyI) DNA ladder (421- 19329 bp, Bioron, Ludwigshafen am Rhein, Germany) was used.

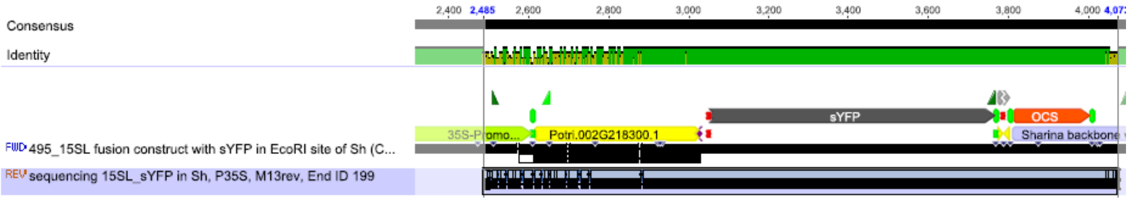
2,400
2,485
2,600
2,800
3,000
3,200
3,400
3,600
3,800
4,000
Consensus
Identity
sYFP
OCS
35S-Promo...
Potri.002G218300.1
Sharina backbone
FWD 495_15SL fusion construct with sYFP in EcoRI site of Sh (C...
REV sequencing 15SL_sYFP in Sh, P35S, M13rev, End ID 199

Supplementary figure 21 .Verification of pPLV_P$_{35S}$_CDS *Potri.2G2183*_sYFP_T$_{OCS}$ via partial Sanger sequencing (described in chapter 2.6.9). Sequenced was with the primer M13rev (see Table 21, page 52). The alignment against the reference plasmid was performed with Geneious (described in chapter 2.6.11). pPLV is named as Sharina.

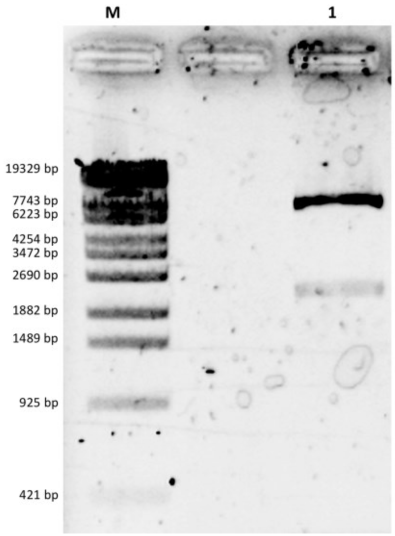
M
1
19329 bp
7743 bp
6223 bp
4254 bp
3472 bp
2690 bp
1882 bp
1489 bp
925 bp
421 bp

pCXUN_P_{35S}_CDS-sYFP_T_{OCS}

Digestion with KpnI/SacI:

8978 bp

2271 bp

Supplementary figure 22. Verification of a C-terminal fusion of *Potri.2G2183* and sYFP in a pCXUN binary vector T – DNA between a 35S promoter and OCS terminator. The construct was verified with *KpnI/SacI* restriction digestion (Lane 1). Expected were 2271 bp and 8978 bp. As marker (Lane M, 6 µl) the Phage Lambda DNA/Eco130I (StyI) DNA ladder was used. Further details are given in the M&M.

6.3.6 *Verifications of Potri.2G2183 promoter constructs*

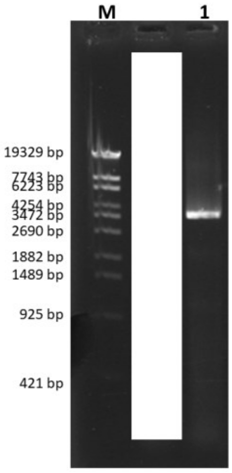
M
1
19329 bp
7743 bp
6223 bp
4254 bp
3472 bp
2690 bp
1882 bp
1489 bp
925 bp
421 bp

PCR amplification:

3551 bp

Supplementary figure 23. PCR amplified 3551 bp promoter fragment of *Potri.2G2183* from *Populus trichocarpa* with 5´*KpnI* and 3´*HpaI* overhangs. Expected were 3.551 kb. As marker (Lane M, 6 µl) the Phage Lambda DNA/Eco130I (StyI) DNA ladder was used. Further details are given in the M&M.

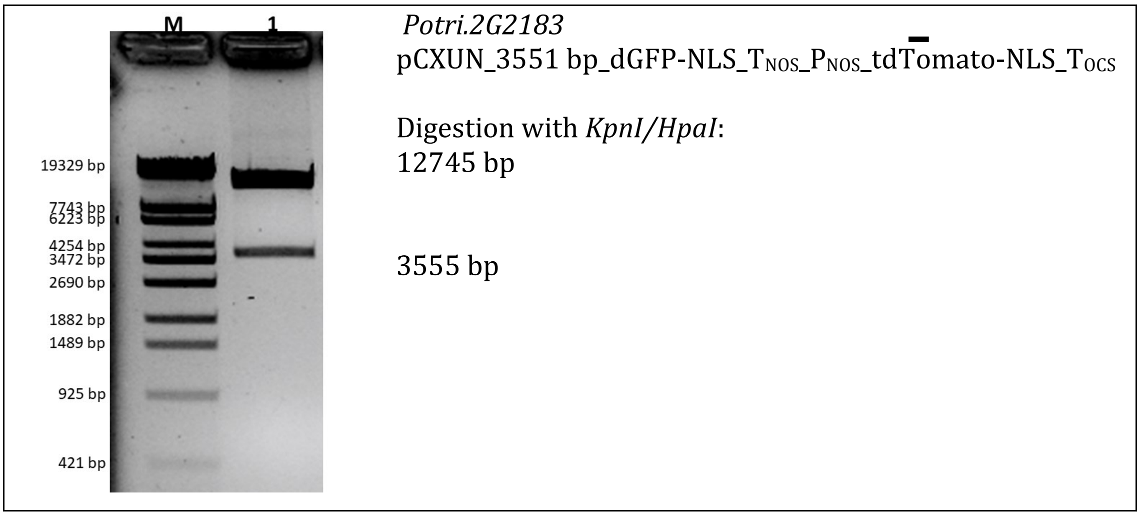
M
1
19329 bp
7743 bp
6223 bp
4254 bp
3472 bp
2690 bp
1882 bp
1489 bp
925 bp
421 bp
Potri.2G2183
pCXUN_3551 bp_dGFP-NLS_T_{NOS}_P_{NOS}_tdTomato-NLS_T_{OCS}
Digestion with *KpnI/HpaI*:
12745 bp
3555 bp

Supplementary figure 24. Verification of a 3551 bp promoter fragment of *Potri.2G2183* in pCXUN with restriction digestion. The promoter region was amplified from *Populus trichocarpa*. The complete cassette consisted of 3551 bp Promoter_T_{NOS}_P_{NOS}_tdTomato-NLS_T_{OCS}. Lane 1: digestion with *KpnI* and *HpaI*, expected were 3555 bp and 12745 bp. As marker (Lane M, 6 µl) the Phage Lambda DNA/Eco130I (StyI) DNA ladder was used. Further details are given in the M&M.

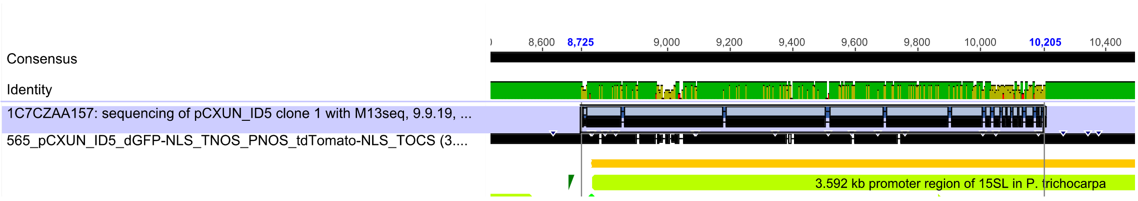
8,600
8,725
9,000
9,200
9,400
9,600
9,800
10,000
10,205
10,400
Consensus
Identity
1C7CZAA157: sequencing of pCXUN_ID5 clone 1 with M13seq, 9.9.19, ...
565_pCXUN_ID5_dGFP-NLS_TNOS_PNOS_tdTomato-NLS_TOCS (3....
3.592 kb promoter region of 15SL in P. trichocarpa

Supplementary figure 25. Verification of a 3551 bp promoter fragment of *Potri.2G2183* from *Populus trichocarpa* via partial Sanger sequencing (described in chapter 2.6.9). Sequenced was with the primer M13seq (see Table 21, page 52). The alignment was performed with Geneious (described in chapter 2.6.11). The sequencing result was aligned against an *In - silico* consensus sequence of *P. tremuloides* and *P. trichocarpa.*

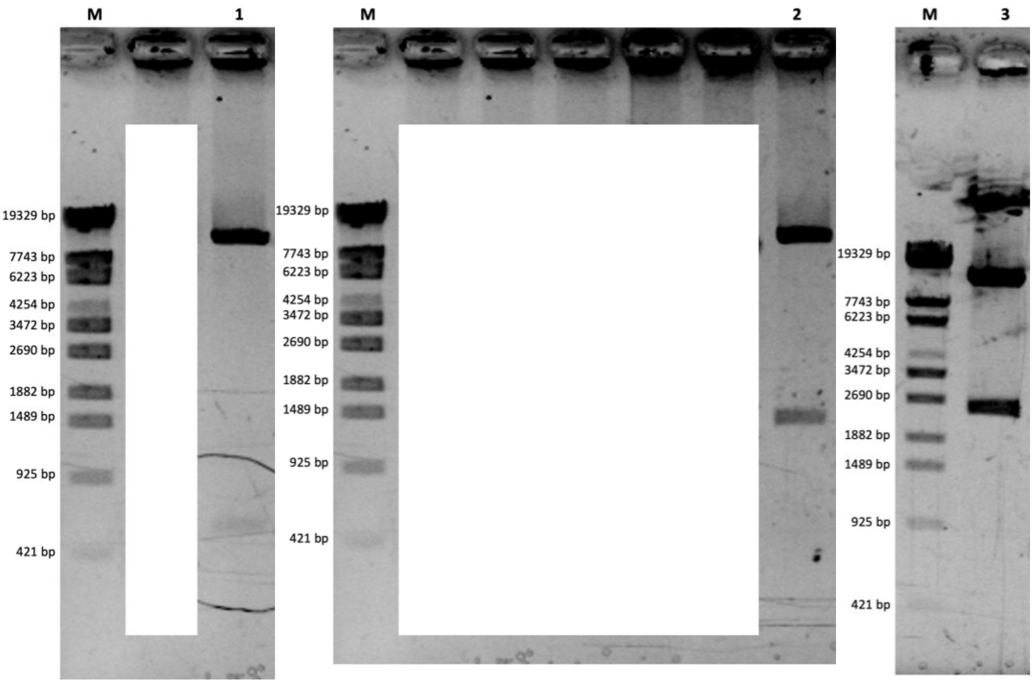
M
1
19329 bp
7743 bp
6223 bp
4254 bp
3472 bp
2690 bp
1882 bp
1489 bp
925 bp
421 bp
M
2
19329 bp
7743 bp
6223 bp
4254 bp
3472 bp
2690 bp
1882 bp
1489 bp
925 bp
421 bp
M
3
19329 bp
7743 bp
6223 bp
4254 bp
3472 bp
2690 bp
1882 bp
1489 bp
925 bp
421 bp

Supplementary figure 26. Verification of promoter of *Potri.2G2183* truncations in pCXUN with restriction digestion and gel electrophoresis. The promoter region was amplified from *Populus trichocarpa*. Digested was with *KpnI/HpaI* in all cases. Lane 1: A 516 bp promoter. Expected were 520 bp and 12754 bp. Lane 2: A 1289 bp promoter. Expected were 1293 bp and 12754 bp. Lane 3: A 2502 bp promoter. Expected were 2506 bp and 12764 bp. As marker (Lane M, 3 µl) the Phage Lambda DNA/Eco130I (StyI) DNA ladder was used. Further details are given in the M&M.

6.3.7 Verifications of Potri.9G1040 promoter constructs

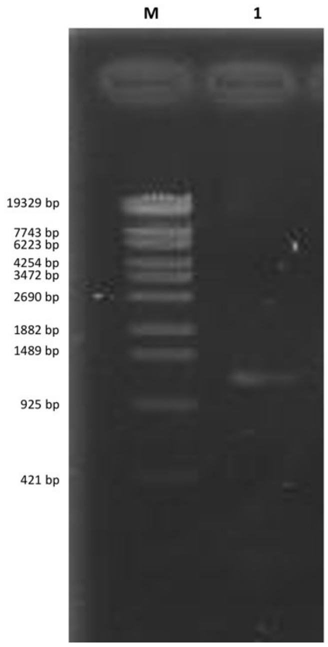
M
1
19329 bp
7743 bp
6223 bp
4254 bp
3472 bp
2690 bp
1882 bp
1489 bp
925 bp
421 bp

PCR amplification:

1.181 bp

Supplementary figure 27. PCR amplification of a 1181 bp promoter fragment of *Potri.9G1040* from *Populus tremula x tremuloides* gDNA. As marker (Lane M, 6 µl) the Phage Lambda DNA/Eco130I (StyI) DNA ladder was used. Further details are given in the M&M.

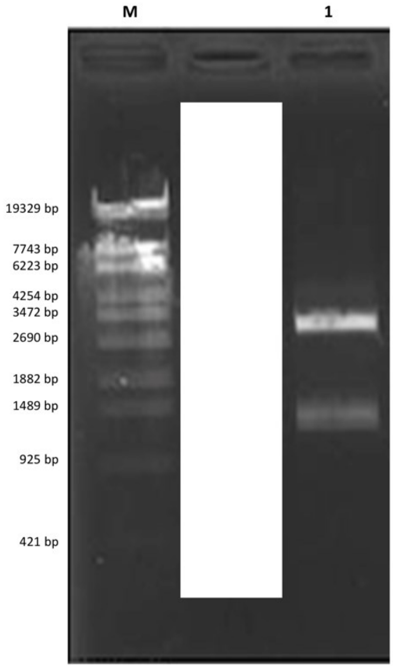
M
1
19329 bp
7743 bp
6223 bp
4254 bp
3472 bp
2690 bp
1882 bp
1489 bp
925 bp
421 bp

In pJET1.2

Digestion with *BglII*:

2.928 kb

1.227 kb

Supplementary figure 28. Verification of a 1.181 bp promoter fragment of *Potri.9G1040* in pJET1.2. The promoter region was amplified from *Populus tremula x tremuloides* gDNA. Digested was with *BglII* and the results of the gel electrophoresis are shown in Lane 1. Expected were 2.928 kb and 1.227 kb. As marker (Lane M, 6 µl) the Phage Lambda DNA/Eco130I (StyI) DNA ladder was used. Further details are given in the M&M.

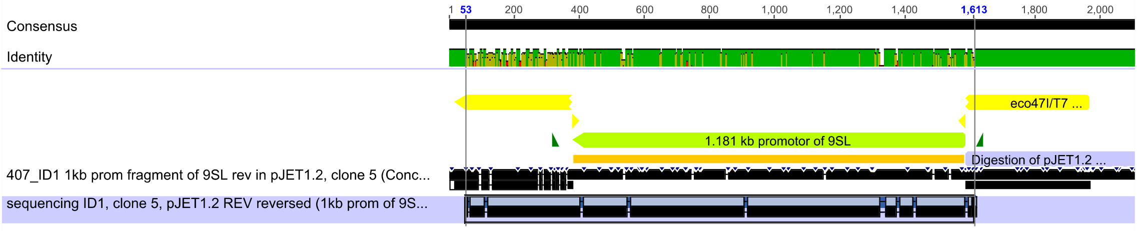
1
53
200
400
600
800
1,000
1,200
1,400
1,613
1,800
2,000
Consensus
Identity
eco47I/T7 ...
1.181 kb promotor of 9SL
Digestion of pJET1.2 ...
407_ID1 1kb prom fragment of 9SL rev in pJET1.2, clone 5 (Conc...
sequencing ID1, clone 5, pJET1.2 REV reversed (1kb prom of 9S...

Supplementary figure 29. Verification of a 1.183 kb promoter fragment of *Potri.9G1040* via partial Sanger sequencing (described in chapter 2.6.9). Sequenced was with the primer pJET1.2rev (see Table 21, page 52). The alignment against the reference plasmid was performed with Geneious (described in chapter 2.6.11). The sequencing result was aligned against an *in-silico* consensus sequence of *P. tremuloides* and *P. trichocarpa.*

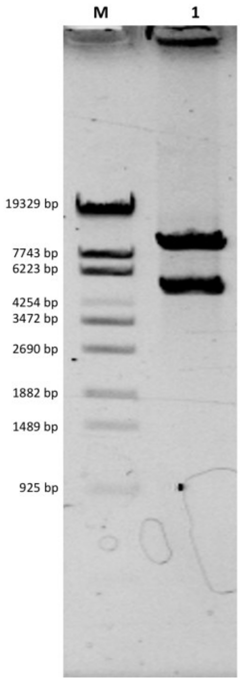
M
1
19329 bp
7743 bp
6223 bp
4254 bp
3472 bp
2690 bp
1882 bp
1489 bp
925 bp

Potri.9G1040
pCXUN_1183 bp_dGFP-NLS_T_{NOS}_P_{NOS}_tdTomato-NLS_T_{OCS}

Digestion with *KpnI/SacI*:

8978 bp

5010 bp

Supplementary figure 30. Verification of a 1.183 kb promoter fragment of *Potri.9G1040* in pCXUN with restriction digestion. The complete cassette consisted of 1.183 kb Promoter_T_{NOS}_P_{NOS}_tdTomato-NLS_T_{OCS}. Lane 1: digested was with *KpnI* and *SacI*, expected were 5010 bp and 8978 bp. As marker (Lane M, 6 µl) the Phage Lambda DNA/Eco130I (StyI) DNA ladder (421- 19329 bp, Bioron, Ludwigshafen am Rhein, Germany) was used.

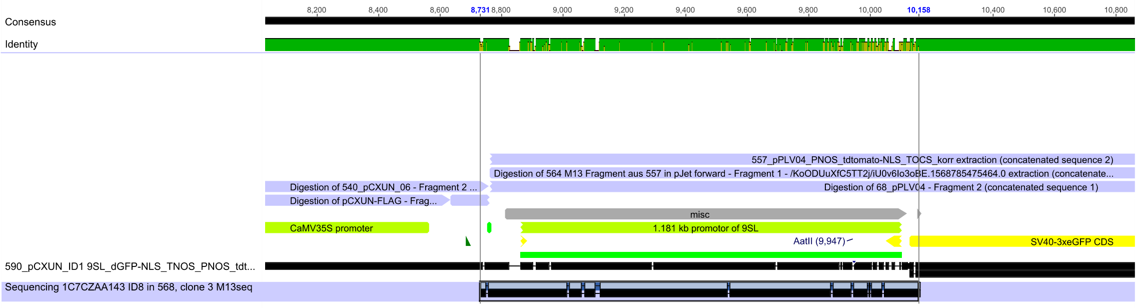
8,200
8,400
8,600
8,731
8,800
9,000
9,200
9,400
9,600
9,800
10,000
10,158
10,400
10,600
10,800
Consensus
Identity
557_pPLV04_PNOS_tdtomato-NLS_TOCS_korr extraction (concatenated sequence 2)
Digestion of 564 M13 Fragment aus 557 in pJet forward - Fragment 1 - /KoODUuXfC5TT2j/iU0v6lo3oBE.1568785475464.0 extraction (concatenate...
Digestion of 540_pCXUN_06 - Fragment 2 ...
Digestion of 68_pPLV04 - Fragment 2 (concatenated sequence 1)
Digestion of pCXUN-FLAG - Frag...
misc
CaMV35S promoter
1.181 kb promotor of 9SL
AatII (9,947)
SV40-3xeGFP CDS
590_pCXUN_ID1 9SL_dGFP-NLS_TNOS_PNOS_tdt...
Sequencing 1C7CZAA143 ID8 in 568, clone 3 M13seq

Supplementary figure 31. Verification of a 1.183 kb (ID1) promoter region of *Potri.9G1040* (9SL) via Sanger sequencing (described in chapter 2.6.9) in pCXUN. The construct consisted of pCXUN_ 1.138 kb promoter_dGFP-NLS_T_{NOS}_P_{NOS}_tdTomato-NLS_T_{OCS}. Sequenced was with the primer M13seq (see Table 21, page 52). The alignment against the reference plasmid was performed with Geneious (described in chapter 2.6.11)

7 References

Agerer, R. (1991). Characterization of Ectomycorrhiza. *Methods Microbiol.* 23, 25–73. doi:10.1016/S0580-9517(08)70172-7.

Agerer, R. (2001). Exploration types of ectomycorrhizae: A proposal to classify ectomycorrhizal mycelial systems according to their patterns of differentiation and putative ecological importance. *Mycorrhiza* 11, 107–114. doi:10.1007/s005720100108.

Akhtar, W., and Veenstra, G. J. C. (2011). TBP-related factors: A paradigm of diversity in transcription initiation. *Cell Biosci.* 1, 23. doi:10.1186/2045-3701-1-23.

Allen, B. L., and Taatjes, D. J. (2015). The Mediator complex: A central integrator of transcription. *Nat. Rev. Mol. Cell Biol.* 16, 155–166. doi:10.1038/nrm3951.

Allen, M. F. (1991). *The Ecology of Mycorrhizae*. doi:10.1097/00010694-199204000-00011.

Alpizar, E., Dechamp, E., Espeout, S., Royer, M., Lecouls, A. C., Nicole, M., et al. (2006). Efficient production of Agrobacterium rhizogenes-transformed roots and composite plants for studying gene expression in coffee roots. *Plant Cell Rep.* 25, 959–967. doi:10.1007/s00299-006-0159-9.

Amaranthus, M. P., and Perry, D. A. (1994). The functioning of ectomycorrhizal fungi in the field: linkages in space and time. *Plant Soil* 159, 133–140. doi:10.1007/BF00000102.

An, G., Costa, M. A., and Ha, S. B. (1990). Nopaline synthase promoter is wound inducible and auxin inducible. *Plant Cell* 2, 225–233. doi:10.1105/tpc.2.3.225.

Anand, A., Krichevsky, A., Schornack, S., Lahaye, T., Tzfira, T., Tang, Y., et al. (2007). Arabidopsis VIRE2 INTERACTING PROTEIN2 Is Required for Agrobacterium T-DNA Integration in Plants. *PLANT CELL ONLINE* 19, 1695–1708. doi:10.1105/tpc.106.042903.

Arnebrant, K., Ek, H., Finlay, R. D., and Söderström, B. (1993). Nitrogen translocation between Alnus glutinosa (L.) Gaertn. seedlings inoculated with Frankia sp. and Pinus contorta Doug, ex Loud seedlings connected by a common ectomycorrhizal mycelium. *New Phytol.* 124, 231–242. doi:10.1111/j.1469-8137.1993.tb03812.x.

Aslanidis, C., and de Jong, P. J. (1990). Ligation-independent cloning of PCR products (LIC-PCR). *Nucleic Acids Res.* 18, 6069–6074. doi:10.1093/nar/18.20.6069.

Balestrini, R., and Kottke, I. (2016). "Structure and development of ectomycorrhizal roots," in *Molecular Mycorrhizal Symbiosis*, 47–61. doi:10.1002/9781118951446.ch4.

Baluska, F., Mancuso, S., and Volkmann, D. (2006). *Communications in Plants. Neuronal Aspects of Plant Life*. 1st ed. Berlin Heidelberg: Springer-Verlag Available at: https://books.google.de/books?id=DBuPKhFjjz0C&dq=ATF1+APC+MFS&hl=de&lr= [Accessed August 15, 2018].

Barker, R. F., Idler, K. B., Thompson, D. V., and Kemp, J. D. (1983). Nucleotide sequence of the T-DNA region from the A grobacterium tumefaciens octopine Ti plasmid pTi15955. *Plant Mol. Biol.* 2, 335–350. doi:10.1007/BF01578595.

Barrett, L. W., Fletcher, S., and Wilton, S. D. (2012). Regulation of eukaryotic gene expression by the untranslated gene regions and other non-coding elements. *Cell. Mol. Life Sci.* 69, 3613–3634. doi:10.1007/s00018-012-0990-9.

Baskaran, P., Hyvönen, R., Berglund, S. L., Clemmensen, K. E., Ågren, G. I., Lindahl, B. D., et al. (2017). Modelling the influence of ectomycorrhizal decomposition on plant nutrition and soil carbon sequestration in boreal forest ecosystems. *New Phytol.* 213, 1452–1465. doi:10.1111/nph.14213.

Benfey, P. N., and Chua, N. H. (1990). The cauliflower mosaic virus 35S promoter: Combinatorial regulation of transcription in plants. *Science (80-.).* 250, 959–966. doi:10.1126/science.250.4983.959.

Bhullar, S., Chakravarthy, S., Advani, S., Datta, S., Pental, D., and Burma, P. K. (2003). Strategies for development of functionally equivalent promoters with minimum sequence homology for transgene expression in plants: cis-Elements in a novel DNA context versus domain swapping. *Plant Physiol.* 132, 988–998. doi:10.1104/pp.103.020602.

Biłas, R., Szafran, K., Hnatuszko-Konka, K., and Kononowicz, A. K. (2016). Cis-regulatory elements used to control gene expression in plants. *Plant Cell. Tissue Organ Cult.* 127, 269–287. doi:10.1007/s11240-016-1057-7.

Billinton, N., and Knight, A. W. (2001). Seeing the wood through the trees: A review of techniques for distinguishing green fluorescent protein from endogenous autofluorescence. *Anal. Biochem.* 291, 175–197. doi:10.1006/abio.2000.5006.

Binder, A., Lambert, J., Morbitzer, R., Popp, C., Ott, T., Lahaye, T., et al. (2014). A modular plasmid assembly kit for multigene expression, gene silencing and silencing rescue in plants. *PLoS One* 9, 88218. doi:10.1371/journal.pone.0088218.

Birch, R. G. (1997). PLANT TRANSFORMATION: Problems and Strategies for Practical Application. *Annu. Rev. Plant Physiol. Plant Mol. Biol.* 48, 297–326. doi:10.1146/annurev.arplant.48.1.297.

Birnbaum, K., Benfey, P. N., and Shasha, D. E. (2001). cis element/transcription factor Analysis (cis/TF): A method for discovering transcription factor/cis element relationships. *Genome Res.* 11, 1567–1573. doi:10.1101/gr.158301.

Blasius, D., Feil, W., Kottke, I., and Oberwinkler, F. (1986). Hartig net structure and formation in fully ensheathed ectomycorrhizas. *Nord. J. Bot.* 6, 837–842. doi:10.1111/j.1756-1051.1986.tb00487.x.

Bouché, N., and Fromm, H. (2004). GABA in plants: Just a metabolite? *Trends Plant Sci.* 9, 110–115. doi:10.1016/j.tplants.2004.01.006.

Bowen, G. D., and Theodorou, C. (1979). Interactions between bacteria and ectomycorrhizal fungi. *Soil Biol. Biochem.* 11, 119–126. doi:10.1016/0038-0717(79)90087-7.

Bradshaw, H. D., Ceulemans, R., Davis, J., and Stettler, R. (2000). Emerging model systems in plant biology: Poplar (Populus) as a model forest tree. *J. Plant Growth Regul.* 19, 306–313. doi:10.1007/s003440000030.

Breitkreuz, K. E., Shelp, B. J., Fischer, W. N., Schwacke, R., and Rentsch, D. (1999). Identification and characterization of GABA, proline and quaternary ammonium compound transporters from

Arabidopsis thaliana. *FEBS Lett.* 450, 280–284. doi:10.1016/S0014-5793(99)00516-5.

Bresinsky, A., Körner, C., Kadereit, J. W., Neuhaus, G., and Sonnewald, U. (2013). *Strasburger's plant sciences : including Prokaryotes and Fungi*. 1st ed. Springer-Verlag Berlin Heidelberg.

Bright, G. R., Fisher, G. W., Rogowska, J., and Taylor, D. L. (1989). Fluorescence Ratio Imaging Microscopy. *Methods Cell Biol.* 30, 157–192. doi:10.1016/S0091-679X(08)60979-6.

Brownlee, C., Duddridge, J. A., Malibari, A., and Read, D. J. (1983). The structure and function of mycelial systems of ectomycorrhizal roots with special reference to their role in forming inter-plant connections and providing pathways for assimilate and water transport. *Plant Soil* 71, 433–443. doi:10.1007/BF02182684.

Brunner, A. M., Busov, V. B., and Strauss, S. H. (2004). Poplar genome sequence: Functional genomics in an ecologically dominant plant species. *Trends Plant Sci.* 9, 49–56. doi:10.1016/j.tplants.2003.11.006.

Bruns, T. ., and Shefferson, R. . (2004). Evolutionary studies of ectomycorrhizal fungi: recent advances and future directions. *Can. J. Bot.* 82, 1122–1132. doi:10.1139/b04-021.

Cano, C., Dickson, S., González-Guerrero, M., and Bago, A. (2008). "In vitro cultures open new prospects for basic research in arbuscular mycorrhizas," in *Mycorrhiza: State of the Art, Genetics and Molecular Biology, Eco-Function, Biotechnology, Eco-Physiology, Structure and Systematics (Third Edition)* (Springer-Verlag Berlin Heidelberg), 627–654. doi:10.1007/978-3-540-78826-3_30.

Carlson, A. S., Dole, J. M., Matthysse, A. G., Hoffmann, W. A., and Kornegay, J. L. (2015). Bacteria species and solution pH effect postharvest quality of cut Zinnia elegans. *Sci. Hortic. (Amsterdam).* 194, 71–78. doi:10.1016/j.scienta.2015.07.044.

Cartharius, K., Frech, K., Grote, K., Klocke, B., Haltmeier, M., Klingenhoff, A., et al. (2005). MatInspector and beyond: Promoter analysis based on transcription factor binding sites. *Bioinformatics* 21, 2933–2942. doi:10.1093/bioinformatics/bti473.

Chalot, M., and Brun, A. (1998). Physiology of organic nitrogen axquisition by ectomycorrhizal fungi and ectomycorrhizas. *FEMS Microbiol. Rev.* 22, 21–44. doi:10.1111/j.1574-6976.1998.tb00359.x.

Chandra, R., and Kang, H. (2016). Mixed heavy metal stress on photosynthesis, transpiration rate, and chlorophyll content in poplar hybrids. *Forest Sci. Technol.* 12, 55–61. doi:10.1080/21580103.2015.1044024.

Chandra, S. (2012). Natural plant genetic engineer Agrobacterium rhizogenes: Role of T-DNA in plant secondary metabolism. *Biotechnol. Lett.* 34, 407–415. doi:10.1007/s10529-011-0785-3.

Chapagain, P. P., Regmi, C. K., and Castillo, W. (2011). Fluorescent protein barrel fluctuations and oxygen diffusion pathways in mCherry. *J. Chem. Phys.* 135, 235101. doi:10.1063/1.3660197.

Chudakov, D. M., Lukyanov, S., and Lukyanov, K. A. (2005). Fluorescent proteins as a toolkit for in vivo imaging. *Trends Biotechnol.* 23, 605–613. doi:10.1016/j.tibtech.2005.10.005.

Citovsky, V., Kozlovsky, S. V., Lacroix, B., Zaltsman, A., Dafny-Yelin, M., Vyas, S., et al. (2007). Biological systems of the host cell involved in Agrobacterium infection. *Cell. Microbiol.* 9, 9–20.

doi:10.1111/j.1462-5822.2006.00830.x.

Citovsky, V., Lee, L. Y., Vyas, S., Glick, E., Chen, M. H., Vainstein, A., et al. (2006). Subcellular Localization of Interacting Proteins by Bimolecular Fluorescence Complementation in Planta. *J. Mol. Biol.* 362, 1120–1131. doi:10.1016/j.jmb.2006.08.017.

Classification | USDA PLANTS Available at: https://plants.usda.gov/java/ClassificationServlet?source=display&classid=POPUL [Accessed May 13, 2020].

Cohen, J. (1988). *Statistical Power Analysis for the Behavioral Sciences*. 2nd ed. Lawrence Erlbaum doi:10.4324/9780203771587.

Collier, R., Fuchs, B., Walter, N., Kevin Lutke, W., and Taylor, C. G. (2005). Ex vitro composite plants: an inexpensive, rapid method for root biology. *Plant J.* 43, 449–457. doi:10.1111/j.1365-313X.2005.02454.x.

Colpaert, J. V., Wevers, J. . . L., Krznaric, E., and Adriaensen, K. (2011). How metal-tolerant ecotypes of ectomycorrhizal fungi protect plants from heavy metal pollution. in *Annals of Forest Science*, 17–24. doi:10.1007/s13595-010-0003-9.

Corrêa, A., Strasser, R. J., and Martins-Loução, M. A. (2008). Response of plants to ectomycorrhizae in N-limited conditions: Which factors determine its variation? *Mycorrhiza* 18, 413–427. doi:10.1007/s00572-008-0195-0.

Costa, M. D., Campos, A. N. da R., Santos, M. L., and Borges, A. C. (2010). In vitro ectomycorrhiza formation by monokaryotic and dikaryotic isolates of Pisolithus microcarpus in Eucalyptus grandis. *Rev. Árvore* 34, 377–387. doi:10.1590/s0100-67622010000300001.

Curtis, M. D., and Grossniklaus, U. (2003). A Gateway cloning vector set for high-throughput functional analysis of genes in planta. *Breakthr. Technol.* 133, 462–469. doi:10.1104/pp.103.027979.specific.

Cymer, F., Von Heijne, G., and White, S. H. (2015). Mechanisms of integral membrane protein insertion and folding. *J. Mol. Biol.* 427, 999–1022. doi:10.1016/j.jmb.2014.09.014.

Dahlberg, A. (2001). Community ecology of ectomycorrhizal fungi: An advancing interdisciplinary field. *New Phytol.* 150, 555–562. doi:10.1046/j.1469-8137.2001.00142.x.

Daimon, H., Fukami, M., and Mii, M. (1990). Hairy root formation in peanut by the wild type strains of Agrobacterium rhizogenes. *Plant tissue Cult. Lett.* 7, 31–34. doi:10.5511/plantbiotechnology1984.7.31.

Das, A. (2018). Ectomycorrhiza Development: Investigation of Selected Ectomycorrhiza Induced Poplar Genes.

Day, R. N., and Davidson, M. W. (2009). The fluorescent protein palette: Tools for cellular imaging. *Chem. Soc. Rev.* 38, 2887–2921. doi:10.1039/b901966a.

De Rybel, B., van den Berg, W., Lokerse, A. S., Liao, C.-Y., van Mourik, H., Moller, B., et al. (2011). A Versatile Set of Ligation-Independent Cloning Vectors for Functional Studies in Plants. *PLANT Physiol.* 156, 1292–1299. doi:10.1104/pp.111.177337.

de Witte, L. C., Rosenstock, N. P., van der Linde, S., and Braun, S. (2017). Nitrogen deposition changes ectomycorrhizal communities in Swiss beech forests. *Sci. Total Environ.* 605–606, 1083–1096. doi:10.1016/j.scitotenv.2017.06.142.

Deckmyn, G., Meyer, A., Smits, M. M., Ekblad, A., Grebenc, T., Kraigher, H., et al. (2014). Simulating ectomycorrhizal fungi and their role in carbon and nitrogen cycling in forest ecosystems. *Can. J. For. Res.* 44, 535–553. doi:10.1139/cjfr-2013-0496.

Donaldson, L. (2020). Autofluorescence in plants. *Molecules* 25, 2393. doi:10.3390/molecules25102393.

Donaldson, L. A., and Radotic, K. (2013). Fluorescence lifetime imaging of lignin autofluorescence in normal and compression wood. *J. Microsc.* 251, 178–187. doi:10.1111/jmi.12059.

Dreyer, I., Horeau, C., Lemaillet, G., Zimmermann, S., Bush, D. R., Rodríguez-Navarro, A., et al. (1999). Identification and characterization of plant transporters using heterologous expression systems. in *Journal of Experimental Botany* (Oxford University Press), 1073–1087. doi:10.1093/jxb/50.special_issue.1073.

Duddridge, J. A., Malibari, A., and Read, D. J. (1980). Structure and function of mycorrhizal rhizomorphs with special reference to their role in water transport. *Nature* 287, 834–836. doi:10.1038/287834a0.

Duplessis, S., Courty, P. E., Tagu, D., and Martin, F. (2005). Transcript patterns associated with ectomycorrhiza development in Eucalyptus globulus and Pisolithus microcarpus. *New Phytol.* 165, 599–611. doi:10.1111/j.1469-8137.2004.01248.x.

Ebert, P. R., Ha, S. B., and An, G. (1987). Identification of an essential upstream element in the nopaline synthase promoter by stable and transient assays. *Proc. Natl. Acad. Sci.* 84, 5745–5749. doi:10.1073/pnas.84.16.5745.

Esseling, J. J., Lhuissier, F. G. P., and Emons, A. M. C. (2004). A nonsymbiotic root hair tip growth phenotype in NORK-mutated legumes: Implications for modulation factor-induced signaling and formation of a multifaceted root hair pocket for bacteria. *Plant Cell* 16, 933–944. doi:10.1105/tpc.019653.

Fang, R. X., Nagy, F., Sivasubramaniam, S., and Chua, N. H. (1989). Multiple cis regulatory elements for maximal expression of the cauliflower mosaic virus 35S promoter in transgenic plants. *Plant Cell* 1, 141–150. doi:10.1105/tpc.1.1.141.

Felten, J., Kohler, A., Morin, E., Bhalerao, R. P., Palme, K., Martin, F., et al. (2009). The Ectomycorrhizal Fungus Laccaria bicolor Stimulates Lateral Root Formation in Poplar and Arabidopsis through Auxin Transport and Signaling. *PLANT Physiol.* 151, 1991–2005. doi:10.1104/pp.109.147231.

Fischer, R., Vaquero-Martin, C., Sack, M., Drossard, J., Emans, N., and Commandeur, U. (1999). Towards molecular farming in the future: Transient protein expression in plants. *Biotechnol. Appl. Biochem.* 30, 113–116. doi:10.1111/j.1470-8744.1999.tb00900.x.

Fischer, W. ., Kwart, M., Hummel, S., and Frommer, W. B. (1995). Substrate-Specificity and Expression Profile of Amino-Acid Transporters (Aaps) in Arabidopsis. *J. Biol. Chem.* 270, 16315–16320. doi:10.1074/jbc.270.27.16315.

Fitter, A. H., and Moyersoen, B. (1996). Evolutionary trends in root-microbe symbioses. *Philos. Trans.*

R. Soc. B Biol. Sci. 351, 1367–1375. doi:10.1098/rstb.1996.0120.

Forouhar, F., Yang, Y., Kumar, D., Chen, Y., Fridman, E., Park, S. W., et al. (2005). Structural and biochemical studies identify tobacco SABP2 as a methyl salicylate esterase and implicate it in plant innate immunity. *Proc. Natl. Acad. Sci. U. S. A.* 102, 1773–1778. doi:10.1073/pnas.0409227102.

Frettinger, P., Derory, J., Herrmann, S., Plomion, C., Lapeyrie, F., Oelmüller, R., et al. (2007). Transcriptional changes in two types of pre-mycorrhizal roots and in ectomycorrhizas of oak microcuttings inoculated with Piloderma croceum. *Planta* 225, 331–340. doi:10.1007/s00425-006-0355-4.

Fütterer, J., and Hohn, T. (1996). “Translation in plants--rules and exceptions.,” in *Plant molecular biology* (Dordrecht: Springer Netherlands), 159–89. doi:10.1007/978-94-009-0353-1_8.

Gabrielian, A. E., Landsman, D., and Bolshoy, A. (1999). Curved DNA in promoter sequences. *In Silico Biol.* 1, 183–196. Available at: https://content.iospress.com/articles/in-silico-biology/isb00017 [Accessed March 5, 2020].

Gallou, A., De Jaeger, N., Cranenbrouck, S., and Declerck, S. (2010). Fast track in vitro mycorrhization of potato plantlets allow studies on gene expression dynamics. *Mycorrhiza* 20, 201–207. doi:10.1007/s00572-009-0270-1.

Ganguly, S., Clayton, A. H. A., and Chattopadhyay, A. (2011). Fixation alters fluorescence lifetime and anisotropy of cells expressing EYFP-tagged serotonin1A receptor. *Biochem. Biophys. Res. Commun.* 405, 234–237. doi:10.1016/j.bbrc.2011.01.016.

Garbaye, J. (1994). Tansley Review No. 76 Helper bacteria: a new dimension to the mycorrhizal symbiosis. *New Phytol.* 128, 197–210. doi:10.1111/j.1469-8137.1994.tb04003.x.

Geertz, M., and Maerkl, S. J. (2010). Experimental strategies for studying transcription factor-DNA binding specificities. *Brief. Funct. Genomics* 9, 362–373. doi:10.1093/bfgp/elq023.

Gelvin, S. B. (2003). Agrobacterium-Mediated Plant Transformation: the Biology behind the “Gene-Jockeying” Tool. *Microbiol. Mol. Biol. Rev.* 67, 16–37. doi:10.1128/MMBR.67.1.16-37.2003.

Gelvin, S. B. (2010). Plant Proteins Involved in Agrobacterium -Mediated Genetic Transformation. *Annu. Rev. Phytopathol.* 48, 45–68. doi:10.1146/annurev-phyto-080508-081852.

Gelvin, S. B. (2017). Integration of Agrobacterium T-DNA into the Plant Genome. *Annu. Rev. Genet.* 51, annurev-genet-120215-035320. doi:10.1146/annurev-genet-120215-035320.

Gershater, M. C., Cummins, I., and Edwards, R. (2007). Role of a carboxylesterase in herbicide bioactivation in Arabidopsis thaliana. *J. Biol. Chem.* 282, 21460–21466. doi:10.1074/jbc.M701985200.

Gershater, M. C., and Edwards, R. (2007). Regulating biological activity in plants with carboxylesterases. *Plant Sci.* 173, 579–588. doi:10.1016/j.plantsci.2007.08.008.

Gielen, J., Terryn, N., Villarroel, R., and Van Montagu, M. (1999). Complete nucleotide sequence of the T-DNA region of the plant tumour-inducing Agrobacterium tumefaciens Ti plasmid pTiC58. *J. Exp. Bot.* 50, 1421–1422. doi:10.1093/jxb/50.337.1421.

Giron, D., Frago, E., Glevarec, G., Pieterse, C. M. J., and Dicke, M. (2013). Cytokinins as key regulators in plant-microbe-insect interactions: Connecting plant growth and defence. *Funct. Ecol.* 27, 599–609. doi:10.1111/1365-2435.12042.

Gleave, A. P. (1992). A versatile binary vector system with a T-DNA organisational structure conducive to efficient integration of cloned DNA into the plant genome. *Plant Mol. Biol.* 20, 1203–1207. doi:10.1007/BF00028910.

Goodstein, D. M., Shu, S., Howson, R., Neupane, R., Hayes, R. D., Fazo, J., et al. (2012). Phytozome: A comparative platform for green plant genomics. *Nucleic Acids Res.* 40. doi:10.1093/nar/gkr944.

Görgens, J. F., Van Zyl, W. H., Knoetze, J. H., and Hahn-Hägerdal, B. (2005). Amino acid supplementation improves heterologous protein production by Saccharomyces cerevisiae in defined medium. *Appl. Microbiol. Biotechnol.* 67, 684–691. doi:10.1007/s00253-004-1803-3.

Graw, J. (1962). *Genetik*. Berlin Heidelberg 2015: Springer-Verlag doi:10.1007/978-3-642-04999-6_7.

Greene, S. A., and Pohanish, R. P. (2005). *Sittig ' s Handbook of Pesticides and Agricultural Chemicals*.

Grefen, C., Donald, N., Hashimoto, K., Kudla, J., Schumacher, K., and Blatt, M. R. (2010). A ubiquitin-10 promoter-based vector set for fluorescent protein tagging facilitates temporal stability and native protein distribution in transient and stable expression studies. *Plant J.* 64, 355–365. doi:10.1111/j.1365-313X.2010.04322.x.

Gross, G., and Hauser, H. (1995). Heterologous expression as a tool for gene identification and analysis. *J. Biotechnol.* 41, 91–110. doi:10.1016/0168-1656(95)00070-7.

Guo, D., Mitchell, R. J., Withington, J. M., Fan, P. P., and Hendricks, J. J. (2008). Endogenous and exogenous controls of root life span, mortality and nitrogen flux in a longleaf pine forest: Root branch order predominates. *J. Ecol.* 96, 737–745. doi:10.1111/j.1365-2745.2008.01385.x.

Hajdukiewicz, P., Svab, Z., and Maliga, P. (1994). The small, versatile pPZP family of Agrobacterium binary vectors for plant transformation. *Plant Mol. Biol.* 25, 989–994. doi:10.1007/BF00014672.

Halfter, U., Morris, P. C., and Willmitzer, L. (1992). Gene targeting in Arabidopsis thaliana. *MGG Mol. &amp; Gen. Genet.* 231, 186–193. doi:10.1007/BF00279790.

Hanahan, D. (1983). Studies on transformation of Escherichia coli with plasmids. *J. Mol. Biol.* 166, 557–580. doi:10.1016/S0022-2836(83)80284-8.

Hansen, J., Jørgensen, J. E., Stougaard, J., and Marcker, K. A. (1989). Hairy roots - a short cut to transgenic root nodules. *Plant Cell Rep.* 8, 12–15. doi:10.1007/BF00735768.

He, X., Bledsoe, C. S., Zasoski, R. J., Southworth, D., and Horwath, W. R. (2006). Rapid nitrogen transfer from ectomycorrhizal pines to adjacent ectomycorrhizal and arbuscular mycorrhizal plants in a California oak woodland. *New Phytol.* 170, 143–151. doi:10.1111/j.1469-8137.2006.01648.x.

Heim, R., Cubitt, A. B., and Tsien, R. Y. (1995). Improved green fluorescence. *Nature* 373, 663–664. doi:10.1038/373663b0.

Heindl, J. E., Wang, Y., Heckel, B. C., Mohari, B., Feirer, N., and Fuqua, C. (2014). Mechanisms and regulation of surface interactions and biofilm formation in Agrobacterium. *Front. Plant Sci.* 5, 176. doi:10.3389/fpls.2014.00176.

Hellens, R. P., Anne Edwards, E., Leyland, N. R., Bean, S., and Mullineaux, P. M. (2000). pGreen: A versatile and flexible binary Ti vector for Agrobacterium-mediated plant transformation. *Plant Mol. Biol.* 42, 819–832. doi:10.1023/A:1006496308160.

Hellman, L. M., and Fried, M. G. (2007). Electrophoretic mobility shift assay (EMSA) for detecting protein-nucleic acid interactions. *Nat. Protoc.* 2, 1849–1861. doi:10.1038/nprot.2007.249.

Helmisaari, H.-S., Lehto, T., and Makkonen, K. (2000). "Fine Roots and Soil Properties," in (Springer, Dordrecht), 203–217. doi:10.1007/978-94-015-9373-1_24.

Hernandez-Garcia, C. M., and Finer, J. J. (2014). Identification and validation of promoters and cis-acting regulatory elements. *Plant Sci.* 217–218, 109–119. doi:10.1016/j.plantsci.2013.12.007.

Hibbett, D. S., and Brandon Matheny, P. (2009). The relative ages of ectomycorrhizal mushrooms and their plant hosts estimated using Bayesian relaxed molecular clock analyses. *BMC Biol.* 7, 13. doi:10.1186/1741-7007-7-13.

Hibbett, D. S., Gilbert, L. B., and Donoghue, M. J. (2000). Evolutionary instability of ectomycorrhizal symbioses in basidiomycetes. *Nature* 407, 506–508. doi:10.1038/35035065.

Hitchcock, C. J., Chambers, S. M., and Cairney, J. W. G. (2011). Genetic population structure of the ectomycorrhizal fungus Pisolithus microcarpus suggests high gene flow in south-eastern Australia. *Mycorrhiza* 21, 131–137. doi:10.1007/s00572-010-0317-3.

Högberg, M. N. ., Briones, M. J. I., Keel, S. G., Metcalfe, D. B., Campbell, C., Midwood, A. J., et al. (2010). Quantification of effects of season and nitrogen supply on tree below-ground carbon transfer to ectomycorrhizal fungi and other soil organisms in a boreal pine forest. *New Phytol.* 187, 485–493. doi:10.1111/j.1469-8137.2010.03274.x.

Holsters, M., de Waele, D., Depicker, A., Messens, E., van Montagu, M., and Schell, J. (1978). Transfection and transformation of Agrobacterium tumefaciens. *MGG Mol. Gen. Genet.* 163, 181–187. doi:10.1007/BF00267408.

Holtorf, S., Apel, K., and Bohlmann, H. (1995). Comparison of different constitutive and inducible promoters for the overexpression of transgenes in Arabidopsis thaliana. *Plant Mol. Biol.* 29, 637–646. doi:10.1007/BF00041155.

Hutzler, P., Fischbach, R., Heller, W., Jungblut, T. P., Reuber, S., Schmitz, R., et al. (1998). Tissue localization of phenolic compounds in plants by confocal laser scanning microscopy. *J. Exp. Bot.* 49, 953–965. doi:10.1093/jxb/49.323.953.

Hwang, H. H., Gelvin, S. B., and Lai, E. M. (2015). Editorial: "Agrobacterium biology and its application to transgenic plant production." *Front. Plant Sci.* 6, 265. doi:10.3389/fpls.2015.00265.

Iizuka, R., Yamagishi-Shirasaki, M., and Funatsu, T. (2011). Kinetic study of de novo chromophore maturation of fluorescent proteins. *Anal. Biochem.* 414, 173–178. doi:10.1016/j.ab.2011.03.036.

Imoto, A., Yamada, M., Sakamoto, T., Okuyama, A., Ishida, T., Sawa, S., et al. (2021). A clearsee-based clearing protocol for 3d visualization of arabidopsis thaliana embryos. *Plants* 10, 1–7. doi:10.3390/plants10020190.

Iyer, V., and Struhl, K. (1995). Poly(dA:dT), a ubiquitous promoter element that stimulates transcription via its intrinsic DNA structure. *EMBO J.* 14, 2570–2579. doi:10.1002/j.1460-2075.1995.tb07255.x.

Jack, D. L., Paulsen, I. T., and Saier, J. (2000). The amino acid/polyamine/organocation (APC) superfamily of transporters specific for amino acids, polyamines and organocations. *Microbiology* 146, 1797–1814. doi:10.1099/00221287-146-8-1797.

Jain, R. G., Rusch, S. L., and Kendall, D. A. (1994). Signal peptide cleavage regions. Functional limits on length and topological implications. *J. Biol. Chem.* 269, 16305–16310. doi:10.1016/s0021-9258(17)34008-5.

Jian, B., Hou, W., Wu, C., Liu, B., Liu, W., Song, S., et al. (2009). Agrobacterium rhizogenes-mediated transformation of Superroot-derived Lotus corniculatus plants: A valuable tool for functional genomics. *BMC Plant Biol.* 9, 1–14. doi:10.1186/1471-2229-9-78.

Johnson, C. N. (1996). Interactions between mammals and ectomycorrhizal fungi. *Trends Ecol. Evol.* 11, 503–507. doi:10.1016/S0169-5347(96)10053-7.

Jones, M. D., Durall, D. M., and Tinker, P. B. (1998). A comparison of arbuscular and ectomycorrhizal Eucalyptus coccifera : Growth response, phosphorus uptake efficiency and external hyphal production. *New Phytol.* 140, 125–134. doi:10.1046/j.1469-8137.1998.00253.x.

Joubert, P., Beaupère, D., Lelièvre, P., Wadouachi, A., Sangwan, R. S., and Sangwan-Norreel, B. . (2002). Effects of phenolic compounds on Agrobacterium vir genes and gene transfer induction - A plausible molecular mechanism of phenol binding protein activation. *Plant Sci.* 162, 733–743. doi:10.1016/S0168-9452(02)00012-2.

Juven-Gershon, T., and Kadonaga, J. T. (2010). Regulation of gene expression via the core promoter and the basal transcriptional machinery. *Dev. Biol.* 339, 225–229. doi:10.1016/j.ydbio.2009.08.009.

Kamano, S., Kume, S., Iida, K., Lei, K. J., Nakano, M., Nakayama, Y., et al. (2015). Transmembrane Topologies of Ca2+-permeable Mechanosensitive Channels MCA1 and MCA2 in Arabidopsis thaliana. *J. Biol. Chem.* 290, 30901–30909. doi:10.1074/jbc.M115.692574.

Kammerbauer, H., Agerer, R., and Sandermann, H. (1989). Studies on ectomycorrhiza - XXII. Mycorrhizal rhizomorphs of Telephora terrestris and Pisolithus tinctorius in association with Norway spruce (Picea abies): formation in vitro and translocation of phosphate. *Trees* 3, 78–84. doi:10.1007/BF00191537.

Kanhere, A., and Bansal, M. (2005). Structural properties of promoters: Similarities and differences between prokaryotes and eukaryotes. *Nucleic Acids Res.* 33, 3165–3175. doi:10.1093/nar/gki627.

Kanters, C., Anderson, I. C., and Johnson, D. (2015). Chewing up the wood-wide web: Selective grazing on ectomycorrhizal fungi by collembola. *Forests* 6, 2560–2570. doi:10.3390/f6082560.

Kapila, J., De Rycke, R., Van Montagu, M., and Angenon, G. (1997). An Agrobacterium-mediated transient gene expression system for intact leaves. *Plant Sci.* 122, 101–108. doi:10.1016/S0168-9452(96)04541-4.

Karijolich, J. J., and Hampsey, M. (2012). The mediator complex. *Curr. Biol.* 22.

doi:10.1016/j.cub.2012.11.011.

Kaschani, F., Gu, C., Niessen, S., Hoover, H., Cravatt, B. F., and van der Hoorn, R. A. L. (2009). Diversity of Serine Hydrolase Activities of Unchallenged and Botrytis -infected Arabidopsis thaliana. *Mol. Cell. Proteomics* 8, 1082–1093. doi:10.1074/mcp.M800494-MCP200.

Kaschani, F., Nickel, S., Pandey, B., Cravatt, B. F., Kaiser, M., and Van Der Hoorn, R. . L. (2012). Selective inhibition of plant serine hydrolases by agrochemicals revealed by competitive ABPP. *Bioorganic Med. Chem.* 20, 597–600. doi:10.1016/j.bmc.2011.06.040.

Kay, R., Chan, A., Daly, M., and Mcpherson, J. (1987). Duplication of CaMV 35S Promoter Sequences Creates a Strong Enhancer for Plant Genes. *Science (80-.).* 236, 1299–1302. doi:10.1126/science.236.4806.1299.

Kempinski, C., and Chappell, J. (2019). Engineering triterpene metabolism in the oilseed of Arabidopsis thaliana. *Plant Biotechnol. J.* 17, 386–396. doi:10.1111/pbi.12984.

Kennedy, P. (2010). Ectomycorrhizal fungi and interspecific competition: Species interactions, community structure, coexistence mechanisms, and future research directions. *New Phytol.* 187, 895–910. doi:10.1111/j.1469-8137.2010.03399.x.

Kennedy, P. G., Peay, K. G., and Bruns, T. D. (2009). Root tip competition among ectomycorrhizal fungi: Are priority effects a rule or an exception? *Ecology* 90, 2098–2107. doi:10.1890/08-1291.1.

Ketelaar, T., Faivre-Moskalenko, C., Esseling, J. J., De Ruijter, N. C. A., Grierson, C. S., Dogterom, M., et al. (2002). Positioning of nuclei in Arabidopsis root hairs: An actin-regulated process of tip growth. *Plant Cell* 14, 2941–2955. doi:10.1105/tpc.005892.

Khan, A., Fornes, O., Stigliani, A., Gheorghe, M., Castro-Mondragon, J. A., Van Der Lee, R., et al. (2018). JASPAR 2018: Update of the open-access database of transcription factor binding profiles and its web framework. *Nucleic Acids Res.* 46, D260–D266. doi:10.1093/nar/gkx1126.

Khullar, S., and Sudhakara Reddy, M. (2019). "Ectomycorrhizal diversity and tree sustainability," in *Microbial Diversity in Ecosystem Sustainability and Biotechnological Applications: Volume 2. Soil & Agroecosystems* (Springer Singapore), 145–166. doi:10.1007/978-981-13-8487-5_6.

Komori, T., Imayama, T., Kato, N., Ishida, Y., Ueki, J., and Komari, T. (2007). Current Status of Binary Vectors and Superbinary Vectors. *PLANT Physiol.* 145, 1155–1160. doi:10.1104/pp.107.105734.

Kottke, I., and Oberwinkler, F. (1987). The cellular structure of the Hartig net: coenocytic and transfer cell-like organization. *Nord. J. Bot.* 7, 85–95. doi:10.1111/j.1756-1051.1987.tb00919.x.

Kremers, G. J., Goedhart, J., Van Munster, E. B., and Gadella, T. W. J. (2006). Cyan and yellow super fluorescent proteins with improved brightness, protein folding, and FRET förster radius. *Biochemistry* 45, 6570–6580. doi:10.1021/bi0516273.

Krogh, A., Larsson, B., Von Heijne, G., and Sonnhammer, E. L. L. (2001). Predicting transmembrane protein topology with a hidden Markov model: Application to complete genomes. *J. Mol. Biol.* 305, 567–580. doi:10.1006/jmbi.2000.4315.

Kuchma, O., Janz, D., Leinemann, L., Polle, A., Krutovsky, K. V., and Gailing, O. (2020). Hybrid and environmental effects on gene expression in poplar clones in pure and mixed with black locust stands. *Forests* 11, 1–13. doi:10.3390/f11101075.

Kurihara, D., Mizuta, Y., Sato, Y., and Higashiyama, T. (2015). ClearSee: A rapid optical clearing reagent for whole-plant fluorescence imaging. *Dev.* 142, 4168–4179. doi:10.1242/dev.127613.

Lansing, L. (2015). Ectomycorrhiza Repressed Genes: Cellular Localisation of Gene Expression in Aspen Roots and Subcellular Localisation of Encoded Proteins.

Leborgne-Castel, N., and Bouhidel, K. (2014). Plasma membrane protein trafficking in plant-microbe interactions: a plant cell point of view. *Front. Plant Sci.* 5, 735. doi:10.3389/fpls.2014.00735.

Lee, L. Y., and Gelvin, S. B. (2007). T-DNA Binary Vectors and Systems. *Plant Physiol.* 146, 325–332. doi:10.1104/pp.107.113001.

Lepage, B. A., Currah, R. S., Stockey, R. A., and Rothwell, G. W. (1997). Fossil ectomycorrhizae from the middle Eocene. *Am. J. Bot.* 84, 410–412. doi:10.2307/2446014.

Levine, M., and Tjian, R. (2003). Transcription regulation and animal diversity. *Nature* 424, 147–151. doi:10.1038/nature01763.

Lilleskov, E. A., Hobbie, E. A., and Horton, T. R. (2011). Conservation of ectomycorrhizal fungi: Exploring the linkages between functional and taxonomic responses to anthropogenic N deposition. *Fungal Ecol.* 4, 174–183. doi:10.1016/j.funeco.2010.09.008.

Liu, L., Adrian, J., Pankin, A., Hu, J., Dong, X., Von Korff, M., et al. (2014). Induced and natural variation of promoter length modulates the photoperiodic response of FLOWERING LOCUS T. *Nat. Commun.* 5, 1–9. doi:10.1038/ncomms5558.

Liu, Y., Li, X., and Kou, Y. (2020). Ectomycorrhizal fungi: Participation in nutrient turnover and community assembly pattern in forest ecosystems. *Forests* 11, 453. doi:10.3390/F11040453.

Llano, I., Marty, A., Johnson, J. W., Ascher, P., and Gahwiler, B. H. (1988). Patch-clamp recording of amino-activated responses in "organotypic" slice cultures. *Proc. Natl. Acad. Sci. U. S. A.* 85, 3221–3225. doi:10.1073/pnas.85.9.3221.

Long, Y., Kong, D., Chen, Z., and Zeng, H. (2013). Variation of the Linkage of Root Function with Root Branch Order. *PLoS One* 8, 57153. doi:10.1371/journal.pone.0057153.

Lu, K., Wu, B., Wang, J., Zhu, W., Nie, H., Qian, J., et al. (2018). Blocking amino acid transporter OsAAP3 improves grain yield by promoting outgrowth buds and increasing tiller number in rice. *Plant Biotechnol. J.* 16, 1710–1722. doi:10.1111/pbi.12907.

Ma, L. S., Hachani, A., Lin, J. S., Filloux, A., and Lai, E. M. (2014). Agrobacterium tumefaciens deploys a superfamily of type VI secretion DNase effectors as weapons for interbacterial competition in planta. *Cell Host Microbe* 16, 94–104. doi:10.1016/j.chom.2014.06.002.

Majdi, H., Damm, E., and Nylund, J. E. (2001). Longevity of mycorrhizal roots depends on branching order and nutrient availability. *New Phytol.* 150, 195–202. doi:10.1046/j.1469-8137.2001.00065.x.

Mamontova, A. V., Grigoryev, A. P., Tsarkova, A. S., Lukyanov, K. A., and Bogdanov, A. M. (2017). Struggle for photostability: Bleaching mechanisms of fluorescent proteins. *Russ. J. Bioorganic Chem.* 43, 625–633. doi:10.1134/S1068162017060085.

Mamoun, M., and Olivier, J. M. (1993). Competition between Tuber melanosporum and other ectomycorrhizal fungi under two irrigation regimes - I. Competition with Tuber brumale. *Plant Soil* 149, 211–218. doi:10.1007/BF00016611.

Manavella, P. A., and Chan, R. L. (2009). Transient transformation of sunflower leaf discs via an agrobacterium-mediated method: Applications for gene expression and silencing studies. *Nat. Protoc.* 4, 1699–1707. doi:10.1038/nprot.2009.178.

Maniatis, T., Goodbourn, S., and Fischer, J. (1987). Regulation of inducible and tissue-specific gene expression. *Science (80-.).* 236, 1237–1245. doi:10.1126/science.3296191.

Marella, H. H., Nielsen, E., Schachtman, D. P., and Taylor, C. G. (2013). The amino acid permeases AAP3 and AAP6 are involved in root-knot nematode parasitism of Arabidopsis. *Mol. Plant. Microbe. Interact.* 26, 44–54. doi:10.1094/MPMI-05-12-0123-FI.

Marshall, S. D. G., Putterill, J. J., Plummer, K. M., and Newcomb, R. D. (2003). The Carboxylesterase Gene Family from Arabidopsis thaliana. *J. Mol. Evol.* 57, 487–500. doi:10.1007/s00239-003-2492-8.

Martin, F. (2001). Frontiers in molecular mycorrhizal research - Genes, loci, dots and spins. *New Phytol.* 150, 499–505. doi:10.1046/j.1469-8137.2001.00144.x.

Martin, F., Aerts, A., Ahrén, D., Brun, A., Danchin, E. G. J., Duchaussoy, F., et al. (2008). The genome of Laccaria bicolor provides insights into mycorrhizal symbiosis. *Nat. Commun.* 452, 88–93. Available at: https://www.nature.com/articles/nature06556 [Accessed June 19, 2018].

Martin, F., Diez, J., Dell, B., and Delaruelle, C. (2002). Phylogeography of the ectomycorrhizal Pisolithus species as inferred from nuclear ribosomal DNA ITS sequences. *New Phytol.* 153, 345–357. doi:10.1046/j.0028-646X.2001.00313.x.

Martin, F., Duplessis, S., Ditengou, F., Lagrange, H., Voiblet, C., and Lapeyrie, F. (2001). Developmental cross talking in the ectomycorrhizal symbiosis: Signals and communication genes. in *New Phytologist* (Wiley/Blackwell (10.1111)), 145–154. doi:10.1046/j.1469-8137.2001.00169.x.

Martin, F., Kohler, A., and Duplessis, S. (2007). Living in harmony in the wood underground: ectomycorrhizal genomics. *Curr. Opin. Plant Biol.* 10, 204–210. doi:10.1016/j.pbi.2007.01.006.

Martin, F., and Nehls, U. (2009). Harnessing ectomycorrhizal genomics for ecological insights. *Curr. Opin. Plant Biol.* 12, 508–515. doi:10.1016/j.pbi.2009.05.007.

Martins, A. (2008). "In vitro mycorrhization of micropropagated plants: Studies on castanea sativa mill," in *Mycorrhizae: Sustainable Agriculture and Forestry* (Dordrecht: Springer Netherlands), 321–336. doi:10.1007/978-1-4020-8770-7_14.

Massicotte, H. B., Ackerley, C. A., and Peterson, R. L. (1987). Localization of three sugar residues in the interface of ectomycorrhizae synthesized between Alnus crispa and Alpova diplophloeus as demonstrated by lectin binding. *Can. J. Bot.* 65, 1127–1132. doi:10.1139/b87-157.

Mathur, S., Vyas, S., Kapoor, S., and Tyagi, A. K. (2011). The mediator complex in plants: Structure, phylogeny, and expression profiling of representative genes in a dicot (Arabidopsis) and a monocot (Rice) during reproduction and abiotic stress. *Plant Physiol.* 157, 1609–1627. doi:10.1104/pp.111.188300.

Matthysse, A. G. (2014). Attachment of Agrobacterium to plant surfaces. *Front. Plant Sci.* 5, 252.

doi:10.3389/fpls.2014.00252.

McCullen, C. A., and Binns, A. N. (2006). Agrobacterium tumefaciens and Plant Cell Interactions and Activities Required for Interkingdom Macromolecular Transfer. *Annu. Rev. Cell Dev. Biol.* 22, 101–127. doi:10.1146/annurev.cellbio.22.011105.102022.

Meng, F., He, Y., Chen, J., Long, X., Wang, H., Zhu, M., et al. (2021). Analysis of natural variation of the rice blast resistance gene Pike and identification of a novel allele Pikg. *Mol. Genet. Genomics*, 1–14. doi:10.1007/s00438-021-01795-w.

Meyer, P., and Saedler, H. (1996). Homology-dependent gene silencing in plants. *Annu. Rev. Plant Physiol. Plant Mol. Biol.* 47, 23–48. doi:10.1146/annurev.arplant.47.1.23.

Miller, J. B., Pratap, A., Miyahara, A., Zhou, L., Bornemann, S., Morris, R. J., et al. (2013). Calcium/Calmodulin-Dependent Protein Kinase Is Negatively and Positively Regulated by Calcium, Providing a Mechanism for Decoding Calcium Responses during Symbiosis Signaling. *Plant Cell* 25, 5053–5066. doi:10.1105/tpc.113.116921.

Mirabella, R., Franken, C., Van Der Krogt, G. N. M., Bisseling, T., and Geurts, R. (2004). Use of the fluorescent timer DsRED-E5 as reporter to monitor dynamics of gene activity in plants. *Plant Physiol.* 135, 1879–1887. doi:10.1104/pp.103.038539.

Mohanta, T. K., Kumar, P., and Bae, H. (2017). Genomics and evolutionary aspect of calcium signaling event in calmodulin and calmodulin-like proteins in plants. *BMC Plant Biol.* 17, 1–19. doi:10.1186/s12870-017-0989-3.

Moore, L. W., and Chilton, W. S. (1997). Diversity of opines and opine-catabolizing bacteria isolated from naturally occurring Diversity of Opines and Opine-Catabolizing Bacteria Isolated from Naturally Occurring Crown Gall Tumors Downloaded from http://aem.asm.org/ on September 19 , 2014 by SER. *Am Soc Microbiol* 63, 201–207. Available at: http://aem.asm.org/content/63/1/201.short [Accessed June 18, 2018].

Morise, H., Shimomura, O., Johnson, F. H., and Winant, J. (1974). Intermolecular energy transfer in the bioluminescent system of aequorea. *Biochemistry* 13, 2656–2662. doi:10.1021/bi00709a028.

Morris, L. M., Klanke, C. A., Lang, S. A., Lim, F. Y., and Crombleholme, T. M. (2010). TdTomato and EGFP identification in histological sections: Insight and alternatives. *Biotech. Histochem.* 85, 379–387. doi:10.3109/10520290903504753.

Murashige, T., and Skoog, F. (1962). A Revised Medium for Rapid Growth and Bio Assays with Tobacco Tissue Cultures. *Physiol. Plant.* 15, 473–497. doi:10.1111/j.1399-3054.1962.tb08052.x.

Musielak, T. J., Slane, D., Liebig, C., and Bayer, M. (2016). A versatile optical clearing protocol for deep tissue imaging of fluorescent proteins in Arabidopsis thaliana. *PLoS One* 11. doi:10.1371/journal.pone.0161107.

Nagaich, A. K., Appella, E., and Harrington, R. E. (1997). DNA bending is essential for the site-specific recognition of DNA response elements by the DNA binding domain of the tumor suppressor protein p53. *J. Biol. Chem.* 272, 14842–14849. doi:10.1074/jbc.272.23.14842.

Nagaki, K., Yamaji, N., and Murata, M. (2017). EPro-ClearSee: A simple immunohistochemical method that does not require sectioning of plant samples. *Sci. Rep.* 7, 1–9. doi:10.1038/srep42203.

Nanjareddy, K., Arthikala, M. K., Gómez, B. M., Blanco, L., and Lara, M. (2017). Differentially expressed genes in mycorrhized and nodulated roots of common bean are associated with defense, cell wall architecture, N metabolism, and P metabolism. *PLoS One* 12. doi:10.1371/journal.pone.0182328.

Nanjo, T., Futamura, N., Nishiguchi, M., Igasaki, T., Shinozaki, K., and Shinohara, K. (2004). Characterization of full-length enriched expressed sequence tags of stress-treated poplar leaves. *Plant Cell Physiol.* 45, 1738–1748. doi:10.1093/pcp/pci009.

Neb, D. (2017). Bedeutung von SWEET-Genen für den pflanzlichen Zuckerexport in einer Ektomykorrhizasymbiose.

Neb, D., Das, A., Hintelmann, A., and Nehls, U. (2017). Composite poplars: a novel tool for ectomycorrhizal research. *Plant Cell Rep.* 36, 1959–1970. doi:10.1007/s00299-017-2212-2.

Nehls, U., Göhringer, F., Wittulsky, S., and Dietz, S. (2010). Fungal carbohydrate support in the ectomycorrhizal symbiosis: A review. *Plant Biol.* 12, 292–301. doi:10.1111/j.1438-8677.2009.00312.x.

Nickel, S., Kaschani, F., Colby, T., Van Der Hoorn, R. A. L., and Kaiser, M. (2012). A para-nitrophenol phosphonate probe labels distinct serine hydrolases of Arabidopsis. *Bioorganic Med. Chem.* 20, 601–606. doi:10.1016/j.bmc.2011.06.041.

Nishiyama, T., Hatano, H., Kurosaka, M., Bolander, M. E., and Sarkar, G. (2003). Cis-acting intronic elements that regulate cartilage-specific alternative splicing of the type II collagen (Col2) pre-mRNA lie at or near splice site junction sequences flanking exon 2 of the gene. *J. Bone Miner. Res.* 18, 1716–1722. doi:10.1359/jbmr.2003.18.9.1716.

Norkunas, K., Harding, R., Dale, J., and Dugdale, B. (2018). Improving agroinfiltration-based transient gene expression in Nicotiana benthamiana. *Plant Methods* 14, 71. doi:10.1186/s13007-018-0343-2.

Nowak, K., Luniak, N., Meyer, S., Schulze, J., Mendel, R. R., and Hänsch, R. (2004). Fluorescent Proteins in Poplar: A Useful Tool to Study Promoter Function and Protein Localization. *Plant Biol.* 6, 65–73. doi:10.1055/s-2004-815730.

Odell, J. T., Nagy, F., and Chua, N. H. (1985). Identification of DNA sequences required for activity of the cauliflower mosaic virus 35S promoter. *Nature* 313, 810–812. doi:10.1038/313810a0.

Odom, D. T. (2011). Identification of transcription factor-DNA interactions in vivo. *Subcell. Biochem.* 52, 175–191. doi:10.1007/978-90-481-9069-0_8.

Okumoto, S., Koch, W., Tegeder, M., Fischer, W. N., Biehl, A., Leister, D., et al. (2004). Root phloem-specific expression of the plasma membrane amino acid proton co-transporter AAP3. *J. Exp. Bot.* 55, 2155–2168. doi:10.1093/jxb/erh233.

Ortiz-Lopez, A., Chang, H. C., and Bush, D. R. (2000). Amino acid transporters in plants. *Biochim. Biophys. Acta* 1465, 275–280. doi:10.1016/S0005-2736(00)00144-9.

Otsu, N. (1979). THRESHOLD SELECTION METHOD FROM GRAY-LEVEL HISTOGRAMS. *IEEE Trans Syst Man Cybern* SMC-9, 62–66. doi:10.1109/tsmc.1979.4310076.

Palmer, E., and Freeman, T. (2004). Investigation into the use of C- and N-terminal GFP fusion proteins for subcellular localization studies using reverse transfection microarrays. *Comp. Funct. Genomics* 5, 342–353. doi:10.1002/cfg.405.

Patterson, G. H., Knobel, S. M., Sharif, W. D., Kain, S. R., and Piston, D. W. (1997). Use of the green fluorescent protein and its mutants in quantitative fluorescence microscopy. *Biophys. J.* 73, 2782–2790. doi:10.1016/S0006-3495(97)78307-3.

Peay, K. G., Bruns, T. D., Kennedy, P. G., Bergemann, S. E., and Garbelotto, M. (2007). A strong species-area relationship for eukaryotic soil microbes: Island size matters for ectomycorrhizal fungi. *Ecol. Lett.* 10, 470–480. doi:10.1111/j.1461-0248.2007.01035.x.

Peter, M., Courty, P. E., Kohler, A., Delaruelle, C., Martin, D., Tagu, D., et al. (2003). Analysis of expressed sequence tags from the ectomycorrhizal basidiomycetes Laccaria bicolor and Pisolithus microcarpus. *New Phytol.* 159, 117–129. doi:10.1046/j.1469-8137.2003.00796.x.

PhytoMine: Gene Potri.002G079700 P. trichocarpa Available at: https://phytozome.jgi.doe.gov/phytomine/report.do?id=48470182&trail=%7C48470182 [Accessed July 21, 2021].

PhytoMine: Gene Potri.002G218300 P. trichocarpa Available at: https://phytozome.jgi.doe.gov/phytomine/report.do?id=48389230&trail=%7C48389230 [Accessed July 21, 2021].

PhytoMine: Gene Potri.009G104000 P. trichocarpa Available at: https://phytozome.jgi.doe.gov/phytomine/report.do?id=49122789&trail=%7C49122789 [Accessed July 21, 2021].

Phytozome v12.1: Gene Potri.002G079700 P. trichocarpa Available at: https://phytozome.jgi.doe.gov/pz/portal.html#!gene?organism=Ptrichocarpa&searchText=locusName:Potri.002G079700 [Accessed July 21, 2021].

Phytozome v12.1: Gene Potri.002G218300 P. trichocarpa Available at: https://phytozome.jgi.doe.gov/pz/portal.html#!gene?organism=Ptrichocarpa&searchText=locusName:Potri.002G218300 [Accessed July 21, 2021].

Phytozome v12.1: Gene Potri.009G104000 Available at: https://phytozome.jgi.doe.gov/pz/portal.html#!gene?organism=Ptrichocarpa&searchText=locusName:Potri.009G104000 [Accessed July 21, 2021].

Phytozome v12.1: News Available at: https://phytozome.jgi.doe.gov/pz/portal.html#!news [Accessed April 3, 2020].

Pitzschke, A., and Hirt, H. (2010). New insights into an old story: Agrobacterium-induced tumour formation in plants by plant transformation. *EMBO J.* 29, 1021–1032. doi:10.1038/emboj.2010.8.

Platt, T. G., Morton, E. R., Barton, I. S., Bever, J. D., and Fuqua, C. (2014). Ecological dynamics and complex interactions of Agrobacterium megaplasmids. *Front. Plant Sci.* 5, 635. doi:10.3389/fpls.2014.00635.

Pliura, A., Suchockas, V., Sarsekova, D., and Gudynaite, V. (2014). Genotypic variation and heritability of growth and adaptive traits, and adaptation of young poplar hybrids at northern margins of natural distribution of Populus nigra in Europe. *Biomass and Bioenergy* 70, 513–529. doi:10.1016/j.biombioe.2014.09.011.

Porto, M. S., Pinheiro, M. P. N., Batista, V. G. L., Dos Santos, R. C., De Albuquerque Melo Filho, P., and De Lima, L. M. (2014). Plant promoters: An approach of structure and function. *Mol. Biotechnol.* 56, 38–49. doi:10.1007/s12033-013-9713-1.

Pregitzer, K. S., Kubiske, M. E., Yu, C. K., and Hendrick, R. L. (1997). Relationships among root branch order, carbon, and nitrogen in four temperate species. *Oecologia* 111, 302–308. doi:10.1007/s004420050239.

Pregitzer, K. S., Zak, D. R., Loya, W. M., Karberg, N. J., King, J. S., and Burton, A. J. (2007). "The Contribution of Root - Rhizosphere Interactions to Biogeochemical Cycles in a Changing World," in *The Rhizosphere* (Elsevier Inc.), 155–178. doi:10.1016/B978-012088775-0/50009-4.

Prewitt, J. M. S., and Mendelsohn, M. L. (1966). THE ANALYSIS OF CELL IMAGES. *Ann. N. Y. Acad. Sci.* 128, 1035–1053. doi:10.1111/j.1749-6632.1965.tb11715.x.

Pumplin, N., Zhang, X., Noar, R. D., and Harrison, M. J. (2012). Polar localization of a symbiosis-specific phosphate transporter is mediated by a transient reorientation of secretion. *Proc. Natl. Acad. Sci. U. S. A.* 109, E665. doi:10.1073/pnas.1110215109.

Ramesh, S. A., Tyerman, S. D., Gilliham, M., and Xu, B. (2017). γ-Aminobutyric acid (GABA) signalling in plants. *Cell. Mol. Life Sci.* 74, 1577–1603. doi:10.1007/s00018-016-2415-7.

Regierer, B., Fernie, A. R., Springer, F., Perez-Melis, A., Leisse, A., Koehl, K., et al. (2002). Starch content and yield increase as a result of altering adenylate pools in transgenic plants. *Nat. Biotechnol.* 20, 1256–1260. doi:10.1038/nbt760.

Reichel, C., Mathur, J., Eckes, P., Langenkemper, K., Koncz, C., Schell, J., et al. (1996). Enhanced green fluorescence by the expression of an Aequorea victoria green fluorescent protein mutant in mono- and dicotyledonous plant cells. *Proc. Natl. Acad. Sci. U. S. A.* 93, 5888–5893. doi:10.1073/pnas.93.12.5888.

Ridge, C. R., Hinckley, T. M., Stettler, R. F., and Van Volkenburgh, E. (1986). Leaf growth characteristics of fast-growing poplar hybrids Populus trichocarpa x P. deltoides. *Tree Physiol.* 1, 209–216. doi:10.1093/treephys/1.2.209.

Riethoven, J. J. M. (2010). "Regulatory Regions in DNA: Promoters, Enhancers, Silencers, and Insulators," in (Humana Press, Totowa, NJ), 33–42. doi:10.1007/978-1-60761-854-6_3.

Roberts, M. R. (2007). Does GABA act as a signal in plants? Hints from molecular studies. *Plant Signal. Behav.* 2, 408–409. doi:10.4161/psb.2.5.4335.

Rombauts, S., Florquin, K., Lescot, M., Marchal, K., Rouzé, P., and Van De Peer, Y. (2003). Computational approaches to identify promoters and cis-regulatory elements in plant genomes. *Plant Physiol.* 132, 1162–1176. doi:10.1104/pp.102.017715.

Rose, A. B. (2019). Introns as Gene Regulators: A Brick on the Accelerator. *Front. Genet.* 9, 672. doi:10.3389/fgene.2018.00672.

Roshchina, V. V. (2012). Vital Autofluorescence: Application to the Study of Plant Living Cells. *Int. J.*

Spectrosc. 2012, 1–14. doi:10.1155/2012/124672.

Sachs, M. M., and Tuan-Hua, D. H. (1986). Alteration of gene expression during environmental stress in plants. *Annu. Rev. Plant Biol.* 37, 363–376. doi:10.4141/cjps65-072.

Sahoo, D. K., Ranjan, R., Kumar, D., Kumar, A., Sahoo, B. S., Raha, S., et al. (2009). An alternative method of promoter assessment by confocal laser scanning microscopy. *J. Virol. Methods* 161, 114–121. doi:10.1016/j.jviromet.2009.06.011.

Sally, E., and Smith, D. (2008). *Mycorrhizal Symbiosis*. Academic Press.

Samanta, S., and Thakur, J. K. (2015). Importance of mediator complex in the regulation and integration of diverse signaling pathways in plants. *Front. Plant Sci.* 6, 757. doi:10.3389/fpls.2015.00757.

Sambrook, J., Fritsch, E. F., and Maniatis, T. (1989). Molecular cloning: a laboratory manual. *Mol. cloning a Lab. manual.*

Sánchez-Brunete, C., García-Valcárcel, A. I., and Tadeo, J. L. (1994). Determination of residues of phenoxy acid herbicides in soil and cereals by gas chromatography-ion trap detection. *J. Chromatogr. A* 675, 213–218. doi:10.1016/0021-9673(94)85274-X.

Sandelin, A. (2004). JASPAR: an open-access database for eukaryotic transcription factor binding profiles. *Nucleic Acids Res.* 32, 91D – 94. doi:10.1093/nar/gkh012.

Sato, S., Ogasawara, Y., and Sakuragi, S. (1995). “The relationship between growth, nucleus migration and cytoskeleton in root hairs of radish,” in *Structure and Function of Roots* (Springer Netherlands), 69–74. doi:10.1007/978-94-017-3101-0_8.

Schaechter, M. (2009). *Encyclopedia of Microbiology*. doi:10.1016/B978-012373944-5.00036-5.

Schilmiller, A. L., Gilgallon, K., Ghosh, B., Jones, A. D., and Last, R. L. (2016). Acylsugar Acylhydrolases: Carboxylesterase-Catalyzed Hydrolysis of Acylsugars in Tomato Trichomes. *Plant Physiol.* 170, 1331–44. doi:10.1104/pp.15.01348.

Schnakenberg, J. (2020). Analysis of ectomycorrhiza induced gene expression of selected poplar genes expressed in poplar fine roots. Available at: https://media.suub.uni-bremen.de/handle/elib/4596 [Accessed May 13, 2021].

Schneeberger, R. G., Zhang, K., Tatarinova, T., Troukhan, M., Kwok, S. F., Drais, J., et al. (2005). Agrobacterium T-DNA integration in Arabidopsis is correlated with DNA sequence compositions that occur frequently in gene promoter regions. *Funct. Integr. Genomics* 5, 240–253. doi:10.1007/s10142-005-0138-1.

Shahmuradov, I. A., Solovyev, V. V., and Gammerman, A. J. (2005). Plant promoter prediction with confidence estimation. *Nucleic Acids Res.* 33, 1069–1076. doi:10.1093/nar/gki247.

Shaner, N. C., Campbell, R. E. E., Steinbach, P. A., Giepmans, B. N. G., Palmer, A. E., and Tsien, R. Y. Y. (2004). Improved monomeric red, orange and yellow fluorescent proteins derived from Discosoma sp. red fluorescent protein. *Nat. Biotechnol.* 22, 1567–1572. doi:10.1038/nbt1037.

Shao, J. L., Long, Y. S., Chen, G., Xie, J., and Xu, Z. F. (2010). The reversed terminator of octopine synthase gene on the Agrobacterium Ti plasmid has a weak promoter activity in prokaryotes. *Mol. Biol. Rep.* 37, 2157–2162. doi:10.1007/s11033-009-9688-y.

Sharma, P., Kumar, V., Singh, S. K., Thakur, S., Siwach, P., Sreenivasulu, Y., et al. (2017). Promoter Trapping and Deletion Analysis Show Arabidopsis thaliana APETALA2 Gene Promoter Is Bidirectional and Functions as a Pollen- and Ovule-Specific Promoter in the Reverse Orientation. *Appl. Biochem. Biotechnol.* 182, 1591–1604. doi:10.1007/s12010-017-2420-9.

Shelp, B. J., Bown, A. W., and McLean, M. D. (1999). Metabolism and functions of gamma-aminobutyric acid. *Trends Plant Sci.* 4, 446–452. doi:10.1016/S1360-1385(99)01486-7.

Shilo, S., Tripathi, P., Melamed-Bessudo, C., Tzfadia, O., Muth, T. R., and Levy, A. A. (2017). T-DNA-Genome junctions form early after infection and are influenced by the chromatin state of the host genome. *PLoS Genet.* 13, e1006875. doi:10.1371/journal.pgen.1006875.

Shimomura, O., Johnson, F. H., and Saiga, Y. (1962). Extraction, purification and properties of aequorin, a bioluminescent. *J. Cell. Comp. Physiol.* 59, 223–239. doi:10.1002/jcp.1030590302.

Signor, S. A., and Nuzhdin, S. V. (2018). The Evolution of Gene Expression in cis and trans. *Trends Genet.* 34, 532–544. doi:10.1016/j.tig.2018.03.007.

Simard, S. W., Perry, D. A., Jones, M. D., Myrold, D. D., Durall, D. M., and Molina, R. (1997). Net transfer of carbon between ectomycorrhizal tree species in the field. *Nature* 388, 579–582. doi:10.1038/41557.

Smale, S. T., and Kadonaga, J. T. (2003). The RNA Polymerase II Core Promoter. *Annu. Rev. Biochem.* 72, 449–479. doi:10.1146/annurev.biochem.72.121801.161520.

Smith, E. F., and Townsend, C. O. (1907). A PLANT-TUMOR OF BACTERIAL ORIGIN. *Science* 25, 671–3. doi:10.1126/science.25.643.671.

Smith, S. E., Gianinazzi-Pearson, V., Koide, R., and Cairney, J. W. G. (1994). Nutrient transport in mycorrhizas: structure, physiology and consequences for efficiency of the symbiosis. *Plant Soil* 159, 103–113. doi:10.1007/BF00000099.

Smith, S. E., and Read, D. J. (2010). *Mycorrhizal symbiosis.* Available at: https://books.google.de/books?hl=de&lr=&id=qLciOJaG0C4C&oi=fnd&pg=PP1&dq=smith+and+read+mycorrhizal+symbiosis&ots=zqtZj-WClQ&sig=r8Mbl3jsHL-2L6veZZCMqd5NZGs [Accessed June 19, 2018].

Srivastava, A. K., Lu, Y., Zinta, G., Lang, Z., and Zhu, J. K. (2018). UTR-Dependent Control of Gene Expression in Plants. *Trends Plant Sci.* 23, 248–259. doi:10.1016/j.tplants.2017.11.003.

Stachel, S. E., Messens, E., Van Montagu, M., and Zambryski, P. (1985). Identification of the signal molecules produced by wounded plant cells that activate T-DNA transfer in Agrobacterium tumefaciens. *Nature* 318, 624–629. doi:10.1038/318624a0.

Stormo, G. D. (2000). DNA binding sites: Representation and discovery. *Bioinformatics* 16, 16–23. doi:10.1093/bioinformatics/16.1.16.

Stricker, K. B., Hagan, D., and Flory, S. L. (2015). Improving methods to evaluate the impacts of plant invasions: Lessons from 40 years of research. *AoB Plants* 7. doi:10.1093/aobpla/plv022.

Stuhlfelder, C., Mueller, M. J., and Warzecha, H. (2004). Cloning and expression of a tomato cDNA encoding a methyl jasmonate cleaving esterase. *Eur. J. Biochem.* 271, 2976–2983. doi:10.1111/j.1432-1033.2004.04227.x.

Su, Y. H., Frommer, W. B., and Ludewig, U. (2004). Molecular and functional characterization of a family of amino acid transporters from Arabidopsis. *Plant Physiol.* 136, 3104–13. doi:10.1104/pp.104.045278.

Subach, F. V., and Verkhusha, V. V. (2012). Chromophore transformations in red fluorescent proteins. *Chem. Rev.* 112, 4308–4327. doi:10.1021/cr2001965.

Subramoni, S., Nathoo, N., Klimov, E., and Yuan, Z. C. (2014). Agrobacterium tumefaciens responses to plant-derived signaling molecules. *Front. Plant Sci.* 5, 322. doi:10.3389/fpls.2014.00322.

Suzuki, K., Tanaka, K., Yamamoto, S., Kiyokawa, K., Moriguchi, K., and Yoshida, K. (2009). “Ti and Ri Plasmids,” in *Microbial Megaplasmids* (Springer, Berlin, Heidelberg), 133–147. doi:10.1007/978-3-540-85467-8_6.

Takada, S., and Jürgens, G. (2007). Transcriptional regulation of epidermanl cell fate in the Arabidopsis embryo. *Development* 134, 1141–1150. doi:10.1242/dev.02803.

Tedersoo, L., May, T. W., and Smith, M. E. (2010). Ectomycorrhizal lifestyle in fungi: Global diversity, distribution, and evolution of phylogenetic lineages. *Mycorrhiza* 20, 217–263. doi:10.1007/s00572-009-0274-x.

Terskikh, A., Fradkov, A., Ermakova, G., Zaraisky, A., Tan, P., Kajava, A. V., et al. (2000). “Fluorescent timer”: Protein that changes color with time. *Science (80-.).* 290, 1585–1588. doi:10.1126/science.290.5496.1585.

Timonen, S. (1995). Avoiding autofluorescence problems: time-resolved fluorescence microscopy with plant and fungal cells in ectomycorrhiza. *Mycorrhiza* 5, 455–458. doi:10.1007/BF00213448.

Trauth, J., Scheffer, J., S., H., and Taxis, C. (2020). Strategies to investigate protein turnover with fluorescent protein reporters in eukaryotic organisms. *AIMS Biophys.* 7, 90–118. doi:10.3934/BIOPHY.2020008.

Tsai, C. J., Podila, G. K., and Chiang, V. L. (1994). Agrobacterium-mediated transformation of quaking aspen (Populus tremuloides) and regeneration of transgenic plants. *Plant Cell Rep.* 14, 94–97. doi:10.1007/BF00233768.

Tuskan, G. A., DiFazio, S., Jansson, S., Bohlmann, J., Grigoriev, I., Hellsten, U., et al. (2006). The genome of black cottonwood, Populus trichocarpa (Torr. & Gray). *Science (80-.).* 313, 1596–1604. doi:10.1126/science.1128691.

Tzfira, T., and Citovsky, V. (2006). Agrobacterium-mediated genetic transformation of plants: biology and biotechnology. *Curr. Opin. Biotechnol.* 17, 147–154. doi:10.1016/j.copbio.2006.01.009.

Tzfira, T., Li, J., Lacroix, B., and Citovsky, V. (2004). Agrobacterium T-DNA integration: Molecules and models. *Trends Genet.* 20, 375–383. doi:10.1016/j.tig.2004.06.004.

Usadel, B., Obayashi, T., Mutwil, M., Giorgi, F. M., Bassel, G. W., Tanimoto, M., et al. (2009). Co-expression tools for plant biology: Opportunities for hypothesis generation and caveats. *Plant, Cell Environ.* 32, 1633–1651. doi:10.1111/j.1365-3040.2009.02040.x.

Valvekens, D., Montagu, M. V., and Lijsebettens, M. V. (1988). Agrobacterium tumefaciens-mediated transformation of Arabidopsis thaliana root explants by using kanamycin selection. *Proc. Natl.*

Acad. Sci. 85, 5536–5540. doi:10.1073/pnas.85.15.5536.

Vandepoele, K., Quimbaya, M., Casneuf, T., De Veylder, L., and Van Peer, Y. D. (2009). Unraveling transcriptional control in arabidopsis using cis-regulatory elements and coexpression networks1[C][W]. *Plant Physiol.* 150, 535–546. doi:10.1104/pp.109.136028.

Varsha Wesley, S., Helliwell, C. A., Smith, N. A., Wang, M., Rouse, D. T., Liu, Q., et al. (2001). Construct design for efficient, effective and high-throughput gene silencing in plants. *Plant J.* 27, 581–590. doi:10.1046/j.1365-313X.2001.01105.x.

Vayssières, A., Pěnčík, A., Felten, J., Kohler, A., Ljung, K., Martin, F., et al. (2015). Development of the Poplar -Laccaria bicolor Ectomycorrhiza Modifies Root Auxin Metabolism, Signaling, and Response. *Plant Physiol.* 169, 890–902. doi:10.1104/pp.114.255620.

Vector Detail Arabidopsis Stock centre pCXUN-FLAG Available at: https://www.arabidopsis.org/servlets/TairObject?type=vector&id=1001200276 [Accessed May 13, 2020].

Veena, V., and Taylor, C. G. (2007). Agrobacterium rhizogenes: Recent developments and promising applications. *Vitr. Cell. Dev. Biol. - Plant* 43, 383–403. doi:10.1007/s11627-007-9096-8.

Verkhusha, V. V., Kuznetsova, I. M., Stepanenko, O. V., Zaraisky, A. G., Shavlovsky, M. M., Turoverov, K. K., et al. (2003). High stability of Discosoma DsRed as compared to Aequorea EGFP. *Biochemistry* 42, 7879–7884. doi:10.1021/bi034555t.

Verma, V., Ravindran, P., and Kumar, P. P. (2016). Plant hormone-mediated regulation of stress responses. *BMC Plant Biol.* 16, 1–10. doi:10.1186/s12870-016-0771-y.

Voets, L., De La Providencia, I. E., Fernandez, K., Ijdo, M., Cranenbrouck, S., and Declerck, S. (2009). Extraradical mycelium network of arbuscular mycorrhizal fungi allows fast colonization of seedlings under in vitro conditions. *Mycorrhiza* 19, 347–356. doi:10.1007/s00572-009-0233-6.

Voinnet, O., Rivas, S., Mestre, P., and Baulcombe, D. (2003). An enhanced transient expression system in plants based on suppression of gene silencing by the p19 protein of tomato bushy stunt virus. *Plant J.* 33, 949–956. doi:10.1046/j.1365-313X.2003.01676.x.

Vollenweider, H. J., Fiandt, M., and Szybalski, W. (1979). A relationship between DNA helix stability and recognition sites for RNA polymerase. *Science (80-.).* 205, 508–511. doi:10.1126/science.377494.

Wagner, S., Behera, S., De Bortoli, S., Logan, D. C., Fuchs, P., Carraretto, L., et al. (2015). The EF-Hand Ca 2+ Binding Protein MICU Choreographs Mitochondrial Ca 2+ Dynamics in Arabidopsis. *Plant Cell* 27, 3190–3212. doi:10.1105/tpc.15.00509.

Wallander, H., Ekblad, A., and Bergh, J. (2011). Growth and carbon sequestration by ectomycorrhizal fungi in intensively fertilized Norway spruce forests. *For. Ecol. Manage.* 262, 999–1007. doi:10.1016/j.foreco.2011.05.035.

Wang, B., and Qiu, Y. L. (2006). Phylogenetic distribution and evolution of mycorrhizas in land plants. *Mycorrhiza* 16, 299–363. doi:10.1007/s00572-005-0033-6.

Wasserman, W. W., and Sandelin, A. (2004). Applied bioinformatics for the identification of regulatory elements. *Nat. Rev. Genet.* 5, 276–287. doi:10.1038/nrg1315.

Waters, J. C. (2009). Accuracy and precision in quantitative fluorescence microscopy. *J. Cell Biol.* 185, 1135–1148. doi:10.1083/jcb.200903097.

Wells, C. E., and Eissenstat, D. M. (2002). Beyond the roots of young seedlings: The influence of age and order on fine root physiology. *J. Plant Growth Regul.* 21, 324–334. doi:10.1007/s00344-003-0011-1.

Wood, D. W., Setubal, J. C., Kaul, R., Monks, D. E., Kitajima, J. P., Okura, V. K., et al. (2001). The genome of the natural genetic engineer Agrobacterium tumefaciens C58. *Science (80-.).* 294, 2317–2323. doi:10.1126/science.1066804.

Wroblewski, T., Tomczak, A., and Michelmore, R. (2005). Optimization of Agrobacterium-mediated transient assays of gene expression in lettuce, tomato and Arabidopsis. *Plant Biotechnol. J.* 3, 259–273. doi:10.1111/j.1467-7652.2005.00123.x.

Wu, M., Wu, S., Chen, Z., Dong, Q., Yan, H., and Xiang, Y. (2015). Genome-wide survey and expression analysis of the amino acid transporter gene family in poplar. *Tree Genet. Genomes* 11, 83. doi:10.1007/s11295-015-0908-4.

Xiang, T., Wang, S., Li, Y., Zhang, T., Wu, D., and Zhou, S. (2016). Cucumopine Type Agrobacterium Rhizogenes K599 (Ncppb2659) T-Dna Mediated Plant Transformation and Its Application. *Bangladesh J. Bot.* 45, 935–945. Available at: http://www.bdbotsociety.org/journal/journal_issue/2016 September Supplementary/25.pdf.

Xie, H., Guo, X. M., and Chen, H. (2009). Making the most of fusion tags technology in structural characterization of membrane proteins. *Mol. Biotechnol.* 42, 135–145. doi:10.1007/s12033-009-9148-x.

Yamamoto, T., Hoshikawa, K., Ezura, K., Okazawa, R., Fujita, S., Takaoka, M., et al. (2018). Improvement of the transient expression system for production of recombinant proteins in plants. *Sci. Rep.* 8, 1–10. doi:10.1038/s41598-018-23024-y.

Yang, Y., Tang, R. J., Li, B., Wang, H. H., Jin, Y. L., Jiang, C. M., et al. (2015). Overexpression of a Populus trichocarpa H+-pyrophosphatase gene PtVP1.1 confers salt tolerance on transgenic poplar. *Tree Physiol.* 35, 663–677. doi:10.1093/treephys/tpv027.

Yang, Y., Xu, R., Ma, C. J., Vlot, A. C., Klessig, D. F., and Pichersky, E. (2008). Inactive Methyl Indole-3-Acetic Acid Ester Can Be Hydrolyzed and Activated by Several Esterases Belonging to the AtMES Esterase Family of Arabidopsis. *PLANT Physiol.* 147, 1034–1045. doi:10.1104/pp.108.118224.

Yen, J. C., Chang, F. J., and Chang, S. (1995). A New Criterion for Automatic Multilevel Thresholding. *IEEE Trans. Image Process.* 4, 370–378. doi:10.1109/83.366472.

Yin, J. W., and Wang, G. (2014). The Mediator complex: A master coordinator of transcription and cell lineage development. *Dev.* 141, 977–987. doi:10.1242/dev.098392.

Young, J. M., Kuykendall, L. D., Martínez-Romero, E., Kerr, A., and Sawada, H. (2001). A revision of Rhizobium Frank 1889, with an emended description of the genus, and the inclusion of all species of Agrobacterium Conn 1942 and Allorhizobium undicola de Lajudie et al. 1998 as new combinations: Rhizobium radiobacter, R. rhizogenes, R. rubi,. *Int. J. Syst. Evol. Microbiol.* 51, 89–

103. Available at: http://ijs.microbiologyresearch.org/content/journal/ijsem/10.1099/00207713-51-1-89 [Accessed June 18, 2018].

Zack, G. W., Rogers, W. E., and Latt, S. A. (1977). Automatic measurement of sister chromatid exchange frequency. *J. Histochem. Cytochem.* 25, 741–753. doi:10.1177/25.7.70454.

Zajac, J. M., Schubert, M., Roland, T., Keum, C., Samuel, I. D. W., and Gather, M. C. (2018). Time-Resolved Studies of Energy Transfer in Thin Films of Green and Red Fluorescent Proteins. *Adv. Funct. Mater.* 28. doi:10.1002/adfm.201706300.

Zak, D. R., Pellitier, P. T., Argiroff, W. A., Castillo, B., James, T. Y., Nave, L. E., et al. (2019). Exploring the role of ectomycorrhizal fungi in soil carbon dynamics. *New Phytol.* 223, 33–39. doi:10.1111/nph.15679.

Zeng, H., Zhang, Y., Zhang, X., Pi, E., and Zhu, Y. (2017). Analysis of EF-Hand Proteins in Soybean Genome Suggests Their Potential Roles in Environmental and Nutritional Stress Signaling. *Front. Plant Sci.* 8, 1–15. doi:10.3389/fpls.2017.00877.

Zhang, H., Jing, R., and Mao, X. (2017). Functional Characterization of TaSnRK2.8 Promoter in Response to Abiotic Stresses by Deletion Analysis in Transgenic Arabidopsis. *Front. Plant Sci.* 8, 1198. doi:10.3389/fpls.2017.01198.

Zhu, M., Zhang, F., Lv, Z., Shen, Q., Zhang, L., Lu, X., et al. (2014). Characterization of the Promoter of Artemisia annua Amorpha-4,11-diene Synthase (ADS) Gene Using Homologous and Heterologous Expression as well as Deletion Analysis. *Plant Mol. Biol. Report.* 32, 406–418. doi:10.1007/s11105-013-0656-2.

Zhu, W., Sang, Y. L., Zhu, Q., Duan, B., and Wang, Y. (2018). Morphology and longevity of different-order fine roots in poplar (Populus × euramericana) plantations with contrasting forest productivities. *Can. J. For. Res.* 48, 611–620. doi:10.1139/cjfr-2017-0296.

Ziegenhagen, B., Gneuss, S., Rathmacher, G., Leyer, I., Bialozyt, R., Heinze, B., et al. (2008). A fast and simple genetic survey reveals the spread of poplar hybrids at a natural Elbe river site. *Conserv. Genet.* 9, 373–379. doi:10.1007/s10592-007-9349-4.

Zielinski, R. E. (1998). Calmodulin and calmodulin-binding proteins in plants. *Annu. Rev. Plant Physiol. Plant Mol. Biol.* 49, 697–725. doi:10.1146/annurev.arplant.49.1.697.

Zimmer, M. (2002). Green fluorescent protein (GFP): Applications, structure, and related photophysical behavior. *Chem. Rev.* 102, 759–781. doi:10.1021/cr010142r.

Zimmer, M. (2009). GFP: From jellyfish to the Nobel prize and beyond. *Chem. Soc. Rev.* 38, 2823–2832. doi:10.1039/b904023d.

Zuo, Y. C. C., and Li, Q. Z. Z. (2011). Identification of TATA and TATA-less promoters in plant genomes by integrating diversity measure, GC-Skew and DNA geometric flexibility. *Genomics* 97, 112–120. doi:10.1016/j.ygeno.2010.11.002.

Universität Bremen

Versicherung an Eides Statt

Ich, Anneke Immoor,

versichere an Eides Statt durch meine Unterschrift, dass ich die vorstehende Arbeit selbständig und ohne fremde Hilfe angefertigt und alle Stellen, die ich wörtlich dem Sinne nach aus Veröffentlichungen entnommen habe, als solche kenntlich gemacht habe, mich auch keiner anderen als der angegebenen Literatur oder sonstiger Hilfsmittel bedient habe.

Ich versichere an Eides Statt, dass ich die vorgenannten Angaben nach bestem Wissen und Gewissen gemacht habe und dass die Angaben der Wahrheit entsprechen und ich nichts verschwiegen habe.

Die Strafbarkeit einer falschen eidesstattlichen Versicherung ist mir bekannt, namentlich die Strafandrohung gemäß § 156 StGB bis zu drei Jahren Freiheitsstrafe oder Geldstrafe bei vorsätzlicher Begehung der Tat bzw. gemäß § 161 Abs. 1 StGB bis zu einem Jahr Freiheitsstrafe oder Geldstrafe bei fahrlässiger Begehung.

____

Ort, Datum Unterschrift